



**CENTRE OF
EXPERTISE**
DELTA TECHNOLOGY

www.coedeltatechnology.nl

PERKPOLDER TIDAL RESTORATION

FINAL REPORT

CENTRE OF EXPERTISE DELTA TECHNOLOGY
APRIL 2019



PERKPOLDER

TIDAL RESTORATION

FINAL REPORT

CENTRE OF EXPERTISE DELTA TECHNOLOGY

APRIL 2019

AUTHORS

Wietse I. van de Lageweg (HZ University of Applied Sciences)

Joao N. Salvador de Paiva (HZ University of Applied Sciences)

P. Lodewijk M. de Vet (Deltares, TU Delft)

Jebbe J. van der Werf (Deltares)

Perry G. B. de Louw, Martijn Visser, Sandra Galvis Rodriguez (Deltares)

Brenda Walles (Wageningen Marine Research)

Tjeerd J. Bouma (NIOZ Royal Netherlands Institute for Sea Research, HZ University of Applied Sciences)

Tom J.W. Ysebaert (Wageningen Marine Research, NIOZ Royal Netherlands Institute for Sea Research)

DATE	LOCATION	VERSION AND STATUS
April 2019	Middelburg, Utrecht, Yerseke	Final

Photo on cover: Perkpolder in April 2017, during field trip



TABLE OF CONTENTS

LIST OF FIGURES	6
LIST OF TABLES	12
MANAGEMENT SAMENVATTING	14
EXECUTIVE SUMMARY	19
1 INTRODUCTION	22
1.1 Plan Perkpolder	22
1.2 Administrative background	23
1.3 Monitoring and research	23
1.4 Problem statement	24
1.5 Goals	24
1.6 Research questions	26
1.6.1 Morphology and hydrodynamics	26
1.6.2 Groundwater	26
1.6.3 Vegetation and soil	26
1.6.4 Benthic macrofauna and birds	26
2 MORPHOLOGY AND WATER MOVEMENT	28
2.1 Introduction	28
2.2 Methods	29
2.2.1 Height measurements in subtidal and inter tidal areas	29
2.2.2 Sediment thickness in shallow intertidal area	30
2.2.3 Cross-section inlet intertidal and supra tidal	33
2.2.4 Flow velocities inlet and water levels	33
2.2.5 Suspended Sediment	34
2.3 Results	35
2.3.1 Sediment import analysis based on measured concentrations and computed discharges	35
2.3.2 Morphological changes	42
2.3.3 Delft3D modelling	56
2.3.4 Sediment balance in the basin and foreshore areas	59
2.3.5 Comparison of hypsometry with other tidal basins	61
2.4 Discussion	64
2.5 Conclusions	65
2.6 Reccomendations	66
3 GRO(U)NDWATER	68
3.1 Inleiding	68
3.2 De kwelvoorziening	69
3.2.1 Doel en werking van de kwelvoorziening	69
3.3 Het meetnet	73
3.3.1 Inleiding	73
3.3.2 Stijghoogte	75
3.3.3 Grensvlak zoet-zout grondwater	76
3.3.4 Afvoer kwelvoorziening: debiet en zoutgehalte	77

3.4	Meetresultaten 2015 – 2018	77
3.4.1	Meetresultaten stijghoogte	77
3.4.2	Meetresultaten grensvlak zoet-zout grondwater	81
3.4.3	Meetresultaten debiet en zoutgehalte kwelvoorziening	82
3.5	Operationeel beheer en onderhoud kwelvoorziening	86
3.5.1	Inleiding	86
3.5.2	Operationeel beheer van de kwelvoorziening	86
3.5.3	Beheer en onderhoud van de kwelvoorziening	89
3.6	Monitoring: uitwerking en analyse meetgegevens	90
3.6.1	Inleiding	90
3.6.2	Monitoringplan, onderhoud en uitvoeren van de metingen	90
3.6.3	Verwerking, presentatie en analyse meetgegevens	92
3.7	Lange termijn effecten op zoetwaterlens	97
3.7.1	Inleiding	97
3.7.2	Opzet en scenario's	97
3.7.3	Resultaten	98
3.8	Conclusies en aanbevelingen	98
3.8.1	Conclusies	98
3.8.2	Aanbevelingen	99
3.9	Extended Abstract	100
4	VEGETATION AND SEDIMENT DEVELOPMENT	103
4.1	Introduction	103
4.2	Results	106
4.2.1	Research question 1	107
4.2.2	Research question 2	117
4.2.3	Research question 3	130
4.2.4	Research question 4	134
4.3	Conclusions	140
5	COLONIZATION AND DEVELOPMENT OF THE BENTHIC MACROINFAUNAL COMMUNITY	141
5.1	Introduction	141
5.2	Methods	142
5.2.1	The study area	142
5.2.2	Morphological changes	143
5.2.3	Colonization by macrobenthic infauna	144
5.2.4	Comparison of the community structure in the managed realignment area versus natural tidal flats	144
5.2.5	Birds	146
5.2.6	Statistical analysis	146
5.3	Results	147
5.3.1	Morphological changes	147
5.3.2	Colonization by macrobenthic infauna	149
5.3.3	Community structure	149
5.3.4	Environment and traits	154
5.3.5	Birds usage at Perkpolder	163
5.4	Discussion	169

5.5	Conclusion	170
6	EDUCATION	171
6.1	Research projects and final thesis	171
6.2	Excursions for students	172
7	EXPOSURE	173
7.1	Conferences	173
7.2	Newsletters	176
8	REFERENCES	177
	ACKNOWLEDGEMENT	181
9	APPENDICES	182
9.1	Gegevens van meetpunten en monitoringfrequentie	182
9.2	Stijghoogtemetingen	183
9.3	SlimFlex-metingen	206
9.4	Krimpen en groeien van een zoetwaterlens in zoute omgeving	213
9.5	Groundwatermodelling of the freshwater lens of Kloosterzande	214
9.5.1	Perkpolder modelling	214
9.5.2	Model construction	214
9.5.3	Discretization	215
9.5.4	Hydraulic Parameters	217
9.5.5	Boundary conditions	217
9.5.6	Seepage Facility:	218
9.5.7	Recharge	219
9.5.8	Transport parameters	219
9.6	Model Scenarios	219
9.6.1	Reference model	219
9.6.2	Flooding	219
9.6.3	Flooding with seepage facility	220
9.7	Model results	221
9.7.1	Reference model	221
9.7.2	Scenario models	223
9.7.3	Seepage facility operating only during winter period	227
9.8	Conclusions	0

LIST OF FIGURES

<i>Figure 1. Plan Perkpolder, village on former ferry platform (No.1), natural tidal area (No.2), recreational housing with golf course (No.3), and marina (No.4), (source: Bureau Lubbers).....</i>	<i>22</i>
<i>Figure 2. Perkpolder tidal basin, September 6, 2016 (Photo: Edwin Patee, RWS)</i>	<i>24</i>
<i>Figure 3. Composition of an intertidal area (Zagwijn, 1986).</i>	<i>28</i>
<i>Figure 4. Sedimentation measurements in April of 2016, measured during three field campaigns.....</i>	<i>31</i>
<i>Figure 5. Locations of the four cross sections located on the shallow area of the basin.</i>	<i>32</i>
<i>Figure 6. Overview of locations DGPS bed level measurements across the inlet (dots) and Aquadopp velocity measurements (crosses) with the underlying T0 bathymetry.....</i>	<i>34</i>
<i>Figure 7. OBS calibration, unit of turbidity: Raw Fluorescence Units.</i>	<i>36</i>
<i>Figure 8. Left: top view of the inlet with the ADCP measurement locations (circles) and the ADCP projections on the inlet (squares). Right: side view of the inlet with cross-sections divided into different segments to be able to compute discharge.</i>	<i>37</i>
<i>Figure 9. Comparison of discharges based on tidal storage approach and ADCP velocity measurements. Top left: complete water level and discharge time series, top right: scatter diagram, bottom: water level and discharge time series for a single tide on 29 November.</i>	<i>38</i>
<i>Figure 10. Cumulative net sediment fluxes (positive = import into Perkpolder) for different background concentration levels for the period September 2016 – March 2017. Each circle marks a single tide.....</i>	<i>39</i>
<i>Figure 11. Top row: Scatter plots of the net sediment fluxes per tide (positive = import) versus the high water level (left), flood peak discharge (middle) and wind speed (right). Bottom row: now with the trapping efficiency on the vertical axis.....</i>	<i>40</i>
<i>Figure 12. Water levels (first row), discharges (second row), suspended sediment concentrations (third row) and sediment flux (fourth row) for tide with a relatively low (left; 20 September 2016) and high (right; 23 September 2016) sediment import.</i>	<i>41</i>
<i>Figure 13. T0 bathymetry (May/June 2015) in the basin and the division of the areas. Area 1 represents the tidal flat and the artificial creeks in the basin. Area 2 is the pond area, area 3 is the inlet and area 4 is the foreshore just in front of the Perkpolder basin.</i>	<i>43</i>
<i>Figure 14. Elevation maps of the Perkpolder tidal basin, T-1 (December 2013), T0 (June 2015), and T6a (April 2016), T9a(February 2017) and T13a (April 2018). On the image sequence it is possible to observe that the blue areas are becoming lighter meaning that the lower parts are accreting. This is particularly clear at the pond area.</i>	<i>44</i>
<i>Figure 15. Sedimentation erosion map of Perkpolder basin and foreshore between T0 (June 2015) and T13a (April 2018). Darker colours mean higher values of sedimentation (red) or erosion (blue). The pond and some areas of the channels show high sedimentation and the inlet and the beginning of the channels next to the pond show erosion.</i>	<i>45</i>
<i>Figure 16. Hypsometric curves of the Perkpolder tidal basin T-1 (Dec. 2013), T0 (June 2015), T6a (April 2016), T9a (Feb. 2017) and T13a (April 2018). On the y-axis the surface elevation, on the horizontal axis the ratio a/A, where ‘a’ is the area below a given elevation colour, and ‘A’ is the total basin area.</i>	<i>46</i>
<i>Figure 17. Morphological development of the inlet. The horizontal red dashed line represents the water level of 86 cm NAP.</i>	<i>47</i>
<i>Figure 18. The development of the cross-section of the tidal inlet over time. Cross-sectional area is calculated at a water level of NAP +0.86 m (Figure 17).</i>	<i>47</i>
<i>Figure 19. Sedimentation and erosion between T0 (May/June 2015) and T4 (19 April 2016).</i>	<i>48</i>
<i>Figure 20. Sedimentation and erosion between T0 (May/June 2015) and T13a (26 April 2018). In red the values represent sedimentation and in blue the values represent erosion. It is clear that the main</i>	

<i>morphological changes are taking place in the channels which are accreting at the end of the flat and eroding in the transition between the flat and the pond area.</i>	<i>50</i>
<i>Figure 21. Locations of cross-sections.</i>	<i>51</i>
<i>Figure 22. Cross-section over creeks in the tidal flat area, the original surface in orange, the measured surface in July 2016 in blue.</i>	<i>52</i>
<i>Figure 23. Cross-section over tidal flat area, the original surface is represented in orange, the blue line indicates the measured surface in April 2016 and the green line the measured surface in June 2017.</i>	<i>54</i>
<i>Figure 24. Shepard's diagram showing the sediment samples in granulometric classes.</i>	<i>55</i>
<i>Figure 25. Sediment distribution map of Perkpolder.</i>	<i>55</i>
<i>Figure 26. Domain Perkpolder Delft3D model.</i>	<i>56</i>
<i>Figure 27. Comparison of measured and computed velocities at location MP0102. u = velocities normal to the inlet (inflow is positive), v = velocities parallel to the inlet (positive is toward the Northwest).</i>	<i>57</i>
<i>Figure 28. Computed sedimentation in Perkpolder after half a year. (Unit should be [m] instead of [m NAP].)</i>	<i>57</i>
<i>Figure 29. Effect of depth reduction pond and creeks with 50% (Scenario 1) and 100% (Scenario 2) on the computed morphological change after 0.5 year.</i>	<i>58</i>
<i>Figure 30. Effect of changing the inlet width on the computed morphological change after 0.5 year. Scenario 3: 50% decrease, Scenario 4: 50% increase.</i>	<i>59</i>
<i>Figure 31. Sediment balance between the duration of the project. The blue numbers correspond to areas that have lost sediment (inlet and outer area); the red numbers correspond to areas that have gained sediment (basin and pond).</i>	<i>60</i>
<i>Figure 32. Tidal basins part of de-poldering projects around Eastern and Western Scheldt.</i>	<i>62</i>
<i>Figure 33. Hypsometric curves of the tidal basins: Perkpolder (A), Saeftinghe (B), Sieperdaschor (C), Hertogin Hedwigepolder (D), Waterdunen (F), and Rammegors (D). On the y-axis the height, on the horizontal axis the ratio a/A, where 'a' is the area below a given elevation contour, and 'A' is the total basin area.</i>	<i>63</i>
<i>Figure 34. De ligging van de westelijke en zuidelijke kwelvoorziening. Op de detailtekening geven de roze punten de positie van de verticale kwelbuizen weer en in blauw zijn de regelputten weergegeven. Groen geeft de ligging van de sloot weer.</i>	<i>70</i>
<i>Figure 35. Foto van westelijke kwelvoorziening met ligging kwelbuizen en regelputten.</i>	<i>71</i>
<i>Figure 36. Foto van een regelput met stuwplankje.</i>	<i>72</i>
<i>Figure 37. Schematische weergave van de kwelvoorziening met ondergrondse verbinding van kwelbuizen, uitkomende in regelput die vervolgens afwatert op sloot. Δh geeft het stijghoogteverschil weer tussen de stijghoogte in het eerste watervoerende pakket en het gestuwd peil in de regelput; hoe groter Δh, hoe meer grondwater de kwelvoorziening afvoert. Δh kan worden beïnvloed door het stuwpeil in de regelput te veranderen: vergelijk de situatie in de linker figuur (laag peil, grote Δh, hoge afvoer kwelvoorziening) met de situatie in de rechter figuur (hoog peil, kleine Δh, lage afvoer kwelvoorziening).</i>	<i>73</i>
<i>Figure 38. Het huidige grondwatermeetnet Perkpolder.</i>	<i>74</i>
<i>Figure 39. De ligging van de peilbuizen ten opzichte van de kwelbuizen. Pb a ligt tussen 2 kwelbuizen en Pb b bij een kwelbuis. Het effect van een kwelbuis op de stijghoogte is groter dicht bij een kwelbuis dan tussen 2 kwelbuizen.</i>	<i>75</i>
<i>Figure 40. Een dwarsnede waarin de gemeten dikte van de zoetwaterbel (T0) en ligging kwelvoorziening en nieuw getijdegebied.</i>	<i>76</i>
<i>Figure 41. Uitvoering EM-Slimflex in Perkpolder (meetpunt Pb-3a, 22 mei 2015).</i>	<i>77</i>
<i>Figure 42. Het stijghoogteverloop van meetpunt EC-111(diep) voor de periode 2015-juni 2018.</i>	<i>78</i>
<i>Figure 43. Het stijghoogteverloop van meetpunt Pb2 en Pb5 gedurende de periode juni 2015 tot december 2018, met het peil in de regelput (EC-buis), de stijghoogte tussen twee kwelbuizen (a-buis) en bij een</i>	

<i>kwelbuis (b-buis). Duidelijk is het patroon zichtbaar van het aanzetten van kwelvoorziening (lage stijghoogte) en dichtzetten van de kwelvoorziening (hoge stijghoogte).</i>	80
<i>Figure 44. De SlimFlex-metingen voor meetpunt EC-106.</i>	81
<i>Figure 45. Het zoutgehalte (elektrische geleidbaarheid EC) voor het water in de regelput voor meetpunten Pb-2 en Pb-5, voor de gehele meetperiode en ingezoomd voor de maand augustus 2015.</i>	84
<i>Figure 46. Het debiet van 2 regelputten waarop 3 (Pb-2) en 7 (Pb-5) verticale kwelbuizen zijn aangesloten, in liter/dag (boven en midden) en liter/uur (onder).</i>	85
<i>Figure 47. De twee afsluiters (stalen koker met deksel eraf) aan beide zijden van de regelput. Met de blauwe T-sleutel kunnen de spindel-afsluiters open en dicht worden gezet.</i>	87
<i>Figure 48. T-sleutel met aan uiteinde vervangbaar bedieningspunt om spindel-afsluiters te bedienen.</i>	88
<i>Figure 49. Voorbeeld van presentatie van de stijghoogtemetingen. De blauwe lijn zijn de uurwaarden gemeten met Divers en de rode punten geven de handmetingen weer.</i>	93
<i>Figure 50. Voorbeeld van presentatie van de stijghoogtemetingen, ingezoomd via de HTML-file.</i>	93
<i>Figure 51. Voorbeeld van presentatie van de debietgegevens van de kwelvoorziening.</i>	94
<i>Figure 52. Een voorbeeld van presentatie van het zoutgehalte van de afvoer van de kwelvoorziening.</i>	95
<i>Figure 53. Twee voorbeelden van presentatie van de EM-SlimFlex metingen van het zoet-zout grensvlak. Ten opzichte van EC-106 laat EC-101 een veel grotere variatie in absolute waarden zien en ook enige variatie in de diepte van het grensvlak. Dit is vermoedelijk een meetartefact.</i>	96
<i>Figure 54. Artist impression of the development of Perkpolder next to the recreation housing (left; http://www.vnsc.eu/uploads/cache/perkpolder-hulst-1.jpg) and a schematic drawing raising the question how long it will take before this situation is realised (right).</i>	103
<i>Figure 55. Schematisation of two positive feedback loops, showing how lack of drainage may cause bare tidal flats to remain bare, and drained tidal flats to rapidly develop vegetation.</i>	104
<i>Figure 56. Photograph of the mesocosms setup.</i>	108
<i>Figure 57. Schematic diagrams showing erosion and accretion treatments.</i>	109
<i>Figure 58. Percentage of surviving, toppled and dead seedlings during the mesocosm experiments. (a) Constant Rate (CR) treatment groups, (b) Intermittent Supply (IS) treatment groups</i>	111
<i>Figure 59. Spartina seedling survival in response to salinity (15 PPT versus 28 PPT) and drainage (poor vs. well drained) and inundation period (3 hours per tide vs. 6 hours per tide).</i>	112
<i>Figure 60. The location of Perkpolder and the Mega-Marsh-Organs (MMO) set up. A) the location of MMO within Perkpolder; B) an aerial view of Perkpolder, the red star in A and red circle in B shows where the MMO's have been set up; C) drainage system for dewatering in one of the drained MMO boxes; D) picture of the MMO in the field; and E, schematic of MMO set up.</i>	113
<i>Figure 61. Spartina anglica seedling survival during the 6 weeks field experiment in Perkpolder. The overall survival of seedlings was significantly higher in the drainage groups (orange) than the groups without drainage (blue). Longer disturbance-free period (seedling age) and higher elevation (less inundation) also facilitates seedling survival.</i>	114
<i>Figure 62: A conceptual diagram showing the importance of drainage in controlling alternative state shifts in salt marsh ecosystems.</i>	115
<i>Figure 63: Anecdotal evidence that drainage relief facilitates salt marsh establishment. a) Salt marsh establishment near a channel at a low pioneer tidal flat (Chongming Island, the Yangtze estuary, China); b) establishment of seedlings first took place near drainage channels (Chongming Island, the Yangtze estuary, China); development of a heterogeneous marsh pattern in creeks at (c) the Chongming Island, the Yangtze estuary and (d) the Scheldt estuary (Paardenschor, Belgium); e) aerial image showing a large tidal flat that remained unvegetated for a long time (years) despite high elevation and being surrounded by old marshes; the only fringes of marsh vegetation are distributed alongside tidal channels (Paardenschor, Belgium, the Scheldt Estuary; Source: Google Earth, 2017).</i>	116

<i>Figure 64: Schematic overview of the 15 locations where SED-sensors were placed and where soil properties are regularly measured (see Table 2 for timing). At locations 3, 6, 9 & 12 we also measure tidal amplitude. We measured the survival of planted Spartina and Scirpus seedlings at location 1 to 15.</i>	<i>119</i>
<i>Figure 65. Bulk density values measured in 2016, 2017, and 2018 at 200 equally spaced sampling points in Perkpolder (upper panel). The lower panel shows the differences between 2018 and 2016 (negative change in blue and positive change in red).</i>	<i>120</i>
<i>Figure 66. Elevation values measured in 2016, 2017, and 2018 at 200 equally spaced sampling points in Perkpolder (upper panel). The lower panel shows the differences between each set of two years (negative change in blue and positive change in red) and the overall change in elevation over the time period.</i>	<i>120</i>
<i>Figure 67. Mud content values measured in 2016, 2017, and 2018 at 200 equally spaced sampling points in Perkpolder (upper panel). The lower panel shows the differences between each set of two years (negative change in blue and positive change in red) and the overall change in mud content over the time period. .</i>	<i>121</i>
<i>Figure 68. Correlations between the eight sediment characteristics with a red background showing statistically significant correlations. The values have been averaged by point over all sampling periods. The map shows the locations of the fifteen points. Mud content is derived from median grain size and bulk density is derived from water content.</i>	<i>123</i>
<i>Figure 69. Bulk density values for 2 cm layers (0 to 16 cm total depth) at the 15 points. There was gap in sampling in 2016.</i>	<i>126</i>
<i>Figure 70: Sediment dynamics at three mini transects at Perkpolder.</i>	<i>127</i>
<i>Figure 71: Sediment availability shown in a. sediment delivery (g/L), suspended in water column and b. Daily sedimentation (g/m²), trapped sediment converted to a daily value.</i>	<i>129</i>
<i>Figure 72. Location of 4 seed nets and the 15 astro-turf mats (i.e., placed near SD-sensors) within Perkpolder.</i>	<i>131</i>
<i>Figure 73. Results on seed availability as trapped in the nets.</i>	<i>133</i>
<i>Figure 74. impression of seedling survival experiment from 2015 until 2018 in Perkpolder.</i>	<i>134</i>
<i>Figure 75: Results of seedling survival experiment 2015-2016 in Perkpolder.</i>	<i>135</i>
<i>Figure 76. a, Schematic of the layout of one mesocosm (view from the top), green part represents for the plant clump, with 5cm distance to the cliff. b, Photograph of one of the mesocosms showing view from the cliff side.</i>	<i>136</i>
<i>Figure 77. Number of shoots expansion to cliff side.</i>	<i>137</i>
<i>Figure 78. Percentage of shoots expansion to cliff side (comparison of different species of Sanymud sediment).</i>	<i>137</i>
<i>Figure 79. Spartina patches planted in the MMO at Perkpolder.</i>	<i>138</i>
<i>Figure 80. Regrowth of S. anglica tussocks at harvest in the field experiment in Perkpolder. The survival of tussocks showed no significant difference between drainage or elevation groups; Plant height, shoot numbers and dry biomass was only affected by elevation per se, with no significant difference effect from drainage treatment or interactive effect of drainage and elevation.</i>	<i>139</i>
<i>Figure 81. Map of the Perkpolder managed realignment site in the Scheldt estuary (southwest of The Netherlands) with the twenty-four macrobenthic infauna sampling stations and the two-hundred sediment characteristic sampling stations. Red line indicates the original dike, yellow the new dike.</i>	<i>143</i>
<i>Figure 82. Map of the Scheldt estuary with 24 macrobenthic infauna sampling stations sampled between 2015-2018 in the managed realignment area (black dots) and 62 macrobenthic sampling stations sampled between 2010-2014 within the low dynamic mid litoral ecotope (red dots).</i>	<i>145</i>
<i>Figure 83. Sediment characteristics: Box plots of changes in median grain size, silt content, deposit mud layer, elevation, penetration resistance, erosion resistance, bulk density and chlorophyll-a in time within the managed realignment area.</i>	<i>148</i>

Figure 84. Variation in the mean (\pm se) species richness (A), total abundance (B) and biomass (C) with proportional representation of the taxa in the managed realignment area (Autumn 2015 till Autumn 2018) and in the MWTL data between 2010 and 2014.	152
Figure 85. nMDS-plot showing changes in benthic community composition from autumn 2015 till autumn 2018 at the managed realignment Perkpolder based on abundance data (open circles) towards a community composition found at nearby tidal flats (closed circles). Each point represents a sampling station. Distance between points is a measure of dissimilarity in benthic community composition. The eclipse (red = realignment area, black = nearby tidal flats) denote the 95% confidence interval for each sampling moment.	153
Figure 86. DCA (left) and CCA (right) ordination diagram of species abundance per sampling moment. Community structure was significantly affected by sampling moment ($F_{6,119} = 21.76$, $p=0.001$) and season ($F_{1,124} = 5.56$, $p=0.002$) which explained 21.6% and 6.2% of the variability.	154
Figure 87. Presence, abundance and biomass of feeding, position, size and life traits averaged over the sampling moments. For the explanation of the trait legends, see Table 16.	155
Figure 88. Presence, abundance and biomass of reworking, mobility, reproductive period and P/B traits averaged over the sampling moments. For the explanation of the trait legends, see Table 16.	156
Figure 89. Average of 23 taxa included in the trait-based analysis at each sampling moment +/- standard deviation (vertical lines black lines).	156
Figure 90. Average of sediment characteristics: elevation (NAP m), mud depth (cm) penetration resistance (N), chlorophyll content (unit?), bulk density (g/cm^3), median grain size (μm), very fine sediment content (%) by sampling moment and standard deviations in grey lines.	157
Figure 91. Coefficient heat map for trait-based analysis of taxa abundance. Refer to Table 3 for explanation of traits and levels. A, B, and C are separate models as all the coefficients traits could not be included in one model because of restricted degrees of freedom. (A) is the best model by AIC. The stars indicate significant ($p<0.1$) interactions between a trait and an environmental variable.	158
Figure 92. Average number of observed birds foraging and resting in the managed realignment area (75 ha) between September 2017 and September 2018.	164
Figure 93. Diet and occurrence (ind. ha^{-2}) of the top ten waders found in Perkpolder between September 2017 and September 2018. The location of the blue circle in the triangle indicate the diet composition. Distance to each corner represents relative importance of shellfish, worms or other macrobenthic organisms within their diet. Diet data was obtained from Leopold et al. 2004. The size of the circles indicates the relative density of species. The green circle indicate the benthic community composition and total biomass (size of the circles) in autumn 2018.	165
Figure 94. Average number of observed birds foraging and resting on the dikes surrounding the managed realignment area between September 2017 and September 2018.	166
Figure 95. Number of people observed on the dikes surrounding Perkpolder. The west side is a bike path. On the east and south dike access is not permitted. For part of this stretch (yellow) it is known how many people visit do walk or bike here. At four occasions in time one dog was observed on the dike.	167
Figure 96. Mireille Martens (BSc. student HZ) busy with field measurements (April 2016).	172
Figure 97. Example of a poster presentation resulting from the Perkpolder project.	173
Figure 98: Model cross section representation.	215
Figure 99: Discretization and boundary conditions. In blue - general head boundary, green – rivers, yellow – drains, and grey with diagonal hatch - inactive cells. (a) Cross section trough row 4, (b) plant view of layer 10.	216
Figure 100: Zones of assigned hydraulic conductivity (m/d) and inactive cells at the bottom layers representing the Rupel/Boom clay.	217

<i>Figure 101: Assigned boundary conditions of the flooding scenario and the flooding + seepage facility. In blue - general head boundary, green – rivers, yellow – drains, and grey with diagonal hatch - inactive cells. (a) Cross section trough row 4, (b) plant view of layer 10.</i>	<i>220</i>
<i>Figure 102: Modelled freshwater lens in the creek ridge zone with steady state conditions reached after 500 years.</i>	<i>221</i>
<i>Figure 103: Concentration contours between the freshwater limit 0.15 mg/l (blue) and 6 mg/L (red).</i>	<i>222</i>
<i>Figure 104: Groundwater head distributions for winter and summer a) Simulated aquifer freshwater heads (at -14.5 m NAP) and water table along the model section; b) head differences between the water table and the aquifer (>0 downward movement, <0 upward movement). Note: X axis is presented as columns numbers.</i>	<i>223</i>
<i>Figure 105: Observed and simulated concentrations and heads profiles at the monitoring bores EC-102, EC-101 and EC-111 located along the model line. Lines correspond to simulated profiles and points represent average of observed values.</i>	<i>223</i>
<i>Figure 106: Results of scenarios simulations at different simulations times.</i>	<i>225</i>
<i>Figure 107: Groundwater head distributions after 6 months for scenarios. a) Simulated aquifer freshwater heads (at -20.5 m NAP) and water table along the model section; b) head differences between the water table and the aquifer (>0 downward movement, <0 upward movement). Note: X axis is presented as columns numbers.</i>	<i>226</i>
<i>Figure 108: Groundwater head distributions after 100 years for scenarios. a) Simulated aquifer freshwater heads (at -20.5 m NAP) and water table along the model section; b) head differences between the water table and the aquifer (>0 downward movement, <0 upward movement). Note: X axis is presented as columns numbers.</i>	<i>226</i>
<i>Figure 109: Observed and simulated head profile at monitoring location PB-2 for the reference, flooding and seepage scenarios.</i>	<i>227</i>
<i>Figure 110: Results of scenarios simulations at different simulations times with the seepage facility operating 6-months a year, during the winter period.</i>	<i>228</i>
<i>Figure 111: Groundwater head distributions after 100 years for scenarios. a) Simulated aquifer freshwater heads (at -20.5 m NAP) and water table along the model section; b) head differences between the water table and the aquifer (>0 downward movement, <0 upward movement). Note: X axis is presented as columns numbers.</i>	<i>228</i>

LIST OF TABLES

<i>Table 1. Overview of morphological measurements in Perkpolder intertidal area and surroundings.</i>	29
<i>Table 2. Overview of sediment thickness measurements in Perkpolder intertidal, and creeks.</i>	32
<i>Table 3. Overview of height measurement of inlets cross-section (higher parts).</i>	33
<i>Table 4. Overview of water level and velocity measurements.</i>	34
<i>Table 5. Sediment balance in the Perkpolder basin and its foreshore between 2015 and 2018.</i>	60
<i>Table 6. Tidal basins, with tidal range, and distribution of channels, flats and marshes (values indicated with * are predictions other values are based on 'Waternormalen' from Rijkswaterstaat). Basins in italics are not yet open.</i>	63
<i>Table 7. Enkele details van de westelijke en zuidelijke kwelvoorziening.</i>	71
<i>Table 8. original time plan as presented in the project plan</i>	106
<i>Table 9: Sedimentation treatments every week during the 6-week course of the mesocosm experiments.</i>	110
<i>Table 10: overview of field measurements.</i>	118
<i>Table 11. Coefficients for explanatory variables for generalized linear models of sediment characteristics from full coverage 200 points. The significance of the explanatory variable coefficient from p values is indicated by the number of stars with 0.05 > * > 0.01 > ** > 0.001 > ***.</i>	122
<i>Table 12. Coefficients for explanatory variables for generalized linear models of sediment characteristics from 15 points. The significance of the explanatory variable coefficient from p values is indicated by the number of stars with 0.05 > * > 0.01 > ** > 0.001 > ***.</i>	124
<i>Table 13. Results of seed trapping on the 15 astro-turf mats placed near SD-sensors, throughout Perkpolder.</i>	132
<i>Table 14. Occurrence (% of the total sampled stations) of the observed species/taxon in the managed realignment Perkpolder and on nearby natural tidal flats (MWTL data) sampled between 2010-2014.</i>	150
<i>Table 15. Density (ind. m⁻², mean ± se) of the observed species/taxon in the managed realignment Perkpolder and on nearby natural tidal flats (MWTL data) sampled between 2010-2014.</i>	151
<i>Table 16. Traits of species/taxa used in the traits-based multivariate analysis. Traits for rare species were not included. Feeding: O=omnivore, SDF=surface deposit feeder, SSDF= subsurface deposit feeder, FF= filter feeder; Position: 1=epifauna, 2=shallow (0-5cm), 3=middle (5-15 cm), 4=deep (.15 cm); Life: 1= short, 2= medium, 3= long; Size: 1= small (<0.001g), 2= medium (0.001-0.01g), 3=large (0.01-0.14g); Reworking: E=epifauna biodiffuser, S= surficial biodiffuser, DC= downward conveyor, UC= upwards conveyor, G=gallery biodiffusor; Mobility: 1= sessile, 2=limited, 3=free; Reproductive period: S= Semelparous, E= episodic, P=Protracted; P/B, 1=low (<1/year), 2=medium (1-3/year), 3=high (>3/year). Traits for C. carinata (Ferreira et al., 2004; Queirós et al., 2013), for Oligochaeta size and position (Ysebaert et al., 2005) lifespan and P/B ratio (Giere, 2006) The other traits are taken from the table by Pieter van Linden.</i>	159
<i>Table 17. The coefficients for the multivariate generalized linear model of taxa presence explained by sediment characteristics. Significant negative coefficients are highlighted in blue, significant positive coefficients are highlighted in red. The significance levels are: 0.1 > * > 0.05 > ** > 0.01 > ***</i>	160
<i>Table 18. The coefficients for the multivariate generalized linear model of taxa abundance explained by sediment characteristics. Significant negative coefficients are highlighted in blue, significant positive coefficients are highlighted in red. The significance levels are: 0.1 > * > 0.05 > ** > 0.01 > ***</i>	161
<i>Table 19. The coefficients for the multivariate generalized linear model of taxa biomass explained by sediment characteristics. Significant negative coefficients are highlighted in blue, significant positive coefficients are highlighted in red. . The significance levels are: 0.1 > * > 0.05 > ** > 0.01 > ***</i>	162
<i>Table 20. The coefficients for the multivariate generalized linear model of taxa abundance explained by point, year, season, and an interaction between year and season. Both point and season were treated as factors, and while the coefficient for season is for sp is for spring, we did not include all the coefficients for</i>	

the points as these were largely not significant. Significant negative coefficients are highlighted in blue, significant positive coefficients are highlighted in red. The significance levels are: 0.1 > * > 0.05 > ** > 0.01 > ***

	163
Table 21. Number of birds observed in the managed realignment Perkpolder (75 ha) during low tide and percentage showing foraging behaviour between September 2017 and September 2018.	168
Table 22. Overview of student projects as part of the Perkpolder project.	171
Table 23: Model discretization.	215
Table 24: Boundary conditions applied to the model.	218
Table 25: Transport parameters.	219

MANAGEMENT SAMENVATTING

Inleiding

Op 17 januari 1995 ondertekenden Nederland en Vlaanderen een verdrag over de tweede verruiming van de vaargeul naar de haven van Antwerpen. Onderdeel van dit verdrag was natuurcompensatie. In een bestuursovereenkomst hebben de regionale overheden afspraken gemaakt over de uitvoering van een natuurcompensatieprogramma, waarin de veerhaven Perkpolder (onder voorbehoud) was opgenomen. Het voorbehoud betrof andere gebruiksmogelijkheden. In samenspraak tussen Provincie Zeeland, gemeente en Rijkswaterstaat is in 2004 besloten tot de gebiedsontwikkeling Perkpolder, waarin naast natuurontwikkeling, tevens woningbouw, een jachthaven en een golfbaan waren opgenomen. In 2015 voltooide Rijkswaterstaat de realisatie van een nieuw buitendijks natuurgebied van 75 ha groot.

Rijkswaterstaat wil als waterbeheerder weten of het nieuwe natuurgebied bijdraagt aan het laag-dynamisch getijdengebied, dat in de Westerschelde onder druk staat. Maar ook of de ondergrondse kwelvoorziening effectief het zoete water voor de landbouw beschermt tegen verzilting. In samenwerking met kennis- en onderzoekspartners is een monitoringprogramma Perkpolder opgesteld onder het Centre of Expertise Deltatechnology. Deze partners zijn de HZ University of Applied Sciences, Koninklijk Nederlands Instituut voor onderzoek der Zee (NIOZ), Wageningen Marine Research (WMR) en Deltares. Het monitoringprogramma Perkpolder benoemt de volgende doelen:

WATERBEHEER WESTERSCHELDE EN BEHEER WATERKERINGEN

1. Vaststellen welke biotopen in het buitendijkse natuurgebied Perkpolder tot ontwikkeling komen, en (door Rijkswaterstaat) onderzoeken of in en welke mate deze biotopen bijdragen aan de gestelde natuurdoelen voor het Schelde-estuarium en de instandhoudingsdoelen voor Natura 2000.
2. Kennisontwikkeling ten behoeve van waterveiligheidsbeheer, bijvoorbeeld de morfologische ontwikkelingen van de bres, het voorland en de het nieuwe natuurgebied;
3. Onderzoek doen naar de effectiviteit van de kwelvoorziening die het landbouwkundig gebruik moet waarborgen;

KENNISONTWIKKELING (KORTE TERMIJN)

4. Het ontwikkelen van systeemkennis van de biotische en abiotische factoren na ontpoldering en vergroten van het begrip van de interactie tussen de biotische en abiotische factoren. Deze kennis helpt bij de inrichting van toekomstige gebieden waar het getij wordt hersteld;

ONDERWIJSVERSTERKING

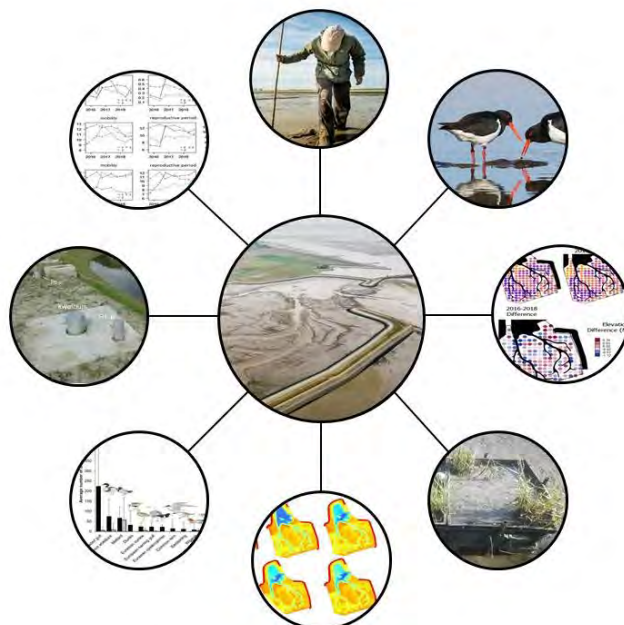
5. Opleiden van meer en beter gekwalificeerde professionals voor de arbeidsmarkt. Daarnaast een investering in de kwaliteit van onderwijs, resulterend in kwaliteitssprong bij studenten en professionals;

KENNISBORGING, KENNISVERSPREIDING EN NETWERKVORMING

6. De kenniscirculatie binnen het werkveld bevorderen, door alle kennis te bundelen binnen de DeltaExpertise-site. De ontwikkeling van een goed functionerend samenwerkingsverband binnen het Centre of Expertise met als doel om na 2018 zelfvoorzienend te zijn.

Uitvoering monitoring

Het natuurgebied Perkpolder wordt sinds 25 juni 2015 twee keer per dag overstromd door zeewater uit de Westerschelde. Het monitoringprogramma richtte zich op morfologische en ecologische ontwikkelingen en de grondwaterveranderingen. De morfologische monitoring omvat jaarlijkse hoogtemetingen om de erosie- en sedimentatiepatronen in kaart te brengen. Ook is het numerieke model Delft3D ingezet om de morfologische veranderingen te kunnen relateren aan het sediment transport in en uit het gebied. Halfjaarlijkse opnames van de bodemgemeenschap en vogelpopulaties zijn gedaan om de ecologische ontwikkelingen te monitoren. Naast de ontwikkelingen in het getijbekken werd ook onderzocht of de kwelvoorziening, die de zoute kwel afvoert, naar behoren functioneerde.



Visuele samenvatting van de uitvoering van de monitoring van het Perkpolder gebied. De belangrijkste aspecten van de monitoring zijn de morfologische en ecologische ontwikkelingen, het grondwatersysteem en de effectiviteit van de kwelvoorziening, en onderwijsversterking en kennisverspreiding.

Morfologie

Perkpolder is een laag-dynamisch en slibrijk gebied. Op basis van de monitoring kan geconcludeerd worden dat de morfologische ontwikkeling van het Perkpolder bekken vertraagde naarmate de tijd vorderde. Met betrekking tot de inlaat vonden de belangrijkste veranderingen plaats binnen de eerste maand na de opening ervan. De diepe put bij de inlaat en de intergetijdengebieden lieten voornamelijk sedimentatie zien, terwijl de inlaat en de vooroevergebieden vooral een erosieve trend lieten zien. De kunstmatige krekten vulden zich op aan het uiteinde (zuidelijk deel van het stroomgebied) en erodeerden aan het begin (noordelijk deel van het bekken). De gegraven krekten hadden een uniforme breedte waardoor ze te groot waren in het zuidelijke deel van het bekken en ondermaats waren in het noordelijke deel van het bekken. Delft3D modelberekeningen suggereren dat de aanwezigheid van de diepe put en de aangelegde krekten een aanzienlijk effect hebben op het sedimentatiepatroon in Perkpolder. Voor het grootste gedeelte van het gebied zijn de hoogteverschillen tussen het begin en einde van de meetperiode tussen de 0 m en 0.5 m, maar vooral de diepe put bij de inlaat (meters sedimentatie) en het noordelijke deel van de gegraven krekten (meters erosie) laten grote hoogteverschillen zien.

De sedimentimport in Perkpolder is geschat op basis van OBS-concentratiegegevens voor de periode tussen september 2016 en maart 2017, gecombineerd met geschatte debieten op basis van waterstanden. De sedimentimport varieerde sterk in deze periode en sediment werd ook geëxporteerd gedurende een aantal getijdencycli. Gedurende de vijf maanden met meetgegevens bedroeg de geschatte netto import 13-16 kiloton. Dit correspondeert met 34-40 kiloton/jaar, oftewel 27-100 kubieke meter sediment per jaar inclusief poriën, wat goed overeenkomt met de volumes op basis van de ontwikkeling van de hoogteligging tussen 2016 en 2017. Ten slotte is een 2DH Delft3D-model opgezet om hydrodynamica, sedimentdynamiek en morfodynamiek als gevolg van getij te simuleren. Het model reproduceerde de gemeten snelheden en ontwikkeling van de inlaat redelijk goed en is verder gekalibreerd op de geschatte netto sedimentinstroom en de morfologische veranderingen tussen juni 2015 en april 2016.

Vegetatie

Van nature hebben zich nog geen planten gevestigd in Perkpolder en de monitoring was daarom gericht op de interactie van vegetatie met hoogteligging, bodemdrainage en de bodemgemeenschap. Monitoring toont aan dat vegetatie in Perkpolder niet beperkt wordt door zaad aanvoer: de vestiging wordt op dit moment vooral beperkt door de te lage ligging van het gebied. Experimenten met getransplanteerde *Spartina* rhizomen tonen aan dat deze goed groeien. Experimenten gericht op initiële vegetatie vestiging laten zien dat zaailingen het best overleven in een goed afwaterende grond. De aangelegde geulen dragen dus bij aan de vestiging van slikvegetatie. De experimenten impliceren dat het creëren van kleine topografische onregelmatigheden (bijv. door een ruwere afwerking bij afgraven) om de drainage van de bodem lokaal te vergroten, de initiële vestiging van pioniervegetatie verder kan helpen. Experimenten gericht op vegetatie

vestiging laten verder zien dat zaailingen maar een beperkte mate van sedimentdynamiek kunnen verdragen. Ze zijn toleranter ten aanzien van sediment depositie in vergelijking met erosie. Toekomstige restauratieprojecten analoog aan Perkpolder hebben baat bij de aanwezigheid van geulen, een heterogene bodem topografie en beschutting om sedimentdynamiek te minimaliseren.

Bodemdieren

De ontwikkeling van de bodemgemeenschap na het getijherstel in Perkpolder is bemoedigend. Een biologisch actief slikkengebied heeft zich binnen een kort tijdsbestek gevormd. Binnen drie jaar vertoont de benthische macro-faunagemeenschap een ontwikkeling naar een gemeenschap die wordt aangetroffen op natuurlijke slikken en platen in de Westerschelde. Het is de verwachting dat een kenmerkende benthische gemeenschap zal ontstaan binnen enkele jaren in plaats van binnen enkele decennia, zoals de oorspronkelijke hypothese luidde. Het gebied wordt ook vaak bezocht door vogels die bij laag water foerageren en tijdens hoogtij op de omliggende dijken rusten.

Grondwater en kwelvoorziening

Uit de grondwatermetingen is gebleken dat het kwelsysteem effectief is. Dit betekent dat het systeem in staat is om de zoute kwel effecten van het nieuwe getijdengebied te compenseren. Dit doet het SeepCat-systeem door de extra grondwaterdruk als gevolg van het hogere peil in het getijdengebied te verlagen door zout grondwater op 15 meter diepte af te voeren. SlimFlex-metingen laten drie jaar na het openen van het gebied geen veranderingen zien in de zoetwater-zoutwaterovergang. Bovendien is gebleken dat het kwelsysteem ook kan worden gebruikt om de zoetwaterlens te laten groeien door extra verlaging van de stijghoogte toe te passen tijdens periodes met een neerslagoverschot. Modelresultaten suggereren dat de zoetwaterlens in 100 jaar 50% kleiner zou zijn in afwezigheid van het kwelsysteem. Op basis van de metingen en modellering wordt aanbevolen om het kwelsysteem permanent te openen, omdat een afsluiting van het systeem tijdens de zomermaanden op de lange termijn (> 25 jaar) een negatief effect heeft op de zoetwaterlens. Daarnaast is het van groot belang dat het monitoringprogramma wordt voortgezet om de werking van het kwelsysteem en eventuele lange termijn effecten te kunnen volgen.

Onderwijsversterking en kennisverspreiding

Studenten zijn actief betrokken bij het Perkpolder project om zo de volgende generatie waterprofessionals te trainen. Er zijn excursies met studenten naar Perkpolder gebied georganiseerd om het project te demonstreren en actueel waterveiligheid en -beheer te laten zien. Studenten namen ook deel in het project door veldcampagnes uit te voeren en door onderzoek te doen via BSc- en MSc-scriptieprojecten (zie hoofdstuk 6 voor meer informatie over de betrokkenheid van studenten). De kennis die is verkregen als onderdeel van het project is ingebed in meerdere onderwijsmodules (bijvoorbeeld Eco-Engineering) aan de HZ University of Applied Sciences. Poster en mondelinge presentaties op symposia (bijvoorbeeld

Scheldesymposium) en conferenties hebben gezorgd voor verspreiding van de projectbevindingen naar het werkveld. Er is een video gemaakt over de kwelinstallatie (SeepCat) die online gepubliceerd is. De installatie was ook te zien tijdens de Proeftuin Zoetwater Zeeland 2017 Dag en is besproken in een artikel in De Volkskrant. Om de kenniscirculatie in het veld verder te bevorderen worden de projectresultaten gerapporteerd op de Delta Expertise site en verspreid via de nieuwsbrief Zuidwestelijke Delta in 2019.

Ten slotte

Perkpolder biedt een unieke gelegenheid om de abiotische en biotische veranderingen in een gebied dat transformeert van een zoetwater agrarisch gebied naar een zoutwater getijdegebied te volgen en te bestuderen. Er is niet veel bekend over deze overgang, dus deze kennis is zeer waardevol met betrekking tot toekomstige projecten voor het herstel van getijden, zoals de Hedwige-Prosper polder. Concreet geeft de huidige monitoring belangrijke inzichten in het ontwerp van de inlaat, de afmetingen van de kunstmatige getijdekreeken, de topografie van de slikken en hoe deze van invloed zijn op de morfologische en ecologische ontwikkeling na getijdeherstel. Daarnaast is unieke kennis verkregen over de effectiviteit van een kwelinstallatie. Het consortium heeft de intentie om de monitoring in Perkpolder voort te zetten met als doel een beter inzicht te krijgen in de middellange (4-10 jaar) effecten van getijherstel op abiotische en biotische factoren.

EXECUTIVE SUMMARY

The Netherlands and Flanders signed a treaty concerning the second extension of the waterway to the Port of Antwerp on January 17, 1995. Part of this treaty was the compensation of nature in the Western Scheldt region for the period of 1998-2008. In total six project locations in the Western Scheldt (category A) and a large number of projects behind the sea defense (categories B and C) became a part of this nature compensation program. Perkpolder is one of the category A projects. In 2004 a memorandum of understanding was signed, which became the start of *Plan Perkpolder*. In this plan, the size of the natural area is 75 hectares with also areas for housing, a marina and a golf course foreseen as part of the entire project.

Rijkswaterstaat is responsible for the realization of tidal nature in *Plan Perkpolder*. Other partners in the Centre of Expertise Delta Technology consortium are HZ University of Applied Sciences, Royal Netherlands Institute for Marine Research (NIOZ), Wageningen Marine Research (WMR) and Deltares. The Perkpolder consortium is interested in pursuing a number of goals with this project:

1. Increasing the body of knowledge on water safety management (i.e. development of inlet and stability of the foreshore) and groundwater development (i.e. effectivity of the seepage discharge installation) following tidal intrusion;
2. Increasing the body of knowledge on the biotic and abiotic factors and their relations in the first years during the transition from a fresh-water agricultural area to a salt-water tidal area;
3. Training of young professionals by improving the knowledge of teachers to be supported by state-of-the-art case studies;
4. Promoting knowledge circulation within the field by combining all the knowledge within the Delta Expertise site.

The Perkpolder tidal basin is flooded twice a day by sea water from the Western Scheldt since June 25th 2015. The monitoring program has focused on morphological and ecological developments and the groundwater changes in the Perkpolder tidal basin. In addition to developments within the tidal basin, the effects of saline groundwater on the surrounding agricultural areas are investigated. To reduce the impact of saline water a unique seepage discharge system is constructed around the Perkpolder tidal basin, at the landward side of the dyke.

The morphological development of the Perkpolder basin and its contiguous areas slowed down in time. Regarding the inlet, the main changes took place within the first month after the opening of it. The pond and the tidal flat areas were mainly accreting and the inlet and the foreshore area were mainly eroding due to the channel formation. The man-made creeks were filling up at the end (southern part of the basin) and eroding at the beginning (northern part of the basin) of the tidal flat. Since the initial cross section was the

same trough out the creeks, they were oversized at the southern part of the basin and undersized at the northern part of the basin, on the transition between the pond and the tidal flat. Using Delft3D simulations, it was shown that the design of the morphological template has a large impact on the rates of morphological change for many years after the initial opening.

The sediment import into Perkpolder was estimated based on OBS concentration data and discharges estimates for the period between September 2016 and March 2017. The sediment import varied strongly in time and sediment was also being exported for a number of tides. Over the 5 months of measurement data, the estimated net import was 13-16 kilotons, or 5000-6000 cubic meters of sediment excluding porosity. These findings correspond to 34-40 kilotons/year, which is good agreement with the 16-48 kilotons/year estimated from the bed level development between 2016 and 2017. Lastly, a 2DH Delft3D model was set up to simulate hydrodynamics, sediment dynamics and morphodynamics due to tidal forcing. The model reproduced the measured velocities and development of the inlet reasonably well and was further calibrated on the estimated net sediment influx and the morphological changes between June 2015 and April 2016.

From the groundwater measurements it was concluded that the seepage system was functioning well enough to compensate the effects of the new tidal area. SlimFlex measurements show no changes in the freshwater-saltwater transition three years after opening the area. Moreover, the seepage system can also be used to grow the freshwater lens by additional lowering of the hydraulic head during times of precipitation surplus. Modelling results suggest that the freshwater lens would be 50% smaller in 100 years in the absence of the seepage system. Based on the measurements and modelling, it is recommended to open the seepage system permanently because a closure of the system during the summer months has a negative effect on the freshwater lens on the long term (> 25 years).

The vegetation monitoring shows that seedlings survive best in a well-drained soil without sediment dynamics. Yet, seedlings can tolerate some moderate sediment dynamics. They are more tolerant to accretion compared to erosion. Monitoring demonstrates that there is no seed limitation in Perkpolder. Artificially constructing drainage conditions or providing longer disturbance-free period could be an efficient management strategy to facilitate marsh restoration at early stages and shift in state from bare tidal flat to vegetated marsh. Our results imply that creating even small topographic irregularities to increase soil drainage may help the initial establishment of young marsh plants. Restoration projects such as Perkpolder may be able to obtain such heterogeneous topography by providing small scale drainage structures and gullies or creating artificial hummocks based on bioplastics might for example be an option.

From a benthic community perspective, the development of the managed realignment Perkpolder is encouraging. A biologically active intertidal area has formed within a short time frame. Within 3 years, the benthic macroinfaunal community shows a development towards a community found on natural tidal

mudflats and is expected to reach a stable community in years rather than decades. The area is also frequently visited by birds, which forage during low tide and rest on the surrounding dikes during high tide.

Students were actively involved in the Perkpolder project to train the next generation of water professionals. Excursions with students to the Perkpolder area were organized to showcase the project and demonstrate water safety and management practices. Students also participated by conducting field campaigns as well as by doing research through multiple BSc and MSc thesis projects (see Section 6 for details on the student involvement). The knowledge obtained as part of the project is embedded in multiple teaching modules (e.g. Eco-Engineering) at the HZ University of Applied Sciences. Poster and oral presentations at symposia (e.g. Scheldesymposium) and conferences have provided dissemination of the project findings to the working field. A video was made about the seepage installation ([SeepCat](#)) and published online. The installation also featured during the Proeftuin Zoetwater Zeeland 2017 Day and was discussed in a De Volkskrant article. To further promote knowledge circulation within the field, the project findings will be reported on the Delta Expertise site and synthesized in Zuidwestelijke Delta newsletter in 2019.

Perkpolder has provided a unique opportunity to monitor and study the biotic and abiotic changes in an area transforming from a freshwater agricultural area to a tidal salt-water natural area. Not much is known concerning this transition, thus this knowledge is very valuable in respect to future tidal restoration projects, such as the Hedwige Prosper managed realignment. Specifically, the current monitoring provides important insights into the design of the inlet, the dimensions of the man-made tidal creeks, the topography of the tidal flats and how these affect the morphological and ecological development following tidal restoration. Additionally, unique knowledge is obtained on the effectiveness of a seepage installation. It is important to note that the monitoring in Perkpolder will be continued with the aim to better understand the medium-term (4-10 years) effects of tidal recovery on abiotic and biotic factors.

1 INTRODUCTION

1.1 PLAN PERKPOLDER

Starting from 2003 the ferry between Kruiningen (Zuid-Beveland) and Perkpolder (Zeeuws-Vlaanderen) became out of service, which was caused by the opening of the Western Scheldt tunnel. This fact was a starting point for the development of *Plan Perkpolder* to prompt the social-economic development of the area. This plan combines the development of real estate, recreational facilities and nature restoration. The regional development plan utilized the concepts developed within the EU project titled *ComCoast* (Interreg IIIb North Sea; Hamer, 2007). The site of Perkpolder was one of the ten pilot locations along the North Sea, and aimed to develop a safe and sustainable coastal zone attractive for living, doing business and recreational activities. The plan includes the following climate adaptation concepts developed within the *ComCoast* project: (1) an elevated former ferry platform, high enough to provide safety for the next 200 years with a rising sea level; (2) the newly developed salt march that acts as a natural buffer to lower the wave load on the dyke. Figure 1 offers an impression of the plan at Perkpolder. The former ferry terminal platform is elevated and transformed into a small village (No. 1). A salt-water tidal area will develop on the southeast side (No. 2). On the west side of the village an area designated for a golf course and housing is planned (No. 3), and the former ferry port will be transformed into a marina (No. 4).

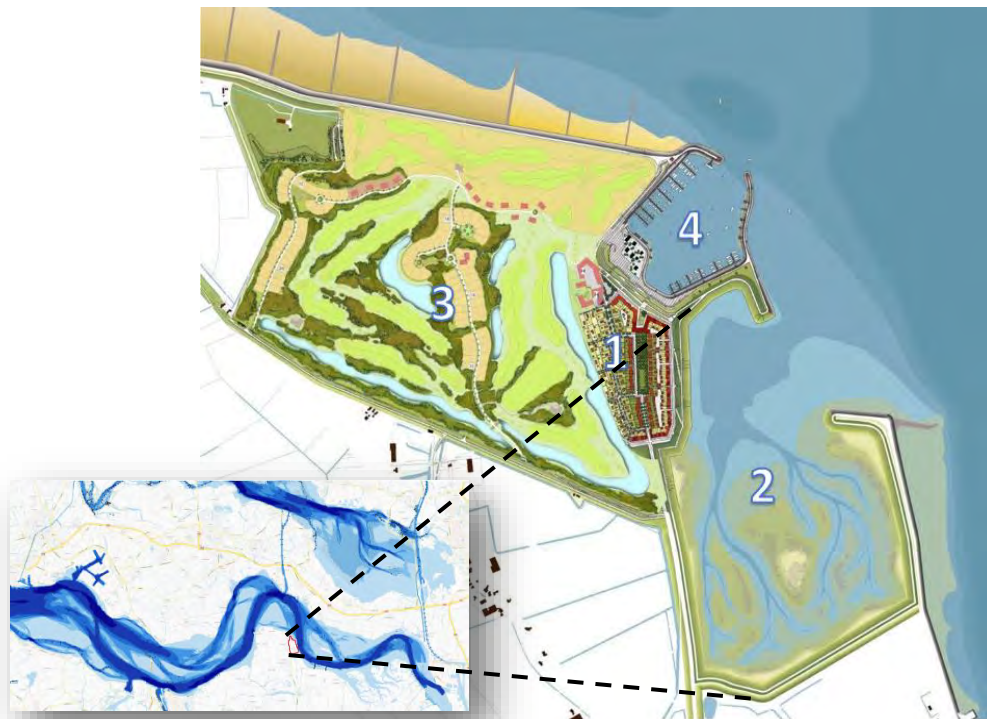


Figure 1. *Plan Perkpolder, village on former ferry platform (No.1), natural tidal area (No.2), recreational housing with golf course (No.3), and marina (No.4), (source: Bureau Lubbers).*

1.2 ADMINISTRATIVE BACKGROUND

On January 17, 1995 the Netherlands and Flemish Region signed a treaty concerning the second extension of the waterway to the Port of Antwerp. Part of this treaty was the compensation of nature in the Western Scheldt region for the period of 1998-2008. The compensation of nature was adopted in the program titled “Natuurcompensatie Westerschelde (NCW)”. In total six project locations in the Western Scheldt (category A) and a large number of projects behind the sea defense (categories B and C) became a part of this nature compensation program (NCW-eindrapportage, 2008). Perkpolder is one of the category A projects, and the executing agency of the Ministry of Infrastructure and the Environment (further mentioned as: “Rijkswaterstaat”) is responsible for the realization and monitoring of this project.

In the original agreement between the national and local governments in the Netherlands, concerning the execution of the NCW program, only the ferry port in Perkpolder was a part of the environmental compensation (total area is 10 hectares). To increase the impact on natural development the ferry terminal and the polder at the southeast site were also included in the program, which resulted in a total of 40 hectares (NCW-eindrapportage, 2008). In beginning of 2000 the local municipality of Hulst took the initiative to start an initiative for social-economic development of the region around Perkpolder. In 2004 a memorandum of understanding was signed, which became a start of *Plan Perkpolder*. In this plan the size of the natural area was increased to 75 hectares, and the port area was planned to be transformed into a marina (Figure 1). Out of these 75 hectares, 40 hectares are a part of the NCW-program, and 35 hectares are a part of the so-called “Natuurpakket Westerschelde (NWP)” (Verbeek, 2005). This environmental compensation package is a part of the development outline signed by the Dutch and Flemish governments, which focuses on an integrative approach to safety, accessibility to the Port of Antwerp, and natural development (Verbeek, 2005). In this outline 600 hectares of estuarine nature are to be added to the Western Scheldt by 2010.

1.3 MONITORING AND RESEARCH

Since June 25th 2015 the Perkpolder tidal basin is flooded twice a day by sea water from the Western Scheldt (Figure 2). The inflow of water has a direct impact on the erosion and sedimentation processes, which gives rise to morphological changes. With the inflow of water benthic macro fauna will start colonizing the area and provide the food for birds. At some point in time the vegetation will have to change in order to settle and increase the stability of the deposited sediment.

This three-year project (from 2016 to 2019) is executed by the Centre of Expertise Delta Technology called CoE-DT further on, has in this project the following partners: Rijkswaterstaat Sea and Delta, Deltares, Wageningen Marine Research, NIOZ Royal Netherlands Institute for Sea Research, and HZ University of Applied Sciences. The research focuses on the morphological and ecological developments, and the

groundwater changes in the Perkpolder tidal basin. In addition to developments inside the tidal basin, the effects of saline groundwater on the surrounding agricultural areas are investigated. To reduce the impact of saline water a unique seepage discharge system is constructed around the Perkpolder tidal basin, at the landward side of the dyke. Deltares is investigating these effects and the functionality of the seepage discharge system. The research is part of the this project although it began earlier, in 2012. The monitoring and research plan is described in De Louw (2014), the monitoring and research in the Perkpolder tidal basin is described in Boersema, et al. (2015).



Figure 2. Perkpolder tidal basin, September 6, 2016 (Photo: Edwin Patee, RWS).

1.4 PROBLEM STATEMENT

Rijkswaterstaat has the responsibility to realize a new tidal environment at Perkpolder (NCW-eindrapportage, 2008). The goal is to create 75 hectares of low-dynamic tidal nature due to the fact that the habitat is disappearing in the Western Scheldt over the last century as caused by human interference in the Scheldt estuary. In addition, this project provides a unique opportunity to monitor and study the biotic and abiotic changes in an area, which transforms from a freshwater agricultural area to a tidal salt-water natural area. Not much is known concerning this transition, thus knowledge is very valuable in respect to future tidal restoration projects.

1.5 GOALS

Rijkswaterstaat is responsible for the realization of tidal nature in Perkpolder. The goal of current research is to determine whether the tidal environment is contributing to the Natura 2000 conservation goals for the Western Scheldt and Saeftinghe (Ontwerpbeheerplan, 2015). Added to that the newly created natural area serves as a compensation measure for the second extension of the waterway to the Port of Antwerp (NCW-eindrapportage, 2008). Rijkswaterstaat is tasked to demonstrate that the area is contributing to the development of a low-dynamic tidal nature.

The development of knowledge and the education of new delta professionals are two important goals of the CoE-DT. This project offers the opportunity to study the real development of a managed realignment site, in which an agricultural area is transformed in a salt-water natural area. This study will contribute to the ongoing research programs on the Hertogin Hedwigepolder. Students involved in this project will expand their knowledge about the modern developments in coastal management and have an opportunity to conduct field work on measuring and observing the changes that are taking place.

The goals of this project are divided into the necessary and desired outcomes as required by Rijkswaterstaat. The necessary project goals for Rijkswaterstaat are indicated by the numbers 1 to 3, while the desired ones with the numbers 4 to 6¹. For the CoE-DT it is the opposite, the objectives 4 to 6 are focusing on the mission of the Centre of Expertise. In this regard objectives of Rijkswaterstaat and CoE-DT complement each other.

In summary the goals of this project are:

WATER MANAGEMENT (LONG TERM) AND SAFETY MANAGEMENT

1. Determine which biotopes will develop in the Perkpolder tidal basin, and to which extent these biotopes will contribute to the agreed environment-related goals for the Scheldt estuary, as well as the conservation goals for Natura 2000 (“instandhoudingsdoelstellingen Natura 2000”)
2. Knowledge development in relation to water safety management (“waterveiligheidsbeheer”), such as the development of the inlet and stability of the foreshore.
3. Knowledge development concerning the effectivity of the seepage discharge installation in order to protect the fresh-water resources for agricultural usage.

KNOWLEDGE DEVELOPMENT (SHORT TERM)

4. The development of knowledge about the biotic and abiotic factors and their relations in the first years of transition from a fresh-water agricultural area to a salt-water tidal area. This knowledge will help to shape the design of future tidal restoration projects;

¹ From the standpoint of Rijkswaterstaat, the knowledge development is not the main objective, but at the same time in many policy documents this ‘knowledge development’ is stressed as being very important, for example: “Deltaprogramma 2016” and “Kennis- en Innovatie Agenda Deltatechnologie 2016-2019”.

EDUCATION ENHANCEMENT

5. Training of young professionals by improving the knowledge of teachers to be supported by state-of-the-art case studies;

NETWORK IMPROVEMENT AND KNOWLEDGE DISSEMINATION

6. Promoting the circulation of knowledge within the field by combining all the knowledge within the site of *DeltaExpertise site*.

1.6 RESEARCH QUESTIONS

1.6.1 MORPHOLOGY AND HYDRODYNAMICS

1. How does the Perkpolder tidal basin compare with the other tidal basins in the vicinity?
2. What are the large-scale height changes in the Perkpolder basin, before and after the opening of the inlet?
3. What is the sedimentation rate at the Perkpolder basin?
4. What are the morphological changes in man-made tidal creeks?
5. How does the inlet develop over time?
6. What are the processes behind the morphological development?

1.6.2 GROUNDWATER

7. What is the effect of the new tidal area on the groundwater system in the adjacent agricultural area? Also, is the implemented mitigation measure called SeepCat compensating the effects properly?
8. What is the tidal propagation in the aquifer below the tidal area?
9. What is the effect of the tides on the salinity of soil and groundwater in the tidal area?

1.6.3 VEGETATION AND SOIL

10. How do abiotic and biotic sediment properties affect seedling survival and lateral expansion?
11. How do these abiotic and biotic sediment properties (that affect vegetation establishment) change in time and space at Perkpolder?
12. What is the role of seed availability and seed dispersal for the vegetation development?
13. What is the pattern of colonization and lateral expansion by pioneer species, along the elevational gradient?

1.6.4 BENTHIC MACROFAUNA AND BIRDS

14. How does the colonization process of benthic macrofauna develop in the de-poldered area?

15. Are the benthic communities in the Perkpolder tidal basin similar to benthic communities in similar ecotopes in the Western Scheldt?
16. How will vegetation establishment affect the benthic macrofauna and vice versa (interactions)?
17. How does the development of Perkpolder tidal basin compare to the development of Rammegors in the Eastern Scheldt? What can be learned about the design of de-polders areas?
18. How is the Perkpolder tidal basin used by birds?

2 MORPHOLOGY AND WATER MOVEMENT

2.1 INTRODUCTION

In this chapter we will discuss the morphological changes following the opening of the Perkpolder tidal basin that took place on June 25, 2015. In the analyses four areas are distinguished: 1) tidal flats with creeks (area 1 in Figure 13), 2) the pond (area 2), 3) the inlet (area 3) and 4) the tidal flat on the seaward side of the inlet (area 4). Secondly, the changes in the cross-section of the inlet are analysed. To obtain a better understanding of the large-scale changes in height, the hypsometric curves of the Perkpolder tidal basin are made before, directly after the opening of the inlet and also every year during the duration of the project. A sediment balance is performed to better understand the possible sediment sinks and sources. Finally, the Perkpolder tidal basin at the time of the opening is compared with other basins in the vicinity.

Besides the morphology, the flow velocities in the inlet are studied and utilized to calibrate a Delft3D model. The model results offer a better understanding of the processes that drive the morphological development in Perkpolder. Subsequently, the model is used to study the effect of the inlet width, the creeks and the pond. The OBS data in the inlet were used to estimate the sediment influx.

In this study the channels are defined below MLW (mean low water, at Perkpolder: -2.06 m NAP), the sand and mud flats or tidal flats are located between MLW and MHW (mean high water; at Perkpolder: +2.56 m NAP). The salt marshes are defined above MHW (Figure 3). The word 'creek' is not only used for tidal streams in the salt marsh, but also in the tidal flat.

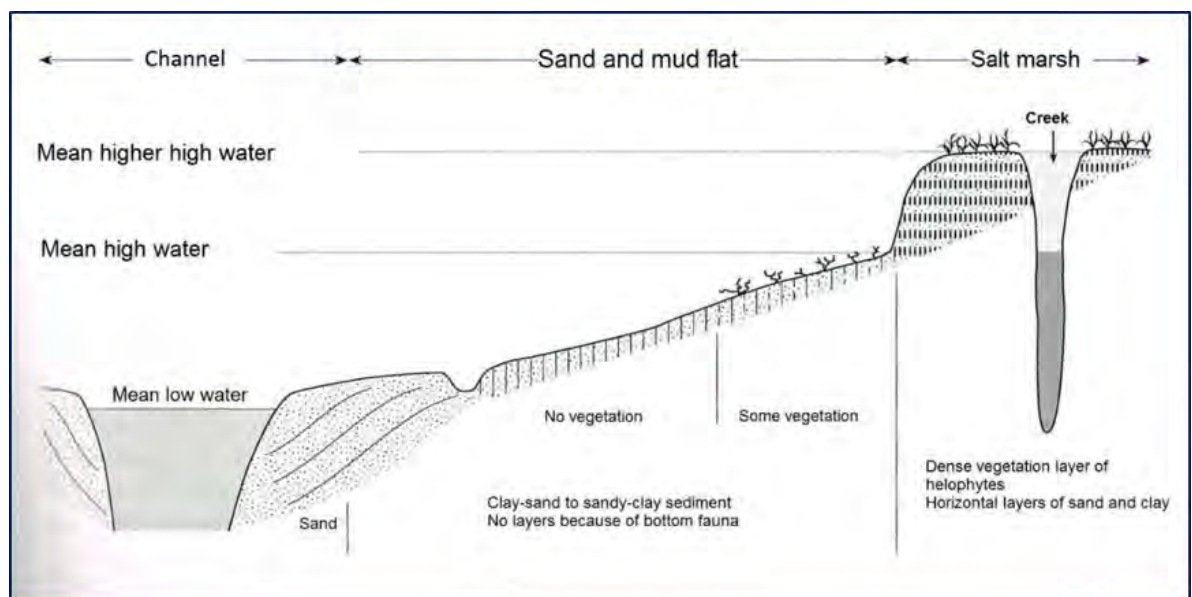


Figure 3. Composition of an intertidal area (Zagwijn, 1986).

2.2 METHODS

2.2.1 HEIGHT MEASUREMENTS IN SUBTIDAL AND INTER TIDAL AREAS

Height measurements in subtidal and intertidal areas were performed by using several measuring technics. The main technics were the Lidar and the multi-beam but also dGPS measurements were used, see Table 1. The first dataset used is a LiDAR measurement of the Perkpolder area during the period when the area was still used for the agricultural purposes (20-12-2013). The second dataset is a composite of multi-beam and DGPS measurements collected in May of 2015 by the contractor, combined with LiDAR data (May of 2015) from the area outside of the Perkpolder basin. It is assumed that this dataset represents the moment just before the levee opening (T0), although it is apparent from the data that this is not the case for the area next to the dike (see Figure 17). This T0 data covered the outer area, inlet and complete intertidal area (see Figure 13). The multi-beam measurements hereafter cover the same area, but without the area to the south of approximately $y = 379$ km RD. Table 1 presents an overview of the available bathymetry data.

Table 1. Overview of morphological measurements in Perkpolder intertidal area and surroundings.

Code	Date	Coverage	Instrument	Resolution
T-1	20-12-2013	Complete area of interest	LiDAR	5 m x 5 m
T0	25-06-2015	Complete area of interest	Multi-beam + DGPS and LiDAR	2 m x 2 m
T1	30-07-2015	Without shallow intertidal area	Multi-beam	1 m x 1 m
T2	17-09-2015	Without shallow intertidal area	Multi-beam	1 m x 1 m
T3	29-10-2015	Without shallow intertidal area	Multi-beam	1 m x 1 m
T4	20-11-2015	Without shallow intertidal area	Multi-beam	1 m x 1 m
T5	08-01-2016	Without shallow intertidal area	Multi-beam	1 m x 1 m
T6	19-04-2016	Without shallow intertidal area	Multi-beam	1 m x 1 m
T6a	April 2016	Complete area of interest	LiDAR + Multi-beam	2 m x 2 m
T7	20-07-2016	Without shallow intertidal area	Multi-beam	1 m x 1 m
T8	31-10-2016	Without shallow intertidal area	Multi-beam	1 m x 1 m

T9	27-01-2017	Without shallow intertidal area	Multi-beam	1 m x 1 m
T9a	February 2017	Complete area of interest	LiDAR + Multi-beam	2 m x 2 m
T10 (1702)	26-04-2017	Without shallow intertidal area	Multi-beam	1 m x 1 m
T11 (1703)	21-07-2017	Without shallow intertidal area	Multi-beam	1 m x 1 m
T12 (1704)	01-12-2017	Without shallow intertidal area	Multi-beam	1 m x 1 m
T13 (1801)	26-04-2018	Without shallow intertidal area	Multi-beam	1 m x 1 m
T13a	April 2018	Complete area of interest	LiDAR + Multi-beam	2 m x 2 m
T14(1802)	26-06-2018	Without shallow intertidal area	Multi-beam	1 m x 1 m
T15 (1803)	06-09-2018	Without shallow intertidal area	Multi-beam	1 m x 1 m

2.2.2 SEDIMENT THICKNESS IN SHALLOW INTERTIDAL AREA

The sedimentation inside the intertidal area was measured by Martens (2016) during three field measurement campaigns in April of 2016 (Figure 4). The method is based on the assumption that the initial bed level (T0, see Table 1) inside the Perkpolder is non-erodible. The sediment thickness was determined by pushing a bamboo stick ($\varnothing = 2$ cm) into the soft sediment layer until it touched the solid surface underneath, it is assumed that this surface is the bed level as of the June 25, 2015 (T0). The sedimentation thickness was recorded at 545 locations and determined by the average of five measurements (Figure 4).

At six cross-sections (Figure 21) over the artificial tidal creeks, the sedimentation thickness is measured to obtain a more detailed picture concerning the sedimentation in the creeks. These measurements were executed on July 11, 2016. The sediment thickness was measured utilizing the same method as described above, also the surface level was measured with a DGPS.

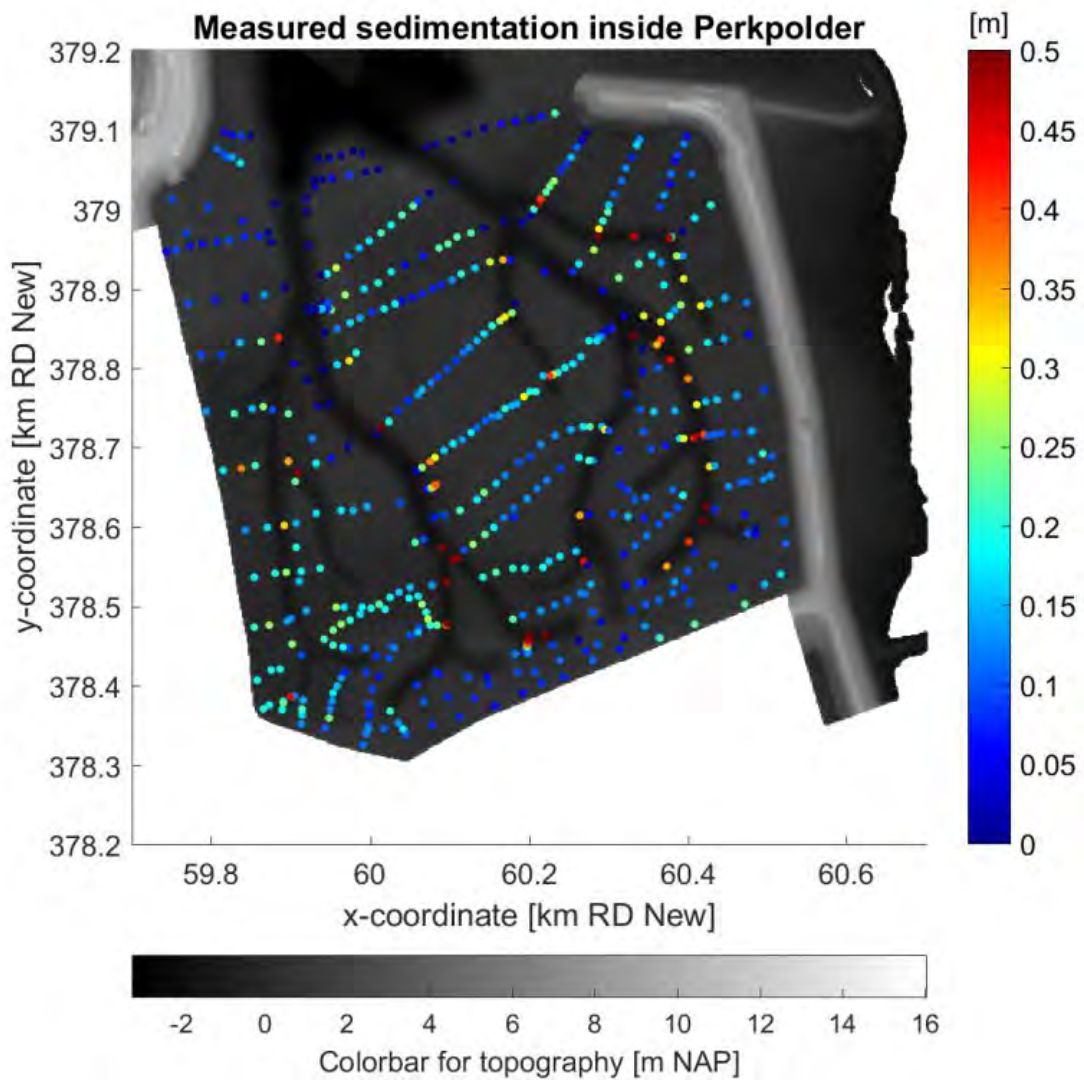


Figure 4. Sedimentation measurements in April of 2016, measured during three field campaigns.

Later, in 2017, the cross sections over the creeks and the sediment thickness were replaced by four cross sections over the entire basin, Figure 5. Besides sediment thickness and DGPS, shear stress, with a shear vane, was also measured and sediment samples were collected to be later analysed. Table 2 provides an overview of sediment thickness measurements in Perkpolder intertidal area and its creeks.

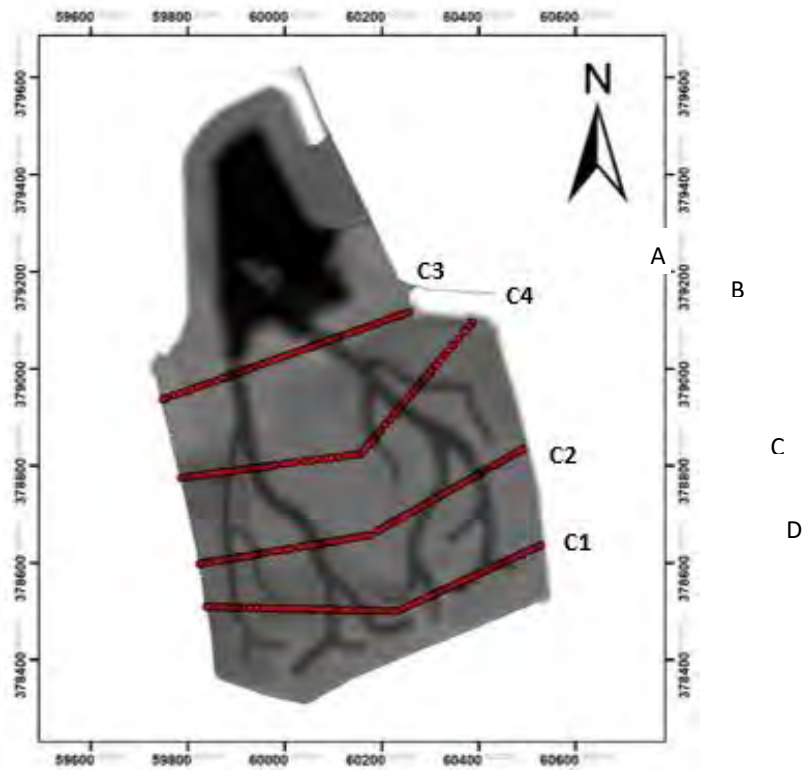


Figure 5. Locations of the four cross sections located on the shallow area of the basin.

Table 2. Overview of sediment thickness measurements in Perkpolder intertidal, and creeks.

Unit	Date	Coverage	Instrument	Resolution
m	04-2016 (3x)	Shallow intertidal area (Part 3)	Bamboo stick	545points/50 ha
m NAP	11-07-2016	Six cross-section over creeks	Bamboo stick, DGPS	1point/m
m NAP	April 2017	Three cross sections	Bamboo stick, DGPS, shear stress and sediment	1point/m to 1point/10m
m NAP	June 2017	Four cross sections	Bamboo stick, DGPS, shear stress and sediment	1point/m to 1point/10m

m NAP	October 2017	Four cross sections	DGPS	1point/m to 1point/10m
m NAP	December 2017	Four cross sections	DGPS	1point/m to 1point/10m
m NAP	April 2018	Four cross sections	DGPS	1point/m to 1point/10m
m NAP	June 2018	Four cross sections	DGPS	1point/m to 1point/10m

2.2.3 CROSS-SECTION INLET INTERTIDAL AND SUPRA TIDAL

To have a complete coverage of the tidal inlet between the two dykes, the multi-beam measurements (Table 1) were extended with a measurement in the higher parts of the inlet cross-section. The bed levels across the inlet were measured by HZ-student Van Vliet (2015) on 25-11-2015 using Differential Global Positioning System (DGPS; Figure 6) and later by Brunetta (2017), see Table 3. The DGPS measurement points were concentrated on the northern part and southern part; the inner channel was too deep to measure and covered by the multi-beam measurements. It is assumed that morphological changes in these higher parts of the inlet, close to the two dyke heads is limited, therefore only two measurement were taken.

Table 3. Overview of height measurement of inlets cross-section (higher parts).

Unit	Date	Coverage	Instrument	Resolution
m NAP	25-11-2015	Intertidal and supratidal part of inlets cross-section	DGPS	153points/400 m
m NAP	17-04-2017	Intertidal and supratidal part of inlets cross-section	DGPS	153points/400 m

2.2.4 FLOW VELOCITIES INLET AND WATER LEVELS

Figure 6 shows the locations of 3D Aquadopp velocity measurements (deployed by Rijkswaterstaat) from 25 November to 1 December 2015 (10-minute data), on six locations and with 0.1 m bins over the water depth. In addition, the 10-min water level data from the Walsoorden tidal station (xRD = 60.3 km, yRD = 379.7 km) just north of Perkpolder intertidal area was used, Table 4.

Table 4. Overview of water level and velocity measurements.

Unit	Date	Coverage	Instrument	Resolution
m/s	25-11-2015 until 1-12-2015	Intertidal part of inlet cross-sections	Aquadopps	6 points – 10 min
m NAP	Continuous	Point measurements at Walsoorden	Pressure sensor	10 min

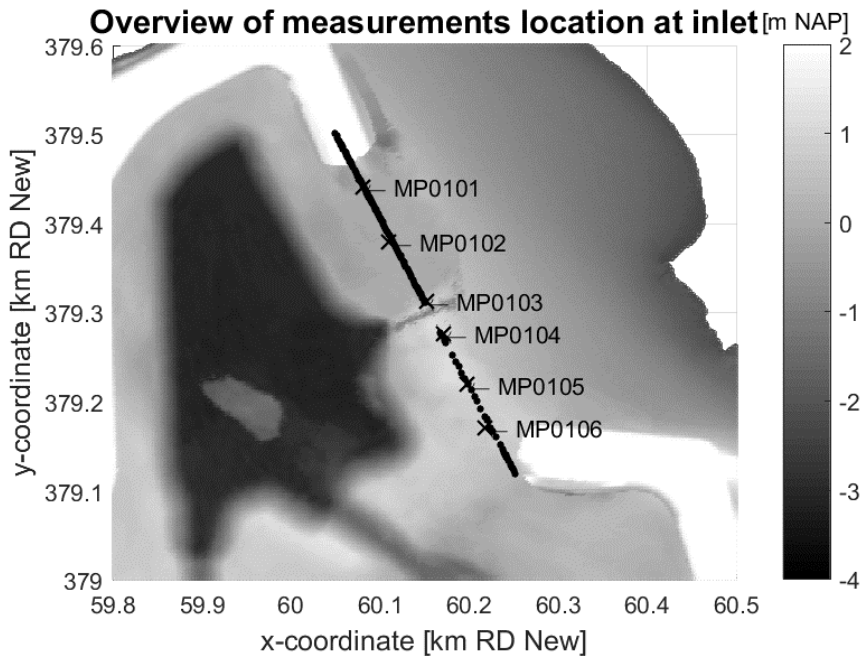


Figure 6. Overview of locations DGPS bed level measurements across the inlet (dots) and Aquadopp velocity measurements (crosses) with the underlying TO bathymetry.

2.2.5 SUSPENDED SEDIMENT

At the inlet OBS measurements performed to determine the turbidity and sediment concentrations and from that to estimate the sediment influx in the basin. Adding to this in 2017 two samples, April and June, regarding the suspended sediment were collected. The suspended sediment was collected at four different locations, outside and inside the basin. Bamboo sticks with 3 bottles at different heights were used to collect the suspended sediment. The sediment was later filtered using a filter machine and then weighed, see Brunetta (2017).

2.3 RESULTS

2.3.1 *SEDIMENT IMPORT ANALYSIS BASED ON MEASURED CONCENTRATIONS AND COMPUTED DISCHARGES*

2.3.1.1 INTRODUCTION

To analyse temporal fluctuations in the sediment import/export of Perkpolder, concentration measurements are performed since September 16, 2016 in the mouth of Perkpolder. When these sediment concentrations are combined with discharge estimates, sediment fluxes can be derived. The questions to be answered with this analysis are:

1. Is there predominantly an import or export of sediment?
2. How variable are these sediment fluxes over time?
3. What drives this temporal sediment flux variation (meteorological and/or astronomical forcing)?
4. How does this sediment exchange compare to the observed morphological development of Perkpolder?

To answer these questions, turbidity measurements from an Optical Back Scatter (OBS) instrument were converted to suspended sediment concentrations, based on a calibration procedure with samples taken from the field. Discharge estimates were derived from a tidal storage (“komberging”) approach, which is a simple mathematical equation that combines the high-resolution bathymetric data with water level measurements. This approach is legitimate as Perkpolder has a relatively small surface area (i.e. the water level within the basin equals the water level outside the basin). In this way, no numerical computations were required. The sediment fluxes are the direct result of multiplying the concentration estimates with the derived discharges. Finally, the net sediment import estimate is combined with the measured morphological change to have a sediment balance.

There are some limitations to be defined for the analysis. First, a single station is considered to provide representative concentration measures for the full opening of Perkpolder. Second, the instrument was exposed part of the tidal period (sensor height NAP+1.0 m). This implies that no closed sediment balance could be derived, unless estimates are made for the concentrations when the instrument was exposed. Nevertheless, still useful insights could be derived to answer the defined questions.

2.3.1.2 DERIVATION SUSPENDED SEDIMENT CONCENTRATIONS

With a calibration procedure, the OBS turbidity measurements were converted to suspended sediment concentrations (Figure 7). Both a linear as a parabolic fit are presented. Clearly, the parabolic fit, which is enforced through the origin (i.e., $y = c \cdot x^2$), is much better in line with the tendency of the measurement data. This parabolic relationship was used to derive concentration time series (in g/L) from the OBS turbidity measurements. The deviation between the data and the fit gives an indication of the accuracy of the derived

time series. It is noted that the difference in concentration between the two most turbid samples used in the concentration procedure is almost a factor two, so the high concentration range was calibrated only with a few samples. Furthermore it is noted that the highest concentration in the calibration procedure is smaller than the concentrations actually measured at Perkpolder (see Figure 7). Therefore, some conservatism is required when considering the precise calibration results, but these are more than sufficient for the aims of this study.

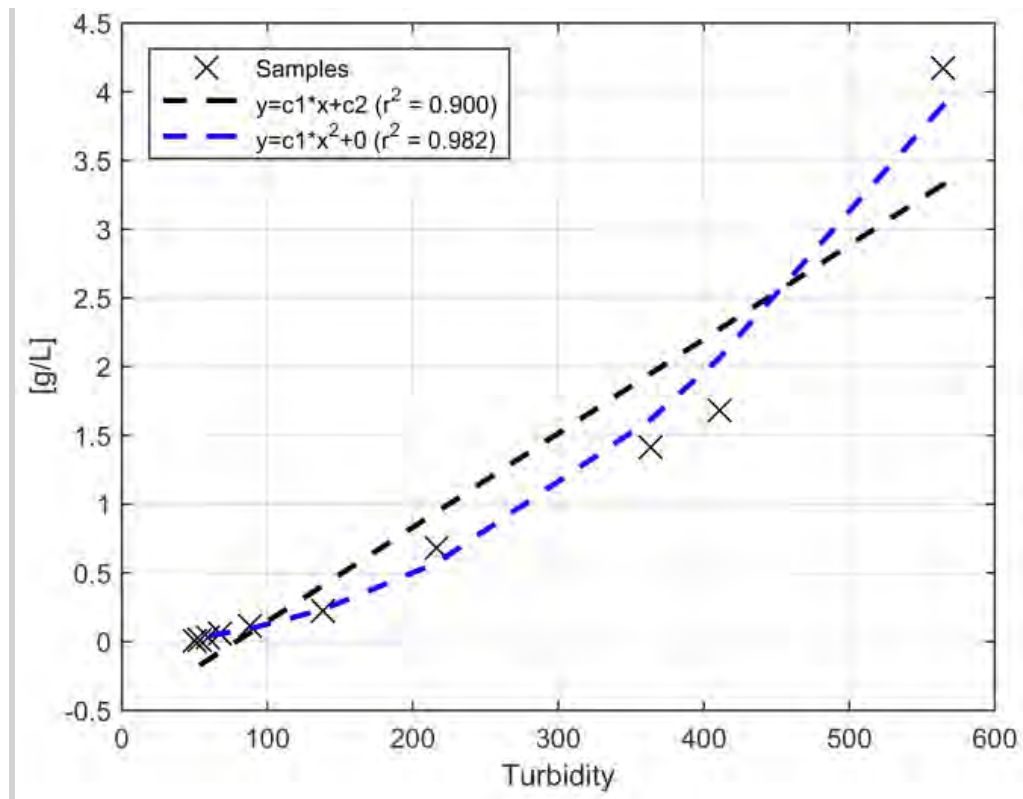


Figure 7. OBS calibration, unit of turbidity: Raw Fluorescence Units.

2.3.1.3 DERIVATION DISCHARGES

As Perkpolder has a small surface area, the discharges in the mouth of Perkpolder are the direct consequence of the area of the basin and the water level variations in the Western Scheldt:

$$Q(t) = A(z) \frac{dz}{dt} \quad (1)$$

in which $A(z)$ represents the wet area of Perkpolder for a certain water level z (hypsometric curve), and dz/dt represents the water level gradient over time. In this formulation, positive discharges are directed into Perkpolder. For the area of Perkpolder at a certain reference level, the high resolution bathymetric LiDAR/multibeam data were used. Bathymetric data of the years 2015, 2016 and 2017 were all used in this

analysis. The water level gradients over time were derived from the nearby located water level station Walsoorden. The inflow and outflow discharges were derived with this equation.

To assess the accuracy of the discharge time series, the estimates derived from this approach were compared to discharges reconstructed from the five-day flow measurement campaign from 25 November to 1 December 2015. First, the ADCP instruments were projected onto the cross-section between the two tips of the levees. Second, the cross-section was divided into sections based on the nearest ADCP. This is visualised in Figure 8. By multiplying the velocity measurements with the (water level dependent) cross-sectional area of each segment, the discharge through each segment was approximated. The discharges through all segments were combined to estimate the total discharge into the Perkpolder. A small correction of $0.02 \text{ m}^3/\text{s}$ (roughly 0.01% of peak discharges) was applied to ensure volume conservation within the basin (zero cumulative flow discharge over the measurement period).

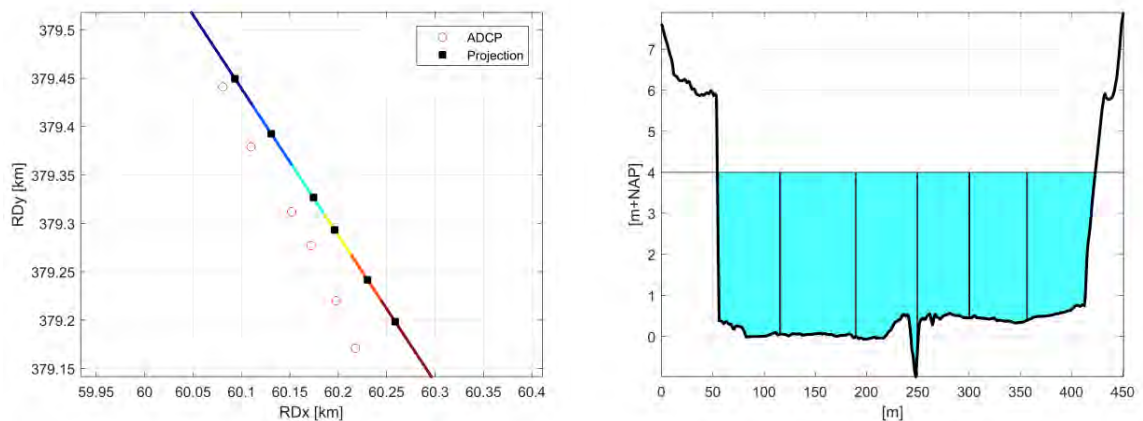


Figure 8. Left: top view of the inlet with the ADCP measurement locations (circles) and the ADCP projections on the inlet (squares). Right: side view of the inlet with cross-sections divided into different segments to be able to compute discharge.

Figure 9 compares discharges derived from the tidal storage approach to discharges derived from the ADCP measurements. As the ADCPs were elevated above the lowest point of the cross-section, the instruments emerged part of the tidal cycle. Therefore, the discharges could not be measured over the full tidal cycle. The two approaches give very similar discharges. Only the peak flood discharges in the tidal storage approach are slightly lower compared to the ADCP approach for several tides. However, the validation ADCP approach is not necessarily better than the tidal storage approach, as also the ADCP approach contains inaccuracies. But the fact that both approaches give such similar results, provides much confidence in the applicability of the tidal storage approach to answer the posed questions. The big advantage of this approach is that now a long continuous time series of the discharges can be derived (as long as water level data is available and bathymetry data is representative).

Figure 9 shows a clear flood dominance: the peak flood discharges are substantially larger than the peak ebb discharges. This is a direct consequence of the shape of the vertical tide: the water levels rise faster than they fall (flood is shorter than ebb). With the discharge time series reliable estimates for the tidal prism (total inflow of water per tide) can be made for Perkpolder. Depending on the HW level, the tidal prism varies between 1.0-2.6 M m³, with an average value of 1.7 M m³.

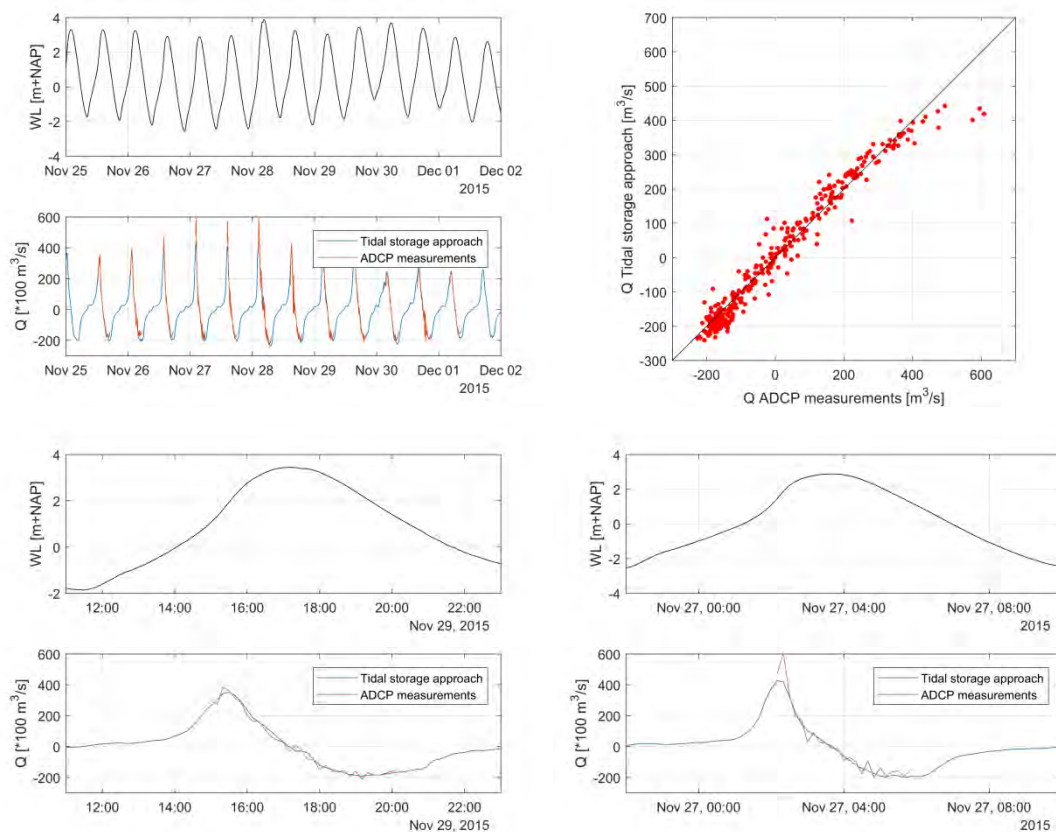


Figure 9. Comparison of discharges based on tidal storage approach and ADCP velocity measurements. Top left: complete water level and discharge time series, top right: scatter diagram, bottom: water level and discharge time series for a single tide on 29 November.

2.3.1.4 SEDIMENT FLUXES

The sediment fluxes can be estimated from the concentration and discharge time series. The fact that the OBS instrument emerged more than half of the tidal cycle was overcome by assuming a constant concentration of zero, 0.2 g/l or 1 g/l at times of exposure. The averaged suspended sediment concentration in the channel at Hansweert varies between 30 and 50 mg/l (van der Wal et al., 2010).

Figure 10 presents the cumulative sediment fluxes over the measurement period, for various background concentrations. Although there are differences between the different background concentration values, the net pattern is very similar. This does not exclude the possibility that substantial errors were introduced by the emergence of the instruments, e.g. due to a correlation between the in- and outflow velocities and concentrations at times of instrument exposure. A value of 0.2 g/l was used as a background value in the further analyses.

There is predominantly an import of sediment, 5-6 k m³ (without porosity) or 13-16 kilotons over the complete measurement period using a sediment density of 2650 kg/m³. This corresponds to 34-40 kilotons/year or 13-15 k m³/year (corrected for the lack of data from Nov 19 to Dec 21). This sediment import time series will be compared to the SED sensor results in Section 4.2.2.4.

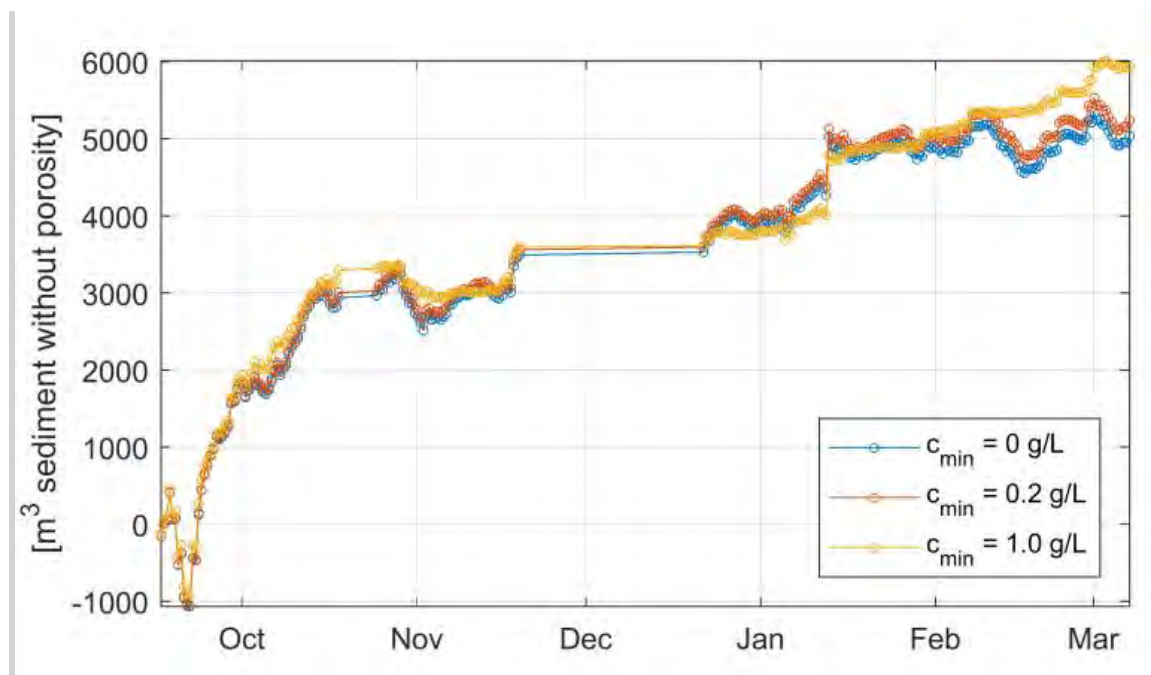


Figure 10. Cumulative net sediment fluxes (positive = import into Perkpolder) for different background concentration levels for the period September 2016 – March 2017. Each circle marks a single tide.

Figure 10 shows that the fluxes are not constant over time. To investigate what drives these temporal fluctuations, the net sediment import/export per tide were plotted against the HW level (representative for total quantity of water entering Perkpolder), maximum flood discharge (representative for local hydrodynamic forcing) and the wind speed (representative for wind events), see Figure 11. The negative correlations imply that that an increase in that variable implies a decrease in the other variable. For the sediment fluxes, these parameters show a lot of scatter, with absolute correlation coefficients smaller than 0.18. Concerning the trapping efficiency (net flux divided by the inflow flux; positive is import; lower panels

in Figure 11), the HW level and the peak flow discharge show slightly stronger relationships. Lower HW levels and lower peak flood discharges appear to result in more import of sediment into Perkpolder.

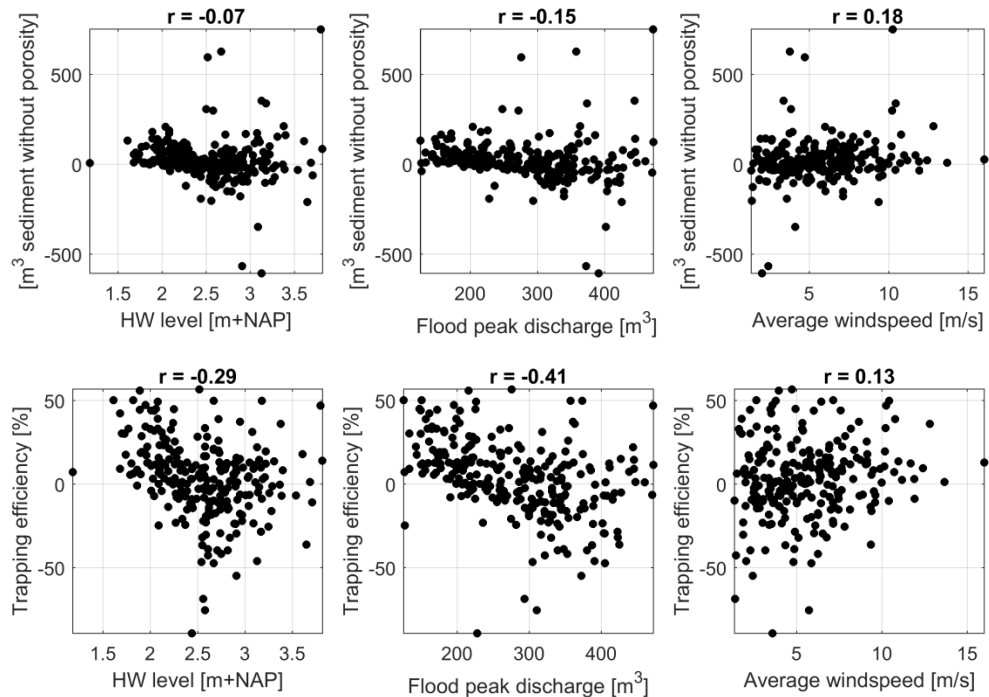


Figure 11. Top row: Scatter plots of the net sediment fluxes per tide (positive = import) versus the high water level (left), flood peak discharge (middle) and wind speed (right). Bottom row: now with the trapping efficiency on the vertical axis.

A closer look to the data of two tides, one with a substantial net flux (23 September 2016) and another tide with a much smaller net flux (20 September 2016), is provided in Figure 12. Both tides faced mild wind conditions: 5 m/s and 2 m/s, respectively. Important insights can be gathered from these two tides. Although the tide of 23 September is one of the major importing tides, the peak discharges are not very large compared to other tides (see Figure 9). The concentrations during this tide were quite substantial (about 2 g/L on average), but much less compared to the tide of 20 September. Based on this, it can be concluded that it is not necessarily a strong tidal flow or a high concentration which results in a large inflow of sediment. The “key of success” of the tide of 23 September is the suspended sand concentration variation over time. In contrast to the tide of 20 September, the sediment concentrations reduced during the tide, causing almost half the concentrations during the outflow phase. The lower outflow concentration implies there is substantially more sediment settled within Perkpolder compared to the amount of sediment resuspended during this specific tide. This observation is in line with the main tendency in Figure 12, in which also higher trapping efficiencies are found for lower tides.

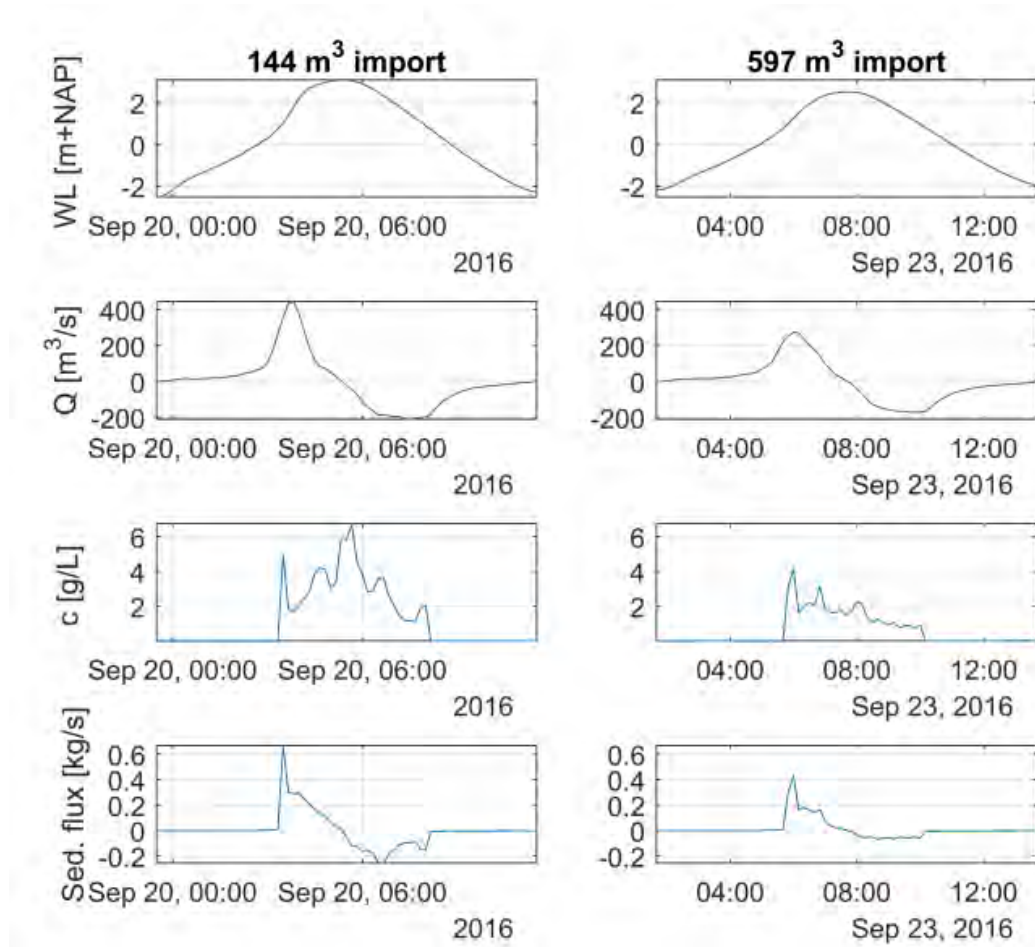


Figure 12. Water levels (first row), discharges (second row), suspended sediment concentrations (third row) and sediment flux (fourth row) for tide with a relatively low (left; 20 September 2016) and high (right; 23 September 2016) sediment import.

2.3.1.5 LINK TO MORPHOLOGICAL CHANGES WITHIN PERKPOLDER

To link the sediment important analysis to the bed level changes, the dry bulk density needs to be known. The dry bed density ($\rho_{dry,b}$) is the mass of soil (excluding water) per volume as a whole. It is related to the wet bulk density (ρ_b) as follows:

$$\rho_{dry,b} = (1 - \varepsilon) \rho_s = \rho_b - \varepsilon \rho_w \quad (2)$$

$$\varepsilon = \frac{(\rho_s - \rho_b)}{(\rho_s - \rho_w)} \quad (3)$$

$$\rho_{dry,b} = \rho_s \frac{(\rho_b - \rho_w)}{(\rho_s - \rho_w)} \quad (4)$$

with ϵ the bed porosity, ρ_s the sediment density ($\sim 2650 \text{ kg/m}^3$) and ρ_w the water density ($\sim 1000 \text{ kg/m}^3$). For a stable sand bed, $\epsilon \sim 0.4$ and $\rho_{\text{dry,b}} \sim 1600 \text{ kg/m}^3$. The dry bed density of (especially) muddy deposits increases in time due to consolidation. The primary consolidation phase takes about 10-50 days to reach a dry bulk density of $\sim 400\text{-}800 \text{ kg/m}^3$, depending on the percentages of sand and clay in the mixture (van Rijn and Barth, 2018). The secondary consolidation process can take up to years during which the dry bulk density increases further. The measured (dry) bulk density in the Perkpolder intertidal area 2017 was typically between 400 and 1250 kg/m^3 , see Figure 65. With this range in bulk density, the 34-40 kilotons/year estimated from OBS and ADCP inlet data correspond to 27-100 km^3/year . This corresponds well to the 2016-2017 observed Perkpolder sedimentation (sum of areas 1 and 2), see Section 2.3.4.

2.3.2 MORPHOLOGICAL CHANGES

This paragraph gives an overview of the morphological changes in the study area. This includes the intertidal areas inside the basin, the pond area, the cross-section of the inlet and the foreshore of the basin including the tidal flat and the new inlet in it.

2.3.2.1 LARGE-SCALE CHANGES IN PERKPOLDER BASIN

The main morphological features present at the Perkpolder basin just after the dike breach are a small inlet channel, a deep basin in the northern part (which in the report is referred as pond) and the artificial creeks on the intertidal area to promote intertidal sedimentation and drainage to favour vegetation growth (see Figure 13).

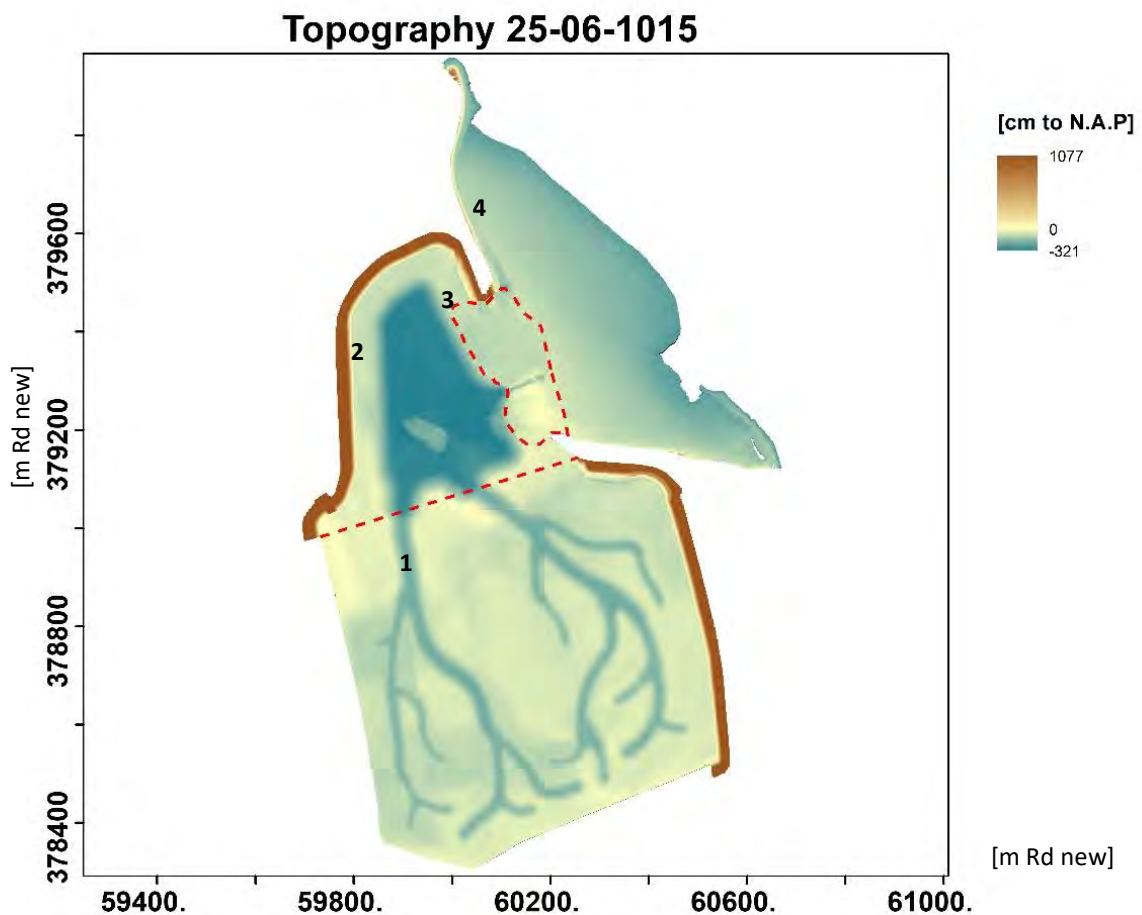


Figure 13. T0 bathymetry (May/June 2015) in the basin and the division of the areas. Area 1 represents the tidal flat and the artificial creeks in the basin. Area 2 is the pond area, area 3 is the inlet and area 4 is the foreshore just in front of the Perkpolder basin.

During the project the basin experienced morphological changes including the erosion of some areas, e.g. the channels, and also the sedimentation of other areas, e.g. the pond area. The maps below (Figure 14) show the bed levels at various moments in time, in December 2013 (T-1), June 2015 (T0), April 2016 (T6a), February 2017 (T9a) and April 2018 (T13a). The most visible changes are the sedimentations processes taking place at the pond (located in the northern part) and at the end of the man-made channels (located on the south part of the area).

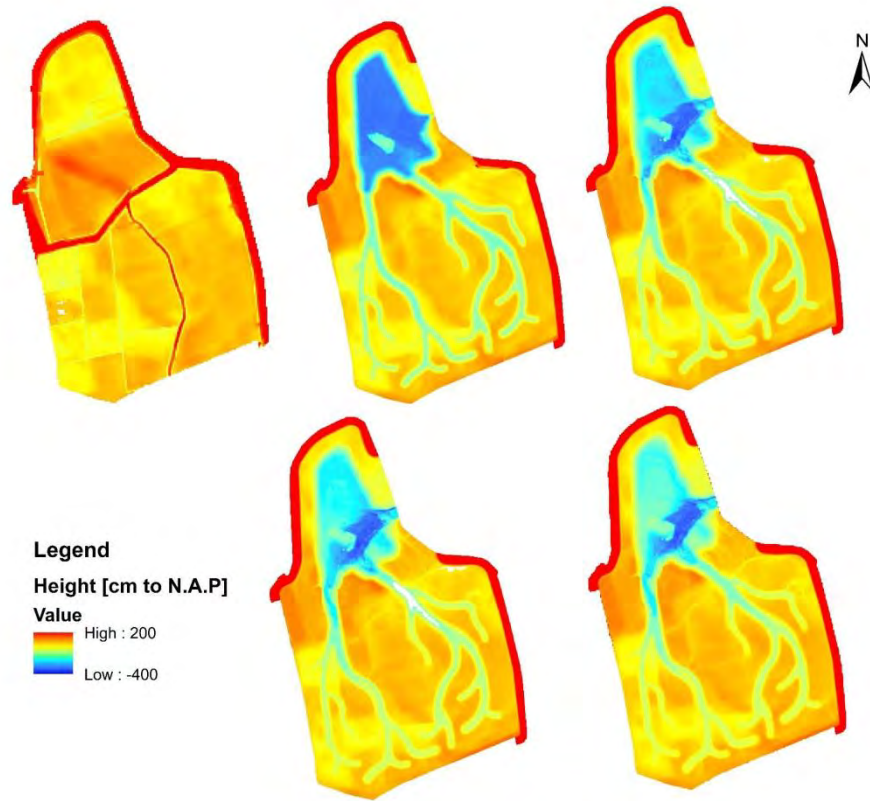


Figure 14. Elevation maps of the Perkpolder tidal basin, T-1 (December 2013), T0 (June 2015), and T6a (April 2016), T9a(February 2017) and T13a (April 2018). On the image sequence it is possible to observe that the blue areas are becoming lighter meaning that the lower parts are accreting. This is particularly clear at the pond area.

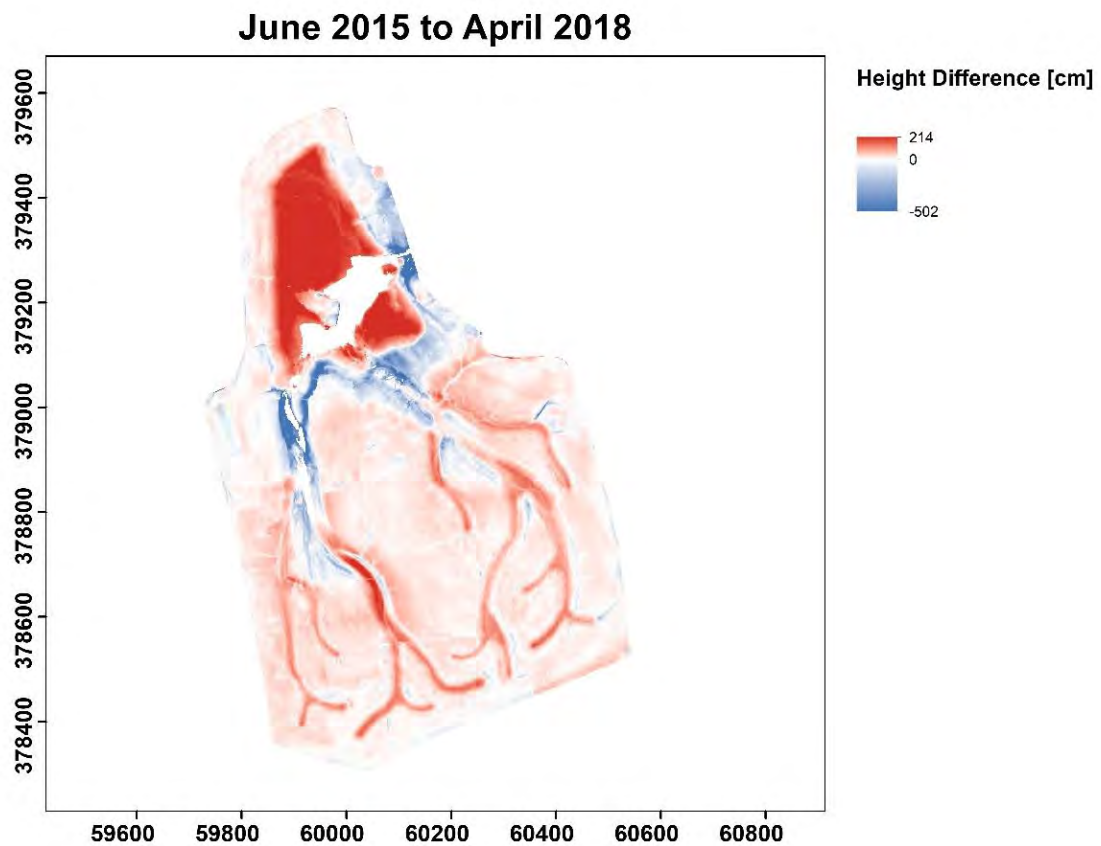


Figure 15. Sedimentation erosion map of Perkpolder basin and foreshore between T0 (June 2015) and T13a (April 2018). Darker colours mean higher values of sedimentation (red) or erosion (blue). The pond and some areas of the channels show high sedimentation and the inlet and the beginning of the channels next to the pond show erosion.

A hypsometric curve is a diagram that presents the proportion of area lower than a certain elevation. The hypsometric curves (Figure 16) show the changes in bed levels of the Perkpolder basin. The differences between T-1 and T0 are due to the excavation work of the contractor, as the dike was not yet opened. The dikes and the top layer of the surface were removed, a basin in the northern part was created and also the creeks in the south. After opening most of the changes are visible in the lower part of the hypsometric curves. This is caused by the large sedimentation in the basin (see also Figure 15 and Figure 19) and the sedimentation of the end part of the creeks around -1.0 m NAP (see also Figure 22).

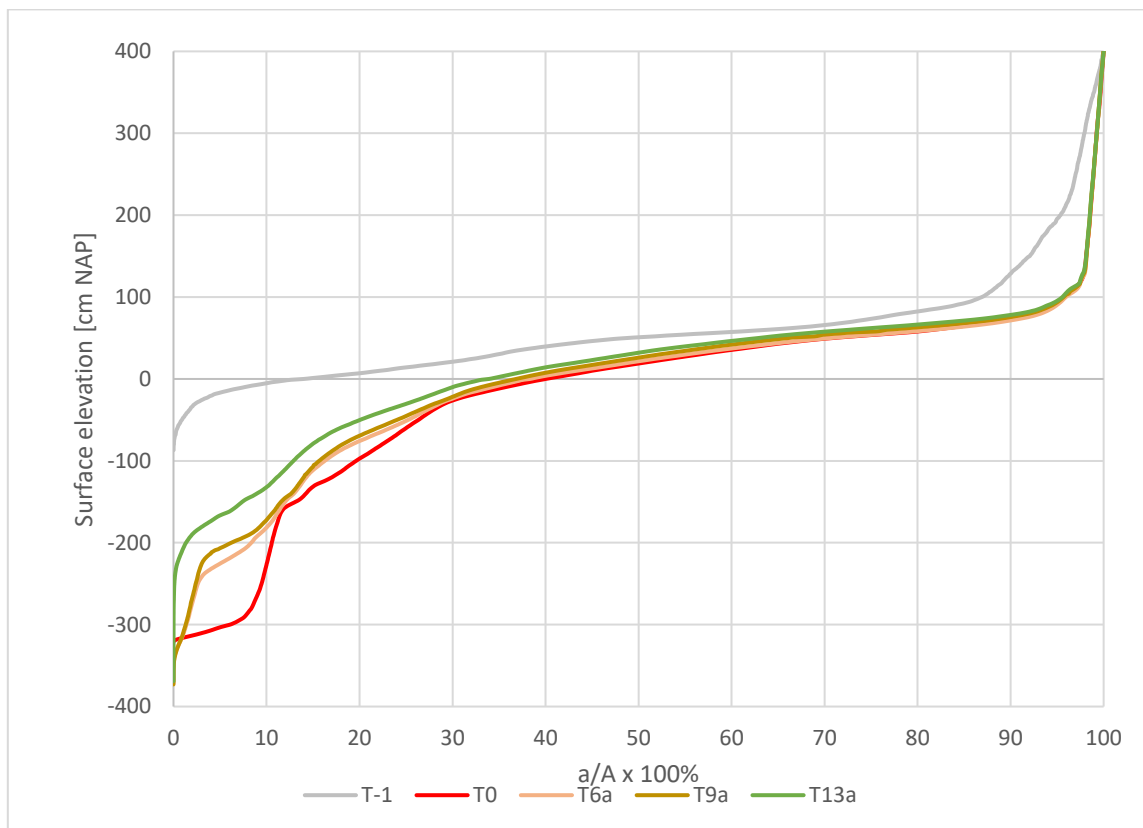


Figure 16. Hypsometric curves of the Perkpolder tidal basin T-1 (Dec. 2013), T0 (June 2015), T6a (April 2016), T9a (Feb. 2017) and T13a (April 2018). On the y-axis the surface elevation, on the horizontal axis the ratio a/A , where 'a' is the area below a given elevation colour, and 'A' is the total basin area.

2.3.2.2 CROSS-SECTION TIDAL INLET

Figure 17 shows how the bed levels at the inlet developed. Figure 18 shows the changes in the cross-sectional area of the inlet over time, below a water level of +86 cm NAP, this is the level on which the water is still only confined to the channel. The main inlet channel has widened and deepened during the period between June (T0) and July (T1) of 2015. After that period, the changes became much smaller, although there is a continuing trend towards an increase of the inlets cross-section (Figure 18).

In the initial phase (T0-T1) a smaller secondary channel developed at the right-hand side of the left dike. Furthermore, this figure shows that the multi-beam and DGPS measurements match well, except for the location of the dikes in the T0 measurements. It is also important to mention that large parts of the cross-section did not change (or very limited changes, <0.1 m). This can be explained by the existence of non-erodible layers (or difficulty eroding layers) due to the presence of old blocks of the hard revetment of the old dyke but also the consolidated clay underneath them, see image of the cover).

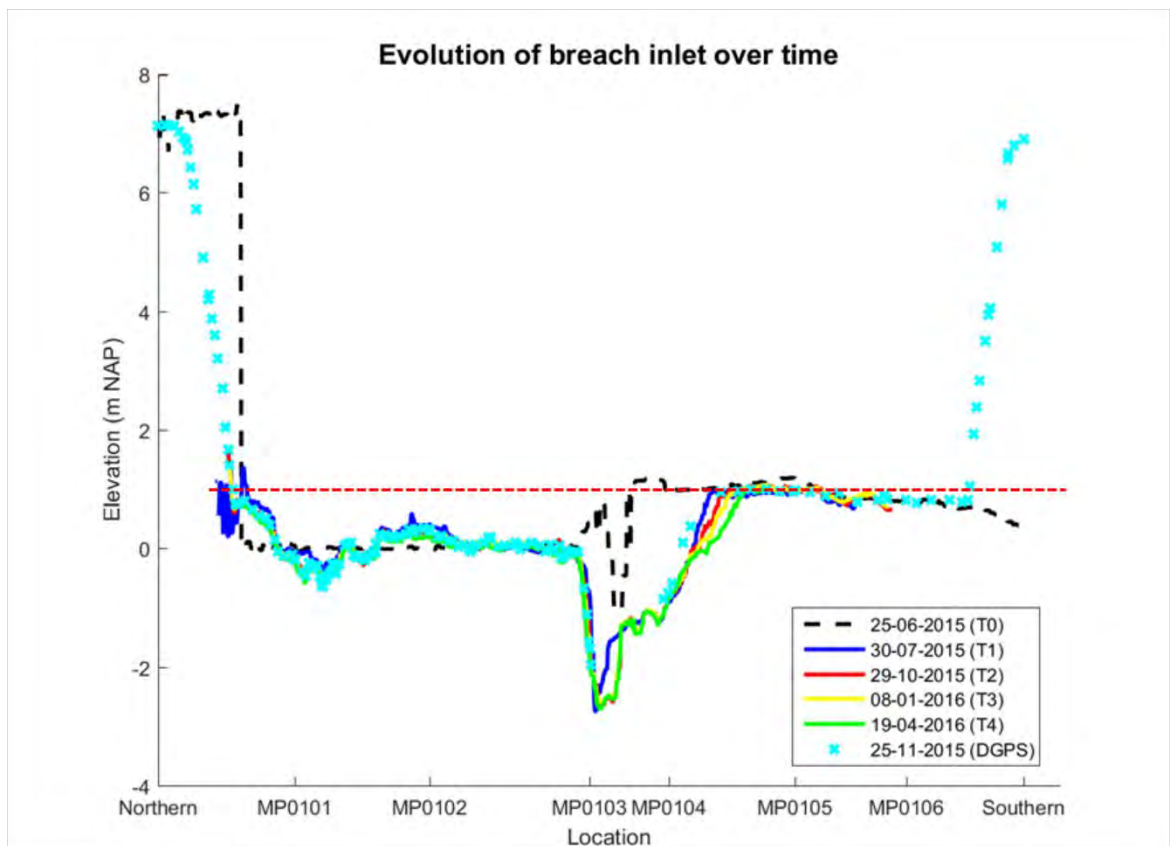


Figure 17. Morphological development of the inlet. The horizontal red dashed line represents the water level of 86 cm NAP.

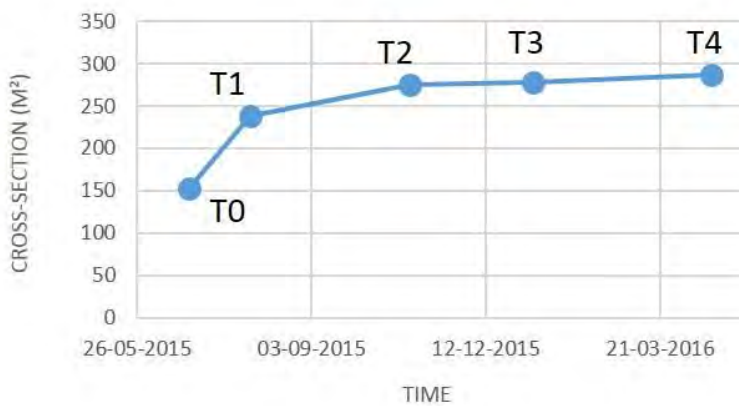


Figure 18. The development of the cross-section of the tidal inlet over time. Cross-sectional area is calculated at a water level of NAP +0.86 m (Figure 17).

2.3.2.3 POND AND OUTER TIDAL FLAT AREA

As mentioned previously, the pond and foreshore area presented some of the main morphological changes. On one hand the foreshore erodes, especially where the new channel is forming, connecting the basin with the Western Scheldt. On the other hand the very deep pond slows down the flow promoting sedimentation in this area. Figure 19 shows the morphological development during the period of May/June 2015 (T0) to 26 June 2018 (T14), or about 36 months. This figure clearly demonstrates the sedimentation of the pond (up to 2 m) and the erosion of the inlet (up to -4 m NAP). The morphological changes are the largest between T0 and T1 when the channel is formed. Another interesting aspect is that the channel initially was turning to clockwise whereas after that initial state all the other measurements show that the channel turned counter-clockwise.

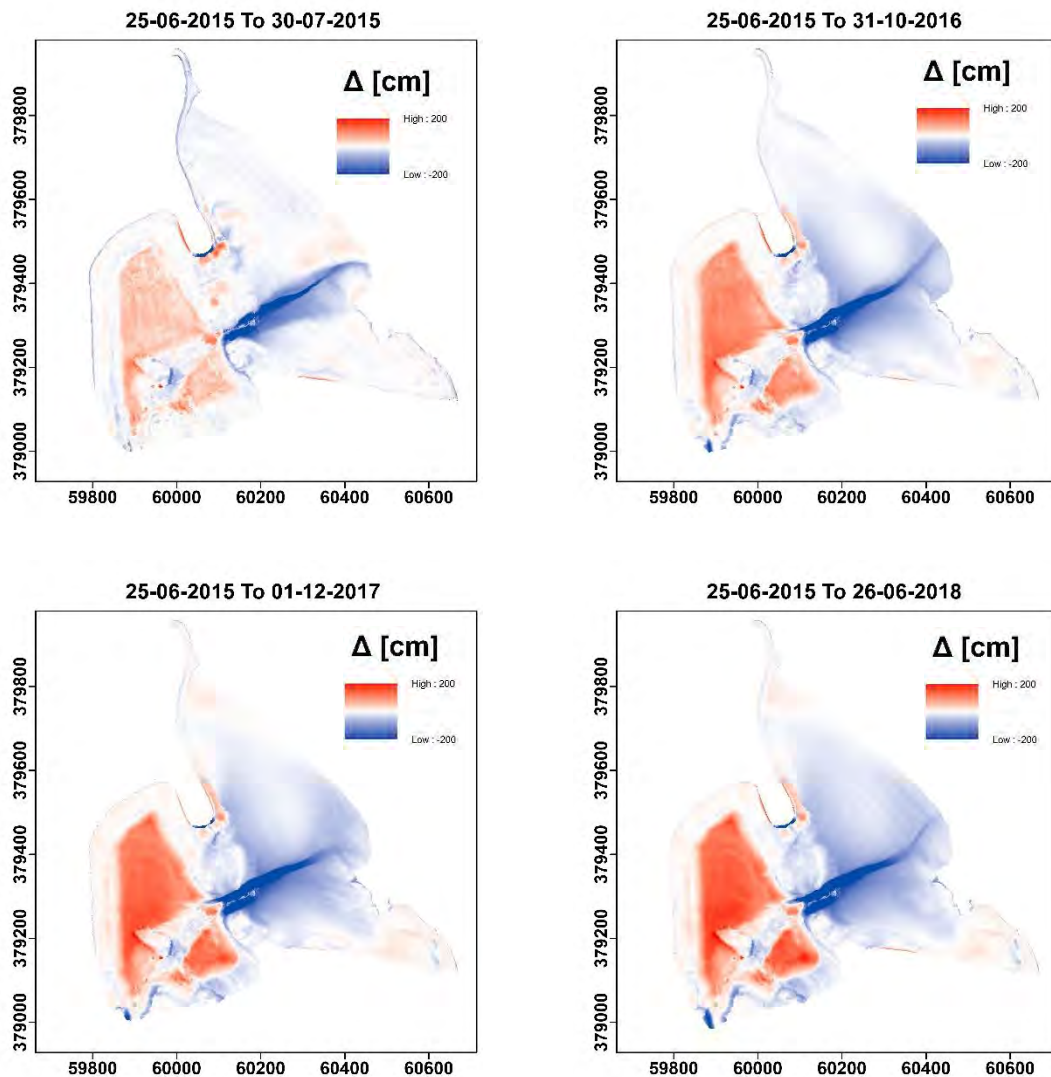


Figure 19. Sedimentation and erosion between T0 (May/June 2015) and T4 (19 April 2016).

Regarding to the pond, inlet and foreshore the maximum rate of accretion was found in the pond with an accretion rate of 0.2 cm.day^{-1} and the maximum erosion rate was found on the inlet with a magnitude of -0.4 cm.day^{-1} . On average the pond (area 2) was accreting with a magnitude of 0.05 cm.day^{-1} , the inlet (area 3) was eroding $-0.05 \text{ cm.day}^{-1}$ and the foreshore (area 4) was eroding with a magnitude of $-0.03 \text{ cm.day}^{-1}$.

2.3.2.4 TIDAL FLAT AND CREEKS

From the beginning it was clear that the main morphological changes, in the intertidal area of the basin, were taking place in the man-made creeks. The sedimentation, during the project, typically varied between 0 and 50 cm, although locally larger values were found. Sedimentation on the tidal flat is much more limited and ranged from 0 to 15 cm. In the northern part of the two main channels we observe that no sedimentation occurs and that the channels are getting wider and also deeper (see Figure 20). On the tidal flat area the maximum erosion rate was found in the channels, $91.3 \text{ cm.year}^{-1}$ and the maximum sedimentation rate was also found in the channels, $51.1 \text{ cm.year}^{-1}$. On average the tidal flat area was accreting with an accretion rate of 3.6 cm.year^{-1} . This last value also suggest that although some morphological changes were taking place in this area they are much less visible than the ones taking place on the foreshore and pond area, as the value is almost three times lower than the other two values, that is also clear from Figure 20.

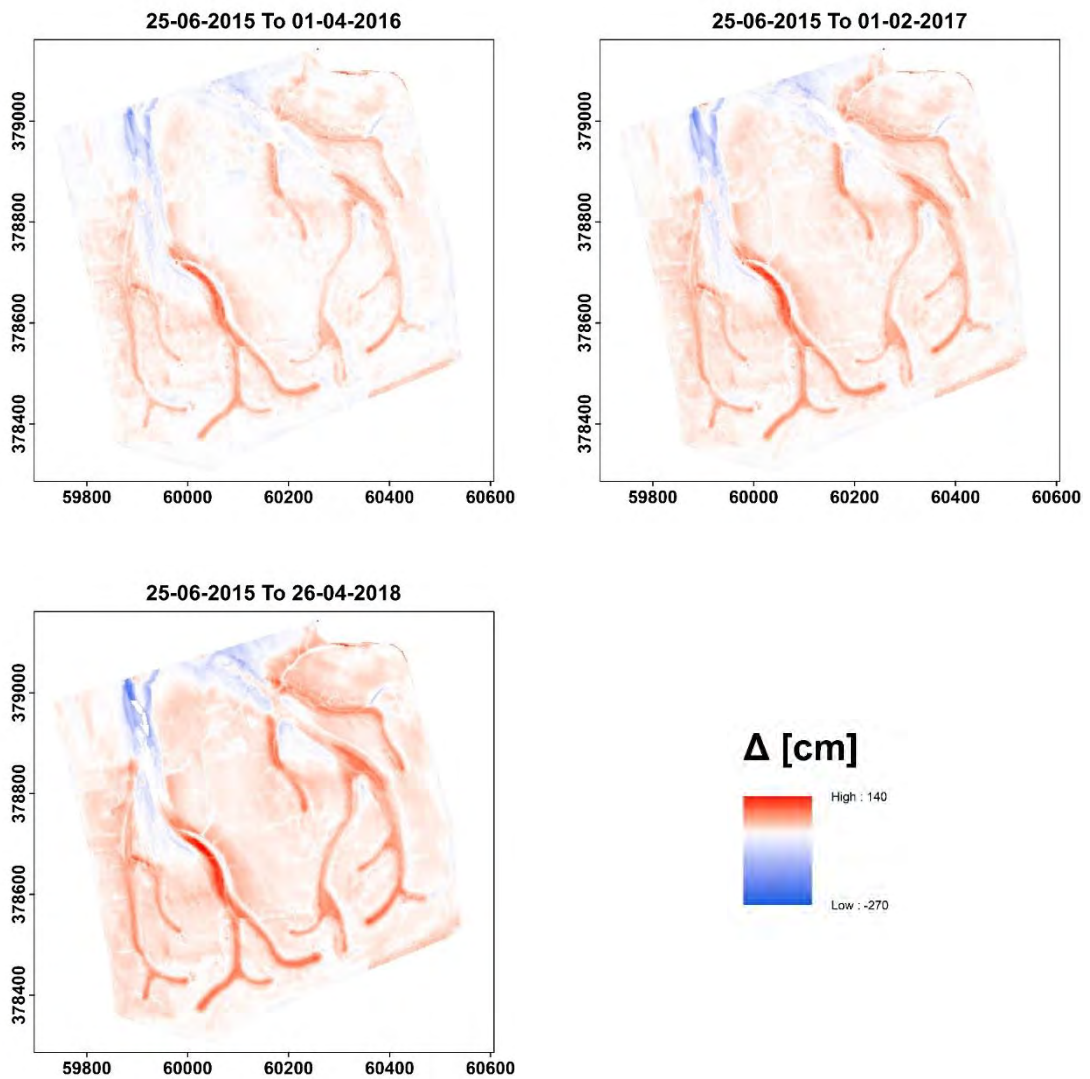


Figure 20. Sedimentation and erosion between T0 (May/June 2015) and T13a (26 April 2018). In red the values represent sedimentation and in blue the values represent erosion. It is clear that the main morphological changes are taking place in the channels which are accreting at the end of the flat and eroding in the transition between the flat and the pond area.



Figure 21. Locations of cross-sections.

To better understand the development of the man-made channels the morphological changes along 6 cross sections of these creeks were also measured, besides the cross sections along the whole basin (Figure 22). The cross-sections show a generally strong sedimentation at the deeper parts of the creeks. Cross-sections closer to the pond demonstrate less sedimentation and more erosion.

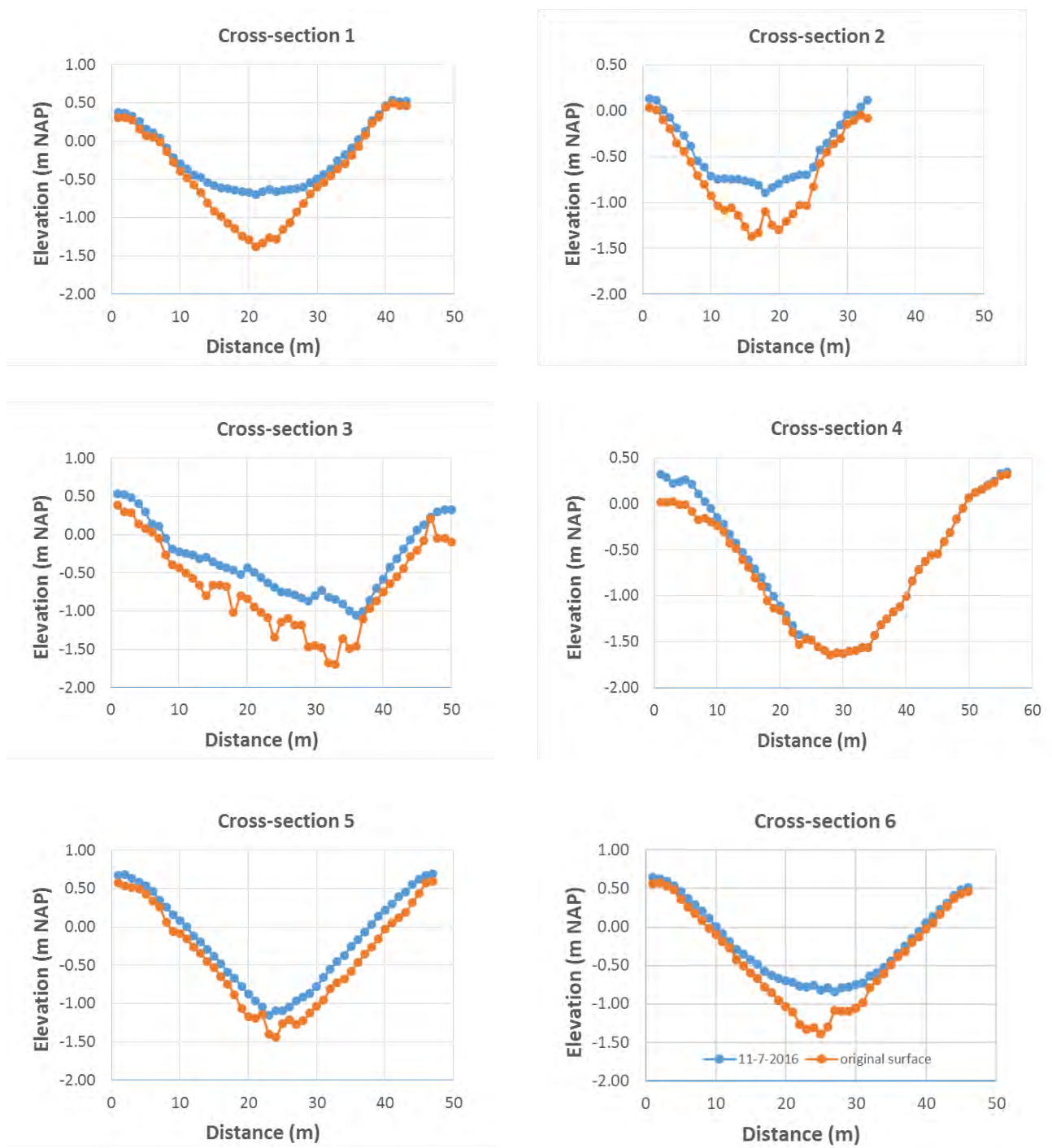
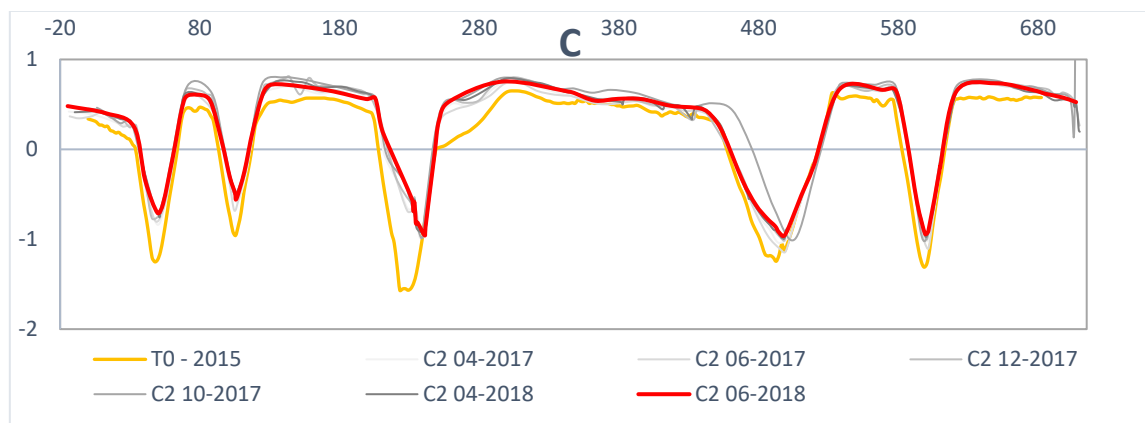
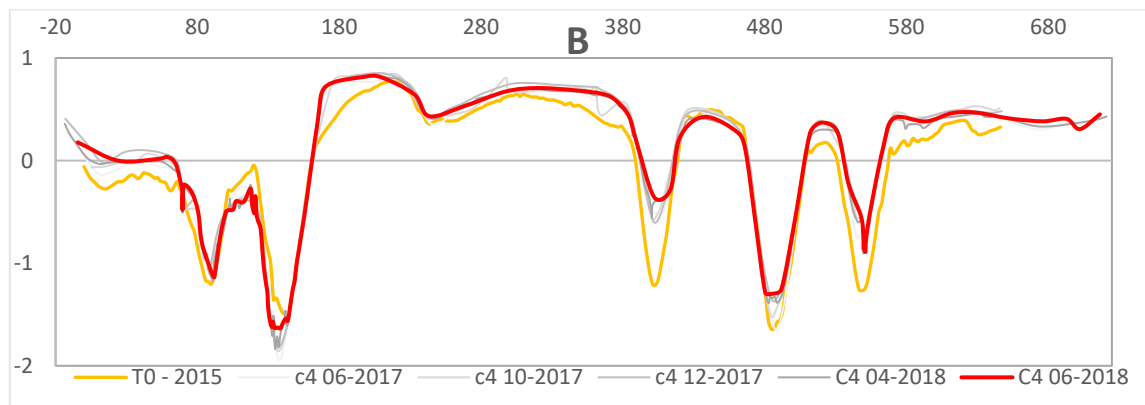
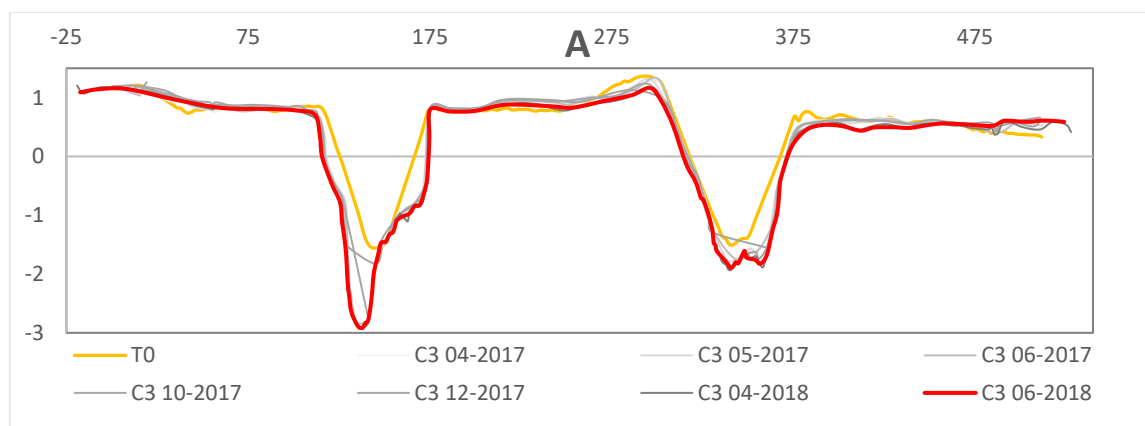


Figure 22. Cross-section over creeks in the tidal flat area, the original surface in orange, the measured surface in July 2016 in blue.

In 2017 and 2018 several cross sections (see Figure 23) were made over 4 locations to analyse the geomorphological characteristics of the creeks but also of the tidal flat. Below, in Figure 23), it is possible to

observe the bed level, represented by the height measured with the DGPS, and the original level. Though accretion is clear, in C1 and C2, it seems higher in the channels than the flat. Cross sections C3 and C4 do not register substantial accretion on the flats and in the channels erosion is visible. From this analysis it is possible to conclude that the cross-section of the man-made creeks were oversized at the end of the creeks and undersized at the beginning of it. Due to this the channels are accreting at the end and eroding in the beginning. These trends are still observed on the last measurements suggesting that the processes are still ongoing.



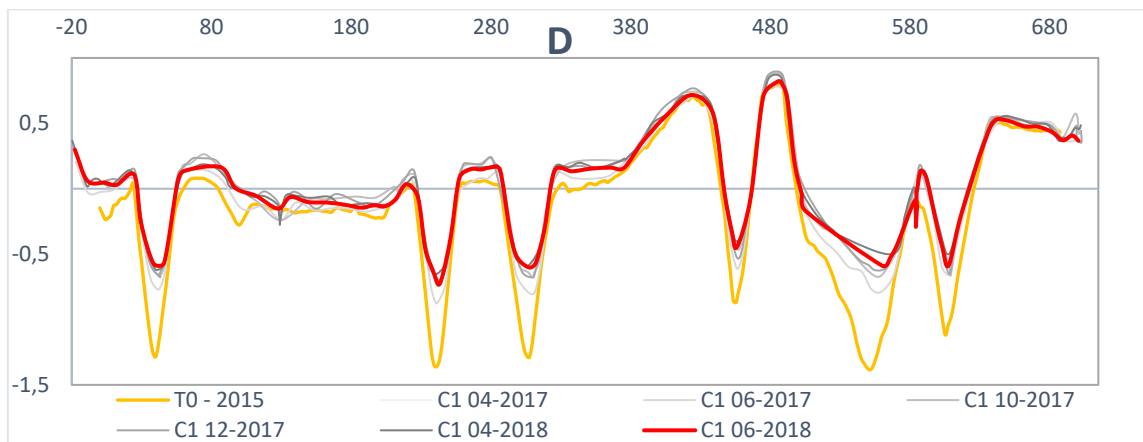


Figure 23. Cross-section over tidal flat area, the original surface is represented in orange, the blue line indicates the measured surface in April 2016 and the green line the measured surface in June 2017.

During the measurements of the mentioned cross sections, sediment samples were also collected and analysed. Figure 24 presents the results regarding sediment characteristics found in the samples. The granulometric classes in which the sediment samples fall are sand, silty sand, sandy silt and clayey silt. Overall, the coarser sediment, characterized by sand, is mainly present at the beginning of the tidal flat (Northern area) whereas the southern part is mainly characterized by clayey silt. Observing the sediment distribution map (Figure 25), it is possible to note that the coarser sediment lies next to the channels area and decreasing, of course, to the inner part; in particular, the coarser sediment is located in the principal tidal creeks. This distribution was expected, because the sediment transport depends on the hydrodynamic energy: the channels are marked by higher energy, so they allow to transport the coarse sediment, while the other parts of the tidal flat are characterized by less energy so only the fine sediment can settle on the distant areas. The sediment granulometric distribution map, Figure 25, is developed by 4 cross sections that, of course, cannot represent perfectly the entire tidal flat, but, relying on it, the area defined by higher energy is the West part, in particular at the beginning of the principal tidal creek, see Brunetta (2017) for more information.

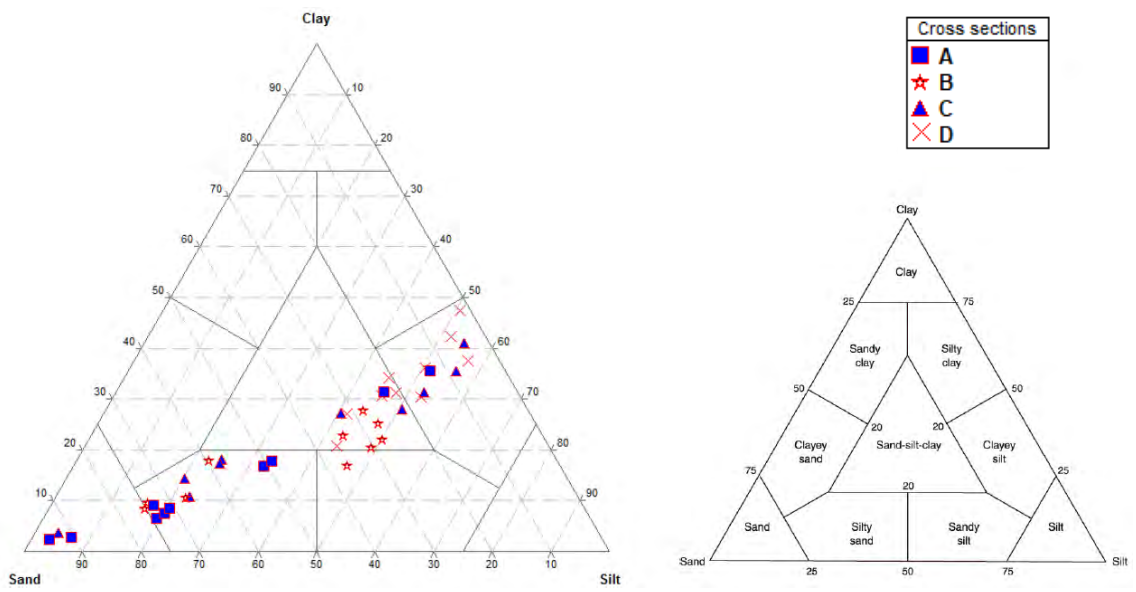


Figure 24. Shepard's diagram showing the sediment samples in granulometric classes.

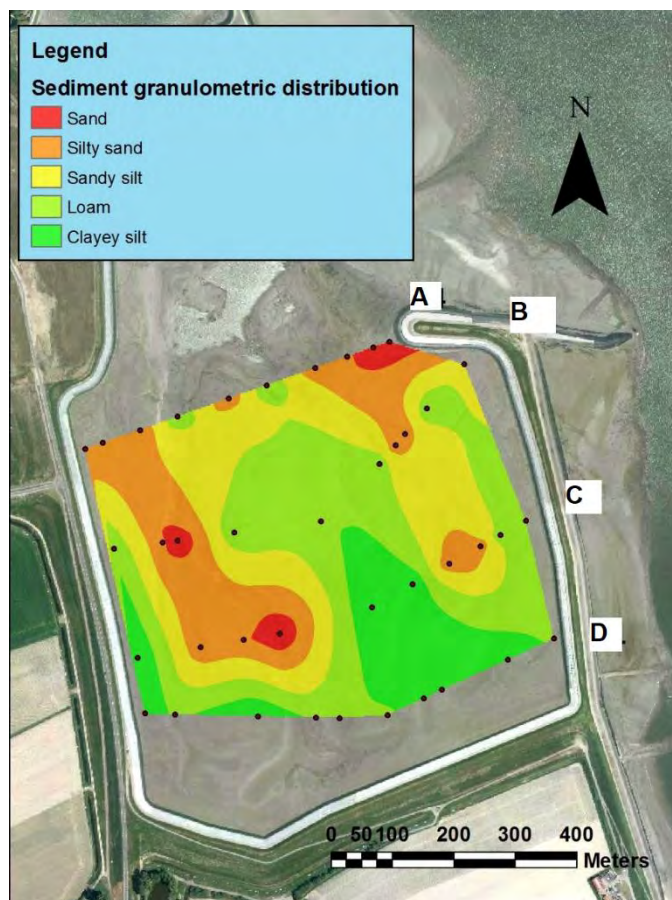


Figure 25. Sediment distribution map of Perkpolder.

2.3.3 DELFT3D MODELLING

2.3.3.1 MODEL SET-UP

A depth-averaged (2DH) Delft3D model was set-up to simulate hydrodynamics, sediment dynamics and morphodynamics under tidal influence. Figure 26 shows the model domain; the grid resolution is ~ 20 m x 20 m. The model can be used to increase the understanding of the development of the Perkpolder area, and to evaluate the design. More information of the Delft3D model can be found in Zhao (2016).



Figure 26. Domain Perkpolder Delft3D model.

The hydrodynamic boundary conditions were obtained from the Delft3D-NeVla model (Vroom et al., 2015) and the mud concentration boundary conditions from the LTV – slib model (Van Kessel et al., 2011). The model considers 1 sand fraction with a median diameter $D_{50} = 0.15$ mm and a dry bed density of 1600 kg/m^3 and 1 mud fraction with a settling velocity $w_s = 1$ mm/s and a dry bed density of 500 kg/m^3 . The model distinguishes between a relatively fast-responding muddy (fluff) layer on top of fully-mixed sediment bed layer consisting of sand and mud.

2.3.3.2 MODEL CALIBRATION AND VALIDATION

The model reproduces the inlet velocities reasonably well with a correlation coefficient, R^2 , between 0.36 and 0.77 and a bias between 0.01 and 0.06 m/s for the six measurement locations. As an example, Figure 27 compares the measured and computed velocities at location MP0102.

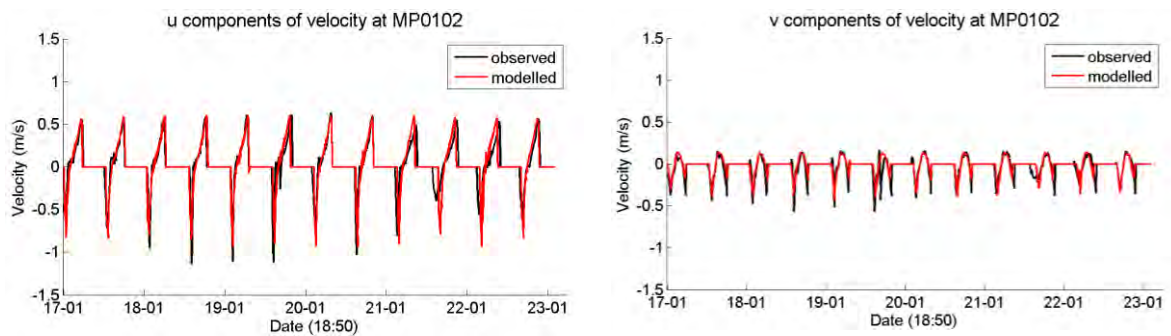


Figure 27. Comparison of measured and computed velocities at location MP0102. u = velocities normal to the inlet (inflow is positive), v = velocities parallel to the inlet (positive is toward the Northwest).

Following this, the settings of the sediment model were calibrated in order to reproduce the net sediment influx. Finally, we compared the measured and computed bed level changes. Figure 28 shows that the general sedimentation patterns are reproduced by the model (the observed sedimentation patterns are shown in Figure 15). The model resolution is too low to reproduce erosions/sedimentation in the creeks, but it shows the measured accretion in the pond and in the higher areas.

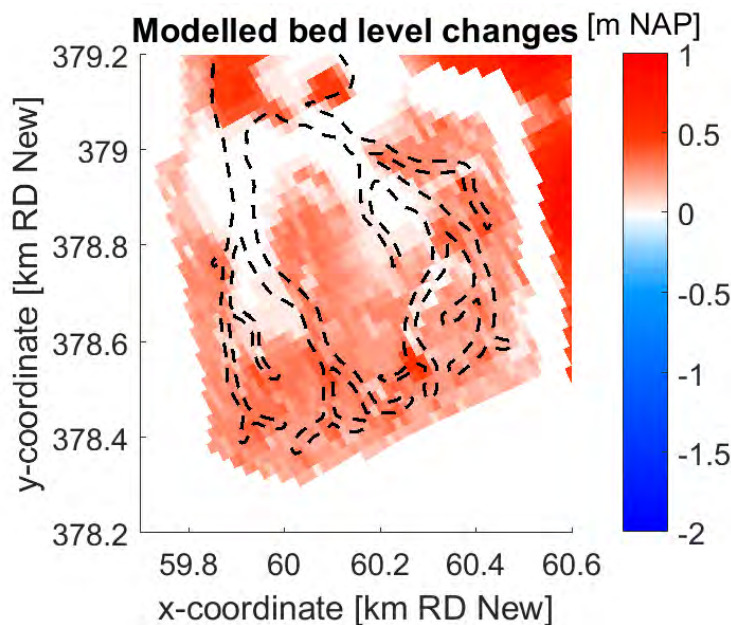


Figure 28. Computed sedimentation in Perkpolder after half a year. (Unit should be [m] instead of [m NAP].)

2.3.3.3 MODEL APPLICATION

We used the Delft3D model in order to better understand the processes that drive the morphological development of Perkpolder. Subsequently, the model was used to study the effect of the inlet width, the creeks and the pond. Figure 29 shows that a 50% reduction of creeks and pond depth leads to a small

reduction of the modelled Perkpolder sedimentation. No creeks and pond results in a very different pattern. It also reduces the total sedimentation, as the net sediment influx is smaller due to the smaller tidal prism. A 50% change in inlet width only seriously affects sedimentation and erosion around the inlet (Figure 30).

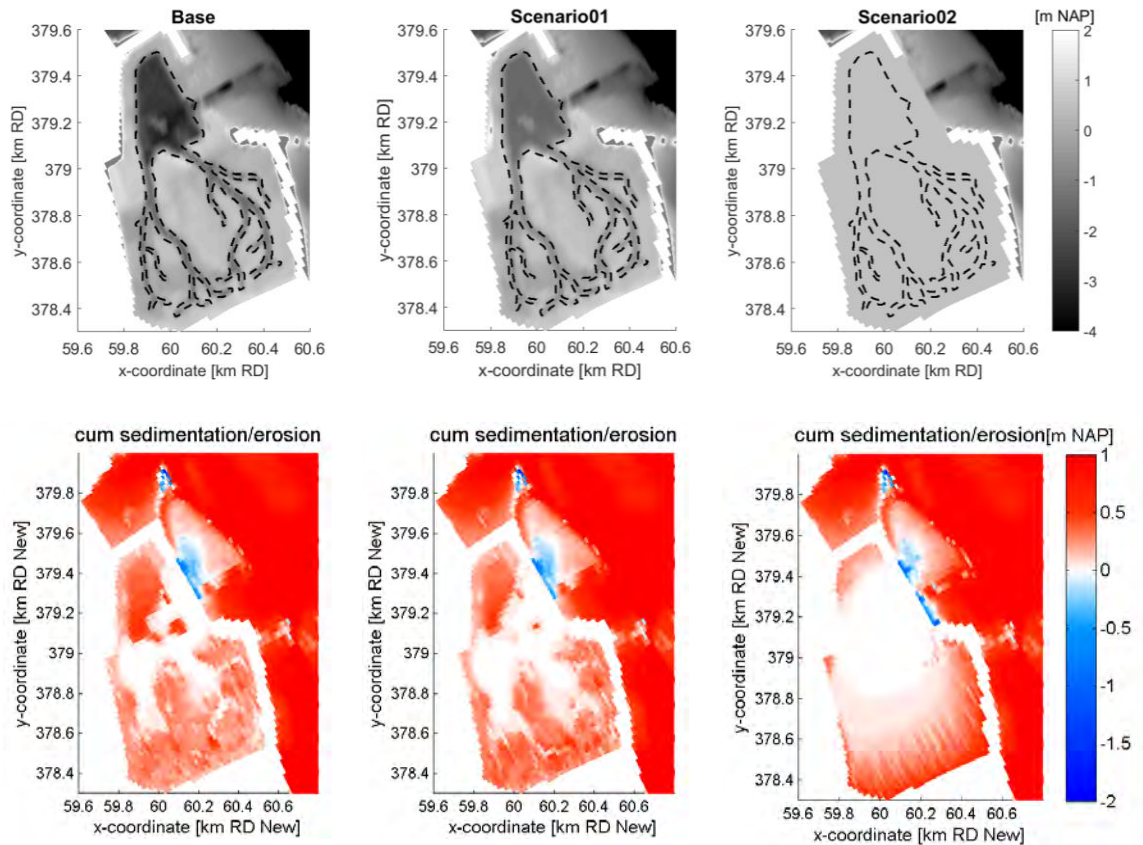


Figure 29. Effect of depth reduction pond and creeks with 50% (Scenario 1) and 100% (Scenario 2) on the computed morphological change after 0.5 year.

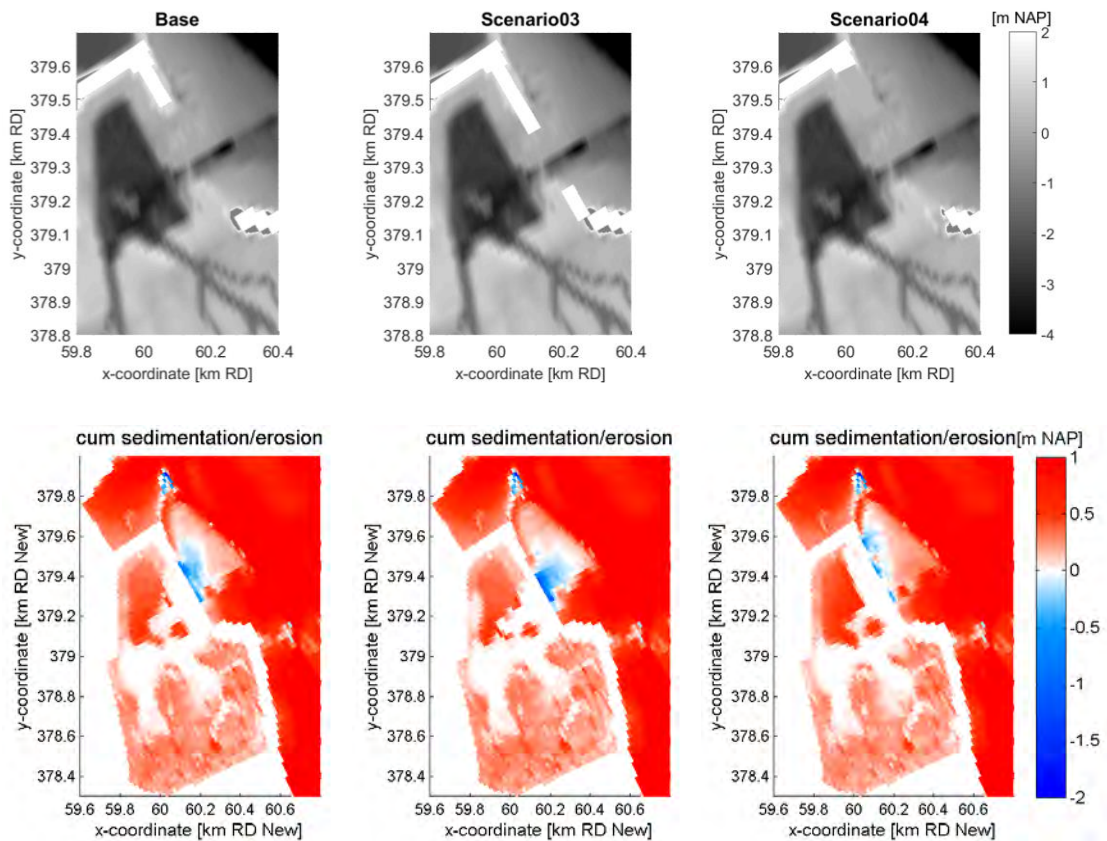


Figure 30. Effect of changing the inlet width on the computed morphological change after 0.5 year. Scenario 3: 50% decrease, Scenario 4: 50% increase.

2.3.4 SEDIMENT BALANCE IN THE BASIN AND FORESHORE AREAS

To better understand the morphological changes taking place in the basin and in the vicinity of it a sediment balance was done. On this sediment balance four main areas were considered the tidal flat in the basin (area 1) the pond (area 2), the inlet (area 3) and the foreshore (area 4), see Figure 31.

From the sediment balance analysis between 2015 and 2018 (Table 5) we can conclude that there is a sediment import of approximately 158 k m^3 in the Perkpolder basin (areas 1 and 2), from which 88 k m^3 are deposited at the pond and the remaining in the tidal flat area. The foreshore area and inlet area (area 3 and 4) are mainly characterized by erosion which amounts to a total of approximately 99 k m^3 . And, this volume can be explained partly by the creation of the inlet of the basin.

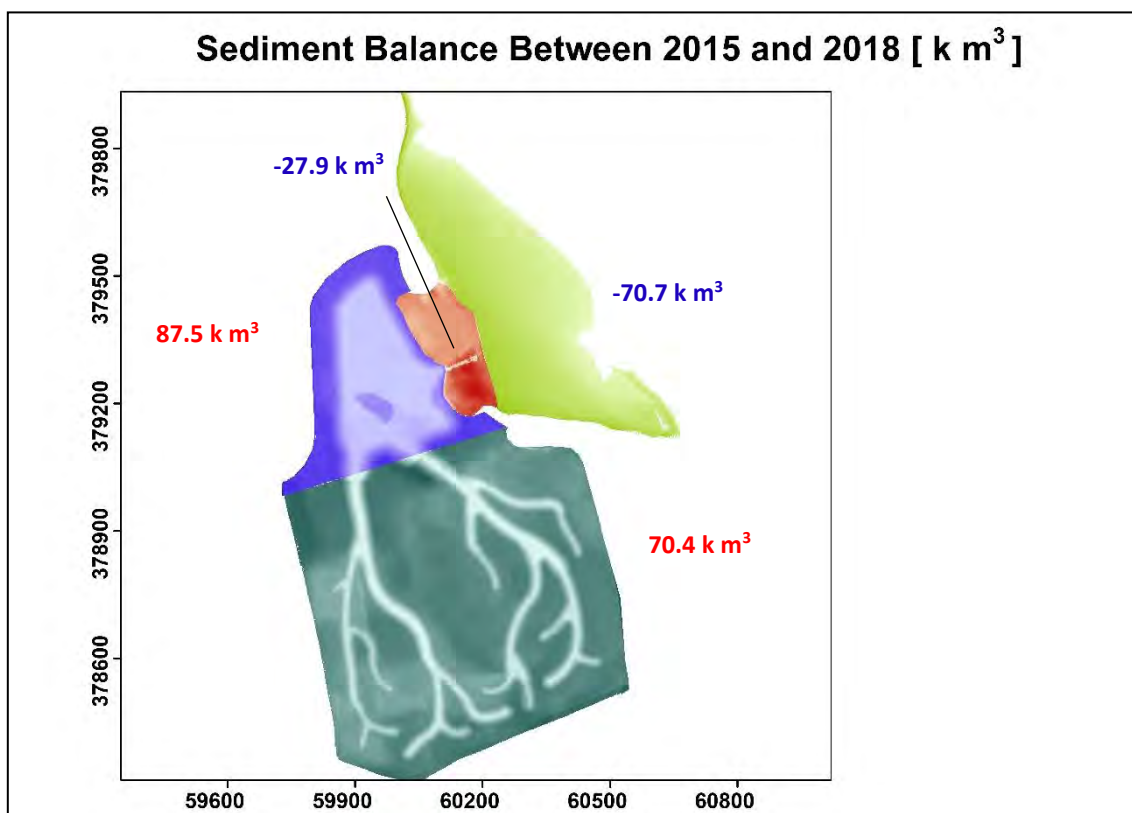


Figure 31. Sediment balance between the duration of the project. The blue numbers correspond to areas that have lost sediment (inlet and outer area); the red numbers correspond to areas that have gained sediment (basin and pond).

Table 5. Sediment balance in the Perkpolder basin and its foreshore between 2015 and 2018.

Area	2015-2016 [k m ³]	2016-2017 [k m ³]	2017-2018 [k m ³]	2015-2018 [k m ³]	2015-2018 [k m ³ /year]
Intertidal area (1)	+27	+26	+17	+70	+23
Pond (2)	+57	+14	+17	+88	+29
Inlet (3)	-20	-6	-2	-28	-9
Foreshore (4)	-51	-15	-5	-71	-24
Total Perkpolder (areas 1 + 2)	+84	+40	+34	+158	+53
Total outer area (areas 3+4)	-71	-21	-7	-99	-33

From Table 5 we can observe that the sediment import on the tidal flat, area 1, is quite constant over the years. It is also the case if we consider the whole Perkpolder area (area 1 and 2) after the first year. The sedimentation in the pond reduces to less than half, after the first year. The inlet and foreshore have a first

adjustment period with large changes. After this period, which corresponded to the first year, the values are greatly reduced and in 2018 are already quite low (10% of the initial values).

The volume analysis also provides insights in the origin of the imported sediment. Areas 3 and 4 (inlet and foreshore area in front of Perkpolder) faced severe erosion over the past years. The inlet and foreshore together eroded 71 k m³ in 2016. This is similar to the total amount of sediment imported to the basin (84 k m³), but the differences in material (sand vs. mud) indicate that foreshore material did not end up in Perkpolder but in the main channel. However in 2017 and 2018, the total erosion in these areas reduced to 21 k m³ and 7 k m³ respectively, which is substantially smaller than the total sediment import into Perkpolder for those years (40 k m³ and 34 k m³). Various explanations can be provided.

1. The intertidal area neighboring Area 4 was an additional sediment source. However, this is not likely to close the sediment balance, as Figure 19 already indicates that the erosion (blue colours) of this intertidal area is very limited.
2. Western Scheldt. The nearby zone of the channel is an unlikely source, as it faced actually sedimentation (red in Figure 19). In contrast, the washload in the water column, present naturally in the channels (~0.05 g/L) can be substantial. Even though the concentrations in the washload are an order less than the concentrations measured locally in the mouth (mainly locally suspended sediment), the washload could be a substantial source of sediment with the large volumes of water entering Perkpolder every tide.
3. Differences in dry bed density (porosity). This is not a source but could also explain the mismatch in volumes. Due to lower dry bed density of freshly settled mud, a volume of sediment eroded in the mouth or delta could result in a larger volume of sediment accreted within Perkpolder. Over time this difference in porosity will reduce due to consolidation. However, it is not likely that this fully explains the difference between sedimentation and accretion, because the agreement was good in 2016.
4. Measurement uncertainties. The Perkpolder has an area of ~70 ha so a bed level error of 1 cm corresponds to 7 k m³.

2.3.5 *COMPARISON OF HYSOMETRY WITH OTHER TIDAL BASINS*

The aim of this section is to better understand how does the Perkpolder basin compared with other basins located in the vicinity of it. This was done to understand the development status of it and also to understand how it can look like in the future. Figure 32 shows five tidal basins in the vicinity of Perkpolder, with some of them not yet open (Hertogin Hedwigepolder and Waterdunen). The basins vary in size and tidal range. The calculated percentages of channels, tidal flats, and salt marshes are based on the definition that was mentioned earlier, and presented in Table 6.

Based on the LiDAR data of the different areas, hypsometric curves are calculated (Figure 33. Hypsometric curves of the tidal basins: Perkpolder (A), Saeftinghe (B), Sieperdaschor (C), Hertogin Hedwigepolder (D), Waterdunen (F), and Rammegors (D). On the y-axis the height, on the horizontal axis the ratio a/A , where 'a' is the area below a given elevation contour, and 'A' is the total basin area.), and for Perkpolder tidal basin the T0 data is used (Figure 13. T0 bathymetry (May/June 2015) in the basin and the division of the areas. Area 1 represents the tidal flat and the artificial creeks in the basin. Area 2 is the pond area, area 3 is the inlet and area 4 is the foreshore just in front of the Perkpolder basin.). Hypsometric curves show the distribution of basin surface area with height. The y-axis represent the height or surface elevation, the x-axis shows the fractional area below a given elevation contour, a/A (Boon & Byrne, 1981), where 'a' is the area below a given elevation, and 'A' is the total basin area.

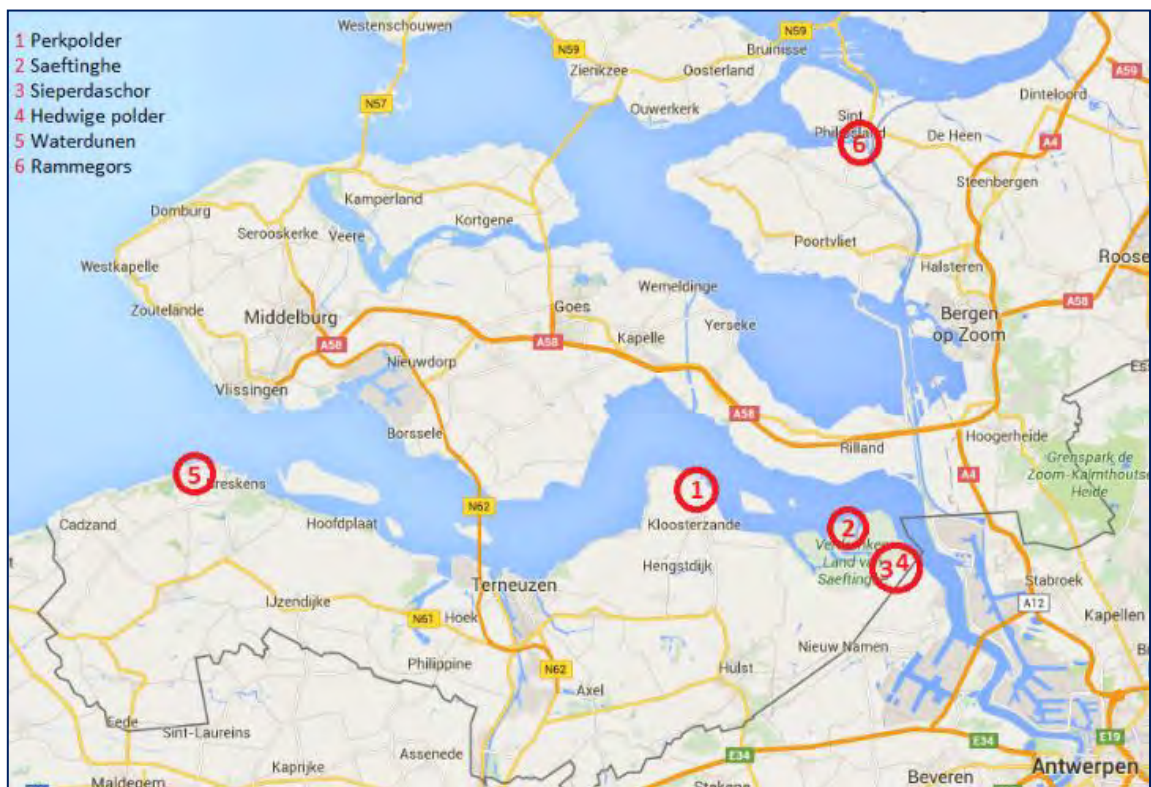


Figure 32. Tidal basins part of de-poldering projects around Eastern and Western Scheldt.

Table 6. Tidal basins, with tidal range, and distribution of channels, flats and marshes (values indicated with * are predictions other values are based on 'Waternormalen' from Rijkswaterstaat). Basins in italics are not yet open.

Tidal basin	Total area (ha)	MLW (m NAP)	MHW (m NAP)	Channel (%)	Tidal flat (%)	Salt march (%)
Perkpolder	75	-2.06	2.56	11	88	1
Saeftinghe	2800	-2.11	2.72	1	47	52
Sieperdaschor	100	-2.11	2.72	0.5	32	67.5
<i>Hedwigepolder</i>	295	-2.22*	2.82*	0	99	1
<i>Waterdunen</i>	250	-0.55*	0.55*	17	20	63
Rammegors	142	-0.20*	1.40*	4.5	72	23.5

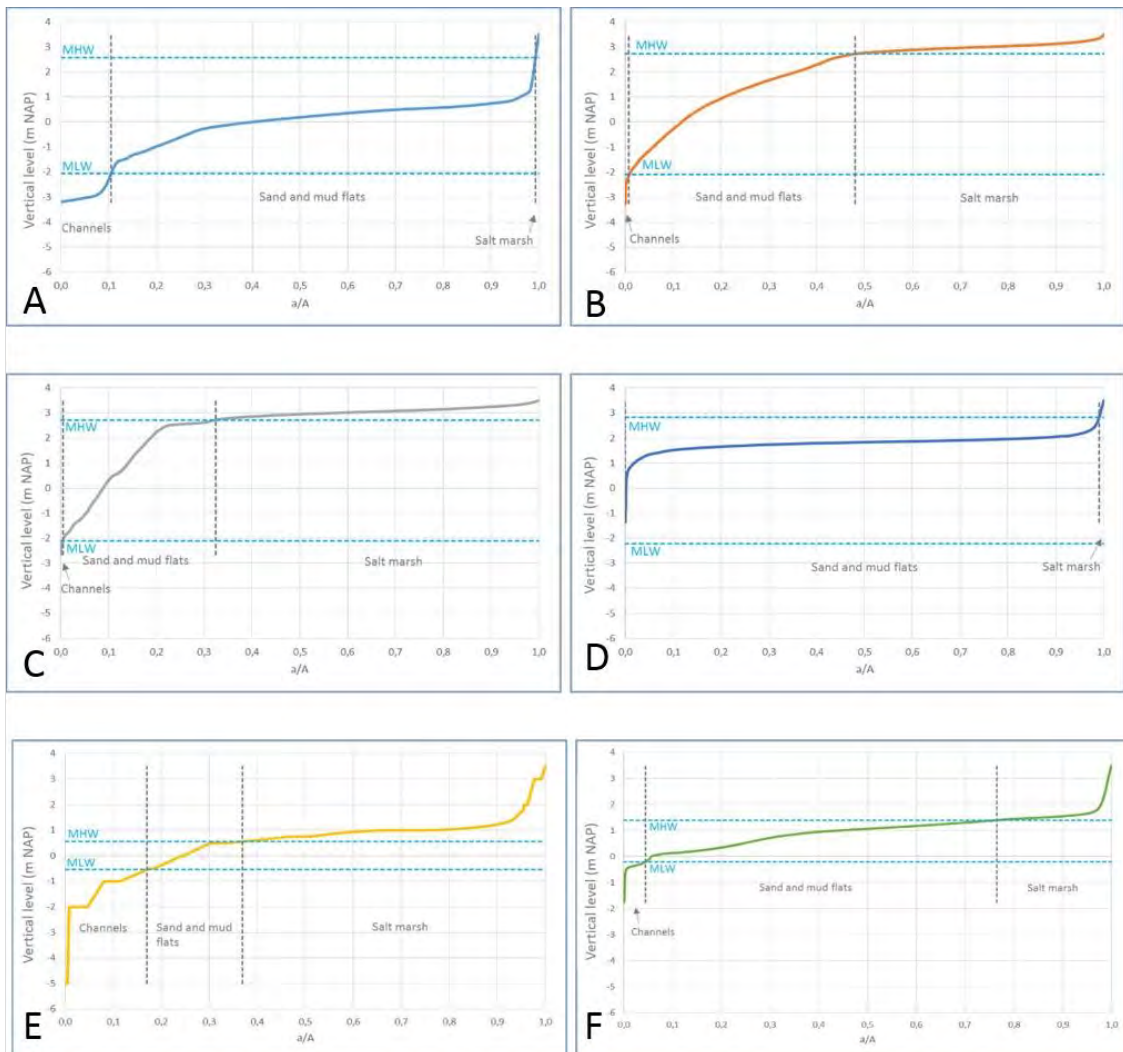


Figure 33. Hypsometric curves of the tidal basins: Perkpolder (A), Saeftinghe (B), Sieperdaschor (C), Hertogin Hedwigepolder (D), Waterdunen (F), and Rammegors (D). On the y-axis the height, on the horizontal axis the ratio a/A , where 'a' is the area below a given elevation contour, and "A" is the total basin area.

The hypsometric curves are used to calculate the percentage of channels, tidal flats and salt marshes (Figure 33). The high percentage of salt marshes is seen in Saeftinghe (52%), Waterdunen (63%) and Sieperdaschor (67.5%), is an indication of a mature tidal basin. On the other hand high coverage of tidal flats is an indication of relatively young basins, e.g. Perkpolder (88%) and Hedwigepolder (99% when opened).

In Figure 33 the hypsometric curves of the six tidal basins are shown including the MLW and MHW water levels. Rammegors and Waterdunen have a human-induced tempered tide as the tidal range is much lower and artificially regulated. Saeftinghe and Sieperdaschor are regarded as reference basins for Perkpolder as both basins have already salt marshes present and it is hypothesised that this will be also the case of Perkpolder in the future. Therefore for Saeftinghe and Sieperdaschor can be considered that they are at a later stage of the succession (from young to mature). At the same time it is clear from Figure 33 that Perkpolder tidal basin will go through great morphological changes if sediment import will not be a limiting factor. One of the reasons for these changes to be much more significant than the expected morphological changes at the Hertogin and Hedwigepolder are the year of the construction of the embankments (poldering), which was much earlier in Perkpolder (1210 AD) than in Hertogin Hedwigepolder at the beginning of last century (1907) therefore subsidence is expected to have a higher effect on the bed level.

2.4 DISCUSSION

There are some uncertainties on the sediment import estimated from the OBS data. First, only a single measurement point is considered as representative for the full cross-sectional area (both over the vertical as along the cross-section). Second, the OBS emerged part of the tidal cycle, which implies a closed sediment balance over the tidal period cannot be made. Furthermore, near bed concentrations are not measured by the OBS, due to the distance between the instrument and the bottom. These limitations affect the total estimates of the sediment import, but have less effect on the temporal variations in sediment import.

The sediment balance for Perkpolder cannot be closed yet. Despite similar in magnitude to the deposited volume in Perkpolder, the sediment eroded outside Perkpolder in the foreshore area is mainly deposited in the deeper channel and is not transported into Perkpolder. The eroded material of the foreshore mainly consists of sand while the deposited material primarily consists of mud. Part of the mismatch between the erosion volumes and the accretion volumes is also explained by the differences in porosity between freshly accreted mud and the porosity of well consolidated sediment prior to erosion. Adding to this, the sediment accretion on the tidal flat is mainly characterized by very fine sediment. Therefore, the sediment that accreted on the tidal flats is expected not (only) to originate from areas 3 and 4 (probably with the exception of the fines that were washed out from these areas).

Looking to the time series derived from the OBS, there are strong temporal fluctuations visible in the net import rates of sediment. A direct comparison between the net fluxes and the high water level, peak discharge and the wind speed did not show strong relations. This does not imply these variables are not important. The relations with these variables are probably more complex. Still, lower high water levels and lower peak discharges appear to be in favour of more positive trapping efficiencies. It is shown it is not necessarily the quantity of water or the magnitude of the sediment concentration being the main driver of the net import or export of sediment. Especially the temporal fluctuation of the sediment concentration within each individual tide is crucial (i.e., the trapping efficiency of each tide). We do not understand yet what is causing this temporal variation in suspended sediment concentrations.

Finally, it is important to mention that the development of the inlet may be constrained by the consolidated clay layer that exists under to old dike footprint. This appears from the very limited erosion for large parts of the cross-section in Figure 17. This clay layer may have limited the lateral expansion of the cross-section of the inlet, as well as the movement of the inlet to other positions.

2.5 CONCLUSIONS

The main conclusions about the morphological development of the Perkpolder basin are the following:

- There is a gradient in grain sizes deposited on the tidal flat. This gradient also relates to the sedimentation and erosion patterns observed in the tidal flat. Coarser grain size deposition was observed at the edges of the tidal flat and in the channels, while finer sediment was mainly observed on the top of the tidal flat and at the highest parts of the tidal flat near the dikes which coincides with the less energetic zones.
- The morphological development of the basin and its nearby areas slowed down in time. Regarding the inlet, the main changes took place within the first month after the opening of it. The pond and the tidal flat areas were mainly accreting and the inlet and the foreshore area were mainly eroding, due to the channel formation. The man-made creeks were filling up at the end (southern part of the basin) and eroding at the beginning (northern part of the basin) of the tidal flat. Since the initial cross section was the same trough out the creeks, they were oversized at the southern part of the basin and undersized at the northern part of the basin, on the transition between the pond and the tidal flat.
- Regarding the design it is also important to mention the role of the pond area and the channels. The pond area, due to its volume, may have induced a delay on the accretion of the higher areas as it acted as a sink for sediment. Regarding the channels besides the adjustments that took place (mainly on the cross section area in the beginning and end) the location of them did not change much suggesting a good initial condition otherwise bigger disturbances were expected to take place, e.g. channel migration.

- The sediment import into Perkpolder was estimated based on OBS concentration data and discharges estimates for the period between September 2016 and March 2017. The sediment import varied strongly in time, and sediment was also being exported for a number of tides. Over the 5 months of measurement data, the estimated net import was 13-16 kilotons or 5-6 k m³ sediment excluding porosity. This corresponded to 34-40 kilotons/year, which is good agreement with the 16-48 kilotons/year estimated from the bed level development between 2016 and 2017.
- A 2DH Delft3D model was set up to simulate hydrodynamics, sediment dynamics and morphodynamics due to tidal forcing. The model reproduces the measured velocities and the inlet reasonably well, and was further calibrated on the estimated net sediment influx and the morphological changes between June 2015 and April 2016. Thereafter, the model was used to better understand how the new intertidal area develops. It was shown that a 50% volume reduction of creeks and pond hardly affects the sedimentation, which is also the case for a 50% change in inlet width. The latter does influence the more local sedimentation and erosion patterns, i.e. close to the inlet.

2.6 RECCOMENDATIONS

Several recommendations result for a possible further research on Perkpolder, which may also be used to improve the monitoring and understanding of future tidal restoration projects:

- The monitoring of the morphodynamics was considered adequate. However a better spatial/temporal coverage is suggested at least for the inlet in the first months since the majority of the changes took place during this period. It is also suggested to enlarge the foreshore area and to do a proper sediment characterization of it to better understand the contribution of this area to the morphological changes in the basin.
- The sediment import analysis can be improved by measuring concentrations for a new period, but now with a lower vertical position of the OBS. If placed as low as possible (NAP+0m), the flood and ebb flows are almost fully covered, which is now not the case, leaving a period of uncertainty for each tide. Furthermore, it could be valuable to have also data at another point in the cross-section or at another elevation, as now only a single point is thought to be representative for the full cross-section. With other instruments, also estimates on the bed load transport rates could be made, for example with acoustic instruments. It could also be possible to gain further insights on the grain size distribution in the water column (e.g., with a LISST or simply taking samples several moments during the tidal cycle).
- The observed strong temporal variations in the sediment exchange between Perkpolder and the Western Scheldt are not well understood. Especially, the fact that lower high water levels and lower peak discharges appear to favour more sediment trapping is intriguing and counter-intuitive. We recommend to set-up and validated a local model to be able to unravel these sediment dynamics,

which will provide value system knowledge applicable to other intertidal area development cases such as the Hedwigepolder.

- We recommend to further test and develop the Delft3D model to improve the understanding of the Perkpolder: i) model calibration using the measured suspended sediment concentrations, 2) improve model input using measured bed composition and density, 3) model validation using the spring 2016, 2017 and 2018 multibeam-LIDAR bed levels, 4) distinction between initial sedimentation mainly related to local erosion of the inlet, and the more long-term development related to the net sediment influx from outside, 5) further model explorations, e.g. effect of waves, initial bed composition and simulation period length.
- Continuing the bathymetry measurements, with LiDAR measurements or other kind of comparable measurements. This would give a better insight and strengthen our knowledge on the trends and conclusions mentioned so far;
- Another campaign of sediment samples would give more information regarding the sediment deposition and its characteristics providing also a better image regarding the sediment movement and exchange with the other areas. It would be very insightful to also know the sediment composition of the present-day inlet and the outer delta.

3 GRO(U)NDWATER

This chapter describes (1) the measured effects of the restoration of the tidal area on the groundwater system of the adjacent agricultural area, (2) the design, mechanism, control and effects of the mitigation measure SeepCat to protect a freshwater lens used by farmers. This chapter is in **DUTCH** since it was written with the purpose to inform the farmers and waterboard about the monitoring program and results and the effects of SeepCat. At the end of this chapter, an extended abstract in English is given which describes the monitoring network and program and the mitigation measure SeepCat. Since it was

3.1 INLEIDING

In het kader van de gebiedsontwikkeling Perkpolder is een getijdengebied ingericht in de Oostelijke Perkpolder waarbij de zeedijk binnenwaarts is verplaatst. Op 25 juni 2015 is de dijk doorgestoken en is het getijdegebied in werking getreden.

Het nieuwe getijdegebied heeft mogelijke effecten op het aangrenzende grondwatersysteem. Een verwachte toename van de stijghoogte in het eerste watervoerende pakket heeft mogelijk voor het aangrenzende gebied tot gevolg (1) toenemende zoute kwel, (2) hogere grondwaterstanden en (3) afnemende zoetwaterbel voor het achterliggende landbouwgebied.

Om mogelijke effecten te kunnen vastleggen, is een nulmeting (T0-meting) uitgevoerd die gestart is in maart 2011. Het doel van deze T0-meting is het in beeld brengen van het grondwatersysteem vóór de ontwikkeling van het getijdegebied voor wat betreft de (1) dieptes van zoet, brak en zout grondwater, (2) stijghoogten en (3) freatische grondwaterstanden. De meetresultaten tot december 2013 (ruim 2.5 jaar aan metingen) zijn gerapporteerd in Buma (2014). De metingen vanaf begin 2014 tot de dijkdoorbraak kunnen tevens tot de T0-meting worden gerekend.

Op basis van de nulmeting en verschillende berekeningen en analyses is geconcludeerd dat ter bescherming van de zoetwaterbel van Kloosterzande een kwelvoorziening nodig is. Deze zoetwaterbel is van belang voor de landbouw. De boeren onttrekken er grondwater uit voor beregening van hun gewassen in droge perioden. Door de ontwikkeling van het getijdegebied is deze zoetwaterbel dichtbij de nieuwe zeedijk komen te liggen en daardoor kwetsbaar geworden voor verzilting. De kwelvoorziening, ook wel SeepCat genaamd, is in 2015 geïnstalleerd. Monitoring is nodig voor een optimale aansturing van de kwelvoorziening, de werking van de kwelvoorziening in de gaten te houden en om effecten te kunnen volgen (eventueel negatieve effecten op tijd te signaleren). De monitoringactiviteiten die hiervoor nodig zijn, zijn beschreven in het monitoringprotocol (De Louw, 2014a) en benodigde aanvullende meetpunten en meetactiviteiten zijn in 2015 uitgevoerd. In De Louw e.a. (2016) zijn de meetresultaten van de meetjaren 2014 en 2015 besproken.

In deze rapportage komen aan bod:

- de monitoringresultaten tot december 2018
- de werking en gewenste sturing van de kwelvoorziening.
- monitoringplan + handvaten uitvoering en analyse metingen voor de komende jaren
- resultaten van grondwatermodellering waarmee de lang termijn effecten op de zoetwaterlens zijn bepaald.

Het waterschap Scheldestromen neemt het beheer van de kwelvoorziening en bijbehorende monitoring begin 2019 van Rijkswaterstaat over. Deze rapportage biedt informatie over het meetnet, de kwelvoorziening en handvaten voor beheer en gebruik van de kwelvoorziening en uitvoering en analyse van de metingen.

3.2 DE KWELVOORZIENING

3.2.1 DOEL EN WERKING VAN DE KWELVOORZIENING

Er wordt verwacht dat de stijghoogte in het eerste watervoerende pakket zal toenemen door de ontwikkeling van het nieuwe getijdegebied met als gevolg toenemende zoute kwel en mogelijk afnemende zoetwaterbel voor het achterliggende landbouwgebied. Uit deze zoetwaterbel in de kreekruig van Kloosterzande wordt in droge tijden zoet grondwater onttrokken voor beregening van landbouwpercelen. Uit onderzoek van Witteveen+Bos (2010) en Royal Haskoning (2012) is geconcludeerd dat een kwelvoorziening nodig is als mitigerende maatregel ter bescherming van de zoetwaterbel. In 2014 is een beknopte second opinion uitgevoerd op het voorgestelde ontwerp van de kwelvoorziening en in overleg met het waterschap Scheldestromen, DLG en aannemer Van Oord is het ontwerp van de kwelvoorziening aangepast (De Louw, 2014b). Het type kwelvoorziening is in de loop van de tijd steeds aangepast. In de beginfase zijn zandpalen voorgesteld, gevolgd door verticale kwelbuizen en daarna een horizontale diepdrain. Gedurende de uitvoering van de second opinion is het type kwelvoorziening weer veranderd van horizontale diepdrain naar verticale kwelbuizen dat daarmee zijn definitieve vorm kreeg. Deze verandering en de argumenten zijn besproken in De Louw (2014b).

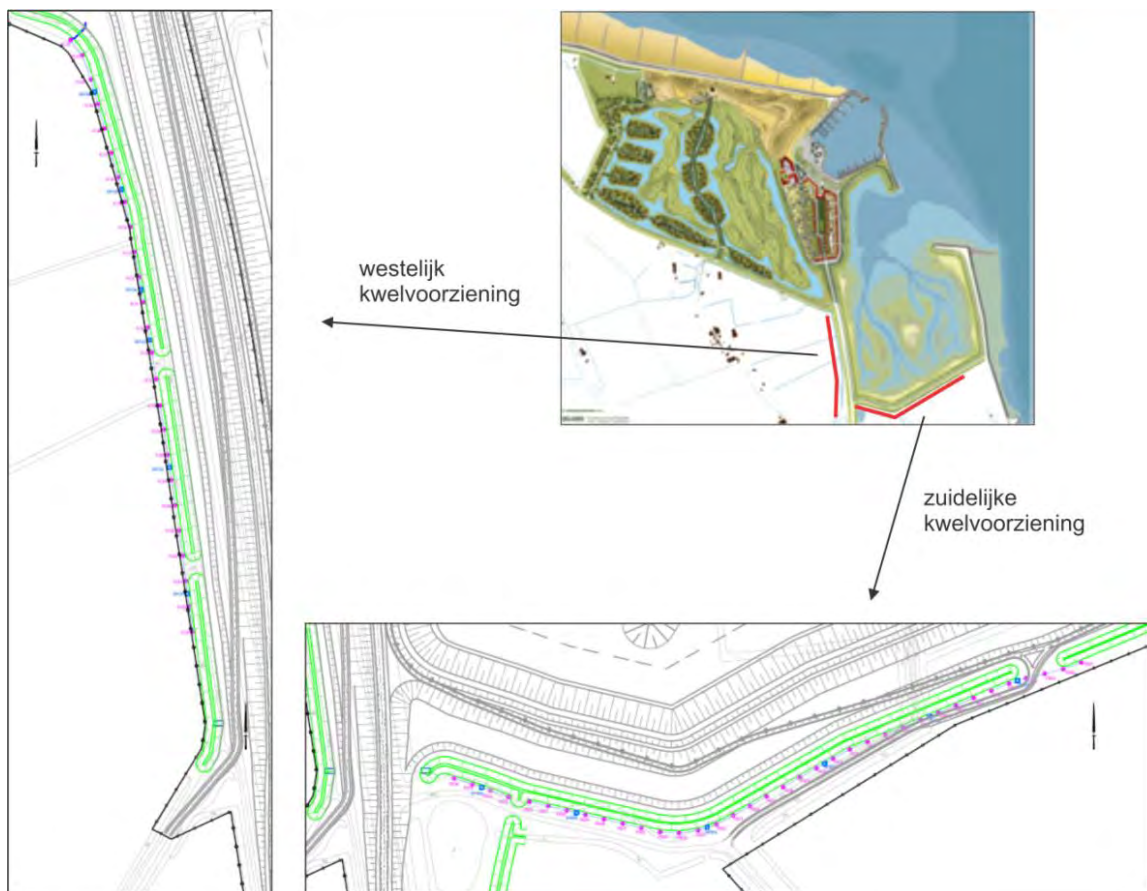


Figure 34. De ligging van de westelijke en zuidelijke kwelvoorziening. Op de detailtekening geven de roze punten de positie van de verticale kwelbuizen weer en in blauw zijn de regelputten weergegeven. Groen geeft de ligging van de sloot weer.

In Figure 34 is de ligging van westelijke en zuidelijke kwelvoorziening te zien met daarop aangegeven alle kwelbuizen en regelputten. De kwelvoorziening ligt vrijwel direct achter de nieuwe zeedijk, direct grenzend aan het landbouwgebied en een sloot (zie Figure 1). De totale lengte van de kwelvoorziening is ruim één kilometer. Figure 35 en Table 7 geven meer details van de kwelvoorziening.

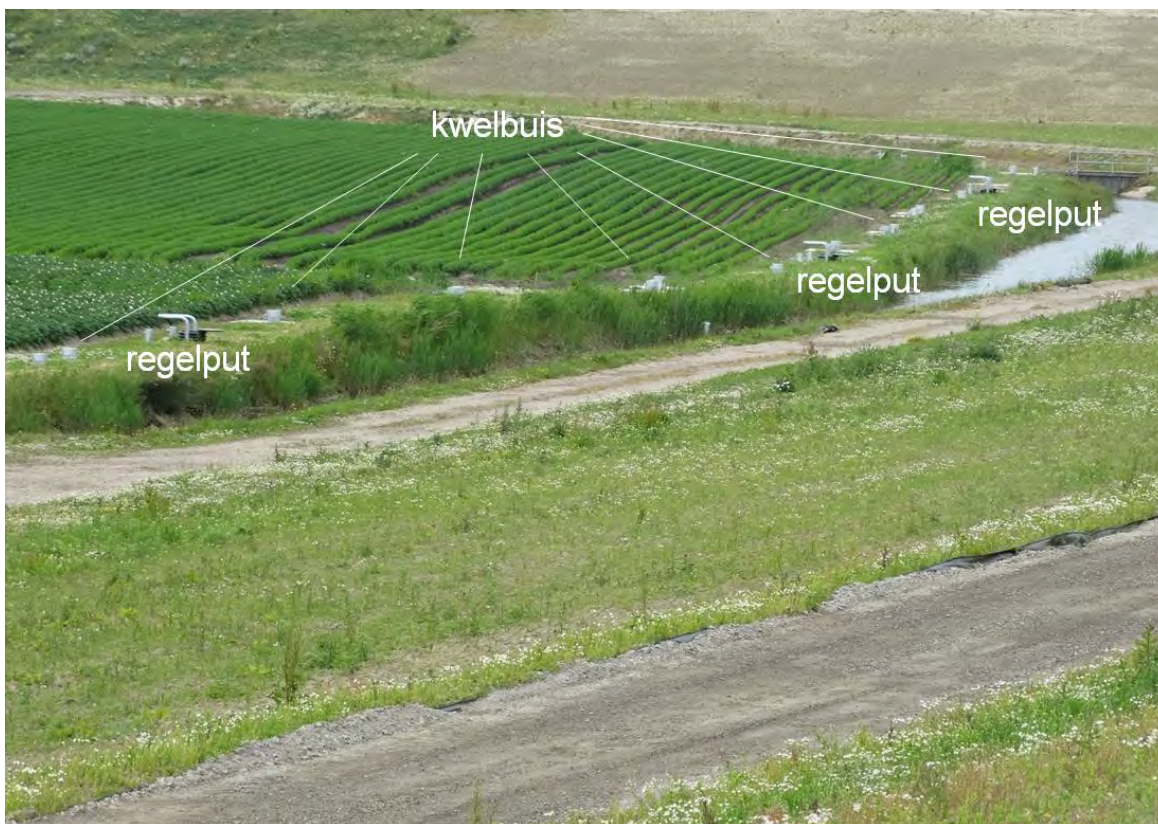


Figure 35. Foto van westelijke kwelvoorziening met ligging kwelbuizen en regelputten.

Table 7. Enkele details van de westelijke en zuidelijke kwelvoorziening.

	Westelijke kwelvoorziening	Zuidelijke kwelvoorziening
Totale lengte	500 m	500 m
Aantal vertical kwelbuizen	25	36
Diepte kwelbuizen	12 m-mv	17 m-mv
Filterdiepte	7 tot 12 m-mv	7 tot 17 m-mv
Filterlengte kwelbuizen	5 m	10 m
Afstand tussen kwelbuizen	20 m	15 m
Aantal kwelbuizen op de regelput	3 tot 5	4 tot 7

De gerealiseerde kwelvoorziening is een onttrekkingsstelsel op basis van vrij verval (door stijghoogtedruk in het eerste watervoerende pakket) bestaande uit een reeks van verticale kwelbuizen die grondwater uit het eerste watervoerende pakket afvoeren. De verticale kwelbuizen zijn over een afstand van ongeveer 80-100 m aan elkaar gekoppeld door middel van een verzamelleiding die uitkomt in een zogenaamde regelput. In de regelput kan het drainageniveau van de kwelbuizen worden ingesteld en daarmee de werking van de kwelvoorziening worden geregeld. De kwelvoorziening wordt geacht de toename van de stijghoogte als gevolg van de inrichting te compenseren om te voorkomen dat de zoetwaterbel krimpt.

De kwelvoorziening voert grondwater af wanneer de stijghoogte hoger is dan het peil in de regelput. Hoe groter het verschil tussen de stijghoogte en het peil in de regelput, hoe meer grondwater de kwelvoorziening afvoert. In Figure 37 is de werking van de kwelvoorziening schematisch weergegeven. Het peil in de regelput kan worden verhoogd met behulp van een stuwplankje (zie Figure 36 en Figure 37) waardoor de kwelvoorziening minder grondwater zal afvoeren. Wanneer de kwelvoorziening helemaal open staat (zonder stuwplankje), dan is het peil in de regelput gelijk aan het oppervlaktewaterpeil en werkt de kwelvoorziening maximaal. Het zomerpeil is ongeveer 20 cm hoger dan het winterpeil. De kwelvoorziening kan per regelput ook worden dichtgedraaid zodat er geen enkel grondwater wordt afgevoerd.



Figure 36. Foto van een regelput met stuwplankje.

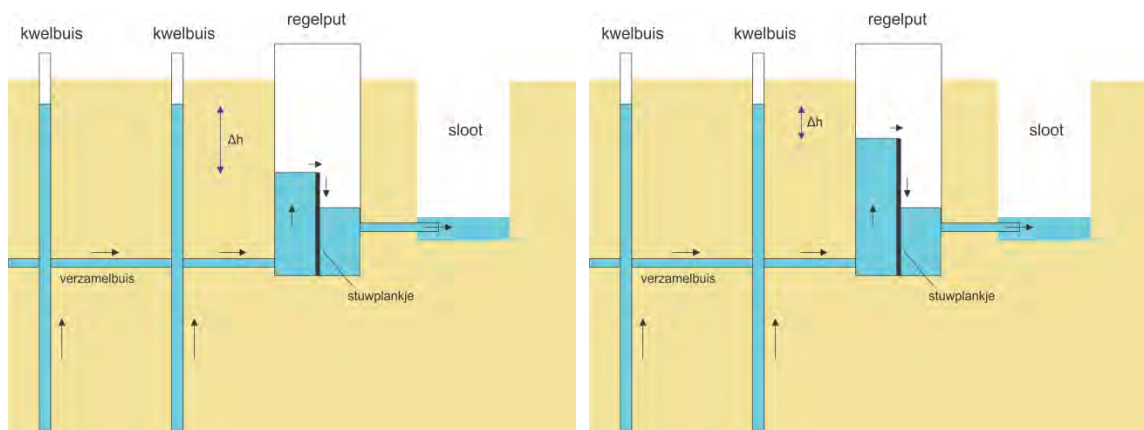


Figure 37. Schematische weergave van de kwelvoorziening met ondergrondse verbinding van kwelbuizen, uitkomende in regelput die vervolgens afwatert op sloot. Δh geeft het stijghoogteverschil weer tussen de stijghoogte in het eerste watervoerende pakket en het gestuwd peil in de regelput; hoe groter Δh , hoe meer grondwater de kwelvoorziening afvoert. Δh kan worden beïnvloed door het stuwpeil in de regelput te veranderen: vergelijk de situatie in de linker figuur (laag peil, grote Δh , hoge afvoer kwelvoorziening) met de situatie in de rechter figuur (hoog peil, kleine Δh , lage afvoer kwelvoorziening).

3.3 HET MEETNET

3.3.1 INLEIDING

Zoals beschreven in het monitoring-protocol kwelvoorziening en nulmeting grondwater Perkpolder richt de monitoring zich op de volgende aspecten van het (grond)watersysteem:

- Stijghoogte eerste watervoerende pakket (en freatische grondwaterstand).
- Zoet-zout grensvlak ofwel dikte zoetwaterbel (SlimFlex-metingen).
- Afvoer kwelvoorziening (debiet en zoutgehalte).

Ten opzichte van de nulmeting zijn de meetpunten grenzend aan de westelijke Perkpolder vervallen (eind 2013) omdat onduidelijkheid ontstond over de verdere ontwikkeling van dit gebied en er voldoende meetjaren beschikbaar waren voor een volwaardige nulmeting. In 2015 zijn er nieuwe meetpunten bijgeplaatst ter hoogte van de kwelvoorziening en aan de rand van Walsoorden.

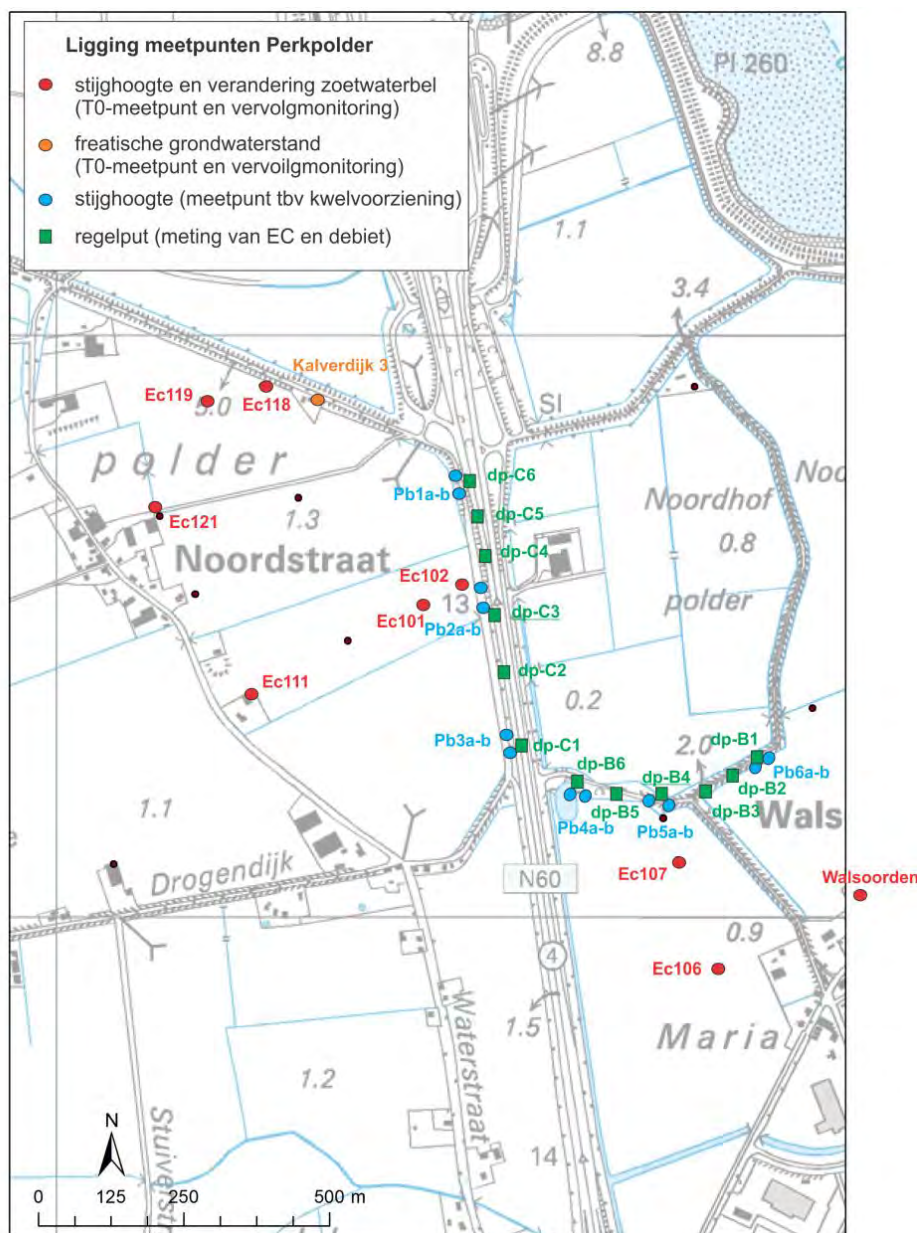


Figure 38. Het huidige grondwatermeetnet Perkpolder.

Figure 38 geeft de ligging van alle meetpunten die deel uitmaken van het huidige monitoringprogramma dat bestaat uit 2 doelen:

- (1) Vervolgmonitoring: het meten van eventuele effecten als gevolg van het getijdegebied
- (2) Monitoring van de werking van de kwelvoorziening en optimale inregeling hiervan.

3.3.2 STIJGHOOGTE

Het nieuwe getijdegebied leidt tot een gemiddeld hoger peil ten opzichte van de oude situatie (polderpeil) waardoor de stijghoogte in het eerste watervoerende pakket ook toeneemt. Uitstralingseffecten naar de omgeving zullen plaatsvinden via de stijghoogte in het eerste watervoerend pakket. Dit is daarmee de belangrijkste parameter om te monitoren. Door een toename van de stijghoogte zal kwel toenemen (in kwelgebieden), infiltratie afnemen (in infiltratiegebieden), grondwaterstanden (mogelijk licht) stijgen en zoetwaterlenzen zullen mogelijk krimpen. Om de uitstralingseffecten goed te kunnen monitoren, zijn de meetpunten geplaatst in raaien op verschillende afstanden van het getijdegebied. Op sommige locaties wordt tevens de freatische grondwaterstand gemeten. Gegevens van de verschillende meetpunten staan weergegeven in Sectie 9.2.

Het doel van de kwelvoorziening is de toename van de stijghoogte in het eerste watervoerende pakket als gevolg van de inrichting te compenseren zodat de zoetwaterbel niet wordt aangetast. Het volgen van de stijghoogte is dus een eerste en directe indicatie of de kwelvoorziening werkt en op basis waarvan de werking van de kwelvoorziening kan worden aangestuurd. Daarom zijn in 2015 nieuwe stijghoogtemeetpunten ter hoogte van de kwelvoorziening geplaatst (zie Figure 38). Op 6 locaties is een stijghoogtemeetpunt geplaatst (a) tussen twee kwelbuizen (aangeduid met code a) en (b) één bij een kwelbuis (aangeduid met code b). Namelijk, het effect van de kwelvoorziening op de stijghoogte is groter bij een kwelbuis dan in het midden tussen twee kwelbuizen (zie Figure 39).

De meeste meetpunten worden ieder uur automatisch gemeten met een zogenaamde 'Diver' (zie Sectie 9.1). Iedere 3 maanden worden Divers uitgelezen en worden handmetingen uitgevoerd. Op 2 meetlocaties ter hoogte van de kwelvoorziening (Pb 2 en Pb 5) wordt de stijghoogte telemetrisch gemeten en kan op elk gewenst moment de huidige meting worden bekeken. Op beide meetlocaties (Pb 2 en Pb 5) gaat het om de stijghoogte tussen twee kwelbuizen (Pb 2a, Pb 5a), bij een kwelbuis (Pb 2b, Pb 5b) en het gestuwde peil in de regelput (Pb 2EC, Pb 5EC).

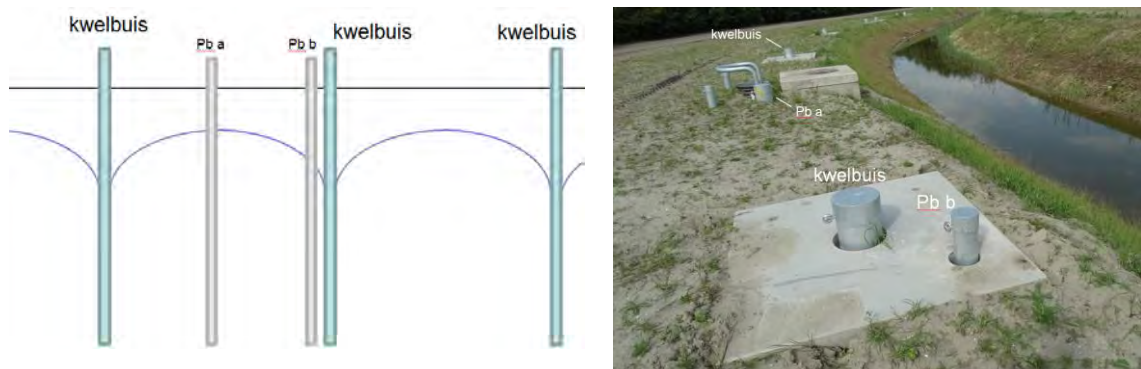


Figure 39. De ligging van de peilbuizen ten opzichte van de kwelbuizen. Pb a ligt tussen 2 kwelbuizen en Pb b bij een kwelbuis. Het effect van een kwelbuis op de stijghoogte is groter dicht bij een kwelbuis dan tussen 2 kwelbuizen.

3.3.3 GRENSVLAK ZOET-ZOUT GRONDWATER

De zoetwaterbel van Kloosterzande wordt door boeren gebruikt om uit te beregenen. Deze zoetwaterbel is met de ontwikkeling van het getijdegebied dicht bij de Westerschelde komen te liggen. Dit is te zien in Figure 40 waarin voor vier locaties de gemeten dikte van de zoetwaterlens staat weergegeven. Veranderingen in de dikte van deze bel dienen daarom te worden gevolgd. Veranderingen van de dikte van de zoetwaterbel gaan veel minder snel dan veranderingen in stijghoogte waardoor de meetfrequentie niet zo groot hoeft te zijn, 1 keer per jaar is voldoende.

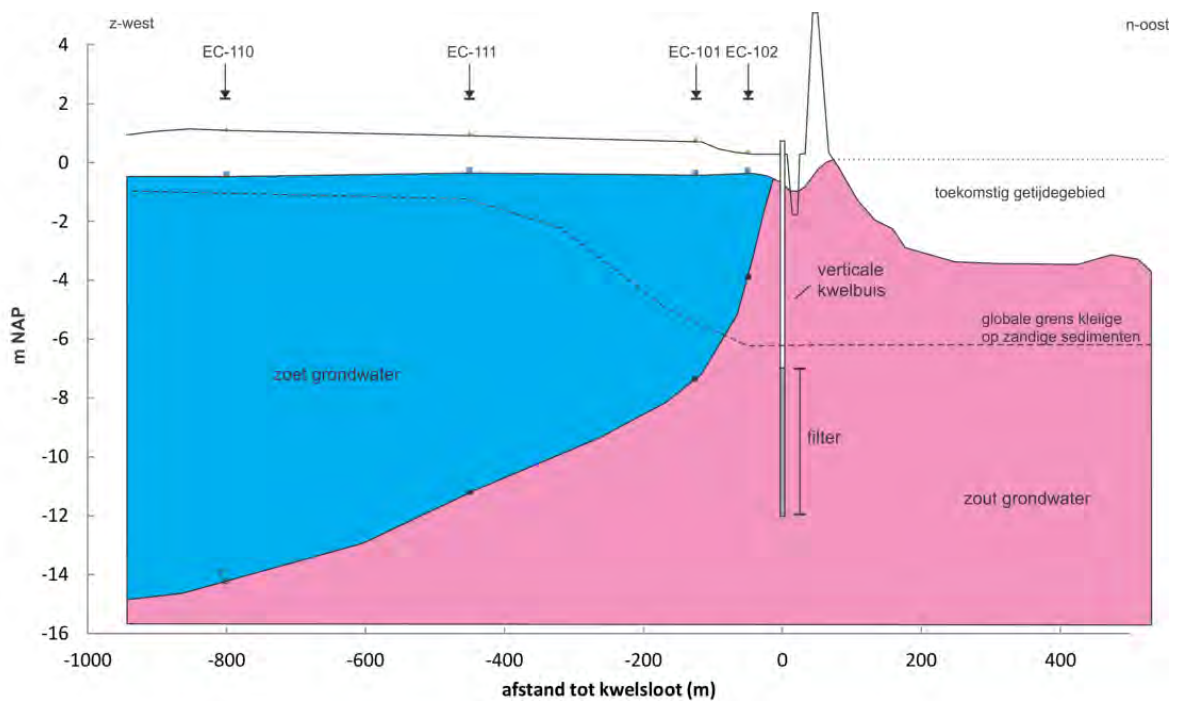


Figure 40. Een dwarsnede waarin de gemeten dikte van de zoetwaterbel (T_0) en ligging kwelvoorziening en nieuw getijdegebied.

De dikte van de zoetwaterbel wordt gemeten met behulp van de EM-Slimflex. De EM-Slimflex wordt in een peilbuis gelaten (zie Figure 41) en voor iedere 5 centimeter wordt een meting verricht. Hierdoor ontstaat een diepteprofiel van de geleidbaarheid van ondergrond en op deze manier kan de overgangszone tussen het zoete en zoute grondwater in beeld worden gebracht.

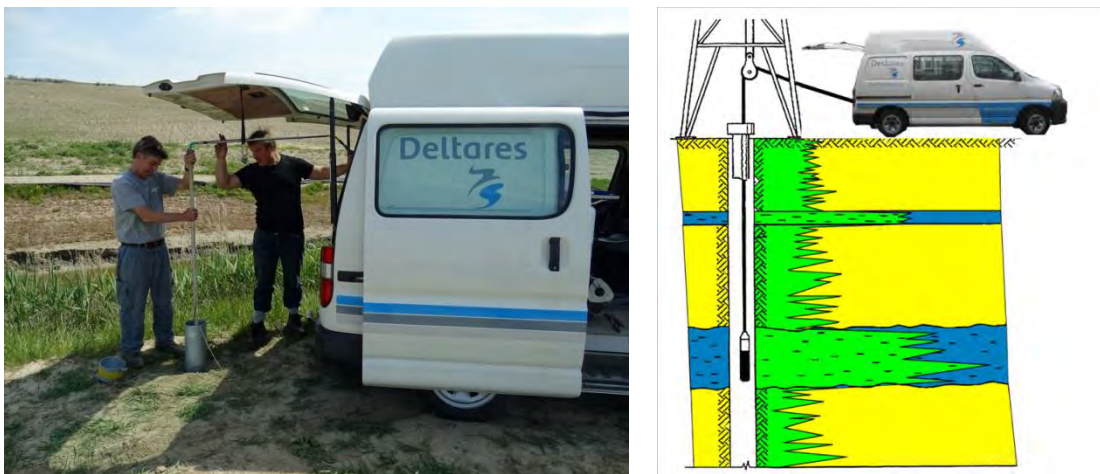


Figure 41. Uitvoering EM-Slimflex in Perkpolder (meetpunt Pb-3a, 22 mei 2015).

3.3.4 AFVOER KWELVOORZIENING: DEBIET EN ZOUTGEHALTE

Het debiet van de verticale kwelbuizen geeft in combinatie met de stijghoogtemetingen een indicatie van de werking van de kwelvoorziening. Daarnaast is het totale onttrekkingsdebiet, samen met het zoutgehalte, van belang voor het bepalen van het lozingsdebiet en de zoutlast op het oppervlaktewater. Veranderingen in zoutgehalte geven overigens ook informatie over de werking van de kwelvoorziening.

Voor 2 regelputten wordt zowel het debiet als het zoutgehalte van de afvoer van de kwelvoorziening automatisch ieder uur en telemetrisch gemeten. Voor de westelijke kwelvoorziening wordt dit gedaan bij meetpunt Pb2 en voor de zuidelijke kwelvoorziening bij meetpunt Pb5. De debietmeter is geplaatst in de horizontale afvoerpijp van de regelput naar de sloot. De debietmeter is van het type Arad-Octave van firma Revaho en maakt gebruik van een dubbele ultrasonische meting voor het meten van het debiet. Tevens wordt het zoutgehalte van de kwelvoorziening in alle regelputten ieder half jaar gemeten. Het handmatig meten van de afvoer van de regelputten is wenselijk maar lastig uit te voeren in verband met het ontbreken van waterdichte stuwplankjes. Immers, de snelheid van peilstijging zou dan kunnen worden gemeten na plaatsen van een stuwplankje. De stijging van het peil is een maat voor het debiet.

3.4 MEETRESULTATEN 2015 – 2018

3.4.1 MEETRESULTATEN STIJGHOOGTE

Periode 2015-2018

In Sectie 9.2 staan voor alle meetpunten de totale beschikbare meetreeksen weergegeven voor het jaar 2015-2018. De hoogfrequente metingen van alle nieuw geplaatste meetpunten zijn gestart ongeveer 1.5

maand vóór dat de dijk is doorgestoken op 25 juni 2015 waardoor een eventueel direct effect als gevolg van het nieuwe getijdegebied in de metingen zichtbaar zou zijn.

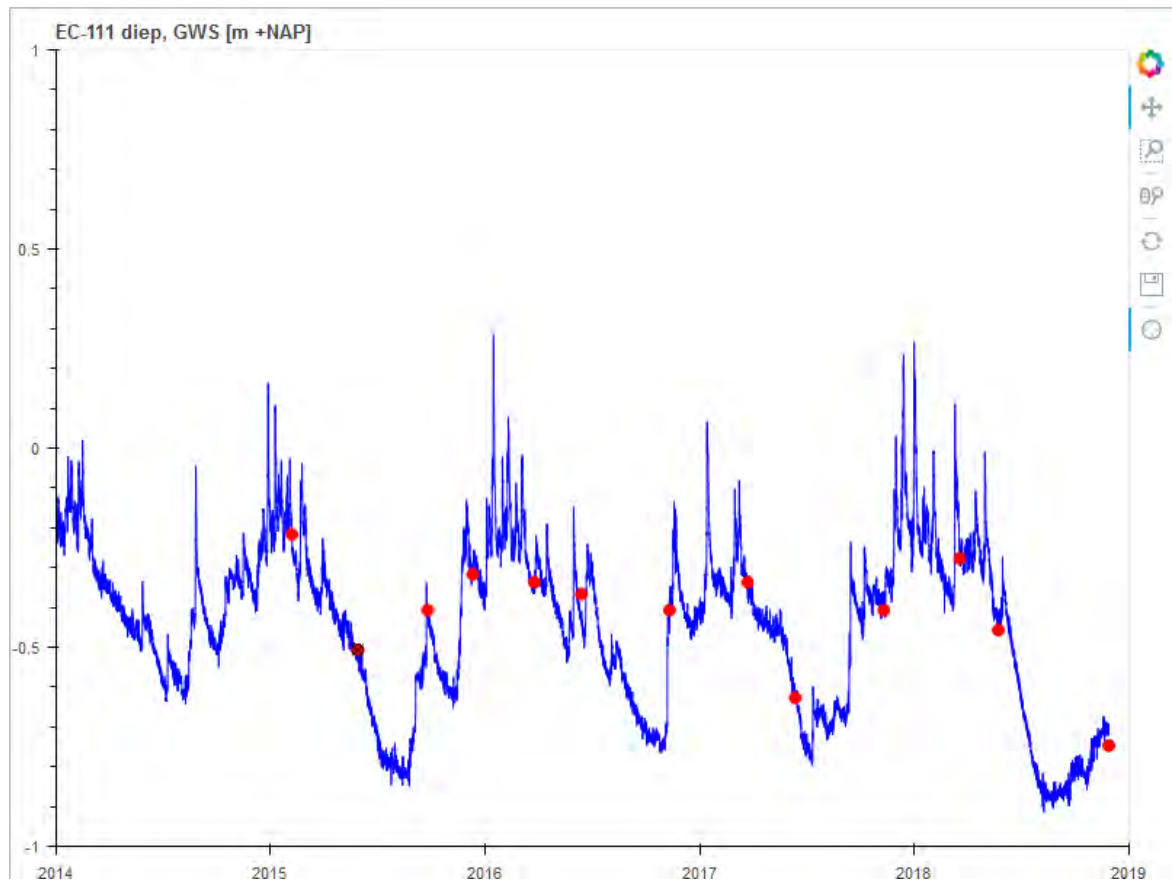


Figure 42. Het stijghoogteverloop van meetpunt EC-111(diep) voor de periode 2015-juni 2018.

Voor meetpunt EC-111(diep) staat het verloop in Figure 42 weergegeven, de overig tijdreeksen staan in Sectie 9.2. Bijna alle diepe meetpunten vertonen een vergelijkbaar verloop door het jaar heen met daarbij een vergelijkbare reactie op neerslag en verdamping. Over het algemeen in de winter en bij ondiepe grondwaterstanden, is de reactie op neerslag sterker. Dit komt doordat er minder water in de onverzadigde zone kan worden geborgen en de grondwaterstand sneller stijgt bij eenzelfde hoeveelheid neerslag.

Meetpunten die afwijken van het algemene patroon worden hieronder opgesomd.

- Meetpunt EC-102 (diep) vertoont na 18 februari 2015 een heel ander patroon dan ervoor. Als de gehele tijdreeks wordt bekeken na deze datum, dan kan worden geconcludeerd dat het meetpunt niet meer goed functioneert. Het meetpunt is afgebroken a.g.v. landbouwwerkzaamheden waardoor er via het maaiveld eenvoudig water in kon stromen. Dit verklaart de snelle stijging en langzaam zakken van de waterstand.. Na reparatie van de peilbuis op 18 maart 2016, lijkt het meetpunt weer

een normaal gedrag te gaan vertonen. Echter, de getijdefluctuatie die in 2014 zichtbaar was, is niet meer zichtbaar. Vanaf 20 oktober 2017 vertoont dit meetpunt weer een getijdefluctuatie en ditmaal veel sterker dan voor de opening. Op deze datum is het meetpunt leeggepompt voor het nemen van grondwater monsters, en waarschijnlijk is hierdoor een bepaalde verstopping in het filter opgeheven. Na deze datum is ook zeer sterk het aan en uitzetten van de kwelvoorziening zichtbaar in het meetpunt en is de getijdefluctuatie 70 cm als de kwelvoorziening uitstaat.

- Meetpunt EC-106 (diep) vertoont een grillig patroon, en wijkt daarmee sterk af van de andere meetpunten. Er is een nieuwe Diver in het meetpunt gehangen en vanaf juni 2016 vertoont het meetpunt weer een normaal patroon.
- Meetpunt EC-121 (diep) vertoont een vergelijkbaar patroon maar laat gedurende de zomerperiode (juli 2015, juli-augustus 2016, juni 2017, juni-september 2018) plotselinge dalingen zien van de stijghoogte. Dit is een bekend patroon en kan worden toegeschreven aan grondwateronttrekkingen uit de zoetwaterbel van Kloosterzande ten behoeve van beregening. De onttrekkingen zijn bevestigd door de akkerbouwer. Tijdens de droge zomer van 2018 is duidelijk meer grondwater onttrokken.

Effect van nieuw getijdegebied en kwelvoorziening

In De Louw e.a. (2016) is uitgebreid ingegaan op het effect van het getijdegebied op de stijghoogte en het effect van de kwelvoorziening. Deze analyse toonde aan dat de kwelvoorziening goed werkt, namelijk hij verlaagt de stijghoogte voldoende goed. Op basis van de metingen tot december 2018, kan nog steeds dezelfde conclusie worden getrokken. In Figure 43 wordt de meetreeks getoond vanaf het moment dat het getijdegebied in werking is getreden tot december 2018. Het effect op de stijghoogte door het openzetten en dichtzetten van de kwelvoorziening is heel goed in de tijdreeks te zien. Ook de momenten van verandering van zomerpeil naar winterpeil of omgekeerd (zie blauwe lijn) zijn in de stijghoogte zichtbaar. Alle andere meetreeksen ter hoogte van de kwelvoorziening laten een vergelijkbaar patroon zien en staan weergegeven in Sectie 9.2.

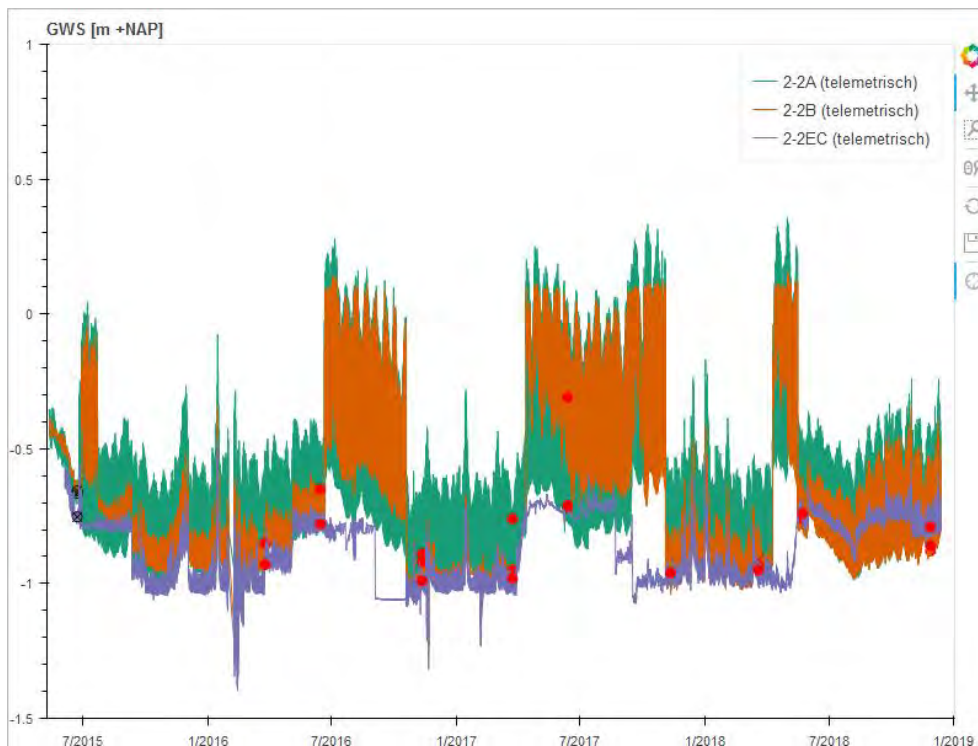
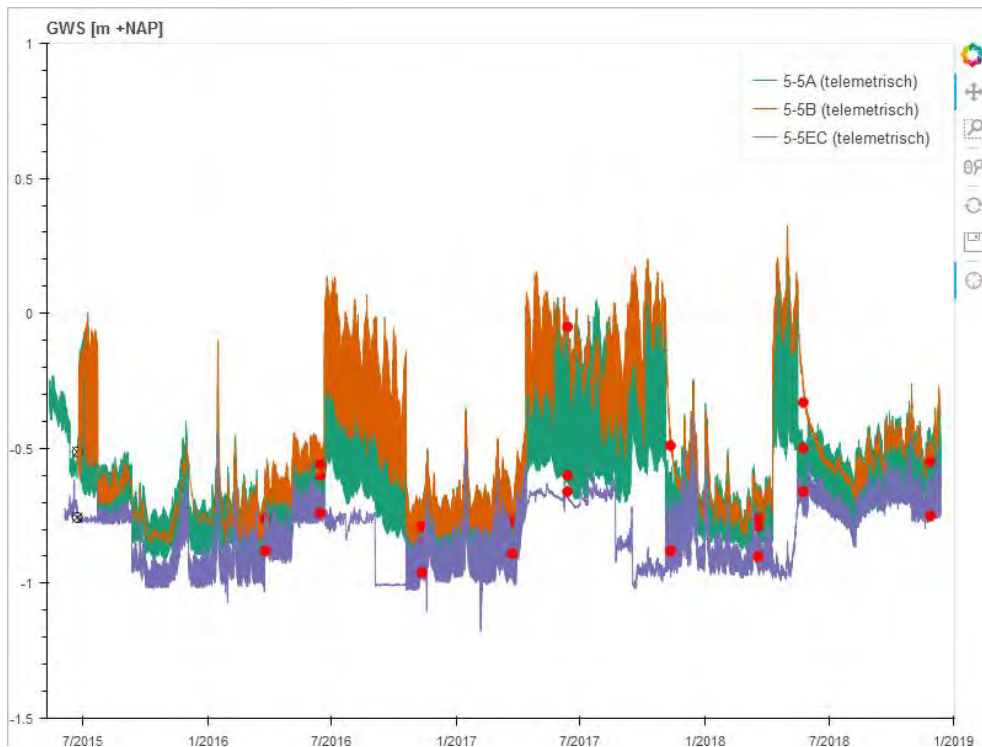


Figure 43. Het stijghoogteverloop van meetpunt Pb2 en Pb5 gedurende de periode juni 2015 tot december 2018, met het peil in de regelput (EC-buis), de stijghoogte tussen twee kwelbuizen (a-buis) en bij een kwelbuis (b-buis). Duidelijk is het patroon zichtbaar van het aanzetten van kwelvoorziening (lage stijghoogte) en dichtzetten van de kwelvoorziening (hoge stijghoogte).

3.4.2 MEETRESULTATEN GRENSVLAK ZOET-ZOUT GRONDWATER

Sinds 2012 wordt regelmatig (1 á 2 keer per jaar) de zoutverdeling van het grondwater gemeten met de SlimFlex. Op 22 mei 2015 zijn ook de nieuw geplaatste meetpunten ter hoogte van de kwelvoorziening en bij Walsoorden bemeaten. Deze meetronde kan als een nulmeting worden gezien. In Figure 44 zijn de SlimFlex-metingen te zien van meetpunt EC-106, de metingen van alle andere meetpunten staan weergegeven in Sectie 9.3. Het zoet-zout grensvlak ligt op -15 m NAP en verandert nauwelijks in de tijd gedurende de nulmeting en ook niet als gevolg van het nieuwe getijdegebied. Ook de andere meetpunten laten een relatief stabiel grensvlak zien (Sectie 9.3). Dit is conform de verwachting en de bevindingen van de PhD-onderzoeken van De Louw (2013) en Pauw (2015). Daarbij dient te worden opgemerkt dat veranderingen van de zoet-zout verdeling in het grondwater vele malen langzamer gaan dan veranderingen van de stijghoogte. Dit komt omdat het bij de zoet-zout verdeling gaat om het daadwerkelijk verplaatsten van waterdeeltjes en bij de stijghoogte gaat het primair om drukverplaatsing.

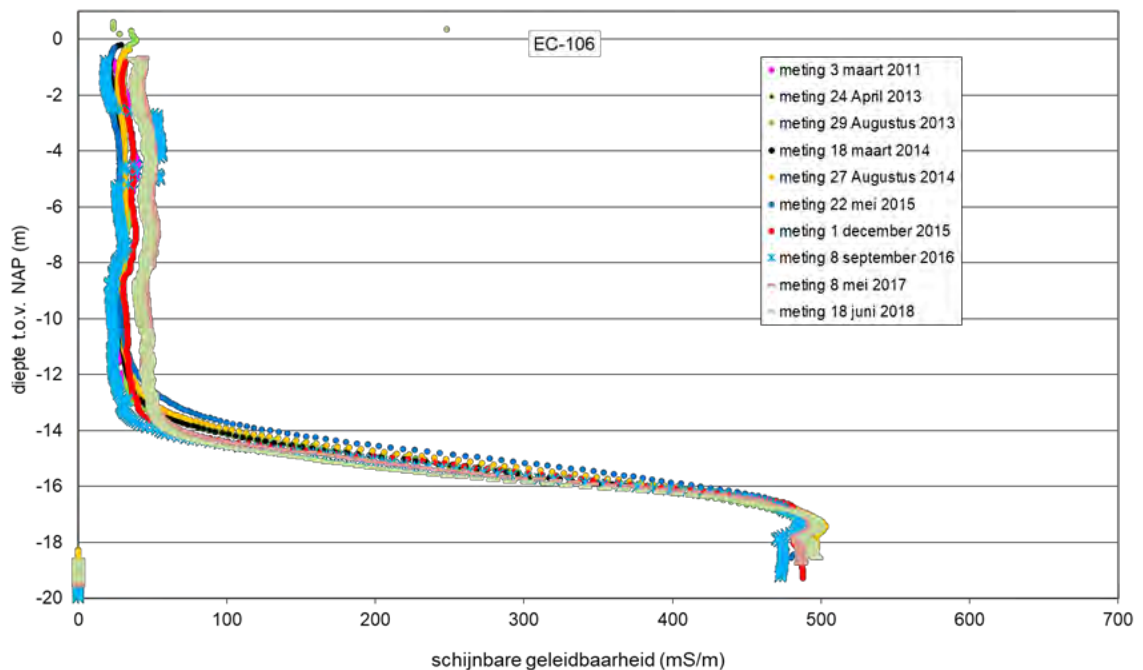


Figure 44. De SlimFlex-metingen voor meetpunt EC-106.

Bij het uitvoeren van de SlimFlex-metingen kunnen er onnauwkeurigheden optreden in de absolute waarde van de meting en de diepteregistratie. Hiervoor zijn een aantal oorzaken aan te wijzen.

- Diepteregistratie wordt onnauwkeuriger bij grotere afstand van de meetwagen tot het meetpunt (afstanden van meer dan 150 meter komen voor i.v.m. toegankelijkheid landbouwpercelen en vermijden gewasschade, bijv. meetpunt EC-107, EC-101);
- De diepte van de meting wordt in het veld gerefereerd ten opzichte van maaiveld. Door landbewerkingen kunnen er maaiveldverschillen optreden van 30 cm waardoor de diepteregistratie kan afwijken;
- Gebruik van verschillende typen SlimFlex-sondes (verschil in spoelafstand en absolute meetwaarden);
- De zonnwind als ook radiogolven (er is een amateur radiostation op korte afstand van de meetpunten, ter hoogte van meetpunt EC111) kunnen de elektromagnetische metingen beïnvloeden waardoor absolute waarden kunnen verschillen.
- Het zogenaamde skin-effect wat inhoudt dat de indringingsdiepte minder groot wordt bij een grotere geleiding.

De Slimflex-metingen zijn gecorrigeerd voor bovengenoemde variaties in diepteregistratie en absolute waarden. Dit is alleen gedaan wanneer met redelijke zekerheid kon worden aangenomen dat variaties zijn veroorzaakt door bovengenoemde oorzaken. Als eerste correctiestap zijn de absolute waarden gestandaardiseerd naar een gemiddeld minimale waarde (zoet bereik) en gemiddelde maximale waarde (zoute deel). Daarna heeft een eventuele verticale correctie plaatsgevonden wanneer uitschieters door lithologische variaties (veelal kleilaagjes) niet op dezelfde diepte worden aangetroffen in de metingen. In de tijd zou de diepte van deze uitschieters namelijk niet mogen veranderen. De gepresenteerde metingen (Figure 44 en Sectie 9.3) laten de gecorrigeerde meetwaarden zien volgens deze methode.

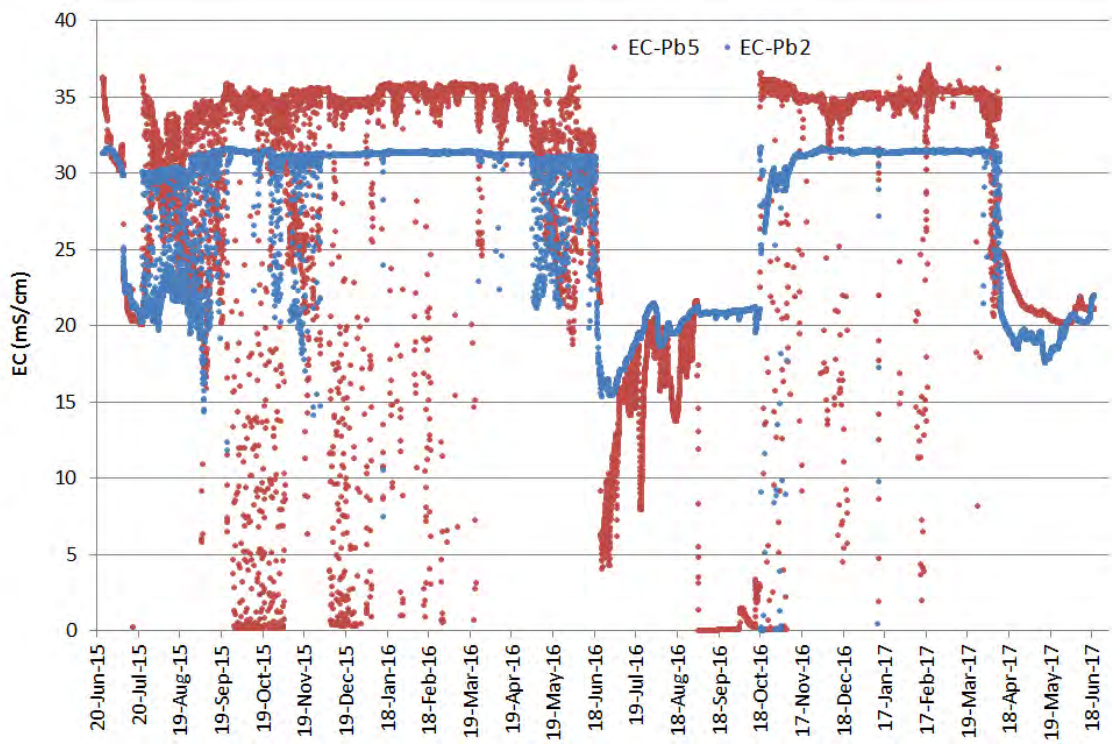
3.4.3 MEETRESULTATEN DEBIET EN ZOUTGEHALTE KWELVOORZIENING

In twee regelputten bij meetpunt Pb-2 en Pb-5 worden het zoutgehalte en de afvoer van de kwelvoorziening automatisch en telemetrisch gemeten. In de onderstaande grafieken staan de meetresultaten weergegeven.

Het zoutgehalte van het water in de regelput laat voor beide meetpunten een relatief constante waarde zien als de kwelvoorziening open staat, ongeveer 35 mS/cm voor de regelput bij Pb5 en 32 mS/cm bij Pb2 (zie Figure 45). Deze maximale waarden komen overeen met het zoutgehalte van het kwelwater. Bij een dichte kwelvoorziening stroomt er oppervlaktewater de regelput in en daalt het zoutgehalte van het oppervlaktewater naar ongeveer 20 mS/cm.

Er wordt een variatie waargenomen die het gevolg is van de getijdewerking (zie Figure 45). Bij hoogtij en daardoor maximale stijghoogte is de afvoer van de kwelvoorziening maximaal en bestaat het water uit 100% kwelwater. Bij een lagere stijghoogte wordt er minder kwelwater afgevoerd en is er meer bijmenging van

het oppervlaktewater waardoor het zoutgehalte daalt. We zien dat voor meetpunt Pb-5 de EC-waarde soms daalt naar de waarde nul. Dit wordt veroorzaakt door het feit dat de EC-diver tijdens eb droog komt te hangen.



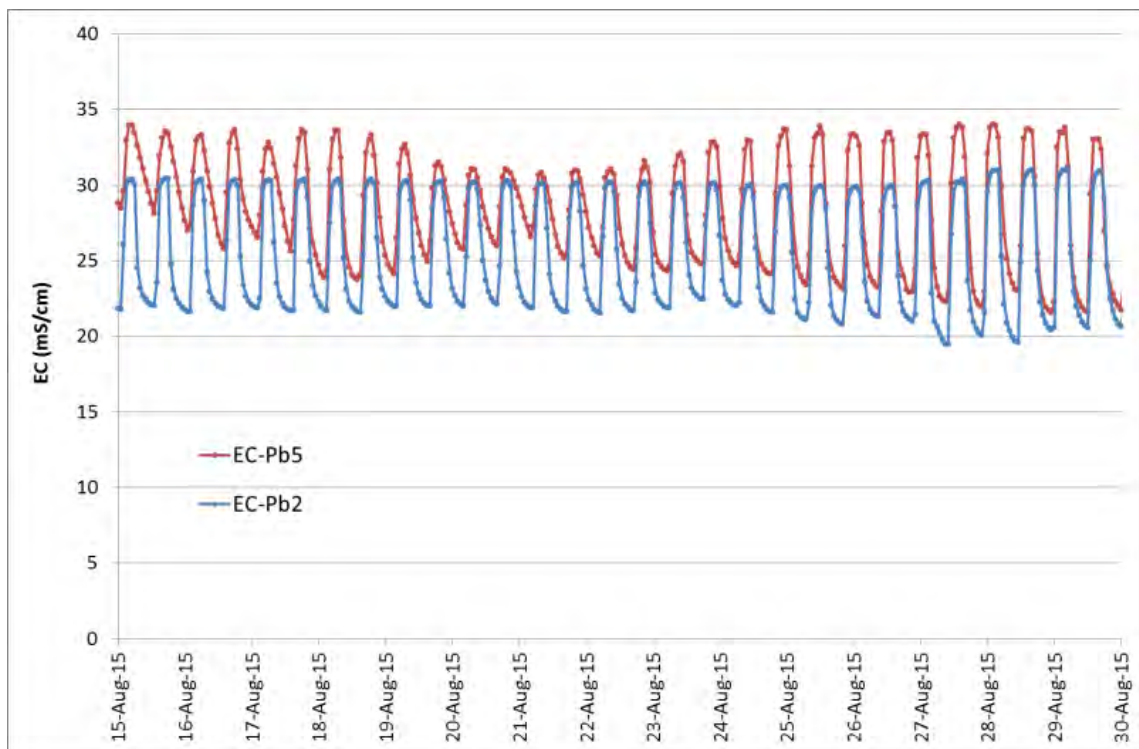
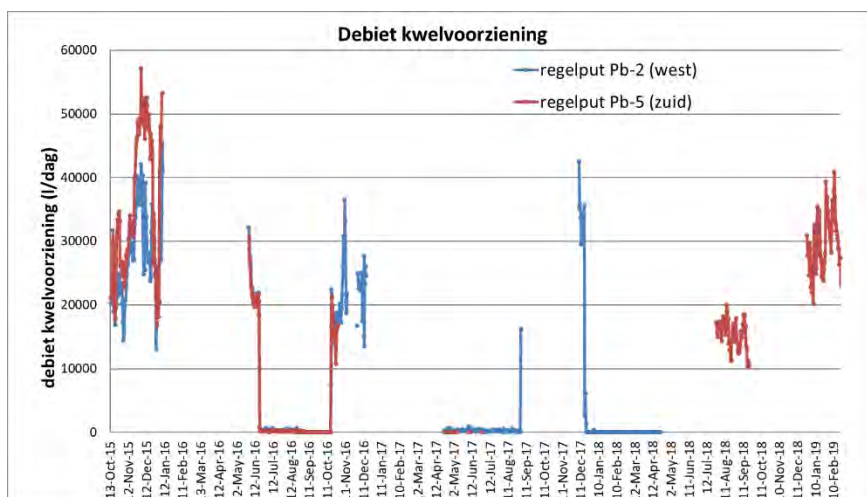


Figure 45. Het zoutgehalte (elektrische geleidbaarheid EC) voor het water in de regelput voor meetpunten Pb-2 en Pb-5, voor de gehele meetperiode en ingezoomd voor de maand augustus 2015.



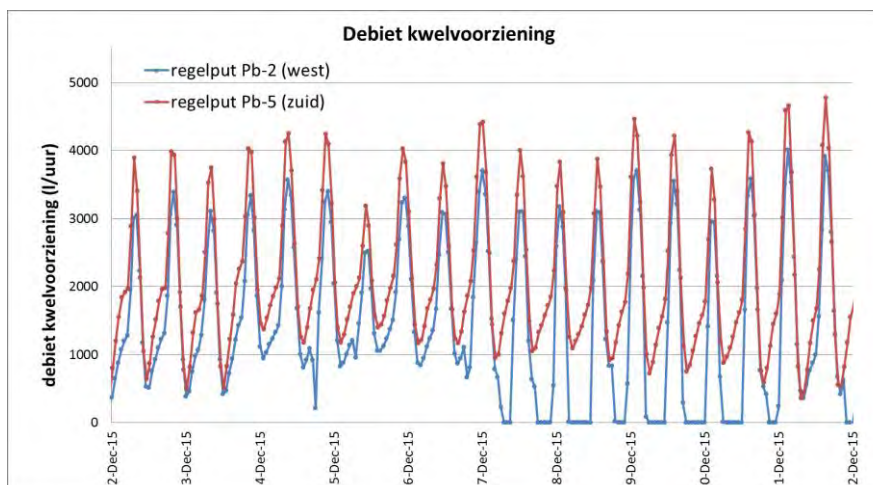
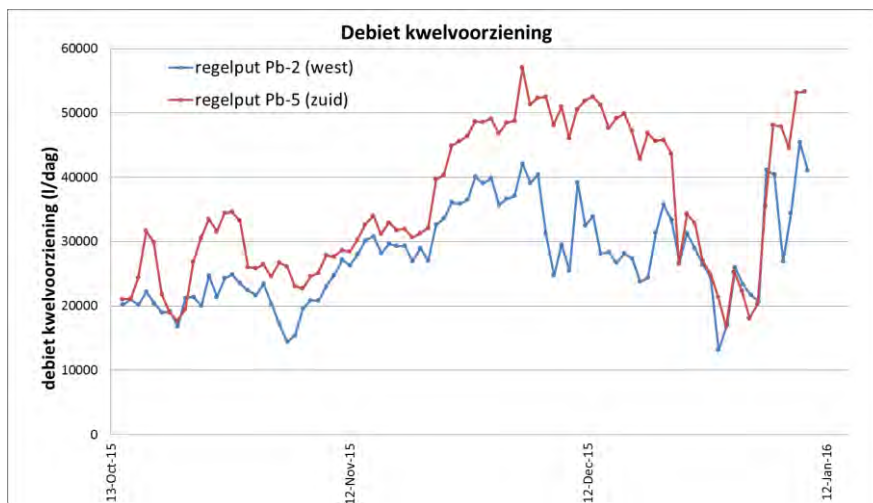


Figure 46. Het debiet van 2 regelputten waarop 3 (Pb-2) en 7 (Pb-5) verticale kwelbuizen zijn aangesloten, in liter/dag (boven en midden) en liter/uur (onder).

De afvoer van de kwelvoorziening is sterk gerelateerd aan de stijghoogte, hoe hoger de stijghoogte, hoe groter de afvoer. Dit is goed te zien in Figure 46 waar het debiet een getijdefluctuatie laat zien; hoogtij leidt tot een hogere stijghoogte en tot een hogere afvoer. In de grafiek is te zien dat voor sommige momenten de afvoer zelfs nul wordt (Pb 2 vanaf 7 december). In dit geval is de stijghoogte lager dan het oppervlaktewaterpeil waardoor er mogelijk weer een kleine hoeveelheid water via de verticale kwelbuis het watervoerend pakket in stroomt. Dit terugstromen wordt niet door de debietmeter geregistreerd en de geregistreerde afvoer is dus een overschatting van het werkelijke netto debiet.

De regelput bij Pb-2 (westelijke kwelvoorziening) voert gemiddeld 28.000 liter per dag af en hierop zijn drie verticale kwelbuizen aangesloten. Op de regelput bij Pb-5 (zuidelijke kwelvoorziening) zijn zeven verticale kwelbuizen aangesloten en deze voert gemiddeld 36.000 liter per dag af. Dit zijn waarden gebaseerd op de metingen in de periode oktober 2015-januari 2016. Wanneer deze waarden worden geëxtrapoleerd naar de

totale kwelvoorziening dan wordt totaal 416 m³/dag afgevoerd. Echter, de netto afvoer zal dus minder zijn omdat er ook water terugstroomt.

In de figuur is te zien dat er erg lange perioden zijn dat er geen afvoermetingen beschikbaar zijn. Dit wordt veroorzaakt door problemen met de stroomvoorziening van het telemetriesysteem. Recentelijk zijn door Broere Berekening de meetpunten uitgerust met zonnepanelen om dit probleem te ondervangen. Echter, helaas is 1 meetpunt momenteel weer niet operationeel. Door de steeds terugkomende problemen met de afvoermetingen wordt aanbevolen deze metingen te stoppen. Metingen van de stijghoogte geven voldoende aanwijzingen dat de kwelvoorziening nog functioneert.

3.5 OPERATIONEEL BEHEER EN ONDERHOUD KWELVOORZIENING

3.5.1 INLEIDING

Het waterschap Scheldestromen neemt in 2019 het beheer van de kwelvoorziening van Rijkswaterstaat over. In dit hoofdstuk wordt het operationeel beheer en beheer en onderhoud van de kwelvoorziening besproken.

De stijghoogtemetingen en debietmetingen laten zien dat de kwelvoorziening goed werkt. Uit de metingen blijkt dat ter plaatse van de kwelvoorziening de stijghoogte meer kan worden verlaagd dan nodig is. Dit biedt perspectief om de zoetwaterbel zelfs wat te laten groeien. Hoe het proces van groeien en krimpen van een zoetwaterbel werkt, wordt geïllustreerd aan de hand van een voorbeeld van het Badon-Ghyben Herzberg principe (zie Sectie 9.4).

3.5.2 OPERATIONEEL BEHEER VAN DE KWELVOORZIENING

De kwelvoorziening heeft twee uiterste standen, (1) dicht of (2) open zonder stuwplankje. Met stuwplankjes in de regelput zou de kwelvoorziening verder kunnen worden ingesteld tussen deze 2 uiterste standen. In sectie 3.2 is uitgelegd hoe dit werkt. Echter, uit tests is gebleken dat er in de regelput behoorlijke lekkage optrad waardoor het gewenste peil in de regelput niet kon worden gehandhaafd. Er trad lekkage op tussen de bodem van de regelput en het onderste plankje en tussen de stuwplankjes zelf.

Als gevolg hiervan en uit praktisch oogpunt is er daarom voor gekozen om niet met stuwplankjes te werken maar de sturing van de kwelvoorziening via het sluiten en openzetten uit te voeren. Daarbij is het, mede uit praktisch oogpunt wat betreft het operationeel beheer van de kwelvoorziening, wenselijk om gedurende lange perioden een bepaalde instelling (open of dicht) te hanteren. Dit is ook wat betreft het effect op de zoetwaterbel een prima uitgangspunt. Namelijk, het gaat voor het groeien of krimpen van de zoetwaterbel om de gemiddelde jaarlijkse stijghoogte en niet om dagelijkse fluctuaties.

Er zijn in totaal 23 afsluiters. Dit zijn er 2 per regelput want aan iedere kant van de regelput komt er een horizontale verzamelbuis uit die kan worden afgesloten (muv 1 regelput waar maar 1 verzamelbuis op uit komt). Het bedienen van de afsluiters is eenvoudig uit te voeren met een T-sleutel (zie Figure 47 en 48).



Figure 47. De twee afsluiters (stalen koker met deksel eraf) aan beide zijden van de regelput. Met de blauwe T-sleutel kunnen de spindel-afsluiters open en dicht worden gezet.

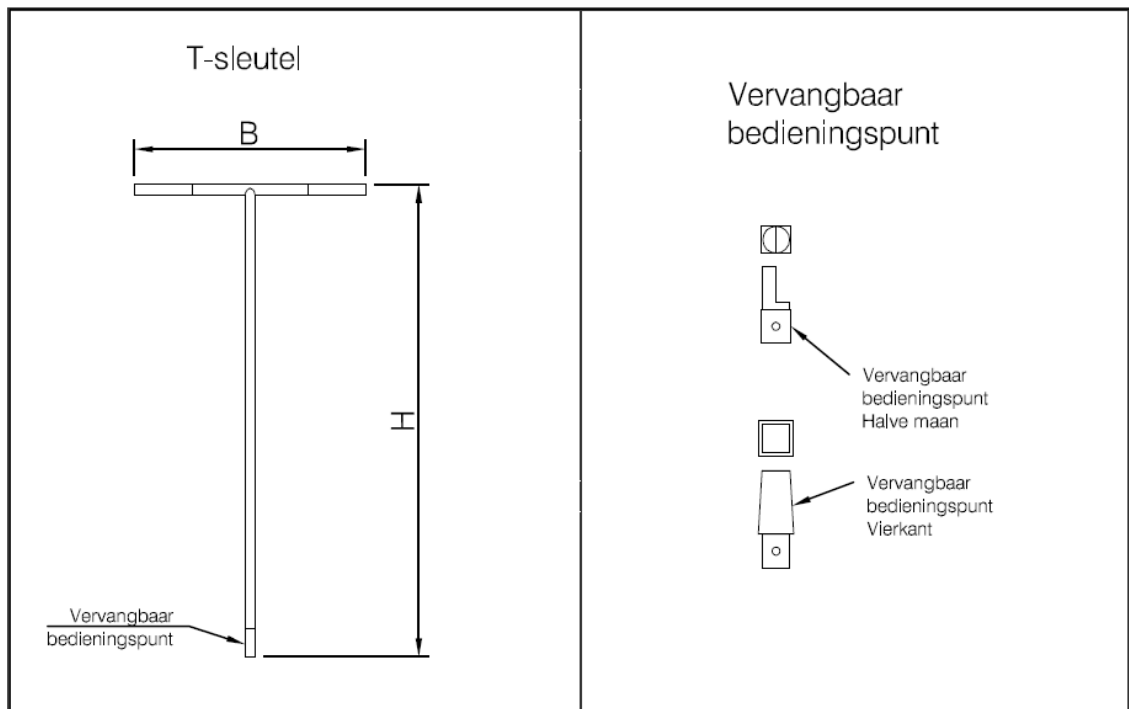


Figure 48. T-sleutel met aan uiteinde vervangbaar bedieningspunt om spindel-afsluiters te bedienen.

De instelmogelijkheden voor de regelput worden dan:

- Kwelvoorziening dicht
- Kwelvoorziening open, geen stuwplankje: peil = polderpeil zomer -0.8 m NAP
- Kwelvoorziening open, geen stuwplankje: peil = polderpeil winter -1.1 m NAP

Op basis van de metingen en inzichten in de effecten van het getijdegebied en kwelvoorziening op de stijghoogte, werd eerder de volgende instelling van de kwelvoorziening voorgesteld:

- Winterperiode: kwelvoorziening helemaal open
- Zomerperiode: kwelvoorziening helemaal dicht

Uit praktisch oogpunt, vallen de zomer- en winterperiode samen met het instellen van het zomer- en winterpeil. Dit is de meest praktische instelling. In de winterperiode is de stijghoogte namelijk het hoogst en zal de grootste verlaging moeten plaatsvinden. Wanneer de kwelvoorziening dan helemaal wordt opengezet, zal er vermoedelijk meer grondwater worden afgevoerd dan nodig is om het effect van het getijdegebied te compenseren en zou de zoetwaterbel zelfs kunnen groeien. Immers, gedurende de winterperiode is er een neerslagoverschot dat de bel kan aanvullen. Het af te voeren kwelwater is zout maar zal in de winterperiode worden verdund door het neerslagoverschot. Bovendien wordt het

oppervlaktewater gedurende de winterperiode niet gebruikt voor beregening. Het dicht zetten van de kwelvoorziening in de zomer heeft dan als voordeel dat er geen extra zoutbelasting van het oppervlaktewater optreedt. Daarnaast zal er in de zomer met het dichtzetten van de kwelvoorziening geen extra verlaging van stijghoogte en grondwaterstand plaatsvinden en daardoor geen extra verdroging. Het is theoretisch zelfs mogelijk dat grondwaterstanden in de zomer iets hoger liggen (door de invloed van het getijdegebied) waardoor er mogelijk minder droogteschade optreedt.

Modelberekeningen (zie sectie 3.7) hebben laten zien dat wanneer de kwelvoorziening in de zomer wordt dichtgezet, het mitigerende effect significant minder is. Daarom wordt op basis hiervan (in tegenstelling tot hierboven vermeld) aanbevolen om de kwelvoorziening het hele jaar open te zetten.

3.5.3 BEHEER EN ONDERHOUD VAN DE KWELVOORZIENING

Bij oplevering van de kwelvoorziening van Van Oord aan Rijkswaterstaat, is een beheer- en onderhoudsplan opgesteld. Er wordt ervan uitgegaan dat dit plan in bezit is van het waterschap en voldoende informatie geeft over het technisch onderhoud en beheer van de kwelvoorziening.

Hieronder worden nog enkele aandachtspunten voor het waterschap gegeven.

- De verticale kwelbuizen en horizontale verzamelbuizen liggen permanent onder water. De kans op verstopping door ijzeroxides wordt daarmee klein geacht. Deze ontstaan wanneer grondwater in contact komt met zuurstof. Er wordt verwacht dat het doorspuiten van de buizen de eerste 10 jaar niet nodig zal zijn. Echter, monitoring van stijghoogte en afvoer is van belang om de werking van de kwelvoorziening te volgen (zie Sectie 3.6). Mocht hieruit blijken dat de kwelbuizen minder water gaan afvoeren of dat de stijghoogte minder wordt verlaagd, dan kan worden besloten de buizen door te spuiten. Hiervoor zijn speciale doorspuitmogelijkheden aangebracht.
- Minimaal tweemaal per jaar (bijvoorbeeld tijdens een meetronde) dient er een visuele inspectie plaats te vinden of alles nog intact is. Wanneer er schade is opgetreden (bijvoorbeeld omver gereden kwelbuizen of regelputten), dient er zo spoedig mogelijk een herstelactie plaats te vinden.
- Momenteel (december 2018) is 1 spindel-afsluiter kapot, bij regelput dp-B1 (aan kant van de Westerschelde). Deze dient zo spoedig mogelijk te worden gerepareerd.
- De zone rond de kwelvoorziening dient vrij te worden gemaakt van overtollige groei van vegetatie. Dit voor beter zicht op de kwelvoorziening en zodat er geen overlast voor aangrenzende landbouwpercelen ontstaat.

3.6 MONITORING: UITWERKING EN ANALYSE MEETGEGEVENS

3.6.1 INLEIDING

Monitoring heeft 2 doelen: (1) het volgen van de werking van de kwelvoorziening en (2) het volgen van de effecten in het aangrenzende landbouwgebied (vervolgmonitoring). De verantwoordelijkheid van de monitoring zal per 1-1-2019 door het waterschap van Rijkswaterstaat worden overgenomen. Uit praktisch oogpunt en afstemming van de meetgegevens, dient de monitoring van de deze twee meetdoelen gezamenlijk te worden opgepakt. Wij adviseren om het gepresenteerde monitoringplan voor beide meetdoelen te blijven uitvoeren zolang de kwelvoorziening operationeel is.

3.6.2 MONITORINGPLAN, ONDERHOUD EN UITVOEREN VAN DE METINGEN

In sectie 3.1 is het meetnet en monitoringplan voor beide meetdoelen uitgebreid besproken. Figure 34 laat de ligging van de verschillende meetpunten zien. In Sectie 9.1 staan de technische gegevens en de monitoringfrequentie. Tevens is aangegeven welk meetpunt voor welk meetdoel bedoeld is: volgen van kwelvoorziening (K) of vervolgmonitoring in aangrenzend landbouwgebied (V). Hieronder worden nog enkele aandachtspunten gegeven voor het meetnet en uitvoering van de metingen en herstel.

Stijghoogte

- De stijghoogte wordt automatisch gemeten met behulp van Divers. Ieder kwartaal dienen de Divers te worden uitgelezen en dient er een handmeting te worden gedaan.
- In alle stijghoogtmeetpunten hangt een Diver. Vaak staat er ook nog een ondiep filter naast. Deze dient altijd handmatig te worden gemeten tijdens de meetrondes.
- Momenteel wordt dit door het bedrijf Colsen BV uitgevoerd, gevestigd in Hulst (<https://www.colsen.nl/>) en de ervaringen met Colsen BV zijn goed.
- Wanneer een Diver niet meer (goed) functioneert, dient deze direct te worden vervangen.
- Het wordt aangeraden om na elke meetronde de meetgegevens uit te werken tot grafieken.
- Bij elke meetronde wordt de Diver uit de peilbuis gehaald. Deze dient zorgvuldig te worden teruggehangen zodat er geen sprong (off-sets) in de data optreedt. Het is namelijk zeer tijdrovend om deze off-sets te corrigeren.
- Het wordt aanbevolen om alle Divers van een nieuw en robuust ophangstelsel te voorzien. Dit is momenteel op een houtje-touwtje manier gebeurd waardoor de kans op off-sets groot is.
- Bij iedere meetronde (ieder kwartaal) dient het meetnet visueel te worden geïnspecteerd. Kapotte meetpunten (bijv. afgebroken peilbuizen) dienen direct te worden gerepareerd. Let daarbij op dat de hoogte ten opzichte van NAP en het maaiveld van het meetpunt opnieuw wordt bepaald.

- Een aantal meetpunten wordt telemetrisch gemeten. Er wordt aanbevolen om maandelijks de meetgegevens te controleren en dit altijd te doen direct na openzetten of dichtzetten van de kwelvoorziening.
- De data van de telemetrische meetpunten kunnen worden bekeken en gedownload via de volgende link: <https://www.telecontrolnet.nl/v3/index.php?s=eijkelkamp>
- Het telemetriesysteem is aangelegd door Eijkelkamp en wordt door hen jaarlijks onderhouden. De kosten hiervoor zijn tot en met 31 december 2018 gedekt. Dit is inclusief kosten voor datatransmissie maar exclusief vervanging van kapotte meetapparatuur.
- Momenteel (februari 2019) zijn een aantal Divers stuk en dienen zo spoedig mogelijk te worden ontvangen. Ook is bij de laatste inspectie op 29 november 2018 gebleken dat er een aantal meetpunten zijn afgebroken en dienen te worden gerepareerd. Ook heeft de kwelvoorziening schade opgelopen en dient deze te worden hersteld.

Afvoer kwelvoorziening: debiet en zoutgehalte

- Van twee regelputten wordt het debiet van de kwelvoorziening automatisch en ieder uur gemeten. Dit gebeurt tevens via een telemetrisch systeem.
- Het systeem is aangelegd door Broere Beregening (<http://www.broereberegening.nl/>)
- De metingen zijn via <https://mymobeye.eu/> te downloaden.
- De afvoermetingen lopen echter niet gesmeerd. Lange perioden zijn er geen afvoermetingen in verband met problemen met het telemetriesysteem. Vermoedelijk zijn dit problemen met de stroomvoorziening (batterijen). Recentelijk zijn door Broere Beregening de meetpunten uitgerust met zonnepanelen om dit probleem te ondervangen. Echter, helaas is 1 meetpunt weer niet operationeel. Er wordt aanbevolen om deze meting te laten vervallen.
- Tevens wordt ieder uur het zoutgehalte van de afvoer van de kwelvoorziening met een CTD-Diver gemeten. De gegevens zijn te bekijken en te downloaden op dezelfde portal als de telemetrische stijghoogtemetingen. De CTD-diver meet tevens het waterpeil in de regelput. Het waterpeil in de regelput bepaalt hoeveel de kwelvoorziening afvoert. Meestal is dit het oppervlaktewaterpeil want de regelput staat in directe verbinding met het oppervlaktewater.
- De afvoermetingen zijn belangrijke metingen voor het volgen van de werking van de kwelvoorziening. Er wordt daarom ondanks de problemen met de afvoermetingen aanbevolen om de metingen voort te zetten en te zoeken naar een robuust meetsysteem.
- De debietmeters dienen jaarlijks te worden schoon gemaakt.

Grensvlak zoet-zout grondwater

- Het grensvlak tussen het zoete en zoute grondwater wordt jaarlijks gemeten met de EM-SlimFlex (zie sectie 3.3). Dit wordt uitgevoerd door Deltares.
- Er wordt aanbevolen om deze metingen jaarlijks voort te zetten.

3.6.3 VERWERKING, PRESENTATIE EN ANALYSE MEETGEGEVENS

Stijghoogtemetingen

De divergegevens dienen eerst te worden gecorrigeerd voor luchtdruk. Deze gegevens worden van het dichtstbijzijnde KNMI-station onttrokken. De link waarmee de gegevens kunnen worden gedownload is <http://projects.knmi.nl/klimatologie/uurgegevens/selectie.cgi>. Er wordt een gemiddelde bepaald van de drie KNMI-stations: 310 Vlissingen, 319 Westdorpe en 340 Woensdrecht.

Daarna vindt de correctie plaats naar NAP. Als er geen verschuivingen plaatsvinden in de ophanghoogte van Diver, dan is deze correctie snel uit te voeren, namelijk gelijk aan de correctie van de vorige meetronde. De handmetingen geven aanwijzingen of er verschuivingen hebben plaatsgevonden en mocht er een off-set zichtbaar zijn, dan is het vaak op de momenten dat de Divers zijn uitgelezen of dat er een SlimFlex-meting is gedaan.

Deltares voert momenteel de verwerking van de stijghoogtemetingen uit en heeft hier een automatische procedure voor gemaakt in Python. Met het Python-script worden automatisch barometrische gegevens onttrokken via link <http://www.knmi.nl/kennis-en-datacentrum/achtergrond/data-ophalen-vanuit-een-script>, correcties voor luchtdruk en NAP uitgevoerd en grafieken gemaakt. Naast figuurtjes van de grafieken, worden de grafieken ook in HTML-format geëxporteerd. Het grote voordeel van deze HTML-bestanden is dat heel eenvoudig kan worden ingezoomd voor een bepaalde periode om de data nauwkeuriger te bekijken. Deze manier van het verwerken van de grote hoeveelheid gegevens wordt sterk aanbevolen.

In onderstaande figuren (Figure 49 en Figure 50) staat een voorbeeld weergegeven hoe de stijghoogtemetingen het beste gepresenteerd kunnen worden.

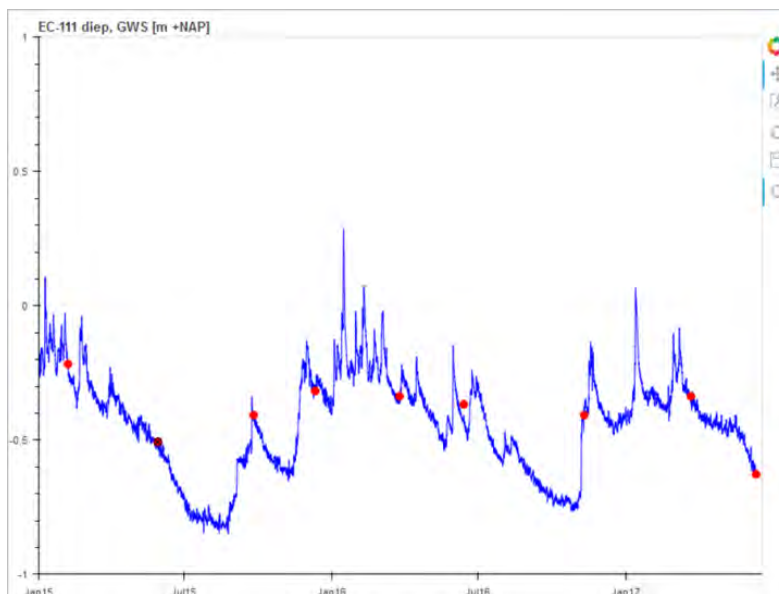


Figure 49. Voorbeeld van presentatie van de stijhoogtemetingen. De blauwe lijn zijn de uurwaarden gemeten met Divers en de rode punten geven de handmetingen weer.

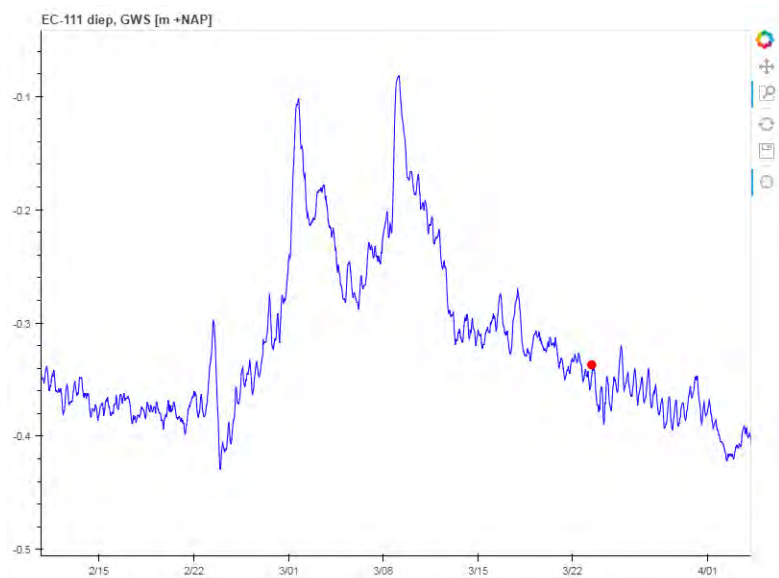


Figure 50. Voorbeeld van presentatie van de stijhoogtemetingen, ingezoomd via de HTML-file.

De stijhoogtemetingen in de nabijheid van de kwelvoorziening geven informatie over de werking van de kwelvoorziening. Met name in de periode rond het open en dichtzetten van de kwelvoorziening kan goed worden bepaald hoe de stijhoogte hierop reageert. Als de stijhoogte naar verloop van tijd minder sterk

daalt of stijgt wanneer de kwelvoorziening respectievelijk wordt open of dicht wordt gezet, is dit een aanwijzing dat de kwelvoorziening minder goed werkt. Op 6 locaties wordt de stijghoogte gemeten en zo kan redelijk nauwkeurig worden bepaald welk deel van de kwelvoorziening niet goed werkt.

Afvoer kwelvoorziening: debiet en zoutgehalte

De debietmeter geeft uurwaarden in liters per uur. Het is aan te bevelen de gegevens te sommeren tot dagwaarden (liter per dag). Dit kan eenvoudig in excel worden uitgevoerd, even als het maken van de grafieken. In onderstaande grafiek staat een voorbeeld weergegeven. Door de regelmatige problemen van de stroomvoorziening, ontstaan er grote gaten in de dataset (zie Figure 51).

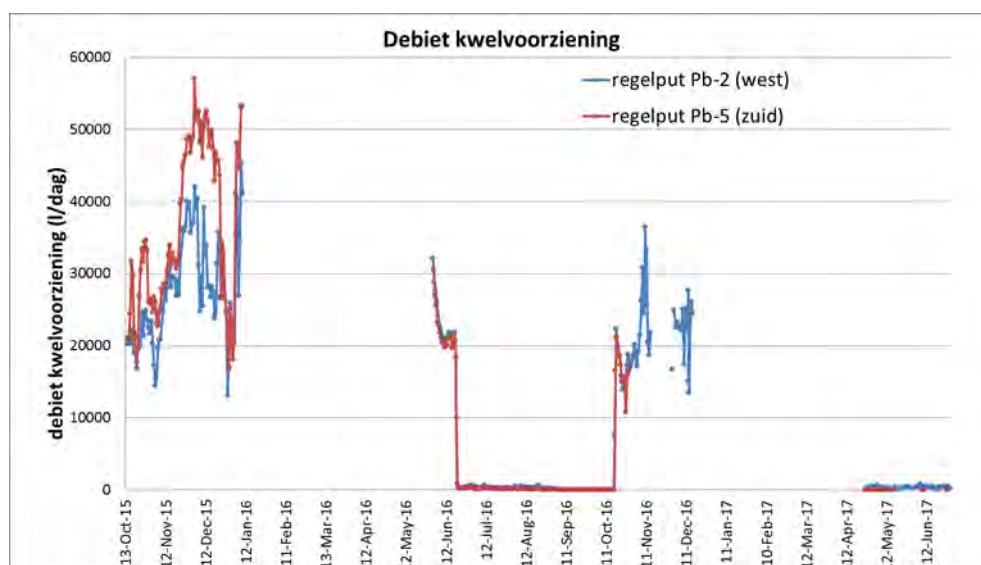


Figure 51. Voorbeeld van presentatie van de debietgegevens van de kwelvoorziening.

Zoals in sectie 3.4 besproken, laat de kwelvoorziening ook een getijdefluctuatie zien, als gevolg van de getijdevariatie van de stijghoogte. De stijghoogte is namelijk de drijvende kracht achter de afvoer van de kwelvoorziening. Daardoor is er ook voor een wat langere periode (gedurende het winterseizoen als de kwelvoorziening open staat), een relatie met de stijghoogte aanwezig (zie bovenstaande figuur). Als de afvoermetingen een dalende trend laten zien, is dat een aanwijzing dat de kwelvoorziening minder goed werkt. Acties zoals het doorspuiten van de kwelbuizen zou dan mogelijk nodig zijn.

De gegevens van het zoutgehalte van de afvoer van de kwelvoorziening kunnen eenvoudig in Excel worden verwerkt tot een grafiek (zie Figure 51). Er hoeven geen correcties worden uitgevoerd. Het is wel belangrijk bij het programmeren van de CTD-diver dat er wordt gekozen voor de optie 'Specifieke elektrische geleidbaarheid'. Effecten van temperatuur op de geleidbaarheid worden dan automatisch gecorrigeerd.

Als de kwelvoorziening open staat, vertoont het zoutgehalte een relatief constant verloop, 35 mS/cm voor de regelput bij Pb5 en 32 mS/cm voor de regelput bij Pb2 (Figure 52). Een dalende trend kan betekenen dat de kwelvoorziening een deel van de zoetwaterlens aan het afvoeren is. Het kan overigens ook betekenen dat de CTD-Diver minder goed functioneert. In het eerste geval, zullen ook de SlimFlex-metingen aanwijzingen geven dat het zoet-zout grensvlak dieper is komen te liggen. In principe betekent het alleen maar goed nieuws als de kwelvoorziening een deel van de zoetwaterlens afvoert, de lens is dan namelijk behoorlijk gegroeid. Er kan dan worden besloten om de kwelvoorziening minder lang open te zetten.

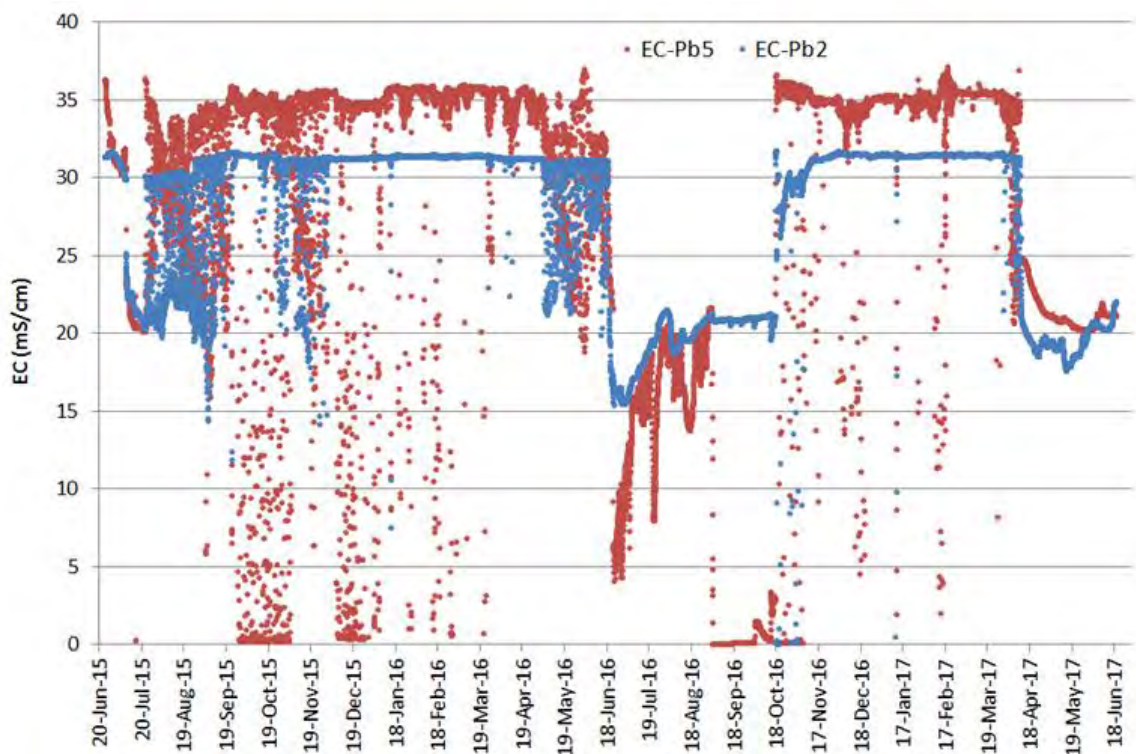


Figure 52. Een voorbeeld van presentatie van het zoutgehalte van de afvoer van de kwelvoorziening.

Grensvlak zoet-zout grondwater

Het grensvlak tussen het zoete en zoute grondwater wordt ieder jaar gemeten (Figure 53). Zoals in sectie 3.4 beschreven, kunnen er bij het uitvoeren van de SlimFlex-metingen onnauwkeurigheden optreden in de

absolute waarde van de meting en de diepteregistratie. Zo goed mogelijk zijn de Slimflex-metingen hiervoor gecorrigeerd wanneer met redelijke zekerheid kon worden aangenomen dat variaties zijn veroorzaakt door bovengenoemde oorzaken. Er wordt bij Deltares gewerkt aan een nauwkeurigere registratie van de diepte en absolute waarden zodat de meting een nauwkeuriger beeld oplevert van de verplaatsingen van het grensvlak. Correcties zijn noodzakelijk om te beoordelen of het grensvlak zich verplaatst. In de onderstaande figuur is te zien, dat er na correctie nog steeds een behoorlijke variatie kan optreden in zowel absolute waarde als de diepte van grensvlak (EC-101). Dit dient met een expertbril te worden beoordeeld, namelijk deze variaties worden door ons ingeschat als het gevolg van de metingen en niet dat ze in werkelijkheid optreden. Met name de meetpunten waar het zoutgehalte ondiep zit (< 6 m), is de variatie groot. De meetpunten met een dieper grensvlak (bijv. EC-106), laat nauwelijks variatie zien. Hier hebben we nog geen verklaring voor gevonden.

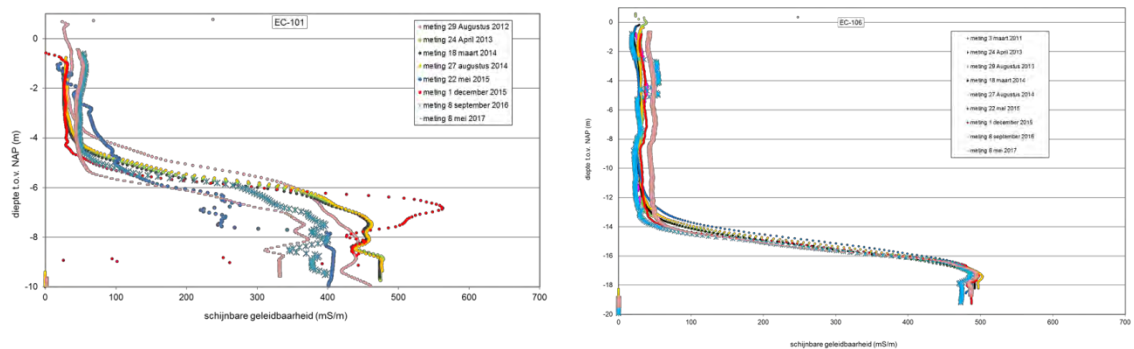


Figure 53. Twee voorbeelden van presentatie van de EM-SlimFlex metingen van het zoet-zout grensvlak. Ten opzichte van EC-106 laat EC-101 een veel grotere variatie in absolute waarden zien en ook enige variatie in de diepte van het grensvlak. Dit is vermoedelijk een meetartefact.

Wanneer er daadwerkelijk significante veranderingen in het grensvlak worden gemeten, dient eerst te worden beoordeeld of dit ook werkelijk gebeurt. Als dat het geval is, dient een mogelijke oorzaak te worden achterhaald. Een dieper grensvlak kan betekenen dat de kwelvoorziening goed werkt, een ondieper grensvlak toont mogelijk aan dat de kwelvoorziening niet voldoende goed werkt. Het wordt aanbevolen om het grensvlak altijd op hetzelfde moment in het jaar te meten. Met name het grensvlak langs de kwelvoorziening kan een grotere variatie vertonen als gevolg van het open (winter) en dicht zetten (zomer) van de kwelvoorziening.

3.7 LANGE TERMIJN EFFECTEN OP ZOETWATERLENS

3.7.1 INLEIDING

Zoals besproken zijn de directe effecten van de ontwikkeling van het getijdegebied en de kwelvoorziening op de stijghoogte relatief eenvoudig uit de meetreeksen te halen. De effecten op de grotere afstand van het getijdegebied manifesteren zich met een vertraging en effecten zijn kleiner, waardoor het veel lastiger is deze uit de meetreeksen te halen. Tijdreeksanalyse biedt soelaas wanneer de reeksen voldoende lang zijn en effecten groter dan enkele centimeters ($\sim > 5\text{cm}$). Nog langzamer gaan de veranderingen van de dikte van de zoetwaterlens.

Om de lange termijneffecten op de zoetwaterlens en in zekere zin ook op de stijghoogte, in beeld te krijgen is een grondwatermodel opgesteld voor een strook van 20 meter breed, loodrecht op het getijdegebied en kwelvoorziening. Het betreft een SEAWAT-model waarbij variabele dichtheidsstroming van water en transport van zout wordt gesimuleerd. Het model is zeer schematisch van opzet om zo conceptueel mogelijk de werking van het grondwatersysteem en de verschillende invloeden in beeld te brengen. Bijvoorbeeld, er is geen ruimtelijke variatie in de geologische opbouw van de ondergrond meegenomen, behalve de aanwezigheid van de zandige kreekkrug waaronder zich de zoetwaterlens heeft gevormd. In Sectie 9.5 staat een uitgebreide beschrijving van de opbouw van het grondwatermodel en worden de resultaten van de simulaties besproken. In deze sectie worden de resultaten samengevat.

3.7.2 OPZET EN SCENARIO'S

In Sectie 9.5 staat de opzet van het grondwatermodel beschreven. De volgende modelscenario's zijn doorgerekend.

- 1 Referentiemodel
- 2 Scenario 1: Invloed van het nieuwe getijdegebied
- 3 Scenario 2: Invloed van het nieuwe getijdegebied met kwelvoorziening, altijd open
- 4 Scenario 3: Invloed van het nieuwe getijdegebied met kwelvoorziening, winter open en zomer dicht

Allereerst is een referentiemodel opgebouwd waarbij de vorming van de zoetwaterlens als gevolg van jarenlange infiltratie is gesimuleerd. Een periode van 750 jaar is doorgerekend en na 500 jaar bleek de zoetwaterlens in evenwicht met de randvoorwaarden. Er heeft een uitgebreide gevoeligheidsanalyse en kalibratie plaatsgevonden om zo goed mogelijk de stijghoogte en dikte van de zoetwaterlens te benaderen. De stijghoogte- en zoutverdeling na 750 jaar zijn als begincondities voor de verdere scenariomodellen ingevoerd.

In scenario 1 wordt het effect van het nieuwe getijdegebied doorgerekend. De effecten op de zoetwaterlens worden na 1, 5, 25 en 100 jaar bepaald. Scenario 2 is gelijk als scenario 1, alleen dan met de kwelvoorziening altijd open en met scenario 3 wordt de kwelvoorziening in de winter open en in de zomer dicht gezet.

3.7.3 RESULTATEN

De resultaten staan uitgebreid in Sectie 9.5 beschreven. Hieronder de belangrijkste bevindingen.

- Op lange termijn (na 100 jaar) heeft het nieuwe getijdegebied een zeer groot effect op de zoetwaterlens (scenario 1). Tot op 1500 m afstand van het getijdegebied is de zoetwaterlens afgenomen (1-3m). Voor de eerste 700 m is de lens zelfs helemaal verdwenen na 100 jaar.
- De korte termijn effecten (< 5 jaar) zijn nauwelijks zichtbaar maar na 25 jaar is de lens zichtbaar gekrompen met > 50% voor de eerste 500 m.
- De kwelvoorziening compenseert de effecten goed. Wanneer de kwelvoorziening het hele jaar open staat (scenario 2) is na 25 jaar de lens overal even dik als in de situatie dat er geen getijdegebied zou zijn. Alleen de eerste 500 m vanaf het getijdegebied neemt de lens iets in dikte af (~1m). Na 100 jaar is de lens is iets meer gekrompen tov de referentiesituatie, namelijk maximaal 2-3 m.
- Wanneer de kwelvoorziening in de winter wordt opengezet en in de zomer wordt dichtgezet, is het mitigerende effect significant minder. Dit scenario laat zien dat de kwelvoorziening het beste het hele jaar open kan worden gezet.
- De modelscenario's laten zien dat het laten groeien van de lens door de kwelvoorziening niet mogelijk blijkt te zijn. De effecten van het getijdegebied zijn toch groter dan op voor hand gedacht. De resultaten tonen aan dat de kwelvoorziening essentieel is om de zoetwaterlens te behouden en te beschermen.
- Er dient te worden opgemerkt dat het grondwatermodel een (semi)2D-opzet betreft met de aanname dat effecten zich uitsluitend loodrecht op het getijdegebied en kwelvoorziening manifesteren. Mogelijk zijn de werkelijke 3D-effecten (iets) kleiner door het meer diffuse karakter hiervan.

3.8 CONCLUSIES EN AANBEVELINGEN

3.8.1 CONCLUSIES

Gedurende het jaar 2015 is de kwelvoorziening gereedgekomen, is het meetnet uitgebreid ten behoeve van de kwelvoorziening en is op 25 juni het nieuwe getijdegebied in werking getreden. Op basis van de meetresultaten kunnen de volgende conclusies worden getrokken.

- Met de uitbreiding van het meetnet rondom de kwelvoorziening voldoet het meetnet aan alle monitoringdoelen (vervolgmonitoring effecten en monitoring werking kwelvoorziening). Er is geen aanleiding om de monitoringcampagne te veranderen.
- De directe zichtbare effecten van het nieuwe getijdegebied manifesteren zich duidelijk in de stijghoogte op de rand van het landbouwgebied (ter hoogte van de kwelvoorziening) en voor enkele meetpunten in het landbouwgebied op korte afstand van het getijdegebied (< 100 m). Ook zijn directe effecten op de freatische grondwaterstand zichtbaar. Er dient te worden opgemerkt dat het hier directe zichtbare effecten betreffen, langere termijneffecten op de stijghoogte die op grotere afstand van het getijdegebied plaatsvinden, kunnen niet uit de huidige meetreeksen worden gehaald. Daarvoor zijn langere meetreeksen nodig die met behulp van tijdreeksanalyse moeten worden geanalyseerd.
- De lange termijneffecten op de zoetwaterlens zijn bepaald met een grondwatermodel. Zonder kwelvoorziening zou de lens voor de eerste 700 m vanaf het getijdegebied, helemaal zijn verdwenen. De kwelvoorziening compenseert de effecten zeer goed, na 25 jaar wordt praktisch dezelfde lens gevonden als zonder getijdegebied. Na 100 jaar is de lens iets dunner (2-3 m).
- De SlimFlex-metingen laten 3.5 jaar na het ontstaan van het getijdegebied geen veranderingen zien in het zoet-zout grensvlak als gevolg van de het nieuwe getijdegebied. Dit is conform de modelresultaten; met de kwelvoorziening zijn er geen veranderingen in het grensvlak waargenomen.
- De metingen van de stijghoogte tonen aan dat de kwelvoorziening goed werkt. De stijghoogte kan ter plaatse van de kwelvoorziening meer worden verlaagd dan nodig is, waardoor mogelijk de zoetwaterbel zou kunnen groeien. Echter, de modelresultaten tonen aan dat de lens op langere termijn niet groeit en zelfs na 100 jaar iets krimpt. Echter, zonder kwelvoorziening zou de zoetwaterlens over 100 jaar voor bijna de helft zijn verdwenen. Hierbij dient te worden opgemerkt dat de effecten zijn bepaald met een (semi) 2D-grondwatermodel en dat daardoor de effecten mogelijk zijn overschat.
- Op basis van de metingen, het testen met de kwelvoorziening en de grondwatermodellering wordt aanbevolen om de kwelvoorziening altijd open te laten staan. Het zomers dichtzetten van de kwelvoorziening heeft een negatieve invloed op de zoetwaterlens op de lange termijn (> 25 jaar).

3.8.2 AANBEVELINGEN

- Spindel-afsluiter bij regelput dp-B1 (aan kant van de Westerschelde) is kapot en deze dient zo spoedig mogelijk te worden gerepareerd.
- De afvoermeting in debietput bij pb2 loopt niet goed. Gezien de regelmatig terugkerende problemen wordt aanbevolen de debietmetingen te stoppen.

- Inspectie van het meetnet dient regelmatig plaats te vinden om tijdig kapotte meetpunten te signaleren. Herstelwerkzaamheden dienen dan zo snel mogelijk plaats te vinden.
- Momenteel zijn de peilbuizen in slechte staat. Het is verstandig alle peilbuizen na te lopen en ze te voorzien van een stalen koker ter bescherming. Ook alle Divers dienen met nieuw draad robuust te worden opgehangen.
- Bij de laatste meetronde in november 2018 bleken 2 Divers kapot (EC102-diep en EC106) en 1 peilbuis met Diver te zijn verdwenen (EC119-diep). Het meetpunt en de Divers dienen zo spoedig mogelijk te worden vervangen.
- Er is schade aan de kwelbuizen en regelputten geconstateerd. Deze schade dient te worden hersteld.
- Tijdreeksanalyse op langere meetreeksen is nodig om niet-direct zichtbare effecten uit de reeks te kunnen filteren. De vervaardigde tijdreeksmodellen kunnen steeds opnieuw worden gebruikt om effecten uit de steeds langer wordende tijdreeksen te analyseren.

3.9 EXTENDED ABSTRACT

The concept and first results of the mitigation measure SeepCat to protect the freshwater lens of Kloosterzande were presented at the SWIM-APCAM conference in Cairns 2016. The extended abstract is given below (In Werner, A.D. (ed.) (2016), Proceedings of the 24th Salt Water Intrusion Meeting and the 4th Asia-Pacific Coastal Aquifer Management Meeting, 4-8 July, 2016, Cairns, Australia).

A self-flowing seepage system to protect a freshwater lens from local sea level rise

ABSTRACT

To restore tidal salt marshes along the Westerschelde (estuary of the North Sea) agricultural land (75 ha) was given back to the sea. A self-flowing seepage system was installed at the border of this new tidal area and the adjacent agricultural area to protect a precious freshwater lens which is used for irrigation. Monitoring results showed that the seepage system is functioning well and that it will even be possible to let grow the freshwater lens.

INTRODUCTION

About 25% of the Netherlands is situated below sea level and pumps are needed to keep the area dry for living and agriculture. These areas are called 'polders'. The first polders originate from around 1000 AD when the reclamation of land from the sea and lakes started in the Dutch coastal area. Below these polder areas, saline groundwater is often found at shallow depth. Freshwater is only found in lenses below sandy dunes or higher elevated fossil creek ridges (Pauw et al., 2015). In the low-lying reclaimed salt marshes, upward seepage of saline groundwater prevents the infiltration of rainwater resulting in very thin rainwater lenses (De Louw, 2013).

The last few years, the opposite of reclamation is happening (de-reclamation); i.e. vulnerable agricultural land is given back to the sea to restore tidal salt marshes. In the southwestern part of The Netherlands, a 75 ha agricultural area called Perkpolder was turned into tidal salt marshes (Figure 1). At 25th of June 2015 the open connection to the sea was realized. The average water level for this new tidal area changed from polder water level (1.0 m below sea level) to average sea level and consequently will affect the groundwater system in the adjacent agricultural area. This can be seen as a local sea level rise of about 1.5 m. Since 2010, hydraulic heads and the fresh-saline interface is being monitored to capture the reference situation and to determine possible effects resulting from the development of the new tidal area.

Below the adjacent agricultural area, a freshwater lens of about 10 to 15 meters provides farmers with fresh groundwater for irrigating their crops. In order to protect this freshwater lens from shrinking, a self-flowing seepage system was designed and installed to compensate the effects resulting from this local sea level rise. In this paper, we will describe the design of this mitigation measure and the monitoring results showing that the self-flowing seepage system is functioning well.

METHODS

The freshwater lens below the agricultural area is one of the Badon Ghyben Herzberg type and will eventually shrink when hydraulic heads below the lens increase caused by the local sea level rise. The task of the self-flowing seepage system is to release the increased pressure in the aquifer preventing the freshwater lens to decrease in size.

The self-flowing seepage system consists of 61 vertical seepage wells with 5-10 m long screens, installed in the aquifer at 12 to 17 m depth. The distance between the wells is 15 to 20 m and the total length of the seepage system is 1100 m. The vertical seepage wells are connected in the subsoil with horizontal tubes which end up in control units. The hydraulic head gradient (Δh) can be regulated by raising or lowering the water level in the control unit using weirs. In this way the discharge of the seepage system can be regulated. Since the hydraulic head in the aquifer is higher than the surface water level in the control unit and ditch, seepage wells are artesian and self-flowing and no pumps are needed to extract the groundwater from the aquifer. The extracted seepage water is discharged into the surface water system and transported to a pumping station (at 1 km) where it is pumped out of the polder into the sea.

A detailed monitoring network was installed for three reasons: (1) monitoring the effects of the new tidal area on the groundwater system in the adjacent agricultural area, (2) monitoring the functioning of the seepage system, and (3) to inform the farmers. At 21 locations the hydraulic head in the aquifer is measured every hour with automatic monitoring devices ('Diver'). At 15 locations the fresh-saline interface (salinity – depth profile) is measured every half a year with the EM-SlimFlex. The discharge of the seepage system as

well as the salinity is measured every hour in two control units which are connected to 3 and 7 seepage pipes.

RESULTS

The tidal fluctuation of the hydraulic head increased from 10 cm (before 25 June) to 60 cm (after 25 June) resulting from the local sea level rise (development of the new tidal area). The increase of the daily mean hydraulic head was 16 cm. The seepage system was closed during the first month to determine direct effects of the local sea level rise where after the seepage system was thrown open. This resulted in a decrease of about 29 cm of the daily mean hydraulic head which show that the hydraulic head could be reduced more than the effects of the local sea level rise which is more than needed. Direct effects in the agricultural area due to the new tidal area and seepage system were only detected for monitoring points within 100-200 m from the tidal area.

The measured average discharge of the seepage system was over the period October – December 2015 410 m³/day and the average salinity was 35 mS/cm. As expected, the EM-SlimFlex measurements in December 2015 didn't show any changes in fresh-saline interface due to the development of the new tidal area. Changes of salinity are induced by transport processes which are far more slowly than changes in hydraulic head caused by pressure transfer.

DISCUSSION AND CONCLUSIONS

From the measurements it was concluded that the seepage system was functioning well enough to compensate the effects of the new tidal area. Moreover, the seepage system could also be used to let grow the freshwater lens by extra lowering the hydraulic head during times of precipitation surplus. Further research (model calculations) will be carried out to verify this and to optimize the regulation of the seepage system.

The situation in Perkpolder which is giving agricultural land back to the sea, can be seen as a local sea level rise for the adjacent area. The Perkpolder can therefore be used as a field laboratory where effects of sea level rise are measured and mitigation measures for sea level rise are tested. Since the system is technically and geohydrologically working well, it could also be applied in other coastal areas, like small ocean islands. Their vulnerable freshwater lenses are seriously threatened by the expected future sea level rise. The seepage system could help to protect their precious freshwater resources.

4 VEGETATION AND SEDIMENT DEVELOPMENT

4.1 INTRODUCTION

The time it takes before vegetation will develop is a key question in many managed realignment (i.e. “ontpoldering”) projects. It is often clear that in tidal areas with sufficiently high sediment concentrations in the water column, marshes will eventually develop. However, for nature development goals and recreate activities in the area, it is desirable to be able to forecast at what time scale these goals are met (Figure 54). It matters to managers and the public perception if ecosystems develop quickly e.g. within less than 5 years, or if this takes much longer, for instance more than 30 years. Being able to better predict the rate of development is desirable to come up with a cost-effective design when a specific type of habitat is required either from nature management perspective (e.g., in case for compensation measures or when public support depends on the type of nature that will develop). To answer this question requires an understanding of the processes that control (i.e., enable and hamper) the initial establishment and subsequent lateral expansion of pioneer species.

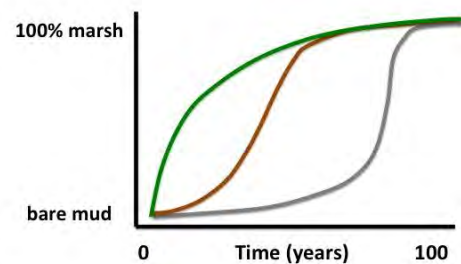


Figure 54. Artist impression of the development of Perkpolder next to the recreation housing (left; <http://www.vnsc.eu/uploads/cache/perkpolder-hulst-1.jpg>) and a schematic drawing raising the question how long it will take before this situation is realised (right).

It is well known that the initial vegetation development depends on a number of abiotic and biotic factors. For example, inundation period, and thus the intertidal elevation, is a major factor controlling seedling survival. Recently, it was shown that short-term mixing of the sediment due to hydrodynamics (e.g. waves) is another important factor that may limit seedling survival to the higher elevations (Bouma et al. 2016; Hu et al. 2015). Much less is however known about how abiotic and biotic ‘sediment’ properties like compaction, drainage, sediment chemistry and bioturbation may affect seedling establishment and lateral expansion. The characteristics and development of the accreting sediment may be expected to be an important factor for the vegetation establishment. As schematised in Figure 55, differences in drainage and sediment compaction may be the driver of two alternative stable states, determining if seedlings establish or not

(Figure 55). From previous projects in the Westerschelde and Zeeschelde it is to be expected that managed realignments result in relatively fast bed level accretion. For instance, sediment accretion followed the construction of groins by Waarde and the managed realignment of Paardenschor and Lillo-Pot project sites. Thus, managed realignment areas are likely to experience high rates of sediment accretion, but will have low rates of soil compaction in the first years of development. As a consequence, tidal marsh development may be lagged as the area is more likely to maintain a poor drained and soft mud.

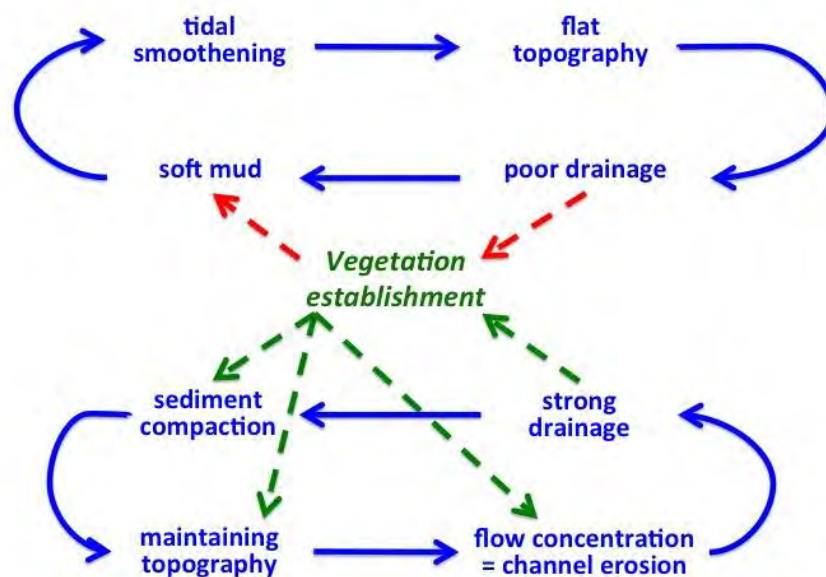


Figure 55. Schematisation of two positive feedback loops, showing how lack of drainage may cause bare tidal flats to remain bare, and drained tidal flats to rapidly develop vegetation.

In this study, we aim to develop generic insights into the factors that control the development rate of sediment and vegetation (i.e., including both establishment and lateral expansion), by answering the following questions:

1. How do abiotic and biotic sediment properties affect seedling survival and lateral expansion
 - Hoe bepalen abiotische en biotische sediment eigenschappen zaailing overleving en laterale uitgroei?*
 - a. *Wat is het interactieve effect van hoogte ligging x bulk-dichtheid (compactie) x drainage*
 - b. *Wat is het effect van bodemchemie? (wordt onderzocht als matching vanuit BE-SAFE project)**
 - c. *Wat is de invloed van bioturbatie? (op het NIOZ uit te voeren studenten onderwerp) **
- *NOTE – As indicated in the original quote, we focus our research on question 1a, as more is already known about 1b and 1c.*

2. How do these abiotic and biotic sediment properties (that affect vegetation establishment) develop over time, and how does this depend on location within Perkpolder?

Hoe ontwikkelen de abiotische sediment eigenschappen die van invloed zijn op zaailing overleving en laterale verspreiding zich binnen Perkpolder?

- a. *Hoe ontwikkelen deze factoren zich in de tijd?*
- b. *Zijn er ruimtelijke patronen te ontdekken in relatie met afstand tot geul / dijk*

3. What is the role of seed availability and seed dispersal for the vegetation development? *

**NOTE – As indicated in the original quote, this is additional work that will only be done if there are sufficient students available to carry out the work*

Wat is de rol van de zaadbeschikbaarheid en zaadverspreiding voor de potentiële vegetatie ontwikkeling?

- a. *Is de zaadaanvoer naar het gebied voldoende om kolonisatie mogelijk te maken?*
- b. *Is er genoeg zaad-retentie en begraving om kolonisatie van alle delen mogelijk te maken?*

4. What is the pattern of colonisation and lateral expansion by pioneer species, along the elevational gradient?

Hoe verloopt de kolonisatie en laterale verspreiding door pionier soorten langs de hoogte gradiënt:

- a. *Is de ontwikkelde Windows of Opportunity theorie te gebruiken om te voorspellen welke delen begroeid raken?*
- b. *Wat is het relatieve belang van zaadverspreiding versus klonale verspreiding voor de kolonisatie in de ruimte?*

Table 8. original time plan as presented in the project plan

	vraag 1A*	vraag 1B**	vraag 1C**	vraag 2A	vraag 2B	vraag 2C	vraag 3A**	vraag 3B**	vraag 4A	vraag 4B-monitor	vraag 4B-exp.	lab work
	mega marsh organs	exp's chemie	exp's bioturbatie	sedimentation	sediment properties	soil chemistry	netten	matten & bodem	vegetatie & inundatie	laterale uitgroei	Spartina & Aster planten	
Mar-15												
Apr-15												
May-15												
Jun-15			studenten**									
Jul-15			studenten**									
Aug-15			studenten**	X	X	X			X	X		X
Sep-15												
Oct-15												
Nov-15				X	X	X			X	X		X
Dec-15												
Jan-16	order											
Feb-16	construct			X	X	X			X	X		X
Mar-16	construct											
Apr-16												
May-16	exp			X	X	X			X	X		X
Jun-16	exp	studenten**										
Jul-16	exp	studenten**										
Aug-16	exp	studenten**		X	X	X	studenten**	studenten**	X	X		X
Sep-16	exp											
Oct-16							studenten**	studenten**				
Nov-16				X	X	X			X	X		X
Dec-16							studenten**	studenten**				
Jan-17												
Feb-17				X	X	X	studenten**	studenten**	X	X		X
Mar-17												
Apr-17												
May-17			studenten**	X	X	X	studenten**	studenten**	X	X	X	X
Jun-17			studenten**									
Jul-17			studenten**								X	
Aug-17				X	X	X			X	X		X
Sep-17												
Oct-17												
Nov-17				X	X	X			X	X		X
Dec-17												
Jan-18												
Feb-18				X	X	X			X	X		X
Mar-18												
Apr-18												
May-18				X	X	X			X	X		X
Jun-18												
Jul-18												
Aug-18				X	X	X			X	X		X
Sep-18												
Oct-18												
Nov-18				X	X	X			X	X		X
Dec-18												

* bestelling kan pas worden geplaatst na dat getekend contract is ontvangen; opbouw kan pas na levering (levertijd ca. 4 wkn na bestelling)
 ** door budget beperkingen alleen mogelijk indien er voldoende studenten beschikbaar zijn

4.2 RESULTS

GENERAL REMARKS AND READING GUIDE

In the Perkpolder project, the NIOZ has worked on four question. Question one focusses on seedling survival and lateral expansion and are reported first. The experiments focussing on the seedling survival experiments as the results of sediment dynamics are published (Cao et al, 2018). To address the second question on the development of abiotic conditions over time a consistent local and spatial sampling survey of the area has been conducted. Again, results are written down in a manuscript and prepared for publication. Questions three and four on the role of seeds availability and dispersal and the patterns of colonisation along the elevation gradient will be discussed thereafter.

Per question a conclusion is given. At the end of the report a summary in the form of bullet point with conclusions can be found.

4.2.1 Research question 1

How do abiotic and biotic sediment properties affect seedling survival and lateral expansion?

MESOCOSM EXPERIMENT 1 - effect of sediment accretion and erosion on seedling survival

To quantify how seedling survival been affected by short-term sediment dynamics, we manipulated a mesocosm experiment. We used a large range of accretion/erosion rates to represent potential short-term sediment dynamics. To quantify the importance of having a disturbance-free period preceding accretion/erosion events, we applied two levels of initially disturbance-free periods: two and nine days.

Spartina anglica seeds were collected from the Oosterschelde estuary and were air-dried and stored over winter in a 4 °C refrigerator with sea water from Oosterschelde estuary until the start of the experiment. The obtained seedlings were planted with an intact seed coat (to avoid damage when transplanting) into salt marsh sediment at 1 cm depth below the surface in individual PVC pots (practical choice, cf. Broome et al., 1974; Schwarz et al., 2015; Bouma et al., 2016). The pots (160 mm height and 110 mm inner diameter) were made from PVC pipes, with open bottoms that allowed for accretion/erosion treatments (see Han et al. 2012 for seagrasses, Balke et al. 2013 for mangroves). Within the pots, punctured polyethylene bags were used to line the bottom, allowing for drainage without losing the sediment. The sediment ($D_{50} = 31.58\mu\text{m}$) used in the pots was collected from the top 20 cm of a salt marsh pioneer mudflat near Rilland-Bath, Oosterschelde estuary, the Netherlands. To prevent possible seedling loss due to grazing by benthic macro-invertebrates (Emmerson, 2000), all collected sediment was put under airtight and waterlogged conditions for two weeks to kill the macrobenthos. Ten randomly chosen pots were sieved to ensure that this treatment was long enough to indeed kill all worms. The pots with sediment were watered with a mix of freshwater and water from the Oosterschelde that had a salinity of 15.8 ppt. All the pots were then left for a week to settle the sediment before adding the seedlings. The unoccupied volume on the top of the pots due to compaction was then replenished with some sediment before the seedlings were planted. The pots with buried seedlings were then transferred to the mesocosms described below.

We used 10 mesocosms, each consisting of 2 big tanks (with inner dimensions 110 × 95 × 60 cm) on top of each other (Figure 56): a top tank that contained pots with plants and was used for tidal inundation, and a bottom tank that served as a water reservoir during low tide. The lower tanks were filled with the prepared brackish water as mentioned above. The pumps in the lower tanks were operated by a timer to flood the upper 'experimental' tanks. An overflow return pipe was used to control inundation height, by providing return-flow of excess water to the lower tank. When the pump was switched off, the upper tank drained via the pump, causing a low tide in the upper 'experimental' tanks. The tidal regime was set by the timer for a semi-diurnal 1.5 h flooding of 50 cm in height in the upper tanks (3 h per day in total), thereby simulating the regular tidal regime of the pioneer zone in salt marshes (Schwarz et al., 2015).

Light to the mesocosms was provided by suspended fluorescent tubes arranged in parallel over the tanks (Figure 56) with 12 h d^{-1} ($550 \mu\text{mol m}^{-2} \text{ s}^{-1}$ PAR), and the temperature was thermostatically controlled in the climate room and maintained at $25 \text{ }^\circ\text{C}$ during the day time and $18 \text{ }^\circ\text{C}$ during night, which is approximately equivalent to the temperatures during seedling establishment in April and May at the field sites (Schwarz et al., 2011).



Figure 56. Photograph of the mesocosms setup.

The pots containing seedlings and the various accretion/erosion treatments were randomly assigned to the 10 upper mesocosm tanks. To compare the response of seedlings in the two different disturbance-free period groups, the two groups of seedlings were given a respite from regular artificial flooding in the mesocosms for 2 and 9 days, respectively, representing the 2- and 9 day disturbance-free periods after germination. These two initial disturbance-free periods were chosen from among the durations of rest periods in a spring-neap tidal cycle, which have been considered to potentially provide windows of opportunity for pioneer seedling settlement (Boorman, 1999; Friess et al., 2012; Balke et al., 2014; Bouma et al., 2014).

Two groups of sedimentation treatments were imposed weekly on seedlings and run for 6 weeks (Table 9): i) “Constant Rate (CR)” consisting of constant net accretion/erosion rates; ii) “Intermittent Supply (IS)” consisting of variable timing and amplitude of accretion/erosion events, in such a manner that the net cumulative changes were identical for all treatments. In total, we applied 1 control, 8 CR treatments, 6 IS treatments (with 2 overlaps with CR treatments) (Table 9). Sediment erosion and accretion events were mimicked by adding or removing sediment from the top of the pots on a weekly basis (Figure 57; see Han et

al. 2012 for seagrasses; Balke et al. 2013 for mangroves). Erosion was simulated by adding 3-mm-thick discs (1-6 discs according to the treatments, i.e., 3 to 18 mm erosion, see Table 9) underneath the pots and gently removing the pushed-up sediment by using a water spray (Figure 57. Schematic diagrams showing erosion and accretion treatments). Accretion was simulated by removing discs that had been previously placed at the bottom of the pots and adding sediment on top around the plants (Figure 57. Schematic diagrams showing erosion and accretion treatments). The previously placed polyethylene bags in the pots enabled us to smoothly lift the sediment cores up and down in the pots without affecting the roots.

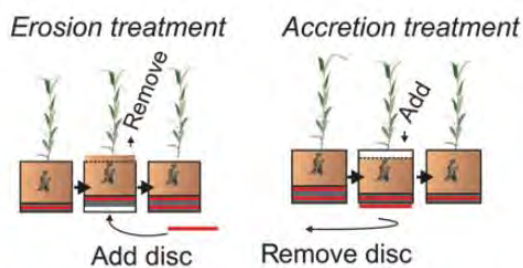


Figure 57. Schematic diagrams showing erosion and accretion treatments.

Each sediment treatment was applied to 12 replicated seedlings per disturbance-free period group (2 days vs. 9 days). All treatments and replicates were randomly assigned to the 10 mesocosms. Survival of the seedlings was surveyed weekly and recorded as surviving, toppled (seedlings that had toppled over but still had visible live shoots or leaves) or dead. Immediately after the weekly monitoring had been completed, the next treatment was applied according to the schedule (Table 9).

Table 9: Sedimentation treatments every week during the 6-week course of the mesocosm experiments.

Treatment type		Treatments in 6 weeks (mm)						Total (mm)
		Week 1	Week 2	Week 3	Week 4	Week 5	Week 6	
Control	CK	0	0	0	0	0	0	0
Constant Rates treatments (CS)	CR-18	-18	-18	-18	-18	-18	-18	-108
	CR-12	-12	-12	-12	-12	-12	-12	-72
	CR-6*	-6	-6	-6	-6	-6	-6	-36
	CR-3	-3	-3	-3	-3	-3	-3	-18
	CR+3	3	3	3	3	3	3	18
	CR+6**	6	6	6	6	6	6	36
	CR+12	12	12	12	12	12	12	72
	CR+18	18	18	18	18	18	18	108
Intermittent Supply treatments	IS-18	-18	0	0	-18	0	0	-36
	IS-12	-12	0	-12	0	-12	0	-36
	IS-6*	-6	-6	-6	-6	-6	-6	-36
	IS+6**	+6	+6	+6	+6	+6	+6	+36
	IS+12	+12	0	+12	0	+12	0	+36
	IS+18	+18	0	0	+18	0	0	+36

'-' and '+' represent erosion and accretion, respectively; '*' and '**' identify the same group of seedlings that were used in our experiments because of the overlapping design.

4.2.1.1 MAIN RESULTS AND CONCLUSION

Among all the treatments, the control (i.e., without any accretion/erosion treatments) resulted in the highest survival rates (100%) throughout the mesocosm experiment (Figure 58a & b). For all the treatments, Cox regression analysis showed that the accretion/erosion-treatments significantly affected the survival of seedlings ($p < 0.01$). The erosion treatments resulted in higher chances of toppling and mortality, on average, than the accretion treatments (Figure 58 a & b).

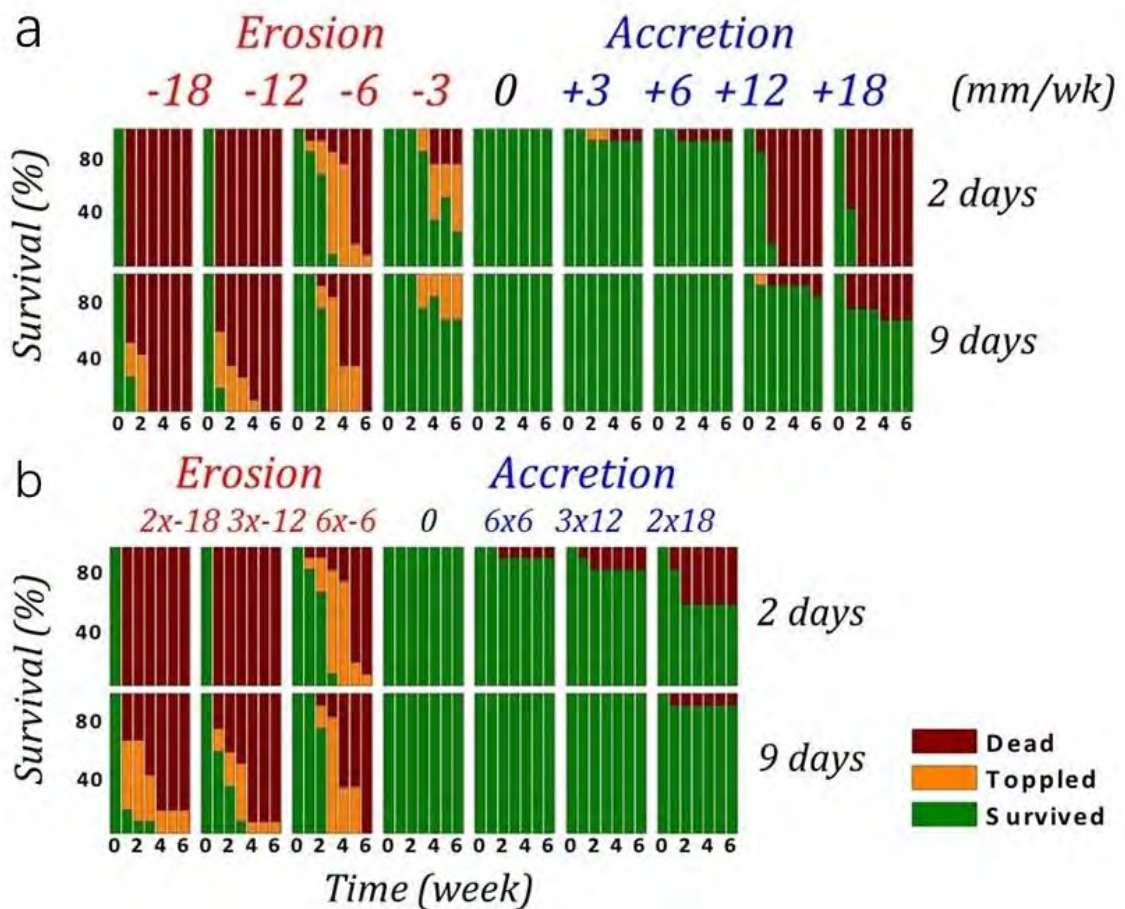


Figure 58. Percentage of surviving, toppled and dead seedlings during the mesocosm experiments. (a) Constant Rate (CR) treatment groups, (b) Intermittent Supply (IS) treatment groups

When focusing on the effects of specific accretion/erosion treatments, it is clear that in the CR (Figure 58a) and IS treatment groups (Figure 58b), the hazards for *Spartina* seedlings became larger with increasing amplitude of the (erosion or accretion) application. Thus, a smaller amplitude in the accretion/erosion treatments resulted in higher survival.

The importance of having a disturbance-free period was studied by comparing seedlings that had reached different disturbance-free times before the first accretion/erosion event was applied. As expected, the survival of seedlings with a 9-day disturbance-free period was found to be significantly higher than that of seedlings with a 2 day disturbance-free period in both CR and IS treatment groups (Figure 58a & b).

MESOCOSM EXPERIMENT 2 - effect of sediment-type & drainage on seedling survival

A mesocosm study has been carried out to quantify the effect of sediment-type (Perkpolder sediment vs. sediment collected at 2 locations in Rammegors) and drainage on seedling survival. The results show that

poor drainage reduce the seedling survival at Perkpolder. The detailed results are available in a student report from Annick van der Laan (University Utrecht), which forms the base for a paper that is currently published.

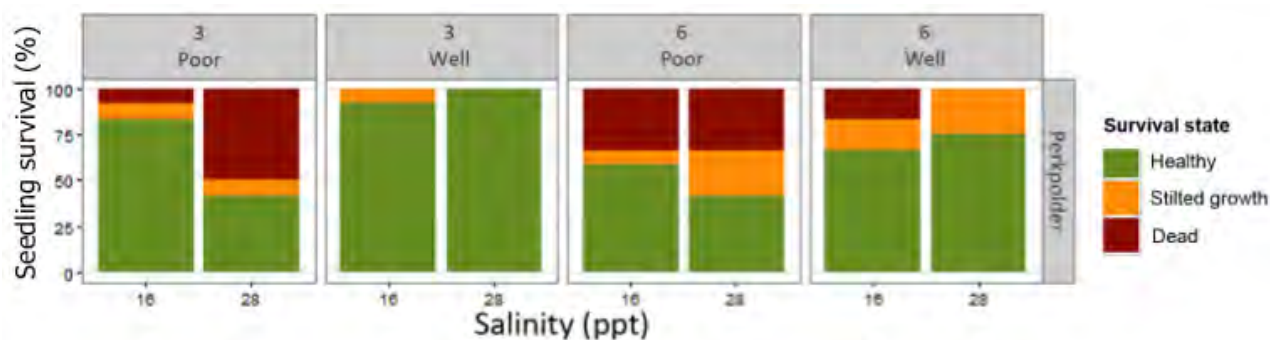


Figure 59. *Spartina* seedling survival in response to salinity (15 PPT versus 28 PPT) and drainage (poor vs. well drained) and inundation period (3 hours per tide vs. 6 hours per tide).

MEGA-MARSH ORGAN EXPERIMENT 1 (MMO-1-2016) – effect of drainage and elevation on plant survival

To investigate the influence of sediment drainage in relation to inundation time on seedling survival for different age class, we manipulated a seedling establishment in the grow season of 2016. Seedlings of *S. anglica*, which is a dominant pioneer species in this part of the estuary, were germinated in a climate chamber kept at 25 °C during the day and 30 °C during the night. Before germination, seeds were soaked in sea water. Fresh water was then used to accelerate germination and to avoid seedlings drying out. All seeds with a visible sprout were identified as seedlings, transplanted to a tray filled with sandy mud in a climate room and watered regularly until they were transplanted into the MMOs in the field. To compare seedlings of different age classes, three batches of seedlings were germinated before transplanting (1-year-, 3-month- and 1-week-old age classes).

MMOs (Figure 60) were used as field mesocosms to study seedlings survival in our study. Each MMO consists of two adjacent boxes (inner dimensions of 75 × 45 × 30 cm each). The design was inspired by but modified and scaled up from the original marsh-organ concept, as introduced by Morris (Morris, 2007; Kirwan and Guntenspergen, 2012; Voss et al., 2013). These original MMOs consisted of narrow PVC pipes used to test growth response in relation to inundation. To identify the potential effects of drainage on seedling survival, one of the two boxes was assembled with a drainage system that facilitates dewatering of the sediment boxes after tidal inundation (Figure 60c). In total, 12 MMOs (i.e., 24 boxes in total, 12 drained & 12 without drainage) were set up on the bare tidal flat at Perkpolder. These MMOs were placed at four elevations (0 cm, 30 cm, 60 cm and 90 cm above MSL, with an inundation duration of 56%, 49%, 45% and 41%,

respectively) with three replicates per elevation (Figure 60d & e). Ten days prior to planting, all boxes were filled with local soft tidal mud (D50 = 27.62m) to allow for natural compaction. The boxes were replenished on the day before transplanting the seedlings.

Before transplantation into the MMOs, seedlings were then carefully washed out from the sediments in which they had germinated in the lab and transplanted within 12 hours. The roots of all seedlings were planted to the depth of 1 cm (practical choice) in the sediment. In order to address the potential competition between relatively big individual plants, we used 6 replicates for the 1-year-old seedlings, 6 replicas for the 3-month-old seedlings and 12 replicas for the 1-week-old seedlings within every experimental treatment group. The experiment was set up in July 2016. A sheltered location was selected (Figure 60a & b), where hydrodynamic forces were not strong enough to disturb our MMO setups and sediment accretion/erosion rates were negligible for the short duration of this experiment. As we did not want to disturb the survival conditions for the potentially vulnerable seedlings in the MMOs by other measurements, only the survival of seedlings was recorded every week during the following 6 weeks. A 6-week period was chosen as experimental period, since age effects were accounted for by planting seedlings of different age classes, rather than by extending the time of the experiment.

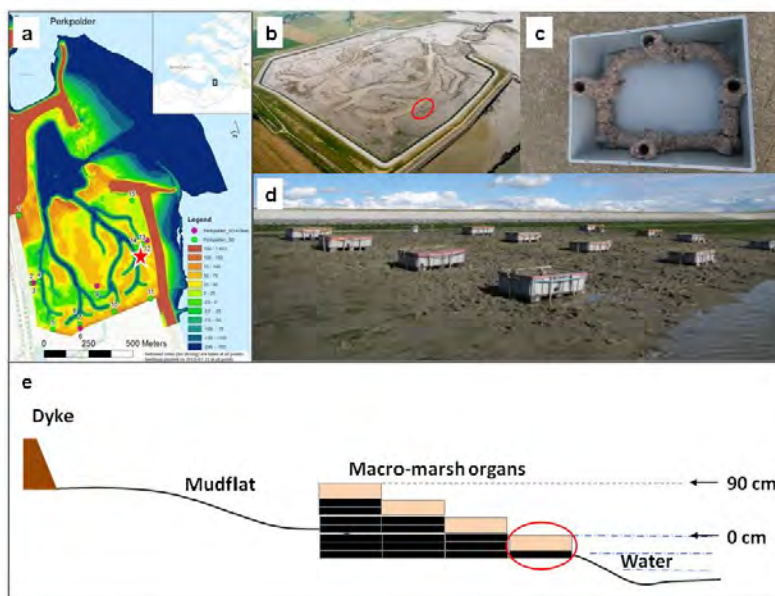


Figure 60. The location of Perkpolder and the Mega-Marsh-Organs (MMO) set up. **A)** the location of MMO within Perkpolder; **B)** an aerial view of Perkpolder, the red star in A and red circle in B shows where the MMO's have been set up; **C)** drainage system for dewatering in one of the drained MMO boxes; **D)** picture of the MMO in the field; and **E,** schematic of MMO set up.

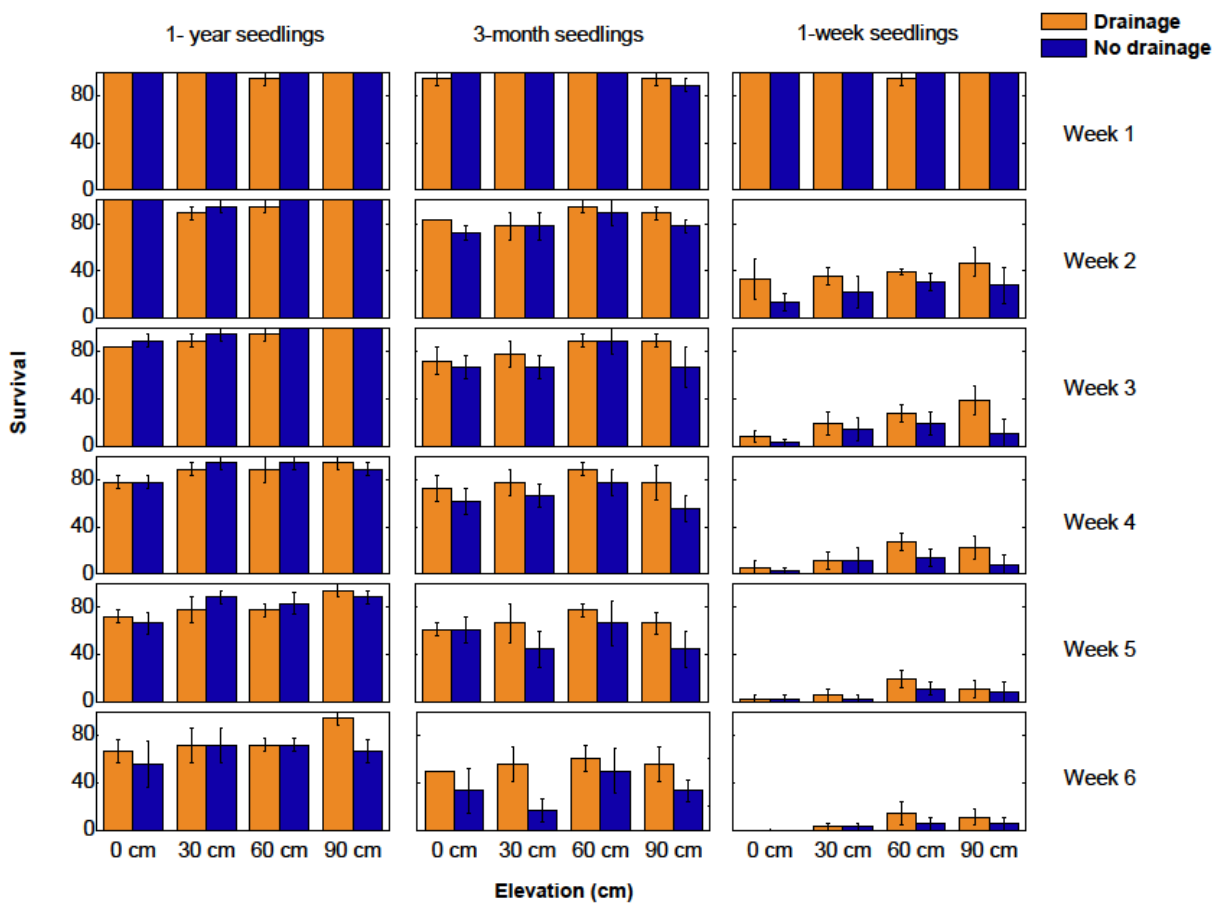


Figure 61. *Spartina anglica* seedling survival during the 6 weeks field experiment in Perkpolder. The overall survival of seedlings was significantly higher in the drainage groups (orange) than the groups without drainage (blue). Longer disturbance-free period (seedling age) and higher elevation (less inundation) also facilitates seedling survival.

Cox regression analysis revealed that, the drainage treatment, elevation and seedling age all significantly affected *S. anglica* seedling survival during our 6 weeks experiment. Compared to groups without drainage treatment, the overall seedling survival was significantly higher in the drainage groups (Figure 61). When looking at the effects of elevation, the risk of seedling die-off is reduced at higher elevations. This means that at higher elevations (i.e. – lower inundation periods) seedling survival is higher.

It is interesting to note that with increasing age and elevation, all our *Spartina* plants became less sensitive to lack of drainage. This indicates that the more time the seedlings have available to develop under favourable conditions, the less vulnerable they become to adverse conditions like e.g. lack of drainage or more inundation.

Based on the results of our study, we postulate that soil drainage can play a pivotal role as driving mechanism for the emergence of alternative stable states (Figure 62):

i). On the left, good soil drainage facilitates salt marsh seedling establishment and growth which may stimulate the formation of channels and consequently further improves soil drainage; hence resulting in self-organized feedbacks.

ii). On the right however, poor drained mudflat hampers seedling establishment due to waterlogging and leads to soft sediment and flat topography due to tidal smoothing, hence inducing a runaway feedback loop that keeps the tidal flat bare.

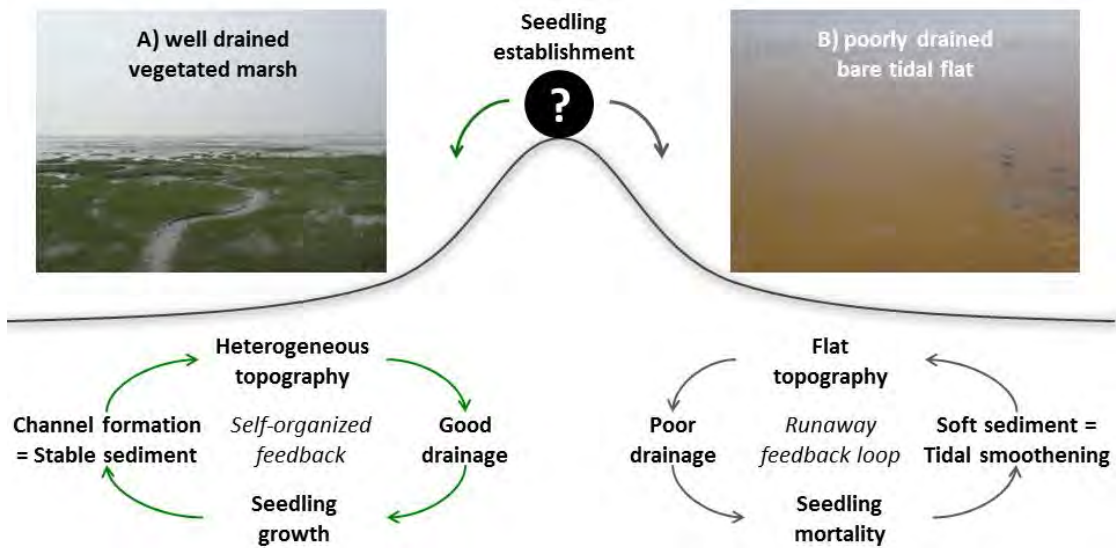


Figure 62: A conceptual diagram showing the importance of drainage in controlling alternative state shifts in salt marsh ecosystems.

Our experimental results highlight a crucial aspect in both these feedback loops: poor drainage kills seedlings due to prolonged waterlogged conditions, whereas good drainage enhances seedling survival. These findings are obviously not sufficient to substantiate all aspects of both proposed feedback loops. However, our conceptual model is supported by various anecdotal evidence from the literatures and the field. For example, Castellanos et al. (1994) demonstrated that at sites in southwest Spain with similar elevation but different drainage conditions, more *Spartina* tussocks were observed at the better drained site. Crooks et al. (2002) observed that similar elevation and drainage at sites in southeast England led to similar mature marshes. In the field, we observed that at some locations, seedling establishment is only present in those areas of the tidal flat with some drainage relief, especially when present at lower elevations with higher inundation frequency (Figure 62). Additionally, both aerial images and field observations show that the establishment of *Spartina* marshes typically first occurs next to existing channels (Schwarz, 2014a) (Figure 63). Whereas previous studies mainly focused on how plants contribute to channel formation or evolution (Temmerman

et al., 2007, Vandenbruwaene et al., 2013), our results highlight the inverse: how topographic heterogeneity and drainage channels may contribute to vegetation establishment.

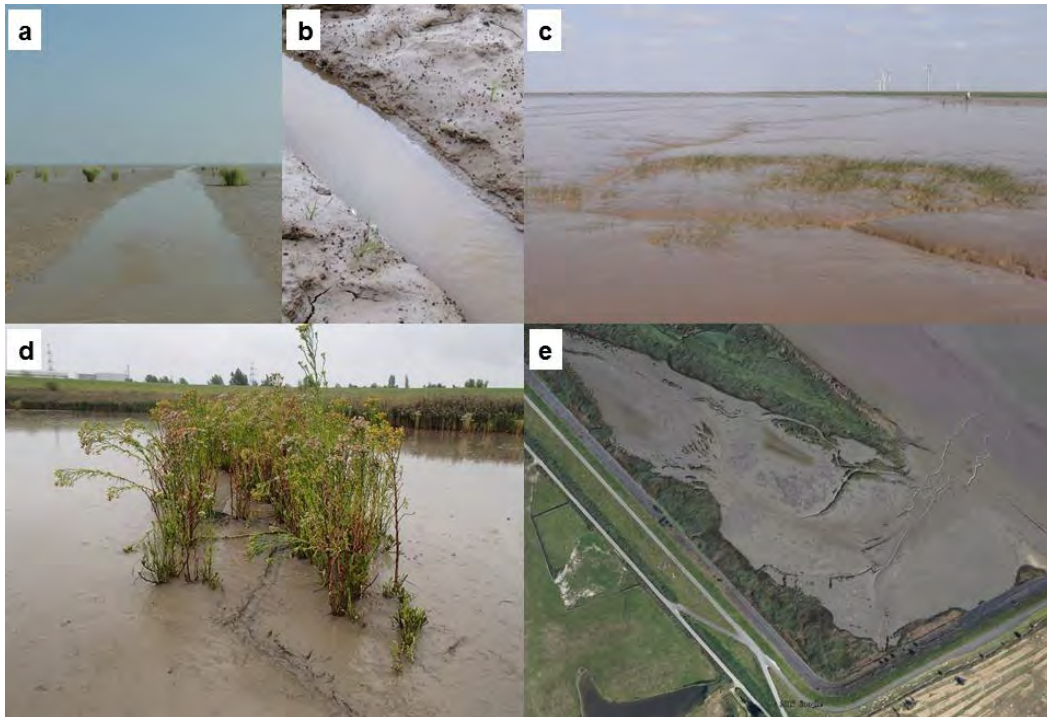


Figure 63: Anecdotal evidence that drainage relief facilitates salt marsh establishment. a) Salt marsh establishment near a channel at a low pioneer tidal flat (Chongming Island, the Yangtze estuary, China); b) establishment of seedlings first took place near drainage channels (Chongming Island, the Yangtze estuary, China); development of a heterogeneous marsh pattern in creeks at (c) the Chongming Island, the Yangtze estuary and (d) the Scheldt estuary (Paardenschor, Belgium); e) aerial image showing a large tidal flat that remained unvegetated for a long time (years) despite high elevation and being surrounded by old marshes; the only fringes of marsh vegetation are distributed alongside tidal channels (Paardenschor, Belgium, the Scheldt Estuary; Source: Google Earth, 2017).

4.2.1.2 OVERALL CONCLUSIONS RESEARCH QUESTION 1

Seedlings survive best in a well-drained soil without sediment dynamics. Yet, seedlings can tolerate some moderate sediment dynamics. They are more tolerant to accretion compared to erosion. The feedback mechanisms we described schematically above have important implications for management options for Perkpolder. Artificially constructing drainage conditions or providing longer disturbance-free period could be an efficient management strategy to facilitate marsh restoration at early stages and shift in state from bare tidal flat to vegetated marsh. Our results imply that creating even small topographic irregularities to increase soil drainage may help the initial establishment of young marsh plants. Restoration projects in

Perkpolder may be able to obtain such heterogeneous topography by, providing small scale drainage structures and gullies or creating artificial hummocks based on bioplastics might for example be an option.

The laboratory survival experiment shows the hazards for *Spartina* seedlings became larger with increasing amplitude of the (erosion or accretion) application. A smaller amplitude in the accretion/erosion treatments resulted in higher survival, with a better survival chance at sedimentation as the plant is able to grow with this sediment change.

Both the results of the laboratory and mega marsh-organ experiment in the field clearly shows that poor drainage reduce the seedling survival at Perkpolder.

4.2.2 Research question 2

How do the abiotic and biotic sediment properties (that affect vegetation establishment) develop over time, and how does this depend on the location within Perkpolder?

To follow how the abiotic conditions develop in time, we monitored sediment properties at 15 locations in Perkpolder (Figure 64) with the timing of sampling as indicated in

Table 10.

The biotic properties in terms of benthic community has been sampled by Tom Ysebaert (WMR). For the abiotic parameters we measured:

- Grain size – Syringe method of top 3 cm
- Bulk Density – Syringe method of top 3 cm
- Elevation - dGPS
- Depth muddy layer – Ruler pushed into sediment till original compact agricultural sediment
- Erodability (i.e. bed shear strength) – Shear vane top 5 mm
- Stiffness (i.e. penetration resistance) – with Eijkelkamp penetrometer

The results in the tree consecutive year since opening in 2015 are shown in Figure 68.

Moreover, short-term changes in bed-level elevation have also been monitored using SED-sensors (Figure 70) which monitor the sediment elevation continuously every minute with a 2 mm resolution (Hu et al. 2015).

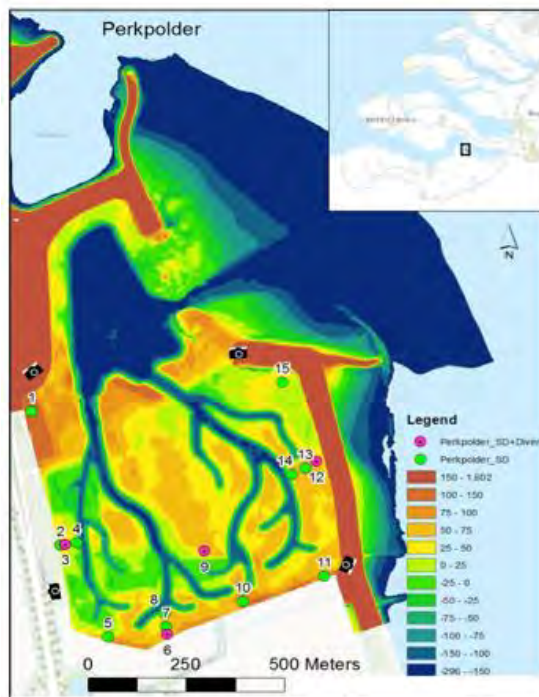
In addition to the measurements at the 15 locations in Perkpolder, a full-spatial-covering sampling survey (Gebiedsdekkende bemonstering) has been performed in September of 2016, 2017 and 2018. Results from this effort has been shown in Figure 65, Figure 66, Figure 67 and Table 11

In addition to the above measurements, NIOZ has taken the additional measurements, which helps to explain the sediment development:

- Turbidity monitoring (OBS)
- Sediment concentration in the water column
- Sediment traps
- Compaction cores from soft-muddy top layer
- Soil redox
- Echosounder / single beam

Table 10: overview of field measurements.

Date	dGPS	SED	Diver	Grain size Top 3 cm	Grain size Core 20cm	Bulkdensity	Depth Mud	Penetrologger	Shear vane	Seeds Net + Mat	Redox	Drone	3D-scan	Camera's	Seedling survival	Mega Marsh Organ	Echosounder
2015/07/09	Orientation		Placed														
2015/07/21	X	Placed		X		X		X							Placement		
2015/08/18				X		X									X		
2015/10/27	X	Removed	Removed	X		X									X		
2015/11/05	X	Replaced	Replaced	X	X	X	X	X				X					
2016/02/12	X			X	X	X	X	X			X						
2016/03/14	X			X	X	X	X	X			X						
2016/04/11				X	X	X	X	X			X						
2016/04/22														Placed			
2016/06/21	X	Replaced	Replaced	X	X	X	X	X								Placed	
2016/09/08	X			X	X	X	X	X	X								
2016/09/29	X			X		X			X								
2016/10/19		Removed								X							
2016/11/21						X				X							
2016/12/20	X	Placed (7)	Replaced	X	X	X	X	X	X	X							
2017/01/17										X							
2017/03/30		Placed (7)	Replaced	X	X	X	X	X	X	X		X	X				
2017/04/18																Spartina placed	
2017/05/18														Placed (Weekly team - Mon)	Monitoring		
2017/07/04															Harvest	Monitoring	
2017/07/27			Replaced	X	X	X		X	X	X Replaced							X
2017/09/25	X			X		X			X							Monitoring	
2017/10/10		Replaced	Replaced	X	X	X	X	X	X	X Out							
2017/11/15																	X
2018/01/19	X	Replace	Replace	X	X	X	X	X	X								
2018/05/01	X			X		X		X	X							X	X
2018/07/26	X			X		X		X	X							X	X
2018/09/25	X			X		X	X	X	X								X
2018/10/30	X			X		X	X	X	X								X
Total area (N=200 points)																	



Continuous monitoring

- 15 SD-Sensors
- 4 Divers (water height; points 3, 6, 9, 12)



Figure 64: Schematic overview of the 15 locations where SED-sensors were placed and where soil properties are regularly measured (see Table 2 for timing). At locations 3, 6, 9 & 12 we also measure tidal amplitude. We measured the survival of planted *Spartina* and *Scirpus* seedlings at location 1 to 15.

4.2.2.1 FULL SPATIAL COVERAGE SAMPLING

The full coverage sampling campaign allowed us to evaluate how the sediment characteristics changed spatially at a fine resolution. We related these spatial distributions to other the spatial features of the site, more specifically the inlet and the two main creeks. In 2016, bulk density was highest near the inlet and the upper creeks and lower throughout the rest of the site, especially in the middle and the bottom left corner (Figure 65). Most of the change over the full period 2016-2018 is occurring in the first two year (2016 and 2017). Hereafter overall not much changes and there is no clear trend. For example, bulk density increased overall in 2017 especially near the creeks. Between 2017 and 2018 bulk density decreased slightly except at the lower edges of the site at the creek outlets and at the upper site near the inlet. The other sediment characteristics also showed patterns driven by distance to the creeks and inlet. Elevation was greatest near the inlet and in the middle of the site, but had the lowest values directly next to or at the creeks (Figure 66). The mud depth layer, mud content, and water content were lowest near the inlet and next to the creeks.

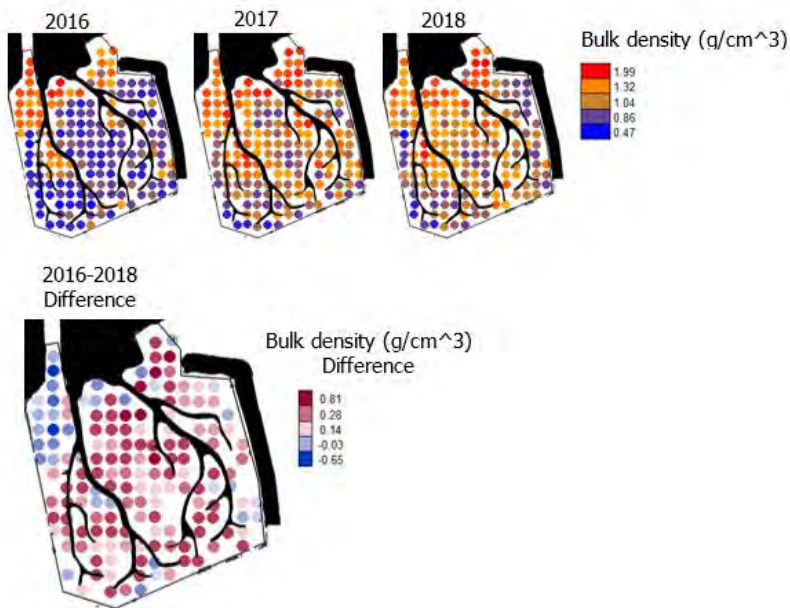


Figure 65. Bulk density values measured in 2016, 2017, and 2018 at 200 equally spaced sampling points in Perkpolder (upper panel). The lower panel shows the differences between 2018 and 2016 (negative change in blue and positive change in red).

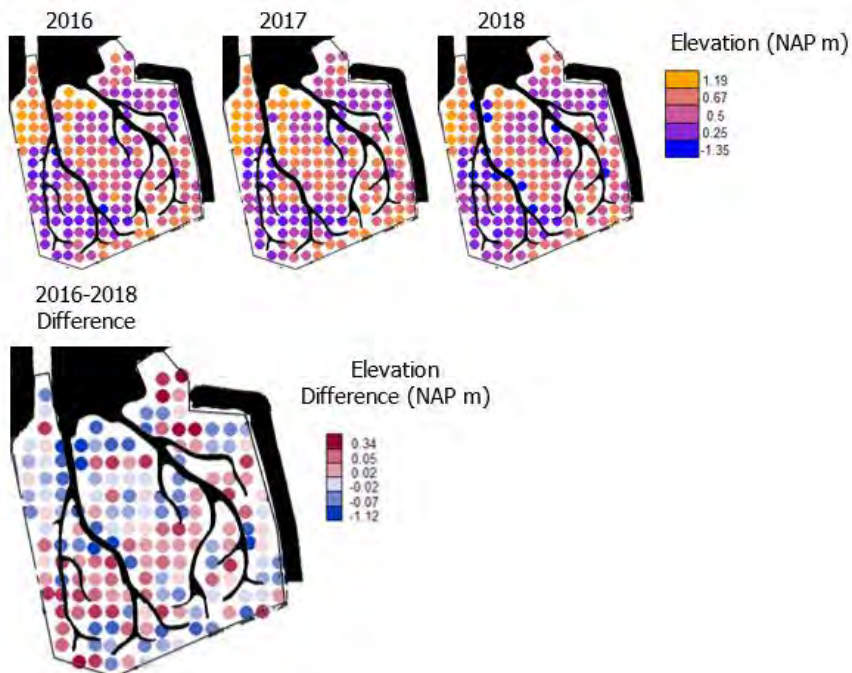


Figure 66. Elevation values measured in 2016, 2017, and 2018 at 200 equally spaced sampling points in Perkpolder (upper panel). The lower panel shows the differences between each set of two years (negative change in blue and positive change in red) and the overall change in elevation over the time period.

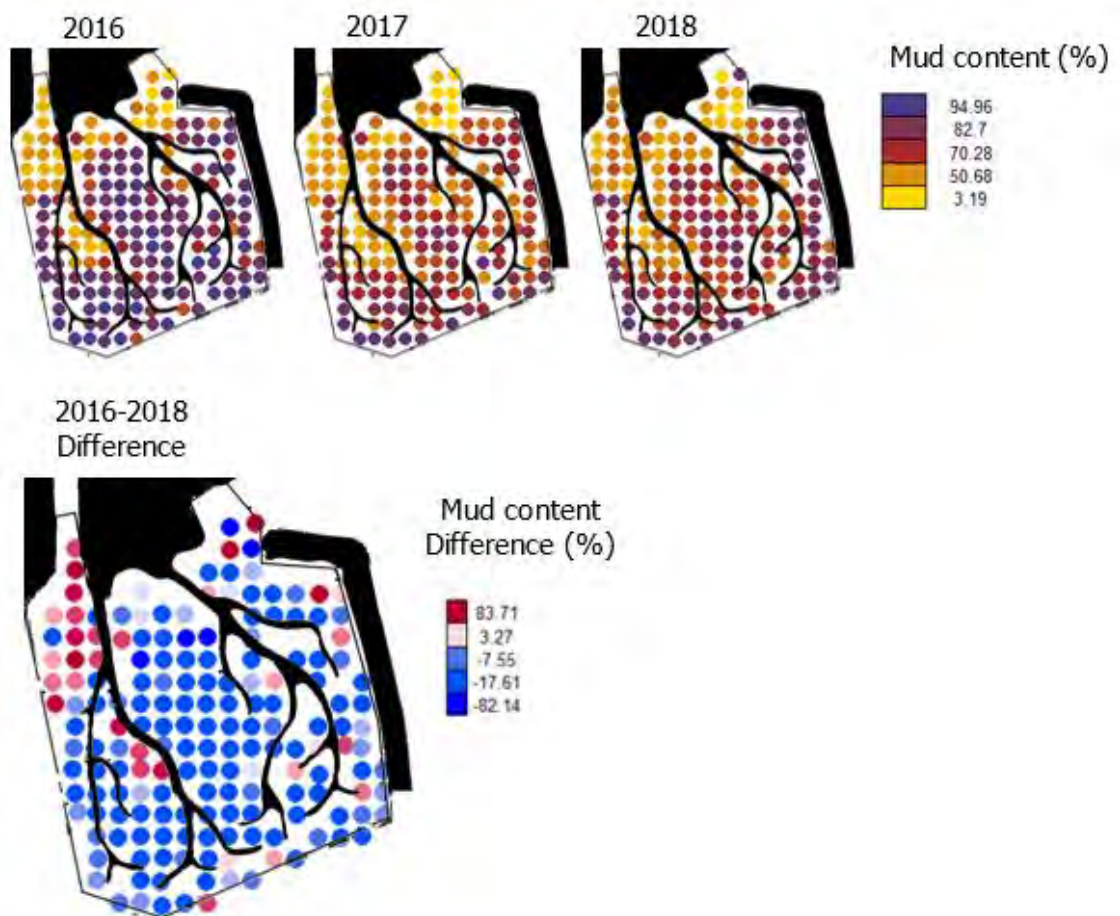


Figure 67. Mud content values measured in 2016, 2017, and 2018 at 200 equally spaced sampling points in Perkpolder (upper panel). The lower panel shows the differences between each set of two years (negative change in blue and positive change in red) and the overall change in mud content over the time period.

Besides the creeks and inlet, another interesting feature was the upper left corner between the wall and the creek which had the highest bulk density, elevation and grain size in 2016. This area tended to change in the direction of the central values for each sediment characteristic over time. For most of the sediment characteristics, it was the only area that changed in a direction opposing that of the rest of the site.

*Table 11. Coefficients for explanatory variables for generalized linear models of sediment characteristics from full coverage 200 points. The significance of the explanatory variable coefficient from p values is indicated by the number of stars with 0.05 > * > 0.01 > ** > 0.001 > ***.*

	year	distance to inlet	distance to creek
elevation	-0.023	0.000	0.006 ***
bulk density	0.1 ***	-0.001 ***	-0.002 ***
water content	-2.594 ***	0.024 ***	0.05 ***
mud depth	-2.929 ***	0.003	0.007
erodability	-0.093	-0.002 ***	-0.006 **
median grain size	6.745 ***	-0.091 ***	-0.078
mud content	-5.318 ***	0.064 ***	0.107 ***

We performed generalized linear models to test the significance of distance to inlet, creek, and year in explaining the variability of the sediment characteristics. Models including distance to inlet and creek had lower AIC compared to models that included sampling station as a factor. Elevation and erodability were the only variables that did not have any significant change over the sampling period. Elevation increased with distance to creek and erodability was higher closer to the inlet and the creeks. Conversely, mud depth only decreased over the sampling period without significant spatial variability. Bulk density, water content, and mud content had high significance across all three explanatory variables.

4.2.2.2 15 LOCAL POINT SAMPLING

We explored the correlations between sediment characteristics using a dataset collected at 15 points (see Figure 68 for point locations). While this dataset did not provide us the full spatial coverage of the 200 points survey, we were able to explore the temporal drivers of variability in the sediment characteristics in addition to spatial ones since these 15 points were sampled more frequently (four times per year) than the yearly full coverage survey from 2016 to 2018.

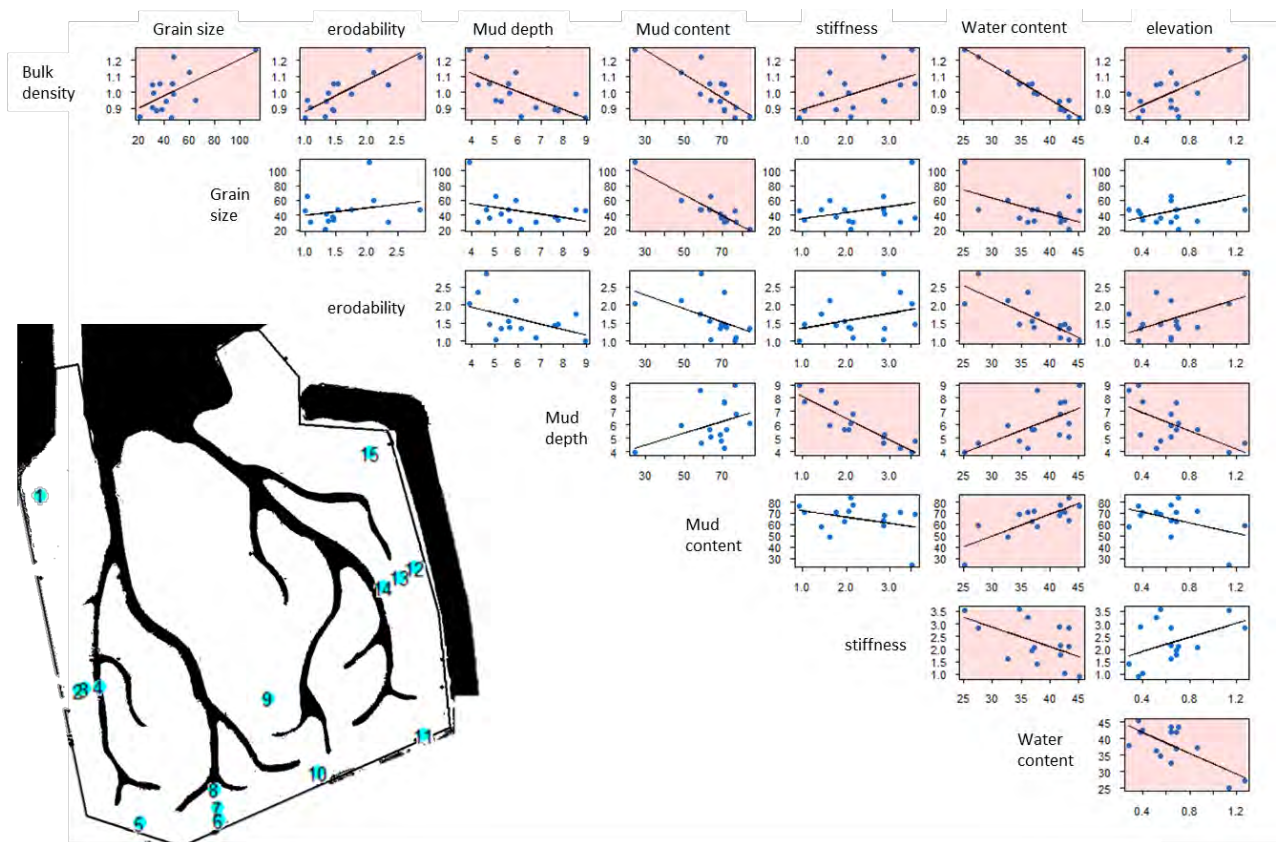


Figure 68. Correlations between the eight sediment characteristics with a red background showing statistically significant correlations. The values have been averaged by point over all sampling periods. The map shows the locations of the fifteen points. Mud content is derived from median grain size and bulk density is derived from water content.

Sediment characteristics were highly correlated. In particular, bulk density and water content showed statistically significant correlations with all the other sediment characteristics, and mud depth and elevation showed significant correlations with five out of the seven variables (Figure 68). It should be noted that bulk density is derived from water content, so it is not surprising that these two variables show opposing trends with each other as well as opposing trends with the other variables. Similarly, mud content is derived from grain size. Bulk density increases with grain size, erodability, stiffness, and elevation; and decreases with mud content, mud depth, and water content. We show an example of inverse trends in sediment characteristics in figure 5, where bulk density and mud content peak and opposite times over the time series of our sampling period. Some other notable trends are the decrease of sediment stiffness with mud depth and the increase of erodability with elevation.

Table 12. Coefficients for explanatory variables for generalized linear models of sediment characteristics from 15 points. The significance of the explanatory variable coefficient from p values is indicated by the number of stars with 0.05 > * > 0.01 > ** > 0.001 > *.**

	distance to creek	distance to inlet	Year	season	Year x season
Water content	-0.05897 ***	0.0051	4.5670	10860 *	-4.543 *
Bulk density	0.001398 **	-0.0001	-0.1756 ***	-420.4 *	0.2085 **
Silt content	-0.157 ***	0.02856 ***	6.5860	14710 *	-7.2940
Grain size	0.004516 ***	-0.0007593 **	-0.1964	-506.5 **	0.2512
Stiffness	0.01372 ***	0.0002	0.4331 **	1.668 ***	-0.0020
Mud depth	-0.02486 **	-0.0009	-1.208 ***	0.5256 **	-0.1764
Erodability	-0.0002	-0.0002	-0.4650	-975.3 ***	0.4831**
Elevation	0.005655 ***	0.0005397 ***	-0.0106	-15.65	0.0078

We examined how the changes in sediment characteristics could be explained by time (year and season) and space (distance to creek or inlet). We ran generalized linear models on each sediment characteristic with the following explanatory variables: distance to creek, distance to inlet, year, season, and an interaction between year and season (Table 12). We tested for other interactions between covariates but did not find any significant ones.

We found that distance to creek explained sediment characteristics much better than distance to inlet. Elevation was the only variable that depended solely on the spatial covariates than the temporal ones. Indeed, while we see some changes in the 200 points campaign over time, we see greater spatial variability than temporal changes. The only other variables besides elevation that have a significant relationship with distance to inlet are median grain size and its derived variable mud content. As in the 200 points survey, mud content increases with distanced to inlet, and vice versa for median grain size. Distance to creek was highly significant for all dependent variables except for erodability. It must be noted that erodability is the characteristic that has the most observation error as the measured values vary greatly from person to person, and this could explain why its greatest explanatory variable is a seasonal effect.

Year is most important for bulk density and mud depth, both decrease over time. Year was also important for sediment stiffness which increased over time. It is interesting that year is a significant explanatory variable for bulk density but not for water content as water content is used to derive bulk density. This could indicate that bulk density is capturing a different aspect of the evolution of the tidal flat than water content.

While season was a significant variable for almost all the sediment characteristics (except elevation), this effect was almost entirely due to differences that occurred in winter (i.e. changes in bulk density, mud

content, depth of mud layer, sediment stiffness). A year and season interaction was significant for water content, bulk density, and erodability.

4.2.2.3 **SEDIMENT COMPACTION OVER TIME**

We wanted to examine how bulk density changed with depth over time. The regular sampling method for the full coverage and 15 points surveys only examines bulk densities of the top 3 cm and we suspected that sediment compaction would be visible in deeper layers. As expected, we found that bulk density increases over depth at all points (Figure 69). We ran a linear model with bulk density as a function of date, point, and layer. We included an interaction between date and layer. As the sampling point in 2015 is so different from those in 2017, we ran the models without the 2015 samples. We found evidence ($p=0.052$) that bulk density increases by date. We found stronger statistical evidence that there is a positive interaction between layer and date ($p=0.035$) which means that bulk density increases faster over time at depth than near the surface. There were also very big differences between points, as is visible in plot 6.

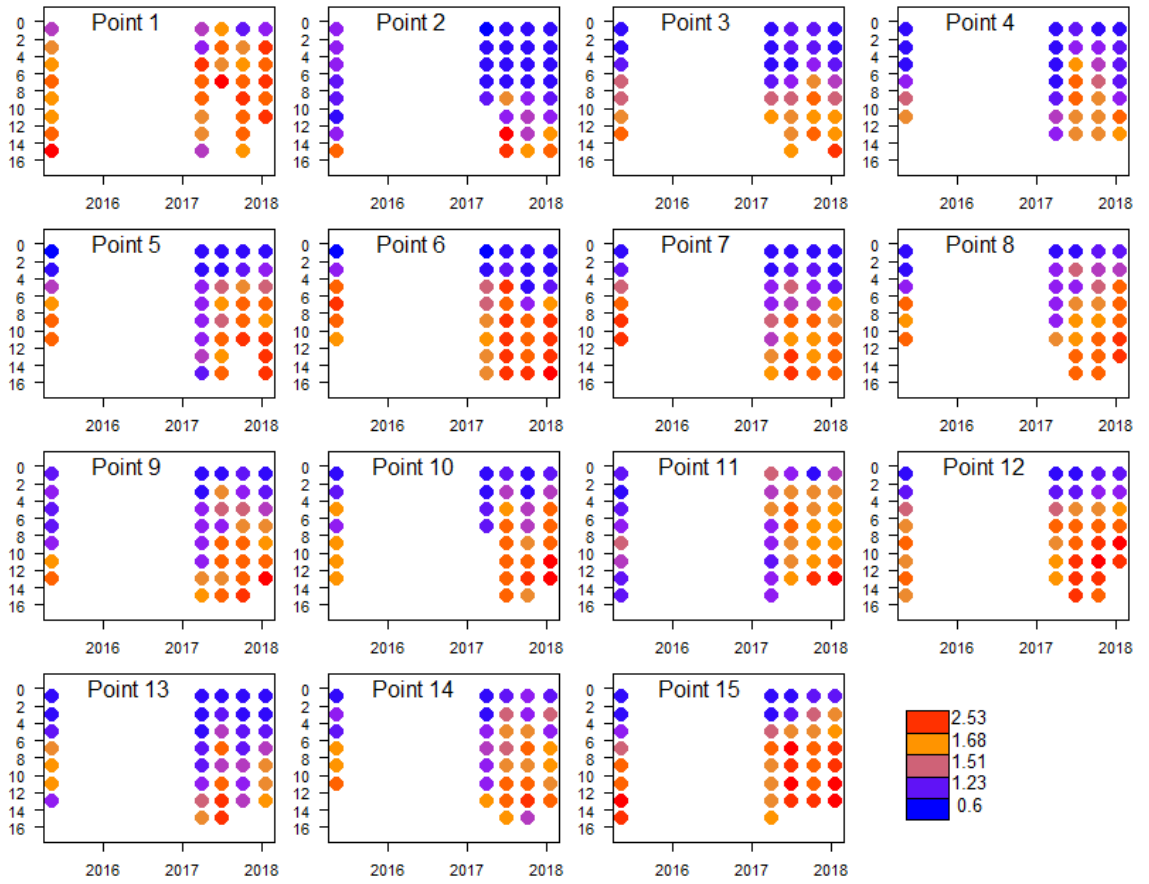


Figure 69. Bulk density values for 2 cm layers (0 to 16 cm total depth) at the 15 points. There was gap in sampling in 2016.

4.2.2.4 SED-SENSOR RESULTS

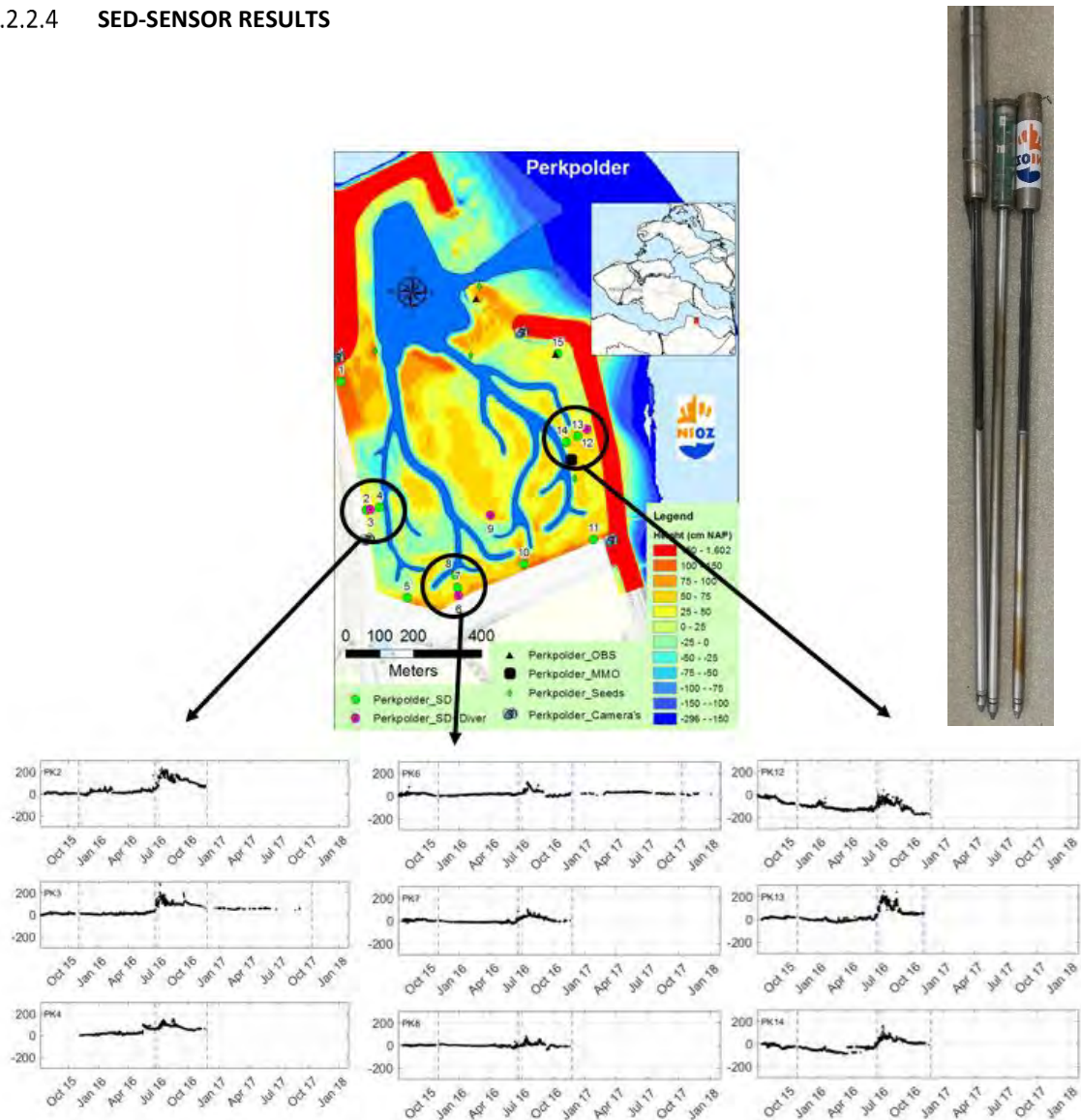


Figure 70: Sediment dynamics at three mini transects at Perkpolder.

Time series of the evolution of the bed, as measured with the SED-sensors, are presented in Figure 70. The measured locations evolved similarly: relatively stable (or erosive for the eastern transect) until July 2016, followed by an accretion event beginning of July. After this accretion event, the bed lowered again. Even though differences are present between the locations, the accretion event of the beginning of July was present at all locations.

As the sediment fluxes were only measured from end of September 2016 until beginning of March 2017 (see Figure 10), the measurement periods of the SEDs did not fully overlap (most SED sensors measured until November 2016). Therefore, a direct comparison between these datasets is not possible over the full

measurement period. Still, Figure 10 indicates that the sediment import rates are everything but constant in time. Half of the import over the measured 6 months was achieved already within the first month (end of September – half of October). However, this period of higher import cannot be observed as an accretion event in the SED time series. Possibly, a window of even higher import rates could explain the substantially higher accretion rates of the beginning of July in Figure 70, but that event was not covered by the sediment fluxes measurements. It is important to note that the lowering of the bed is not necessarily due to sediment export (which is limited in this basin, see Figure 10), as the lowering of the bed could also be partly explained by compaction of the freshly deposited sediments due to gravitation, even though this is a gradual process (order of months).

4.2.2.5 SEDIMENT AVAILABILITY

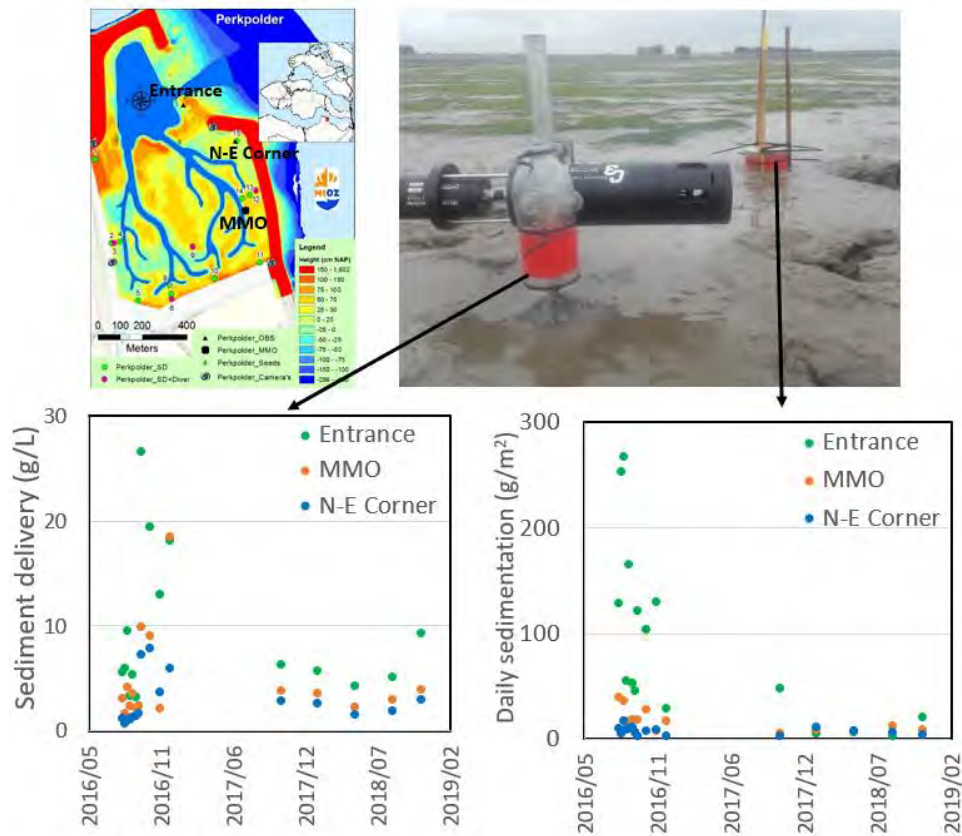


Figure 71: Sediment availability shown in a. sediment delivery (g/L), suspended in water column and b. Daily sedimentation (g/m²), trapped sediment converted to a daily value.

4.2.2.6 OVERALL CONCLUSION RESEARCH QUESTION 2

The bed-level elevation of the tidal flat in Perkpolder are increasing slightly to almost nothing. Moreover, the sediment is gradually compacting and becomes less muddy.

While we did not see sediment accumulation as we expected, the elevation might change more rapidly once the pit at the entrance of the Perkpolder area (sediment used for strengthening the dike) is almost filled and sediment fluxes further into the area might not be reduced because of it. We did see spatial and temporal changes in sediment dynamics over the sampling period. While elevation did not change much over the sampling period, other characteristics like bulk density show that compaction occurred over the time period. A muddy top layer is present, but as the result of a well-drained area with an abundance of creeks the underlying sediment is compacting.

We get a more complete picture of how the area changed over time due to the more frequent sampling of 15 points spread around Perkpolder. This local sampling show opposing patterns for bulk density, mud content, and water content. This is probably due to the 15 points being close to the edges of the site, which had an opposite pattern in sediment dynamics than the middle. Conversely, the greater temporal resolution of the 15-points campaign captured seasonal variability in the sediment characteristics. These different patterns highlight how important it was to have both good spatial and temporal coverage in capturing the full morphological development of the area.

4.2.3 RESEARCH QUESTION 3

What is the role of seed availability and seed dispersal for the vegetation development?

As indicated in the project-offer, we would only work on this additional topic if we would attract *sufficient* students available to carry out the work. So the work on this topic remains limited. However, in the fall of 2016 until January 2017 seed availability has been assessed by trapping seeds in floating nets, in collaboration with a HZ-student. Moreover, seed dispersal throughout the area was measured as seed trapping in astroturf.

4.2.3.1 SEED DISTRIBUTION

Astroturf mats of 0.5 by 0.5 meter were pinned down into the soil on the measurement points (Figure 9) using five pickets. These were left on the locations on the period of one tidal cycle (one month), in the months October, November and December. After one month the Astroturf mats were washed out over a sieve with a micromesh of 450 μ m. Seeds were separated and identified to make up the species composition per sample. This method has been performed earlier at the Paulinapolder and Zuidgors salt-marshes in the Westerschelde and has proven to be effective (Zhu Z, 2014). By deploying the Astro-turf mats in a spatial explicit pattern, we can map the seed arrival for different species in this area.

4.2.3.2 SEED AVAILABILITY

Four nets were placed at the beginning of the channels to measure the seed inflow. These measurements were done in October (2016-10-19), November (2016-11-22) and December (2016-12-22). These nets have a mesh size of 60 μ m and an aluminum frame with a rudder to follow the tidal currents. Styrofoam was attached to the frame and the construction is placed on a pole so it can float along with the water level. The nets were floating under the water surface. In Perkpolder nets were placed on one location where the dike was breached, two locations at the beginning of the channels on the channel banks and one location land inwards on the intertidal area, as shown in Figure 72.

Preliminary results, as partly copied from the student report has been included below (L. Gillissen 2017, Salt Marsh Establishment, Seed settlement and soil properties in the case study of Perkpolder and Rammegors).

The preliminary results suggest that:

- Seeds do reach the area
- The astro turfs may not function optimal as seed trap in the Perkpolder area, as they get clogged by sediment

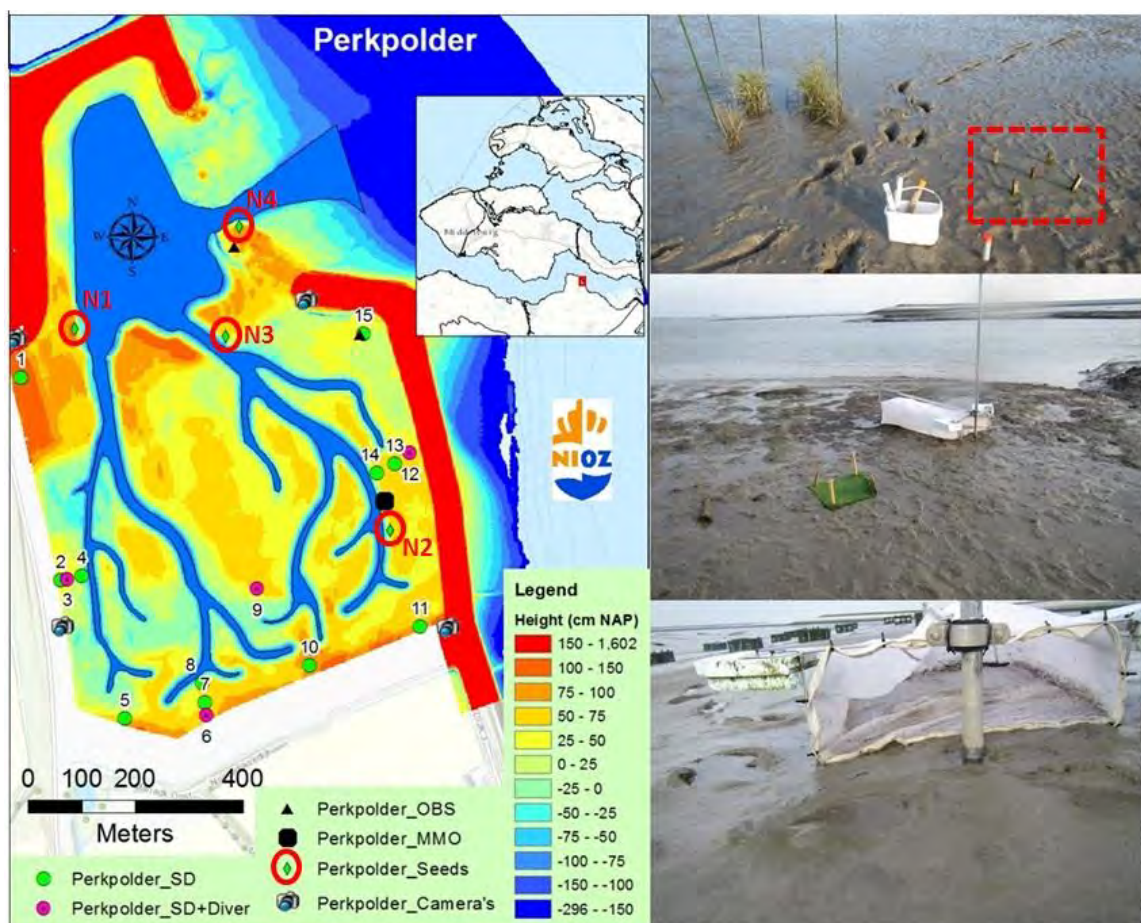


Figure 72. Location of 4 seed nets and the 15 astro-turf mats (i.e., placed near SD-sensors) within Perkpolder.

Table 13. Results of seed trapping on the 15 astro-turf mats placed near SD-sensors, throughout Perkpolder.

24/10/2016	Pk01-M	Pk02-M	Pk03-M	Pk04-M	Pk05-M	Pk06-M	Pk07-M	Pk08-M	Pk09-M	Pk10-M	Pk11-M	Pk12-M	Pk13-M	Pk14-M	Pk15-M
<i>Aster tripolium</i>	0	0	0	0	0	0	3	2	0	0	0	0	0	0	0
<i>Atriplex litoralis</i>	0	0	0	10	7	0	0	2	0	0	8	0	0	0	1
<i>Suaeda maritima</i>	0	0	0	0	2	0	0	1	0	0	0	0	0	0	0
<i>Bolboschoenus maritimus</i>	0	0	0	0	0	0	0	1	0	0	0	1	0	0	0
<i>Atriplex prostrata</i>	0	0	0	0	0	0	0	1	0	0	0	0	0	0	0
Unidentified	0	8	1	1	5	0	0	5	0	2	2	2	0	0	0

22/11/2016	Pk01-M	Pk02-M	Pk03-M	Pk04-M	Pk05-M	Pk06-M	Pk07-M	Pk08-M	Pk09-M	Pk10-M	Pk11-M	Pk12-M	Pk13-M	Pk14-M	Pk15-M
<i>Aster tripolium</i>	0	0	1	3	0	1	0	2	3	0	0	2	3	2	1
<i>Spartina anglica</i>	0	0	0	0	0	0	0	0	0	0	0	0	0	2	0
<i>Atriplex Litoralis</i>	2	0	0	0	0	0	0	1	0	0	2	0	0	0	0
<i>Limonium vulgare</i>	0	0	0	0	0	0	0	1	0	0	0	0	0	0	0
<i>Rhizomes</i>	0	0	1	2	0	0	0	3	0	0	0	0	0	0	0
unidentified	0	1	0	0	0	0	0	1	0	0	0	1	1	0	0

21/12/2016	Pk01-M	Pk02-M	Pk03-M	Pk04-M	Pk05-M	Pk06-M	Pk07-M	Pk08-M	Pk09-M	Pk10-M	Pk11-M	Pk12-M	Pk13-M	Pk14-M	Pk15-M
<i>Aster tripolium</i>	0	1	0	0	0	0	0	2	0	0	0	0	1	0	2
<i>atriplex litoralis</i>	0	0	0	0	0	0	0	0	0	0	8	1	0	0	
<i>puccinellia maritima</i>	0	0	0	0	0	0	0	0	0	0	0	0	0	0	0
<i>bolboschoenus maritimus</i>	0	0	0	0	0	0	0	0	0	4	0	0	0	0	0
<i>spartina anglica</i>	0	0	0	0	0	0	0	0	0	1	0	0	0	0	0
unidentified	0	1	0	0	0	0	0	0	0	0	0	0	0	0	0

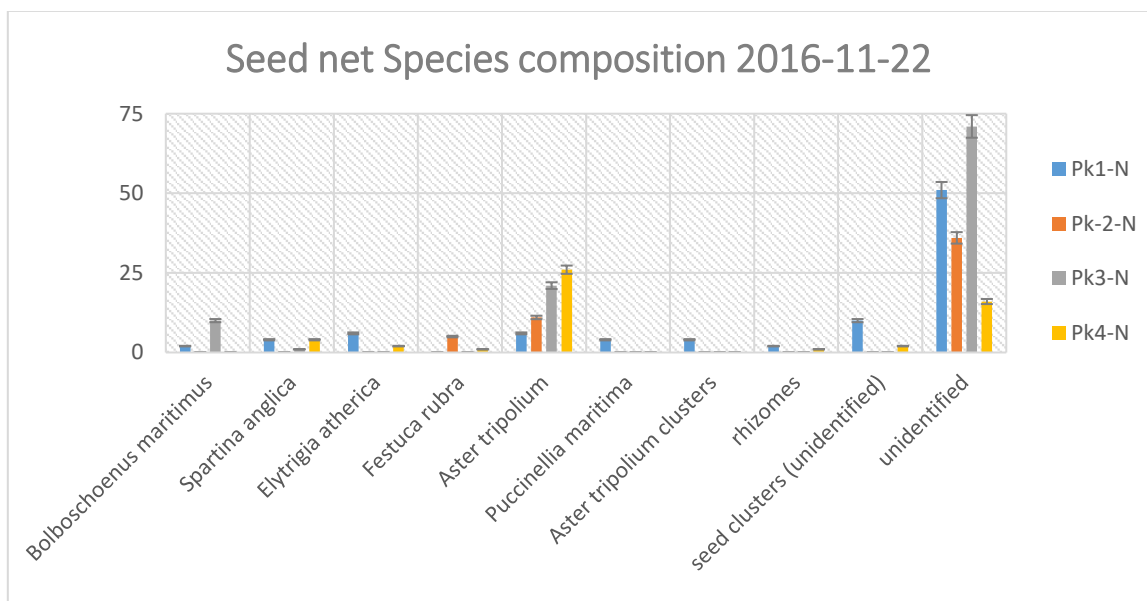
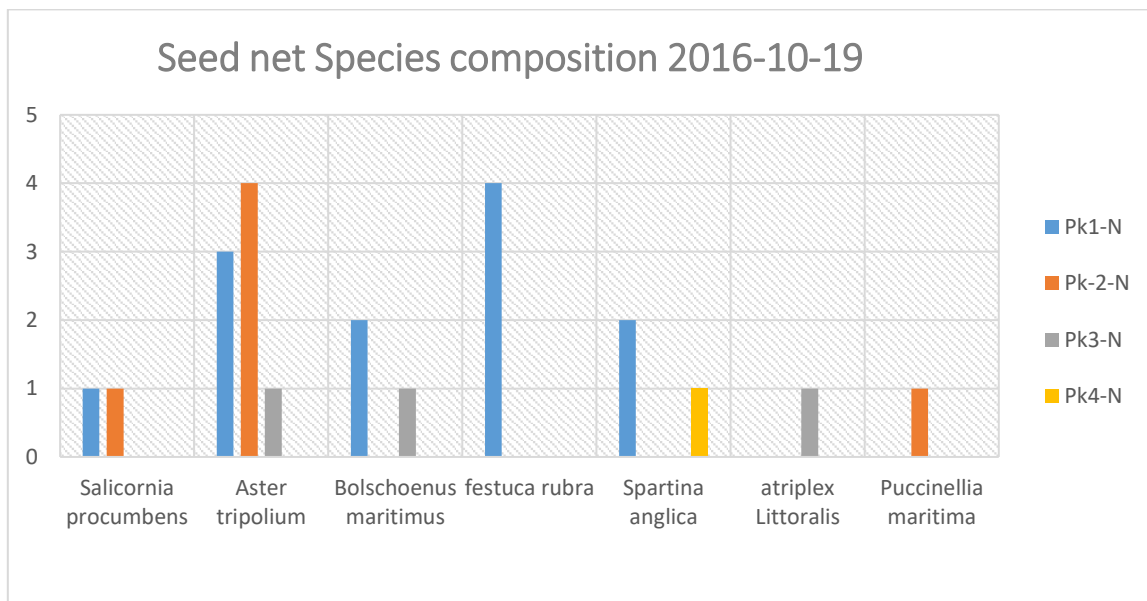


Figure 73. Results on seed availability as trapped in the nets.

Based on these results we can conclude that the area is not seed limited. Seeds are available and reach the new tidal flats of the Perkpolder are and they were able settle.

4.2.4 RESEARCH QUESTION 4

What is the pattern of colonisation and lateral expansion by pioneer species, along the elevational gradient?

4.2.4.1 FIELD EXPERIMENT (2016) – SEEDLING COLONISATION, SURVIVAL & LATERAL EXPANSION

First, we carried out a survival experiment focussing on pioneer-species. At the 15 locations that are monitored throughout the year we planted relatively large *Spartina* and *Scirpus* seedlings (11 weeks old) in July 2015. At each of these 15 locations we therefore established two plots of 1m² each: in one of the plots we planted five *Spartina* seedlings; in the other plot 5 *Scirpus* seedlings. We subsequently monitored their survival over time



Figure 74. impression of seedling survival experiment from 2015 until 2018 in Perkpolder.

The survival curves show that *Scirpus* seedlings die much faster than the *Spartina* seedlings (Figure 75). We were not able to explain spatial variability in *Spartina* seedling mortality (data not shown). So, no relation with elevation or distance to creek or inlet could be found.

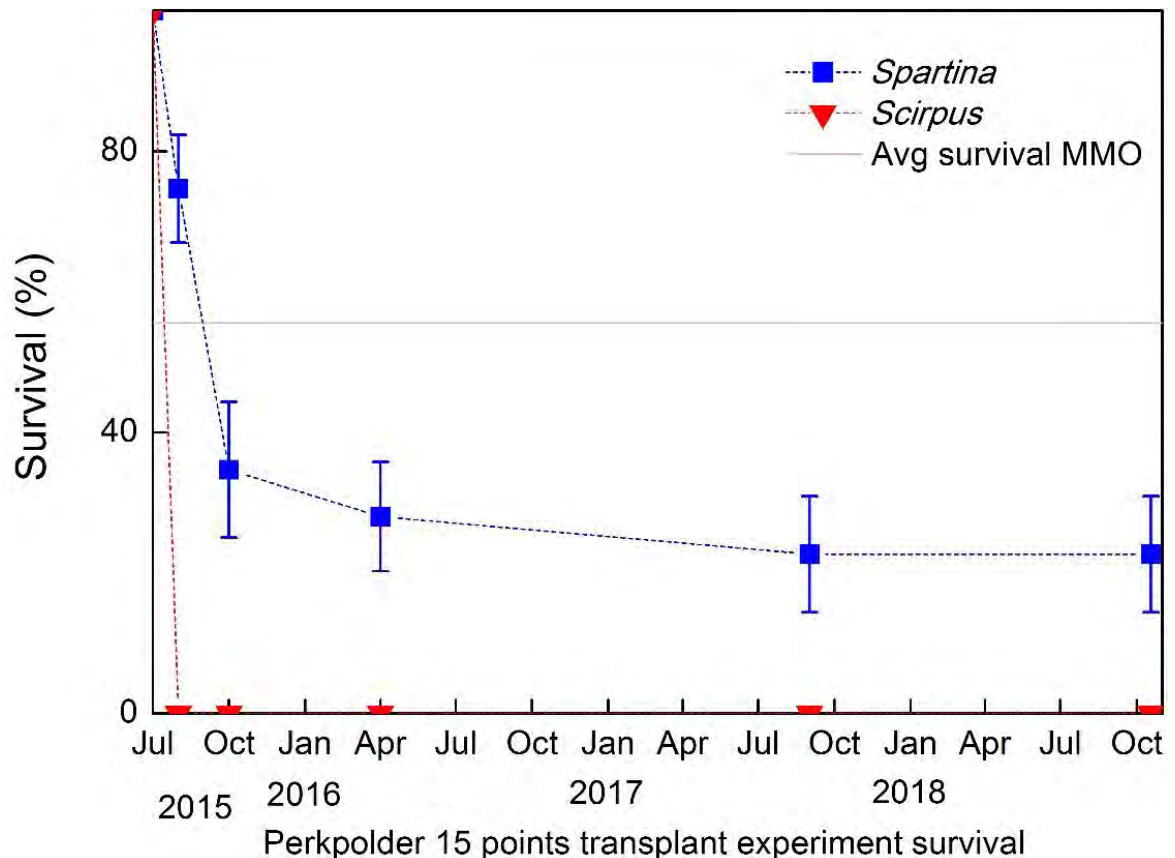


Figure 75: Results of seedling survival experiment 2015-2016 in Perkpolder.

4.2.4.2 LAB EXPERIMENT (2016) – LATERAL EXPANSION IN RELATION TO SEDIMENT TYPE

Identify thresholds in marsh expansion - marsh clump transplanting experiment

In the aims to quantify the edge dynamic thresholds of cliff height in determining transitions between vegetated and bare state, we carried out a marsh clumps transplanting experiment. We especially asked the following questions: i) Are there any thresholds in cliff height for pioneer marsh plants to expansion or retreat? ii) Does these thresholds change in different cliff systems that varies in marsh species?

Mesocosms set up

To test the threshold of cliff height in hampering salt marsh expansion, mesocosms with different cliff heights were set up in a batch of plastic boxes (inner dimensions approximately 75 × 45 × 30 cm). 3 salt marsh species

were used in our experiments, i.e., *Spartina anglica*, *Scirpus maritima*, and *Phragmites australis*. All plant clump samples were collected near Rilland-Bath, in the Westschelde estuary. After irrigated with fresh water for one week each clump was transplanted to a mesocosm using the following design. The size-standardized (20*20cm) plant clump was surrounded by three kinds of prepared sediments (average D50 = 143.64 μ m) with a cliff at the 1/3 length site of the box (Figure 76). Different cliff height was maintained though the experiment period at 0, 2, 4, 8, 16 cm with 5 repetitions each treatment.

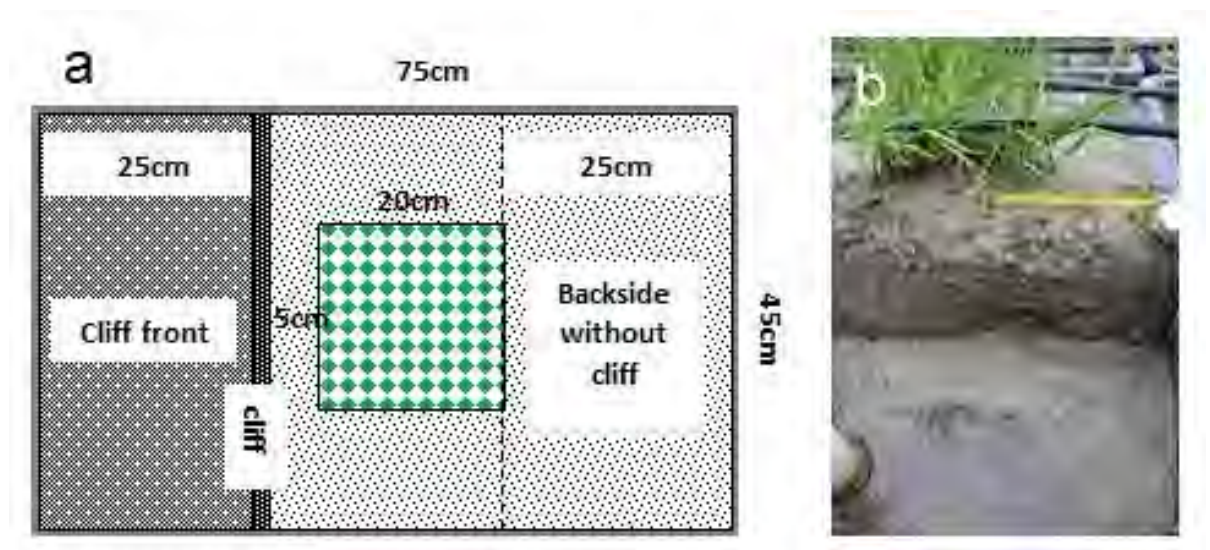


Figure 76. a, Schematic of the layout of one mesocosm (view from the top), green part represents for the plant clump, with 5cm distance to the cliff. b, Photograph of one of the mesocosms showing view from the cliff side.

Growth conditions and measurements

To obtain the parallel illumination and to management the systems more convenient, mesocosms was assembled together in an open outside area with natural lights in NIOZ Yerseke, the Netherlands. Fresh water was used to irrigate plants though the experiment period in consideration of salinity tolerance difference between species. To prevent the cliff height been disturbed during raining or storming, a removable roof was used during bad weather conditions. The plant traits were recorded every week for two months in simulation of the natural expansion time of salt marshes in the field side. Spatially we looked at shoots expansion to the cliff side to compare for lateral expansion from different species and sediment types.

Main results

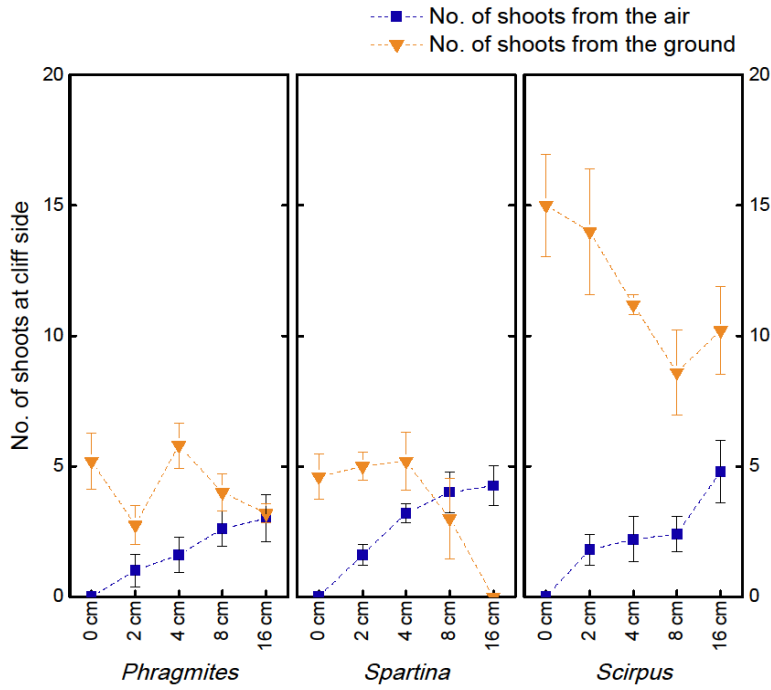


Figure 77. Number of shoots expansion to cliff side.

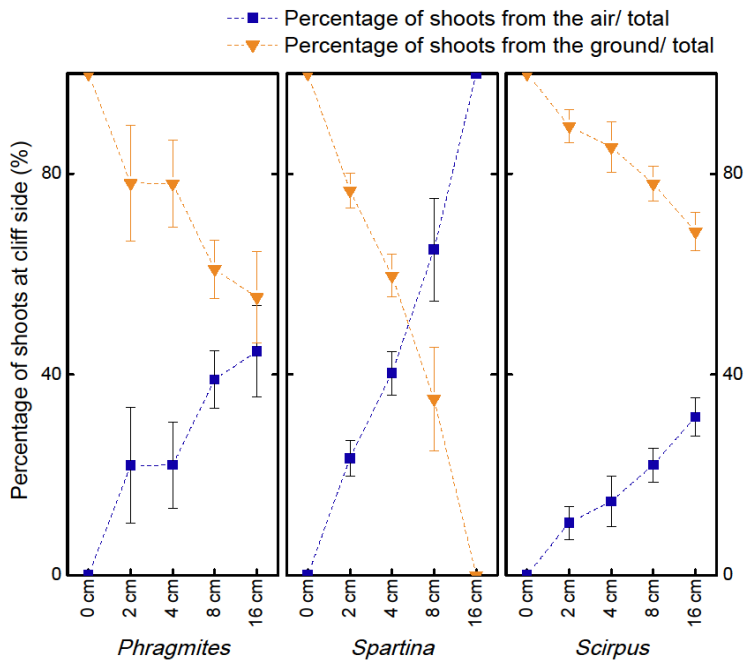


Figure 78. Percentage of shoots expansion to cliff side (comparison of different species of Sanymud sediment).

The most significant results from our marsh expansion experiment is that, both the number and percentage of shoots that expand into the air (cannot outgrow a cliff) increased with cliff height for all three species, while the data of shoots expand to the ground (outgrows a cliff) in front of the cliff shows the opposite (Figure 77 and Figure 78). This means that the cliff height can be a threshold that hampering tidal marsh expansion, especially at the pioneer marsh edge. For example, no *Spartina* shoots could successfully outgrow a 16 cm high cliff (Figure 77 and Figure 78).

Interestingly, we also found that the capacity to outgrow a cliff changes between species. For example, the *Scirpus* outgrows significantly more shoots to the cliff front ground than *Phragmites* and *Spartina* at all cliff height treatments (Figure 78). These results agree with field observations that *Scirpus* marsh fronts seems never develop cliffs and always present gradual transitions from bare tidal flat to vegetation instead of a cliff.

Conclusion

Results suggest that the outgrow of pioneer marsh is affected by cliff height and is species-specific. The marsh restoration in Perkpolder should consider local conditions of the area and use the early-successional species.

MEGA-MARSH ORGAN EXPERIMENT 2 (MMO-2-2017) - effect of sediment-type & drainage on expansion

The aim of the second experiment was to monitor the survival and especially the lateral expansion of *Spartina* patches in the Mega Marsh Organ. In this experiment the consequences of different heights and drainage are monitored.



Figure 79. *Spartina* patches planted in the MMO at Perkpolder.

To compare the potential different effects of sediment drainage and inundation time on the young seedlings and mature marsh plants, we also carried out a follow-up tussock transplant experiment using the same MMO set up. On 18 April 2018, *S. anglica* tussocks transplants were extracted from an existing monoculture marsh from Knuitershoek (51°24'19.91N, 3°58'20.17E), where uniform size soil blocks (20 x 20 x 30 cm) were collected by cut of all above ground vegetation. The tussock transplants were then placed in the above-mentioned 12 MMOs in Perkpolder (12 drained & 12 without drainage boxes) with 2 soil blocks diagonally embedded at each box each elevation. Regrowth of each tussock were harvested at 31 October 2018 by clipping all above ground vegetation as close to the sediment surface as possible. When no above ground present, the tussock was deemed as establishment failure. After measuring above ground vegetation height and recording shoot number of each tussock, all the collected tussocks were then dried at 60 °C in an oven to a constant weight for measuring dry biomass.

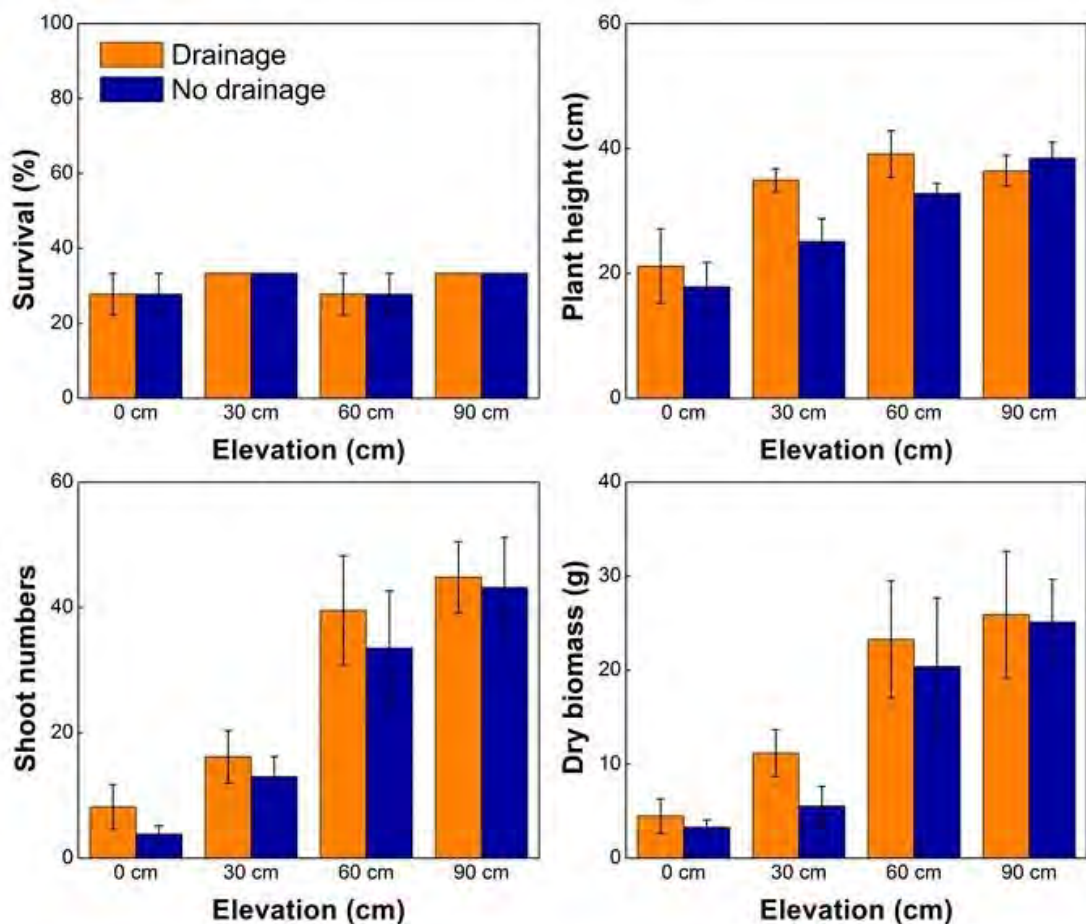


Figure 80. Regrowth of *S. anglica* tussocks at harvest in the field experiment in Perkpolder. The survival of tussocks showed no significant difference between drainage or elevation groups; Plant height, shoot numbers and dry biomass was only affected by elevation per se, with no significant difference effect from drainage treatment or interactive effect of drainage and elevation.

There is a clear effect of the elevation of the MMO on the plant biomass, shoot number and plant height, but survival of the plants seems to be equally low in all MMO, ~30%. No significant effect of poor or good drainage are found on most of the elevation. Only in case of the 30 cm elevation this treatment is significantly different. Results from our previous in situ MMO experiment show that drainage is critical for the survival of salt marsh seedlings, especially those younger ones at their initial establishment phase. This agrees with recent findings by Redelstein et al., (2018), where the authors reported that soil waterlogging can severely reduce seedling root growth and thereby stability of NW European salt marshes. Whereas, our results on marsh tussocks shown that the regrowth of mature marshes was not affected by sediment drainage. This agrees with previous studies that emphasized drainage as an establishment issue and may less important for larger mature plants (for details see Mendelssohn and Seneca 1980; Padgett et al., 1998, 1999). Thus, the overall results of present study show that lack of drainage can be one of the key factors hampering salt marsh seedling establishment.

4.3 CONCLUSIONS

The Perkpolder area is:

- Consisting of well-drained, compacting sediment, perfect for seedling survival.
- Slowly accreting, because of compaction not (yet) elevating.
- All seedlings are vulnerable to sediment dynamics, but are more tolerant to accretion than erosion
- Not seed limited, enough available for settlement. No bottleneck for a future salt-marsh establishment.
- Approximately one meter below ideal elevation for seedling settlement/survival.
- Due to the slow elevation increase the probability for vegetation establishment will increase over time. Eventually the potential for saltmarsh development occurs:
 - Establishment from seeds is essential to kick-start the salt-marsh development and requires stochastic 'good year' events (i.e. Window of Opportunity). However, the clonal expansion will also be important and colonize the area in a much more constant rate after the initial establishment has taken place.
 - Clearly, vegetation establishment is a size/stage-dependent process therefore requiring randomly occurring 'good year' event.
 - Both sediment dynamics and drainage quality have an effect on the earlier life-stage of the pioneer plants and can limit the likelihood of such 'good year' events occurring.

5 COLONIZATION AND DEVELOPMENT OF THE BENTHIC MACROINFAUNAL COMMUNITY

The results described in this chapter are also available as a WMR report (Walles, 2019).

5.1 INTRODUCTION

Intertidal habitats absorb and attenuate wave energy, buffering for flood protection. Under influence of sea level rise intertidal habitats can grow to higher elevations and move inland. Man-made flood defences however prevent inland movement leading to narrowing of these areas, a process known as coastal squeeze. Loss of intertidal habitats combined with rising sea levels results in high maintenance costs of coastal defences and asked for more cost effective and sustainable methods of coastal protection. Managed realignment (setting back defences inland of the original to stimulate rising ground) has become an increasingly common mechanism to compensate for habitat loss and to increase sustainability of flood defences (Esteves, 2014). Landward retreat of coastal defences will result in the formation of newly flooded habitats exposed to tidal inundation. In riverine situations, setting back defences reconnects the river to its flood plain, making room for the river to buffer for increased precipitation reducing flood risks. Creation of intertidal habitats by managed realignment for coastal defence is one of several 'soft' engineering options that could reduce maintenance costs of dikes and at the same time deliver environmental and societal benefits. For future coastal management it is important to understand how newly flooded coastal areas will develop. Will flooded areas develop into productive ecosystems with high ecological and recreational value or remain in an undesirable state for an extended time. Insight in the development of flooded areas may provide decision makers with sufficient knowledge for future implementation of these mitigation measures.

Primary producers like benthic diatoms are the foundation of intertidal flat food webs. They are an important food source for primary consumers like benthic macrofauna such as polychaetes, molluscs and crustaceans. Benthic macrofauna on their turn are a key food source for secondary consumers including fish, crustaceans and birds. As of this, the rate at which the benthic macrofaunal community develops in a newly flooded coastal area is expected to influence total biodiversity and ecosystem functioning.

Previous studies showed initial colonization by benthic macrofauna could occur within days and reach a stable community composition after months or a few years (Moseman et al. 2004; Mazik et al. 2007) but it may also take years to decades (Levin et al. 1996; Craft and Sacco 2003). Colonization and succession depend on local environmental conditions. Characteristics of the sediment is one of the key factor controlling colonization and succession. Garbutt et al. (2006) noted no colonization on agricultural remains whereas rapidly colonization occurred in areas with newly accreted sediments. To understand the development of newly flooded areas, monitoring is necessary as there is no consensus on how newly flooded area are colonized and develop over time.

The managed realignment Perkpolder is one of the first in the Dutch part of Scheldt estuary, undertaken as climate adaptation measure. In the future, other areas will be flooded, such as Hedwige-Prosper. The newly developing intertidal habitat acts as a safety buffer for the surrounding dikes and by means of sedimentation will rise with rising sea-levels. This study assesses initial colonization and development of the benthic macrofaunal community in this newly flooded managed realignment area and the usage of the area by birds. Development of the benthic macrofauna community was compared to the community found in adjacent intertidal areas in the Schelde estuary. Furthermore, the relation between species and community traits and environmental characteristics was investigated. Traits based models were used to examine which traits best explained environmental responses.

5.2 METHODS

5.2.1 THE STUDY AREA

The Scheldt estuary is one of the longest estuaries in NW Europe with a complete salinity gradient. It is a macrotidal system and measures 160 km from the mouth near Vlissingen (The Netherlands) to Gent (Belgium). The study area is located in the Western Scheldt, which is the Dutch part of the River Scheldt connected to the North Sea (Figure 81). The mean tidal range in the Western Scheldt increases from 3.5 m from the mouth of the estuary to 5 m at the Dutch/Belgian border. The mean annual river discharge is $105 \text{ m}^3 \text{ s}^{-1}$ with low summer discharges ($20 \text{ m}^3 \text{ s}^{-1}$) and high winter discharges ($400 \text{ m}^3 \text{ s}^{-1}$). Depending on the river discharge residence time of the water in the estuary range from 1 to 3 months (Soetaert & Herman, 1995). The Western Scheldt has a complex morphology with flood and ebb channels and intertidal mud and sand flats. The average depth of the channel is 15-20 m. The Scheldt estuary is an important Nature 2000-area for a large number of birds. Especially the intertidal flats provide essential feeding grounds for waders, with benthic macrofauna as main food source.

A 75 ha intertidal habitat was created at Perkpolder as a managed coastal realignment project, where new dikes were constructed along the inland perimeter and flooding occurred through a single breach in the original dike (Figure 81). Before flooding, the area was used for agriculture. Prior to inundation channels were dug in the realignment site to ensure water retain in the area to enhance ecological development of the area. On 25th of June 2015 a single breach in the sea defences at Perkpolder allowed 75 ha of farmland to be inundated by the sea for the first time in at least 380 years. The inflow of water had a direct impact on erosion and sedimentation processes, which give rise to morphological changes in the area. The resulting intertidal habitat can be classified as low dynamic mid litoral (25-75% emersion time) located at the poly/mesohaline (average salinity between 10-18) transition zone of the Western Scheldt.

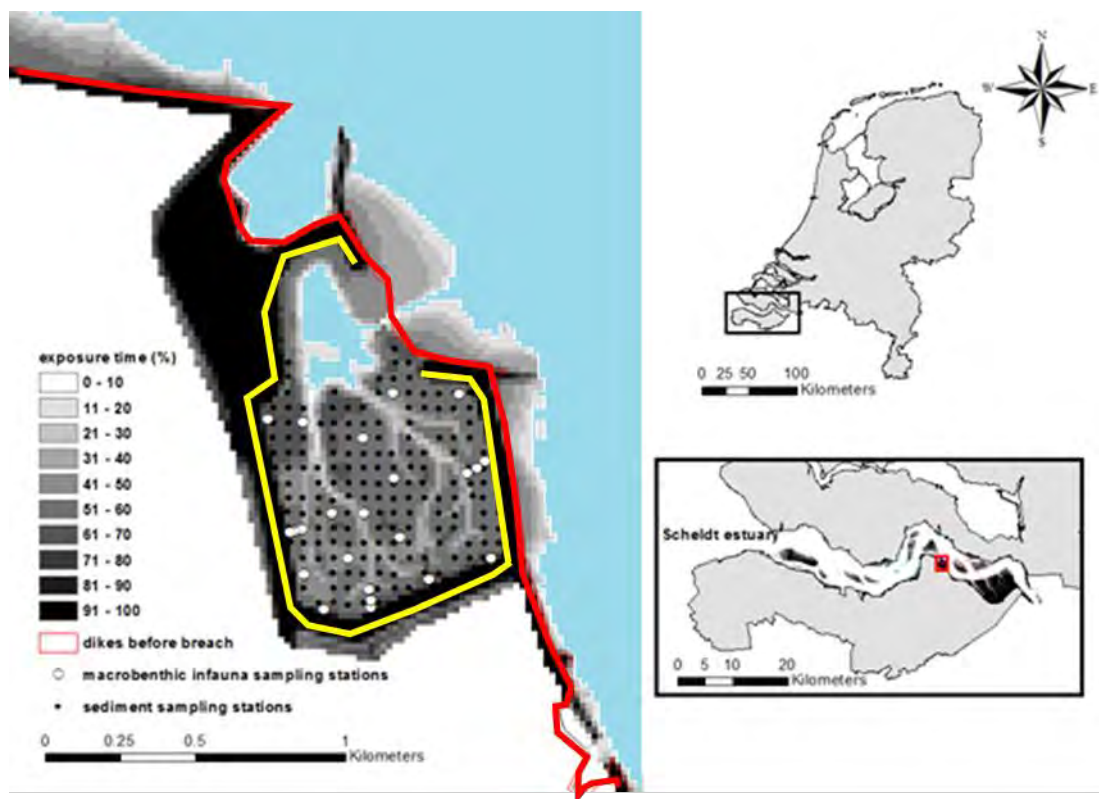


Figure 81. Map of the Perkpolder managed realignment site in the Scheldt estuary (southwest of The Netherlands) with the twenty-four macrobenthic infauna sampling stations and the two-hundred sediment characteristic sampling stations. Red line indicates the original dike, yellow the new dike.

5.2.2 MORPHOLOGICAL CHANGES

To monitor spatial and temporal variation in sediment accumulation and physical properties several sampling campaigns were carried out after inundation of the area. Spatial variation of these parameters was investigated by sampling 200 stations equally spaced throughout the managed realignment in autumn 2016, 2017 and 2018 (Figure 81). Temporal variation was studied by sampling 15 stations in 2015 (n=3 times per year), 2016 (n=6), 2017(n=3) and 2018 (n=4).

At each station a single sediment sample (18.5 cm³) was collected from the upper 3 cm (using a 1.4 in diameter syringe from which the tip was cut off) and stored in a pre-weighed sample bottle. Samples were wet weighed and placed in a freezer for a minimum of 3 days before opening the bottles and freeze dry (Christ® Alpha 1-4) the sediment samples for 4 days. Samples were reweighed after freeze drying. Bulk density of the sediment (g cm⁻³) was calculated as ratio dry weight to the sampled volume. Sediment particle size distribution was determined by laser diffraction (Malvern Mastersizer 2000), from which the median grain size of the sediment D₅₀ (µm) as well as the size distribution (percentage coarse, medium, fine and very fine sand, and silt) was derived. The average depth of the mud layer (cm) on top of the old farmland was randomly measured (n=10) at each station using a ruler. Elevations (m NAP) were measured using a

differential GPS device with a horizontal and vertical measure accuracy of 8 and 13 mm, respectively (Leica GS12, Leica Geosystems AG, Switzerland, correction signal: SmartNet, Leica Geosystems, the Netherlands). Furthermore, average (n=5) sediment penetration resistance (N) and average (n=5) erosion resistance (kPa) of the sediment was measured at each station using a penetrometer and a shear vane, respectively.

5.2.3 COLONIZATION BY MACROBENTHIC INFAUNA

To quantify the colonisation of macrobenthic infauna and their community structure twenty-four stations inside the managed realignment site were sampled (Figure 81). Sampling was first undertaken in autumn 2015, four months after the breach. Subsequent sampling took place annually in spring and autumn for three years. In 2015, 2016 and 2017 samples were collected at sixteen, relatively easy accessible stations situated close to the dike. In 2018 the sampling effort was increased with samples covering also the middle part of the managed realignment site. Macrobenthic infauna was sampled using a 10 cm i.d. corer, i.e. 78 cm² surface area to a maximum depth of 35 cm or to the depth of the former farmland. Three replicates were taken randomly at each station, pooled and sieved in the field through a 1 mm mesh sieve. The residue was preserved in 4% buffered formaldehyde solution and stained with Rose Bengal. In the lab specimens were sorted and identified to the lowest possible taxonomic level, counted, wet weighted and preserved. The number of individuals per species found at each station was converted to density (number of ind. m⁻²). Worm counts were based on the number of heads found in a sample. When only a tail was found it was recorded as 1 individual of this species. Biomass was calculated by converting total wet weight to total ash free dry weight (AFDW) in g m⁻² using species specific conversion factors as described in Craeymeersch and Escaravage (2014). Additional, lugworm *Arenicola marina* densities were counted in the field within 0.25 m² quadrants (n=10) at each sampling station.

At each stations elevation (NAP m), median grain size (µm), sediment size distribution (percentage coarse, medium, fine and very fine sand, and silt), bulk density (g cm⁻³) and depth of mud layer (cm) were determined. Additional, Chlorophyll *a* (µg cm⁻³), as a measure for food availability for benthic animals, was measured by three pooled sediment samples collected from the upper 1 cm of the sediment, using a 1 cm in diameter syringe from which the tip was cut off. The samples were stored in the dark at -80°C after which they were freeze dried and analysed spectrophotometrically according to Aminot and Rey (2000). At 15 stations also sediment penetration resistance (N) and average erosion resistance (kPa) (n=5) of the sediment was measured.

5.2.4 COMPARISON OF THE COMMUNITY STRUCTURE IN THE MANAGED REALIGNMENT AREA VERSUS NATURAL TIDAL FLATS

Since 1992 the Ministry of Transport, Public Works and Water Management is monitoring the benthic fauna of the Western Scheldt as part of a biological monitoring programme (MWTL). To compare community structure in the managed realignment area to that of natural nearby tidal flats, a subset of the MWTL data (based on location and ecotope) was used. The managed realignment area, located on the poly/mesohaline transition zone, can be classified as low dynamic mid littoral ecotope according to the Dutch ecotope system used in Scheldt estuary, the so-called ZES (Zoute Ecotopen Stelsel, Bouma et al. 2005). A total of 62 macrobenthic samples taken between 2010 and 2014, within the low dynamic mid littoral ecotope between $3^{\circ}59.659'E$ and $4^{\circ}6.550'E$ (58000 and 66000 Rijksdriehoek) were used in the analysis (Figure 82).

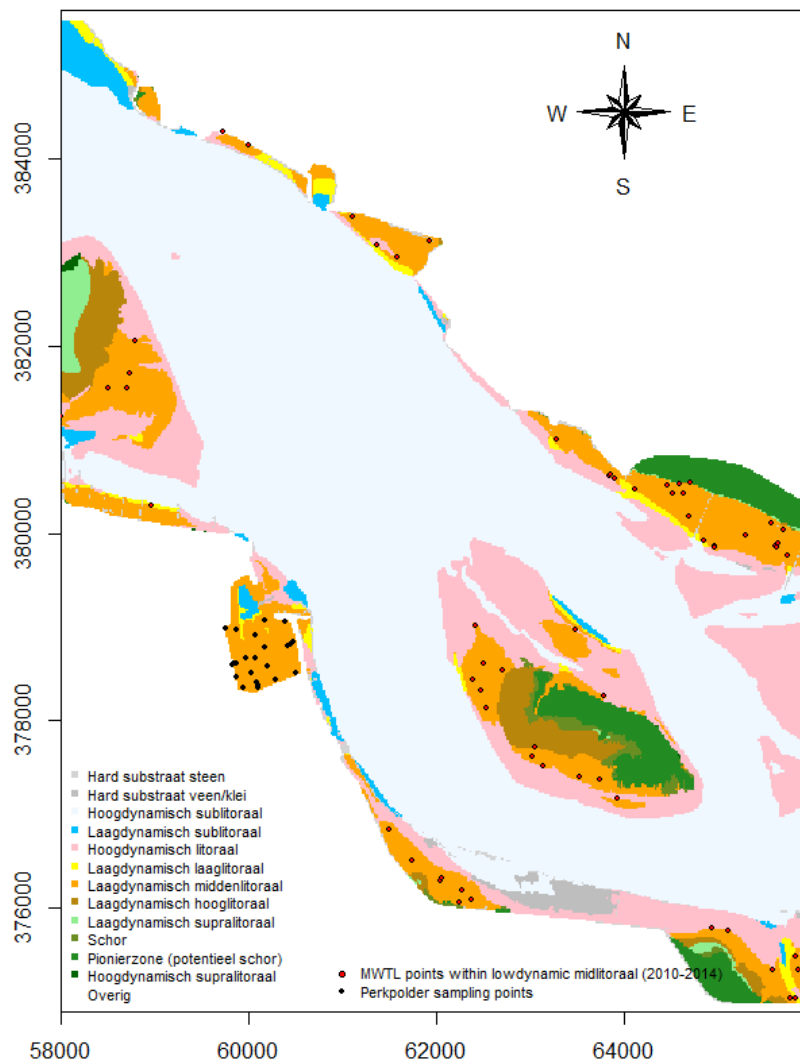


Figure 82. Map of the Scheldt estuary with 24 macrobenthic infauna sampling stations sampled between 2015-2018 in the managed realignment area (black dots) and 62 macrobenthic sampling stations sampled between 2010-2014 within the low dynamic mid littoral ecotope (red dots).

5.2.5 BIRDS

During the first two years, counts of birds in the realignment site were made during low tide on seven occasions during the autumn and winter months (2016: Feb, Mar, 2*Oct, Nov, Dec; 2017: Jan). No attempt was made to establish a reference area on which bird counts would be made. From September 2017 onwards the methodology changed in low and high tide bird counts during each calendar month. Only the data from September 2017 onwards have been analysed. Behaviour of the birds were recorded separately distinguishing foraging birds from resting birds and birds that use the surrounding dike as roosting area. For the top ten waders, diet data was obtained from Leopold et al. (2004) and plotted versus the available food source. During each count all humans and dogs using the surrounding dikes and tidal flat were counted.

5.2.6 STATISTICAL ANALYSIS

5.2.6.1 DEVELOPMENT OF THE COMMUNITY STRUCTURE IN PERKPOLDER

A multivariate analysis was performed to assess the development of the community structure of the macrobenthic infauna. To avoid ambiguity, specimens that had only been determined at class or phylum level were left out for the multivariate analysis of the community composition. Nemertea and Oligochaeta were included. If not all individuals of a genus were identified at the species level, they were merged to the genus level. The species name was then added in parentheses when only one species was identified within the genus in all samples, whereas *spp.* was used when multiple species were present. The community structure was analysed using multivariate statistics using the package ‘vegan’ (Oksanen et al. 2018) in R (R Core Team, 2018). A Bray-Curtis similarity matrix was constructed from fourth root-transformed densities of the macrobenthic taxa with a dummy variable (with a value of 1) to overcome the problems associated with the complete absence of organisms at one station inside the realignment site in autumn 2018. A Non-metric multidimensional scaling (NMDS) was applied to the similarity matrix to represent, as closely as possible, the pairwise (dis)similarity between objects in a two-dimensional space. NMDS is a rank-based approach. This means that the original distance data is substituted with ranks.

Detrended Correspondence Analysis (DCA) was used to detect the length of the environmental gradient. After DCA, Canonical Correspondence Analysis (CCA) was applied and the Monte Carlo permutation test used to reveal the effect of the obtained explanatory variables on macrobenthic infauna species composition. A total of 999 permutations were performed.

5.2.6.2 EXPLANATORY ENVIRONMENTAL VARIABLES

To explore how species and community traits varied with environmental characteristics as well as through time additional multivariate analyses were conducted using the R package “mvabund” (Warton 2011).

Multivariate generalized linear models were used to examine environmental drivers of abundance, biomass, and presence/absence as they allowed to run linear models on all taxa responses simultaneously. Only the 20 most abundant taxa were included in the models. To obtain significance of environmental explanatory variables, ANOVAs were run and resampled 999 times for each model. Two sets of models were run, one with environmental characteristics (elevation, mud depth, penetration resistance, chlorophyll, bulk density, median grain size, and very fine grain fraction) and one with year, season, and sampling station. Model fit was checked using residual plots. For the presence/absence and abundance model a binomial and negative binomial distribution was used respectively.

5.2.6.3 **COMMUNITY TRAITS**

To examine which traits best explained variation across taxa in their environmental response, trait based models were used. For 22 taxa species specific traits were obtained from the BIOTIC database (Marlin, 2016) and from literature. A total of 12 traits were evaluated, including feeding, mobility, size, position in sediment, longevity, bioturbation/bioirrigation, reproductive and productivity traits. Each trait consists of different modalities (e.g. for the trait 'feeding', the modalities are: omnivore, surface deposit feeder, subsurface deposit feeder and filter feeder).

The trait based models were generalized linear models that examined interactions between traits and environmental variables. To test for the significance of interactions between environmental variables and traits ANOVAs were run on the models. Models were compared using the Akaike Information Criterion (AIC).

5.3 **RESULTS**

5.3.1 **MORPHOLOGICAL CHANGES**

5.3.1.1.1 **Area-wide spatial and temporal morphological changes**

The full coverage sampling campaign allowed to evaluate how sediment characteristics changed spatially at a fine resolution. Spatial distributions of bulk density, changes in elevation and sediment characteristics were in general related to the location of the inlet and the two main creeks. In 2016, bulk density (g sediment per sampled cm^{-3}) was highest near the inlet and upper creeks and lower throughout the rest of the site, especially in the middle and bottom left corner (Figure 65). Most change occurred during the first two years (2016 and 2017) followed by almost no changes in 2018. Other sediment characteristics showed patterns driven by the distance to creeks and the inlet. Changes in elevation were larger near the inlet and in the middle of the site, compared to directly next to or at the creeks (Figure 66). The mud depth layer, mud content (Figure 67), and water content were lowest near the inlet and next to the creeks. Besides the creeks and inlet, another interesting feature was the upper left corner between the wall and the creek which had

the highest bulk density, elevation and grain size in 2016. This area tended to change in the direction of the central values for each sediment characteristic over time. For most of the sediment characteristics, it was the only area that changed in a direction opposing that of the rest of the site.

5.3.1.2 SPATIAL AND TEMPORAL MORPHOLOGICAL CHANGES AT THE BENTHIC MACROFAUNA SAMPLING STATIONS

After inundation, sediment with a high percentage of silt deposited in the managed realignment (Figure 83). Whereas the deposited mud layer on top of the former farmland changed in thickness over time, as measured with a ruler, elevation measurements do not reflect these changes as elevations stayed in the order of those recorded four months after the breach. An increase in deposited mud layer in 2016 and 2018 could indicate sedimentation in those years, whereas no large changes seems to occur in 2017. An increase in penetration resistance and a decrease in erosion resistance in time could indicate compaction of the sediment. Sediment density (Bulk density) however shows a decreases over time indicating that the sediment contains more water which is counter intuitive with respect to compaction. Chlorophyll *a* shows a peak in autumn 2016 and 2018.

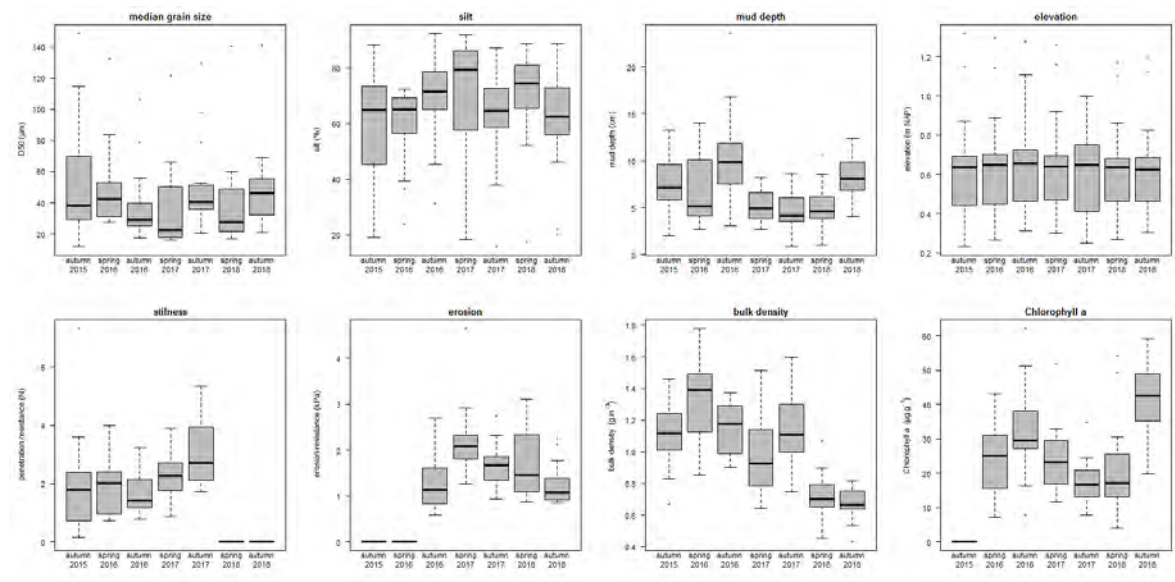


Figure 83. Sediment characteristics: Box plots of changes in median grain size, silt content, deposit mud layer, elevation, penetration resistance, erosion resistance, bulk density and chlorophyll-a in time within the managed realignment area.

5.3.2 COLONIZATION BY MACROBENTHIC INFAUNA

A total number of 61 299 individuals belonging to 39 different taxa were collected in 126 samples taken within the managed realignment area between 2015 and 2018. A rapid colonization was observed as 19 species colonized the realignment area within four months after the breach. During each subsequent sampling campaign new species colonized the area (Table 14). During the first year, all sampling stations exhibited a large number of small opportunistic, highly mobile benthic species, mainly of the class Malacostraca. *Corophium volutator* was by far the most dominant species in abundance and biomass (Table 15). After one year larger sized long living species colonized the area with species from the class Polychaeta dominating the area. The mean number of species per station was on average 10, in same order as found on nearby tidal flats (Figure 84A). Only at one station in autumn 2018, no species were found. Total abundance increased during the first year after the breach followed by a decrease resulting in an average abundance in the order found on nearby tidal flats (Figure 84B). The managed realignment was dominated by Malacostraca and Polychaeta of which *Corophium volutator*, *Pygospio elegans* and *Heteromastus filiformis* respectively contributed most to the total abundance. Biomass (Figure 84C) increased over time. During the first two sampling campaigns malacostraca accounted for the majority of the biomass whereas from autumn 2016 onwards polychaetes and bivalves contributed most to the total biomass. Biomass in autumn 2018 is 63% higher compared to nearby tidal flats. This is mainly due to high abundance of *Heteromastus filiformis* and *Hediste diversicolor* which contribute most to the total biomass.

5.3.3 COMMUNITY STRUCTURE

The benthic community composition showed high dissimilarity between sampling moments inside the realignment site indicating that after three years the community is still changing (Figure 85). The community development shows seasonality and develops in the direction of the community found on nearby tidal flats in the Western Scheldt. Development of the community structure was significantly affected by sampling moment ($F_{6,119} = 21.76$, $p=0.001$) and season ($F_{1,124} = 5.56$, $p=0.002$) which explained 21.6% and 6.2% of the variability, respectively (Figure 86).

Table 14. Occurrence (% of the total sampled stations) of the observed species/taxon in the managed realignment Perkpolder and on nearby natural tidal flats (MWTl data) sampled between 2010-2014.

species/Taxon	Occurrence %							MWTl 2010-2014
	Autumn 2015	Spring 2016	Autumn 2016	Spring 2017	Autumn 2017	Spring 2018	Autumn 2018	
<i>Corophium volutator</i>	100	100	100	100	100	83	22	56
<i>Polydora cornuta</i>	94	31	88	88	50	22	70	11
<i>Nemertea</i>	88	88	50	75	56	13	35	13
<i>Oligochaeta</i>	88	81	38	25			4	11
<i>Limicola balthica</i>	81	69	100	100	75	65	78	89
<i>Pygospio elegans</i>	81	100	100	100	94	91	96	79
<i>Eteone spp</i>	69	56	88	81	88	91	39	44
<i>Alitta succinea</i>	50	63	81	94	94	83	43	2
<i>Aphelochaeta</i>	50	38	75	50	63	43	39	13
<i>Crangon crangon</i>	50	69	13	69	31	61	17	32
<i>Heteromastus filiformis</i>	50	31	100	100	100	100	96	89
<i>Streblospio benedicti</i>	44	6	63	13	44	48	83	60
<i>Pearingia ulvae</i>	38		63	13	44	48	83	60
<i>Chironomidae</i>	31		13	6				
<i>Cyathura carinata</i>	31	31	69	63	94	91	91	58
<i>Nudibranchia</i>	19		6					3
<i>Hediste diversicolor</i>	13	6	81	94	63	83	91	69
<i>Insecta</i>	13	13	19			13	9	2
<i>Scrobicularia plana</i>	6	6	6	13	44	61	83	35
<i>Bivalvia</i>		13			6			21
<i>Gammarus</i>		6		6	6			
<i>Polychaeta</i>		6	6					
<i>Pseudopolydora pulchra</i>		6						
<i>Arenicola</i>			13	13			4	15
<i>Alitta virens</i>			6					
<i>Donax vittatus</i>			6					
<i>Isopoda</i>			6					2
<i>Mya arenaria</i>			6			4	9	5
<i>Bathyporeia pilosa</i>				6		4		29
<i>Platyhelminthes</i>				6				
<i>Carcinus maenas</i>					13		26	3
<i>Cerastoderma edule</i>					13	4	9	11
<i>Ensis</i>					6			2
<i>Gastropoda</i>						4		
<i>Hemigrapsus</i>							22	
<i>Abra tenuis</i>							13	3
<i>Tapes</i>							4	
<i>Corophium</i>								32
<i>Corophium arenarium</i>								29
<i>Tellinoidea</i>								26
<i>Arenicola marina</i>								15
<i>Capitella spp</i>								10
<i>Decapoda</i>								8
<i>Assiminea grayana</i>								6
<i>Marenzelleria</i>								6
<i>Cardiidae</i>								5
<i>Corophiidae</i>								5
<i>Eurydice pulchra</i>								5
<i>Parahaustorius holmesii</i>								5
<i>Abra tenuis</i>								3
<i>Monopseudocuma gilsoni</i>								3
<i>Abra alba</i>								2
<i>Bygides sarsi</i>								2
<i>Capitellidae</i>								2
<i>Crangonidae</i>								2
<i>Enchytraeidae</i>								2
<i>Harmothoe glabra</i>								2
<i>Scolelepis bonnierii</i>								2
<i>Semellidae</i>								2
number of species	19	20	25	21	20	20	24	49

Table 15. Density (ind. m⁻², mean ± se) of the observed species/taxon in the managed realignment Perkpolder and on nearby natural tidal flats (MWTl data) sampled between 2010-2014.

species/Taxon	Density (ind. m ⁻²)							MWTl 2010-2014
	Autumn 2015	Spring 2016	Autumn 2016	Spring 2017	Autumn 2017	Spring 2018	Autumn 2018	
<i>Corophium volutator</i>	13083 ± 2113	23418 ± 4770	14358 ± 1680	17157 ± 3625	10862 ± 2099	1555 ± 561	688 ± 582	4817 ± 1092
<i>Polydora cornuta</i>	622 ± 137	153 ± 71	652 ± 227	233 ± 52	127 ± 46	51 ± 16	138 ± 20	127 ± 31
<i>Nemertea</i>	97 ± 14	209 ± 59	58 ± 11	124 ± 29	113 ± 35	57 ± 14	53 ± 7	127 ± 21
<i>Oligochaeta</i>	670 ± 290	1342 ± 848	707 ± 384	64 ± 12			170 ± 0	1592 ± 1294
<i>Limecola balthica</i>	160 ± 33	2809 ± 879	347 ± 50	509 ± 156	138 ± 27	141 ± 28	160 ± 30	1313 ± 237
<i>Pygospio elegans</i>	157 ± 46	3271 ± 625	1761 ± 394	4886 ± 1016	1684 ± 470	1388 ± 359	1734 ± 547	2459 ± 657
<i>Eteone spp</i>	120 ± 14	85 ± 20	127 ± 20	153 ± 25	167 ± 35	156 ± 24	66 ± 10	120 ± 16
<i>Alitta succinea</i>	159 ± 54	102 ± 28	140 ± 28	314 ± 52	190 ± 36	192 ± 37	64 ± 20	64 ± 0
<i>Aphelocheata</i>	69 ± 16	78 ± 13	103 ± 21	90 ± 23	102 ± 20	76 ± 21	141 ± 49	2094 ± 1690
<i>Crangon crangon</i>	58 ± 16	204 ± 105	42 ± 0	282 ± 146	119 ± 66	188 ± 56	53 ± 11	169 ± 47
<i>Heteromastus filiformis</i>	58 ± 21	17 ± 17	20438 ± 2541	4581 ± 496	6093 ± 502	4342 ± 514	6337 ± 757	1685 ± 211
<i>Streblospio benedicti</i>	79 ± 19	42 ± 0	127 ± 22	99 ± 24	42 ± 0	42 ± 0	42 ± 0	159 ± 43
<i>Peringia ulvae</i>	42 ± 0		373 ± 129	85 ± 42	715 ± 392	270 ± 91	1336 ± 284	510 ± 111
<i>Chironomidae</i>	59 ± 10		149 ± 106	127 ± 0				
<i>Cyathura carinata</i>	127 ± 36	102 ± 49	235 ± 58	178 ± 41	662 ± 155	612 ± 95	726 ± 100	566 ± 73
<i>Nudibranchia</i>	42 ± 0		42 ± 0					96 ± 32
<i>Hediste diversicolor</i>	0 ± 0	42 ± 0	219 ± 56	229 ± 51	191 ± 44	237 ± 46	1203 ± 234	510 ± 89
<i>Insecta</i>	106 ± 64	42 ± 0	495 ± 299			71 ± 14	106 ± 21	64 ± 0
<i>Scrobicularia plana</i>	85 ± 0	42 ± 0	0 ± 0	64 ± 21	127 ± 43	127 ± 31	520 ± 87	191 ± 37
<i>Bivalvia</i>		64 ± 21			42 ± 0			78 ± 8
<i>Gammarus</i>		42 ± 0		42 ± 0	42 ± 0			
<i>Polychaeta</i>		0 ± 0	849 ± 0					
<i>Pseudopolydora pulchra</i>		85 ± 0						
<i>Arenicola</i>			106 ± 64	85 ± 42			0 ± 0	64 ± 0
<i>Alitta virens</i>			42 ± 0					
<i>Donax vittatus</i>			85 ± 0					
<i>Isopoda</i>			42 ± 0					64 ± 0
<i>Mya arenaria</i>			212 ± 0			42 ± 0	42 ± 0	106 ± 21
<i>Bathyporeia pilosa</i>				42 ± 0		85 ± 0		2615 ± 652
<i>Platyhelminthes</i>				42 ± 0				
<i>Carcinus maenas</i>					42 ± 0		71 ± 9	64 ± 0
<i>Cerastoderma edule</i>					64 ± 21	42 ± 0	64 ± 21	182 ± 88
<i>Ensis</i>					85 ± 0			64 ± 0
<i>Gastropoda</i>						42 ± 0		
<i>Hemigrapsus</i>							59 ± 17	
<i>Abra tenuis</i>							127 ± 49	64 ± 0
<i>Tapes</i>							42 ± 0	
<i>Corophium</i>								1583 ± 749
<i>Corophium arenarium</i>								393 ± 94
<i>Tellinoidea</i>								661 ± 168
<i>Arenicola marina</i>								120 ± 22
<i>Capitella spp</i>								85 ± 13
<i>Decapoda</i>								76 ± 13
<i>Assiminea grayana</i>								446 ± 243
<i>Marenzelleria</i>								96 ± 18
<i>Cardiidae</i>								64 ± 0
<i>Corophiidae</i>								4883 ± 4058
<i>Eurydice pulchra</i>								85 ± 21
<i>Parahaustorius holmesi</i>								85 ± 21
<i>Abra tenuis</i>								64 ± 0
<i>Monopseudocuma gilsoni</i>								64 ± 0
<i>Abra alba</i>								64 ± 0
<i>Byligides sarsi</i>								64 ± 0
<i>Capitellidae</i>								3567 ± 0
<i>Crangonidae</i>								64 ± 0
<i>Enchytraeidae</i>								318 ± 0
<i>Harmothoe glabra</i>								64 ± 0
<i>Scolelepis bonnierii</i>								255 ± 0
<i>Semellidae</i>								64 ± 0
average abundance	14984 ± 2189	30291 ± 4325	39088 ± 2937	28661 ± 3682	20398 ± 2112	8438 ± 778	11860 ± 1317	11270 ± 1247

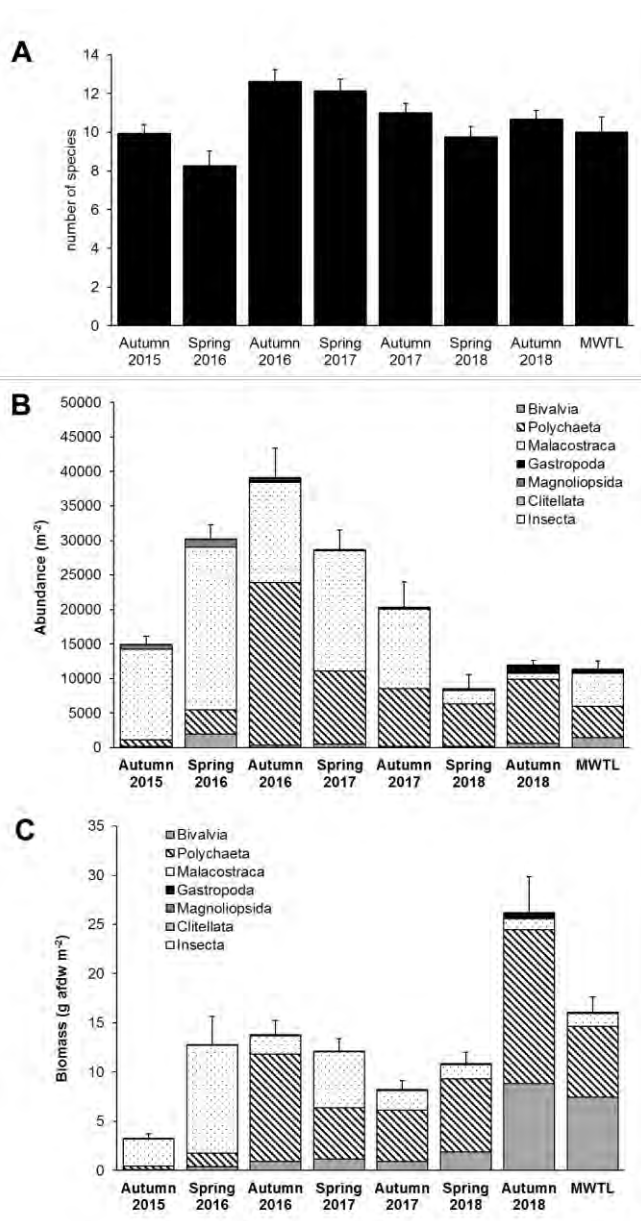


Figure 84. Variation in the mean (\pm se) species richness (A), total abundance (B) and biomass (C) with proportional representation of the taxa in the managed realignment area (Autumn 2015 till Autumn 2018) and in the MWTL data between 2010 and 2014.

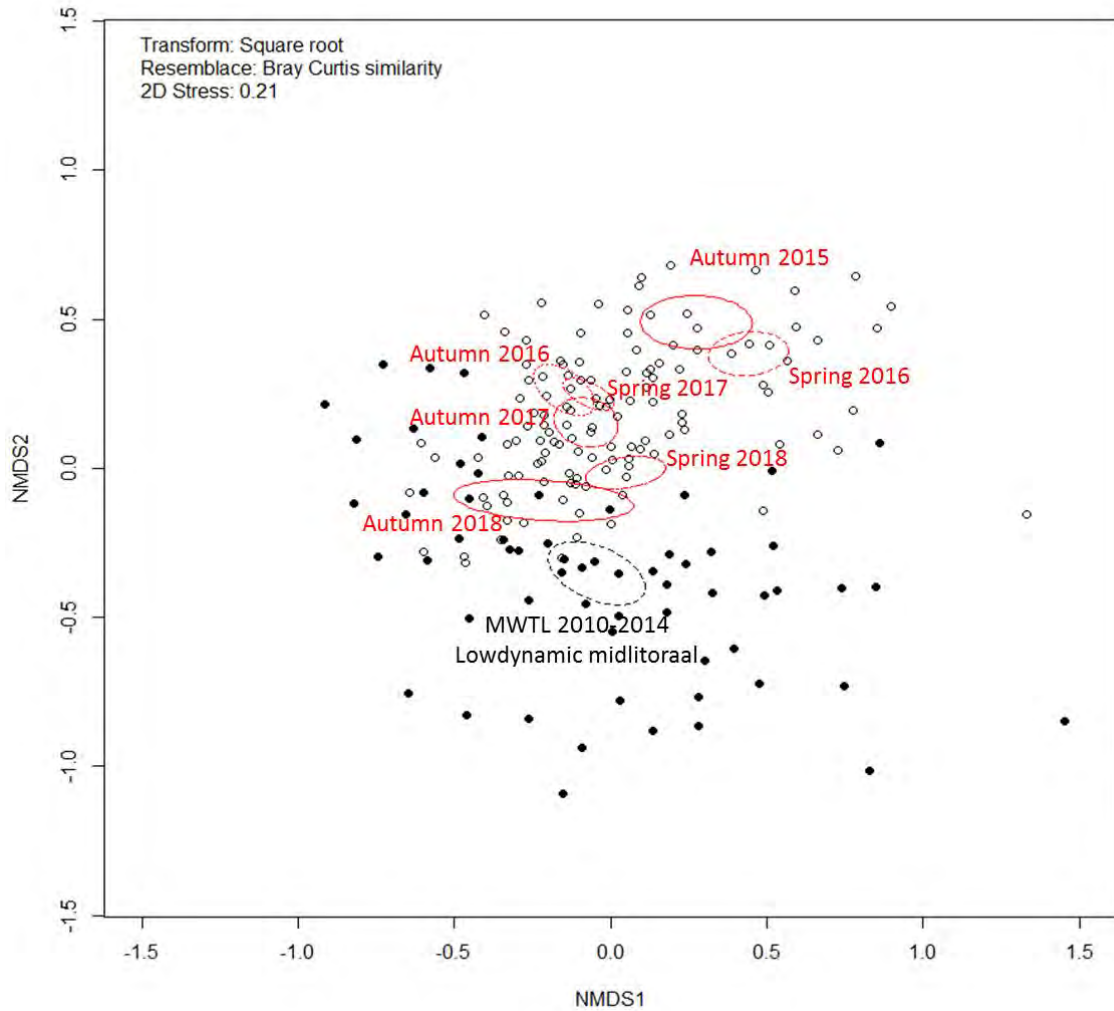


Figure 85. nMDS-plot showing changes in benthic community composition from autumn 2015 till autumn 2018 at the managed realignment Perkpolder based on abundance data (open circles) towards a community composition found at nearby tidal flats (closed circles). Each point represents a sampling station. Distance between points is a measure of dissimilarity in benthic community composition. The ellipse (red = realignment area, black = nearby tidal flats) denote the 95% confidence interval for each sampling moment.

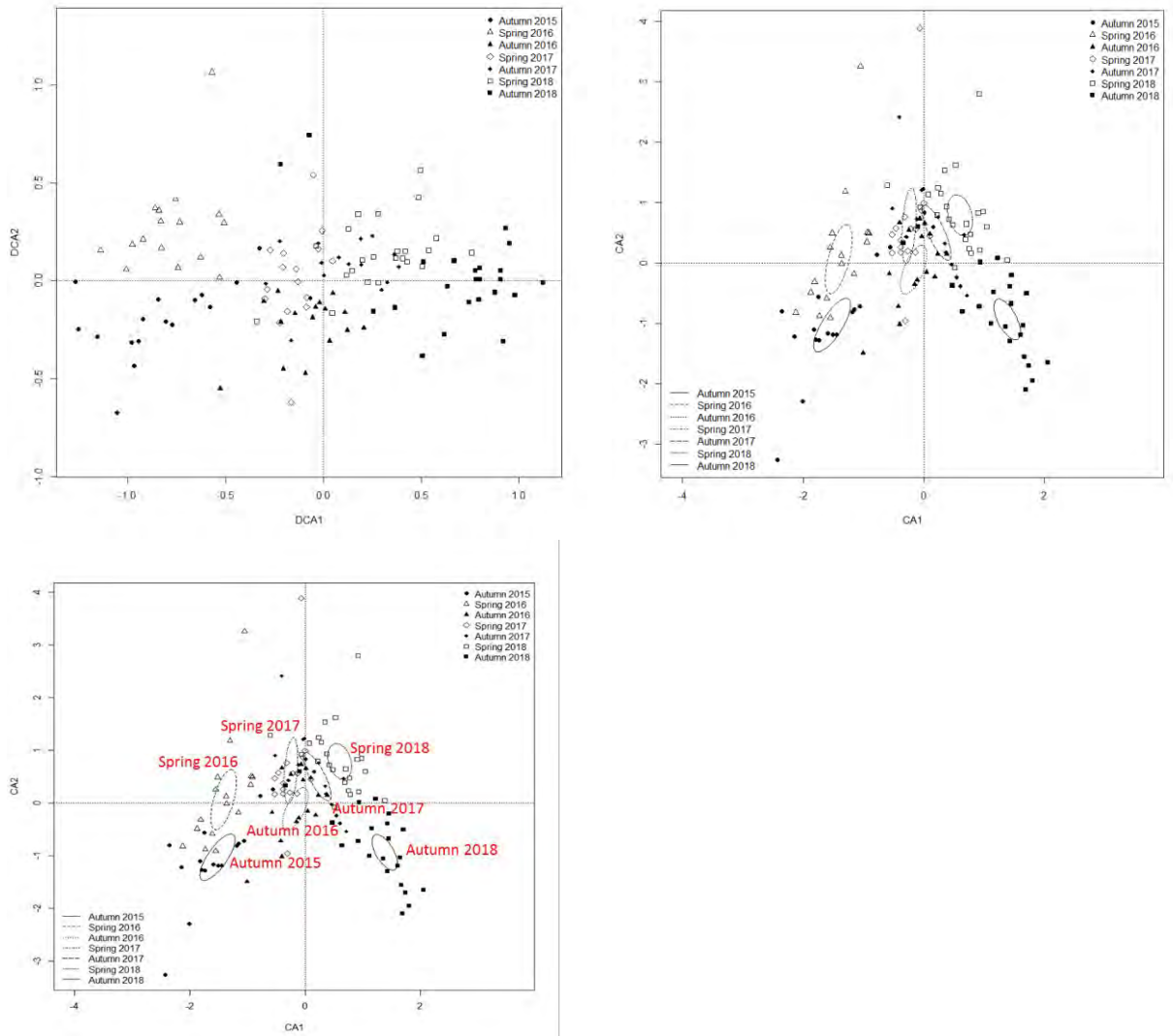


Figure 86. DCA (left) and CCA (right) ordination diagram of species abundance per sampling moment. Community structure was significantly affected by sampling moment ($F_{6,119} = 21.76$, $p=0.001$) and season ($F_{1,124} = 5.56$, $p=0.002$) which explained 21.6% and 6.2% of the variability, respectively.

5.3.4 ENVIRONMENT AND TRAITS

The area was first colonized by small, short-lived (except long-lived Oligochaeta), highly mobile taxa (except polychaete tube dweller *Pygospio elegans*) with high P to B ratios (Figure 87 and Figure 88). These taxa live within the top five centimeters of the surface and are surface deposit feeders (except sub-surface deposit feeding Oligochaeta). Oligochaeta were highly abundant at the beginning of the sampling period, but decreased dramatically starting in Spring 2017 (Figure 89). Over the course of the monitoring period, the community shifted to larger, longer lived, and more productive taxa which correspond mostly to bivalves,

especially *Scrobicularia plana*. A notable decrease in abundance of these shorter lived species, mostly *Corophium volutator*, occurred in 2018 which coincided with a drop in average bulk density of the area (Figure 89 and Figure 90). A spike in chlorophyll in Autumn 2016 coincided with a large increase in *Heteromastus filiformis* abundance as well as an increase in the large benthos category. After autumn 2016, the large benthos category has a stable mean abundance until Autumn 2018 where the abundance of large benthos increases coinciding with the spike in chlorophyll (Figure 87 and Figure 90).

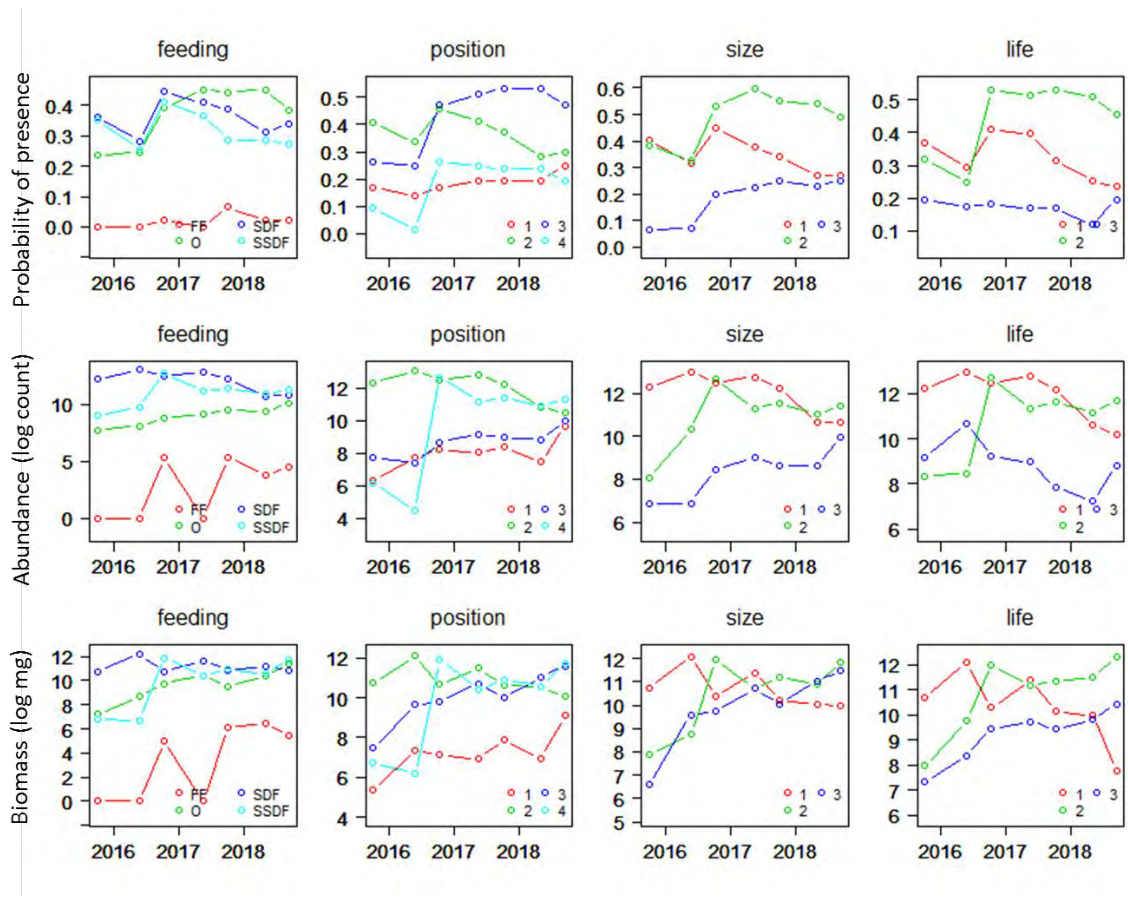


Figure 87. Presence, abundance and biomass of feeding, position, size and life traits averaged over the sampling moments. For the explanation of the trait legends, see Table 16.

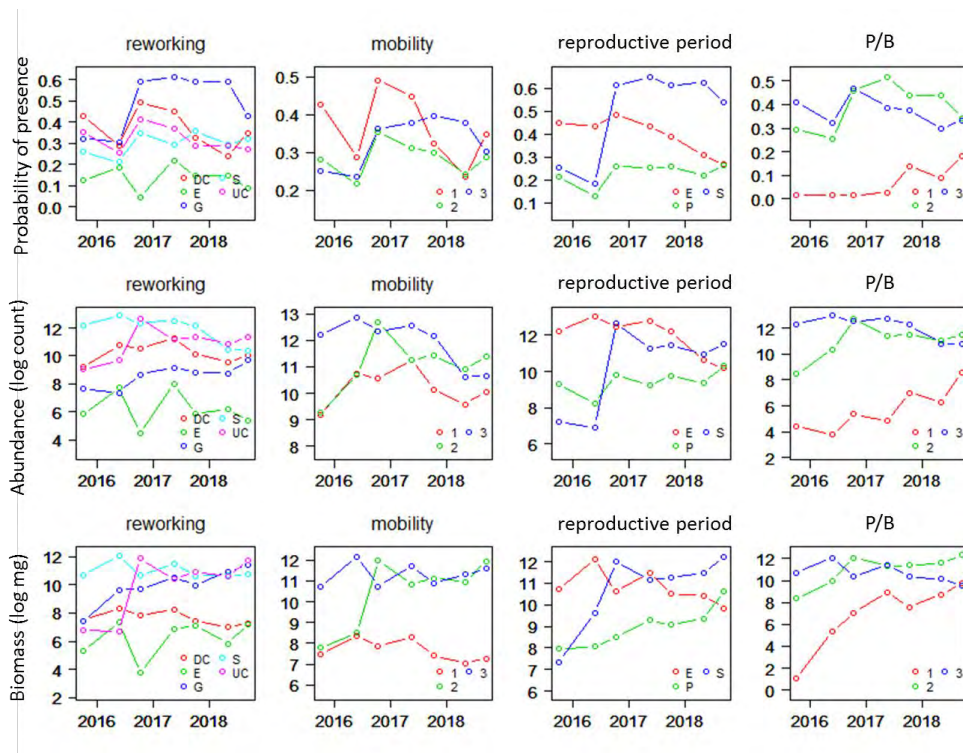


Figure 88. Presence, abundance and biomass of reworking, mobility, reproductive period and P/B traits averaged over the sampling moments. For the explanation of the trait legends, see Table 16.

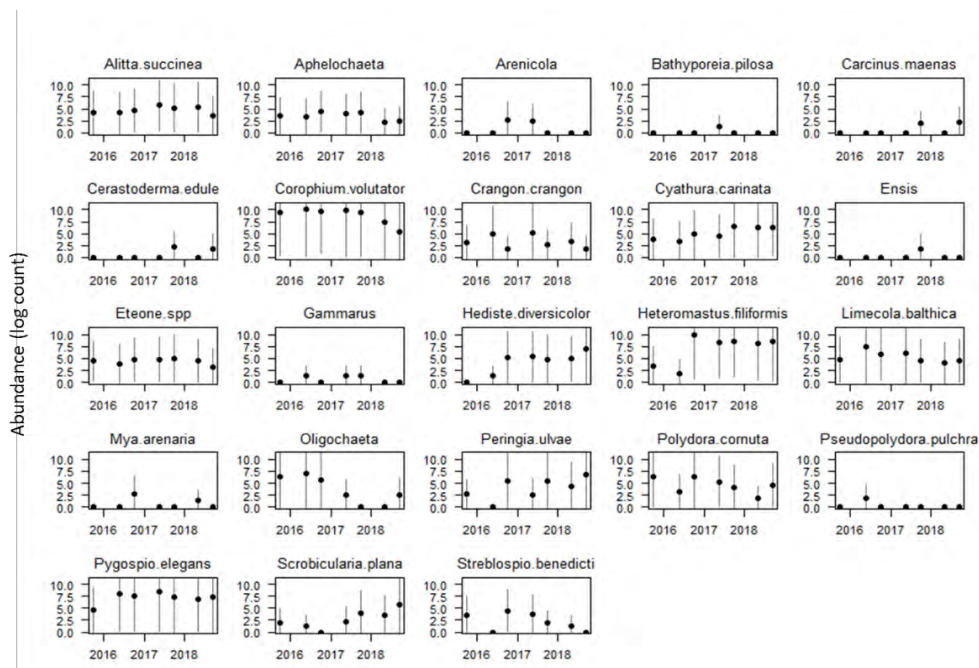


Figure 89. Average of 23 taxa included in the trait-based analysis at each sampling moment +/- standard deviation (vertical lines black lines).

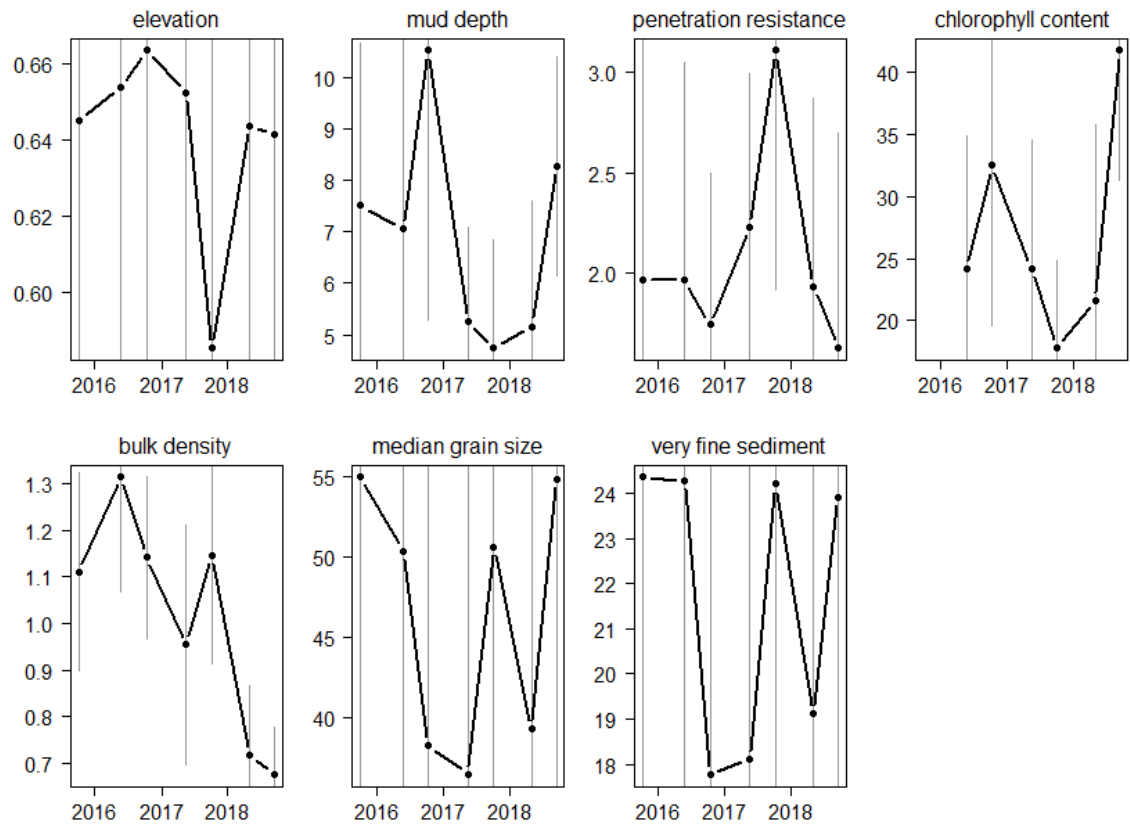


Figure 90. Average of sediment characteristics: elevation (NAP m), mud depth (cm) penetration resistance (N), chlorophyll content (unit?), bulk density (g/cm³), median grain size (μm), very fine sediment content (%) by sampling moment and standard deviations in grey lines.

Bulk density was the sediment characteristic that was most important in explaining taxa abundance, biomass, and presence/absence (Table 17, Table 18, Table 19 and Table 20). It was also one of the sediment characteristics that showed the clearest trend as it decreased over the sampling period (Figure 90). Bulk density had a significant positive effect on the presence of smaller, shorter lived taxa (*C. volutator*, *Oligochaeta*, *P. elegans*) and a negative effect on longer lived and deeper dwelling taxa (*S. plana*, *H. diversicolor*, *H. filiformis*) (Table 17). *Peringia ulvae*, the only abundant epifaunal diatom grazer also was less present with increases in bulk density. As could be expected, chlorophyll had a significant positive effect on *P. ulvae* abundance (Table 18). Chlorophyll had a significant negative relationship with the biomass of *C. volutator* and *P. elegans*, the early dominant small, shorter lived taxa. Mud depth was a significant explanatory variable for both biomass and abundance of deeper dwelling polychaetes, such as *Heteromastus filiformis* and *H. diversicolor*. The only taxon with a significant negative effect of mud depth on abundance and biomass is the polychaete *Alitta succinea*. The very fine sand fragment had a consistent significant

negative effect on *Streblospio benedicti*, though none of the other spionid polychaetes (*P. elegans* and *Polydora cornuta*) had a significant relationship with grain size. Taxa abundances varied more in a temporal scale than over a spatial one (Table 19). The taxa with only a significant seasonal effect are Aphelochaeta, *Crangon crangon*, and *P. cornuta*, which all had decreased abundance in spring. The taxa with a significant year effect only, with the exception of Oligochaeta, increased over the sampling period (*Cyathura carinata*, *H. diversicolor*, and *S. plana*).

The trait-based analysis revealed interactions, or how the benthos trait response changed as the environment changed. Bulk density and penetration resistance had the greatest number of interactions with benthos traits (Figure 89). Chlorophyll content did not have any interactions with the traits, however it had strong positive effects on long-lived taxa and sub-surface deposit feeders, which confirms what we observed from the multivariate generalized linear models. The reworking trait had interactions with both elevation and the very fine sediment fraction, both of which are environmental variables that reflected spatial variability over temporal variability.

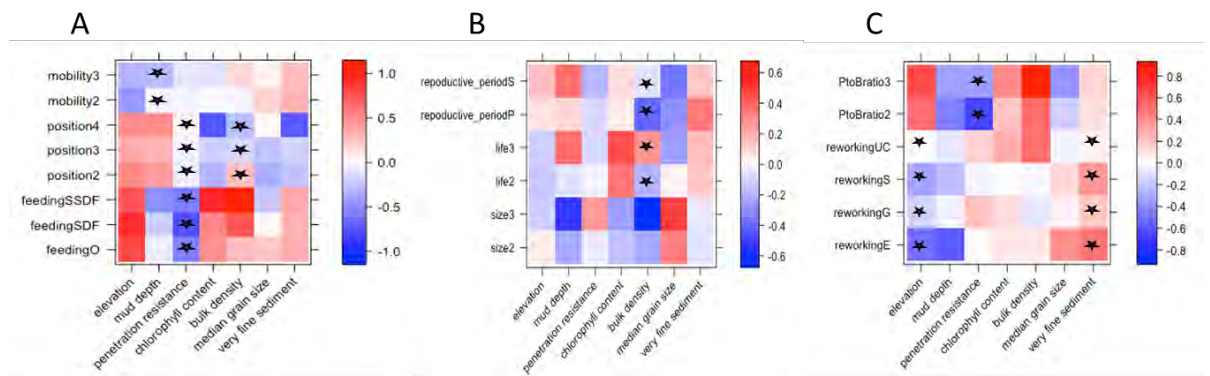


Figure 91. Coefficient heat map for trait-based analysis of taxa abundance. Refer to Table 3 for explanation of traits and levels. A, B, and C are separate models as all the coefficients traits could not be included in one model because of restricted degrees of freedom. (A) is the best model by AIC. The stars indicate significant ($p < 0.1$) interactions between a trait and an environmental variable.

Table 16. Traits of species/taxa used in the traits-based multivariate analysis. Traits for rare species were not included. Feeding: O=omnivore, SDF=surface deposit feeder, SSDF= subsurface deposit feeder, FF= filter feeder; Position: 1=epifauna, 2=shallow (0-5cm), 3=middle (5-15 cm), 4=deep (.15 cm); Life: 1= short, 2= medium, 3= long; Size: 1= small (<0.001g), 2= medium (0.001-0.01g), 3=large (0.01-0.14g); Reworking: E=epifauna biodiffuser, S= surficial biodiffuser, DC= downward conveyor, UC= upwards conveyor, G=gallery biodiffuser; Mobility: 1= sessile, 2=limited, 3=free; Reproductive period: S= Semelparous, E= episodic, P=Protracted; P/B, 1=low (<1/year), 2=medium (1-3/year), 3=high (>3/year). Traits for *C. carinata* (Ferreira et al., 2004; Queirós et al., 2013), for *Oligochaeta* size and position (Ysebaert et al., 2005) lifespan and P/B ratio (Giere, 2006) The other traits are taken from the table by Pieter van Linden.

	Feeding	Position	Size	Life	Reworking	Mobility	Reproductive period	P/B
<i>Alitta succinea</i>	SDF	3	3	2	G	3	S	2
<i>Aphelochaeta</i>	SDF	2	1	2	S	2	E	3
<i>Arenicola</i>	SSDF	4	3	3	UC	2	E	2
<i>Bathyporeia pilosa</i>	SDF	2	1	1	S	3	P	2
<i>Carcinus maenas</i>	O	1	3	3	E	3	P	1
<i>Cerastoderma edule</i>	FF	2	3	3	S	3	P	1
<i>Corophium volutator</i>	SDF	2	1	1	S	3	E	3
<i>Crangon crangon</i>	O	1	2	2	E	3	P	2
<i>Cyathura carinata</i>	O	2	2	2	S	3	P	3
<i>Ensis</i>	FF	4	3	3	S	2	E	1
<i>Eteone</i> spp	O	3	1	2	G	3	P	2
<i>Gammarus</i>	SDF	1	1	1	E	3	P	3
<i>Hediste diversicolor</i>	O	3	3	2	G	3	S	2
<i>Heteromastus filiformis</i>	SSDF	4	2	2	UC	2	S	2
<i>Limecola balthica</i>	SDF	2	2	3	S	2	E	2
<i>Mya arenaria</i>	FF	4	3	3	S	2	P	1
<i>Oligochaeta</i>	SSDF	2	1	3	UC	2	E	3
<i>Peringia ulvae</i>	SDF	1	1	2	S	3	P	3
<i>Polydora cornuta</i>	SDF	2	1	1	DC	1	P	3
<i>Pseudopolydora pulchra</i>	SDF	2	1	1	DC	1	P	3
<i>Pygospio elegans</i>	SDF	2	1	1	DC	1	E	3
<i>Scrobicularia plana</i>	SDF	3	3	3	S	2	P	1
<i>Streblospio benedicti</i>	SDF	2	1	1	DC	1	P	3

Table 17. The coefficients for the multivariate generalized linear model of taxa presence explained by sediment characteristics. Significant negative coefficients are highlighted in blue, significant positive coefficients are highlighted in red. The significance levels are: 0.1 > * > 0.05 > ** > 0.01 > ***

	(Intercept)	elevation	mud depth	penetration resistance	chlorophyll content	bulk density	median grain size	very fine sediment
Alitta succinea	5.38	-1.50	0.01	-0.26	-0.04	-0.35	-0.01 *	-0.03
Aphelochaeta	-2.64	-3.01	0.15	0.56 **	0.00	2.01 **	0.00	0.01
Corophium volutator	-2.45	1.65	0.25	0.56	-0.33 ***	23.14 ***	-0.06	-0.13
Crangon crangon	-0.21	-1.3 *	-0.07	-0.24	-0.01	0.54	0.01	0.04
Cyathura carinata	1.38	-0.15	0.11	0.30	-0.02	-1.8 *	-0.01	0.04
Eteone.spp	2.56	-2.15	0.09	0.23 *	-0.03	0.71	0.01	-0.07 **
Hediste diversicolor	1.33	-0.45	0.04	0.11	0.02	-2.09 **	0.01	0.00
Heteromastus filiformis	6.43	-0.28	0.00	0.54	-0.03	-3.92 ***	-0.01	-0.01
Limecola balthica	0.97	0.09	0.13 *	-0.33	-0.02	0.98	0.00	-0.01
Nemertea	-1.60	-2.56 **	0.07	0.46	-0.01	2.8 ***	0.00	-0.01
Nereis	-1.97	0.20	-0.03	-0.08	0.02	0.68	0.01	0.01
Oligochaeta	-3.16	-0.94	-0.01	-0.69	-0.02	6.58 ***	0.01	-0.14
Peringia ulvae	1.28	-0.15	0.02	-0.28 *	0.01	-1.76 **	0.00	0.01
Polydora cornuta	-5.38	3.17	0.12	0.42	0.06 **	0.75	-0.03	0.05
Pygospio elegans	-2.90	-0.83	0.01	-0.16	0.04	3.51 *	-0.02	0.24
Scrobicularia plana	-0.09	-0.18	-0.12	0.24	0.02	-4.16 ***	-0.02	0.18 ***
Streblospio benedicti	-2.30	0.17	0.41 ***	0.24	-0.02	3.09	-0.02 **	-0.24 ***

Table 18. The coefficients for the multivariate generalized linear model of taxa abundance explained by sediment characteristics. Significant negative coefficients are highlighted in blue, significant positive coefficients are highlighted in red. The significance levels are: 0.1 > * > 0.05 > ** > 0.01 > ***

	(Intercept)	elevation	mud depth	penetration resistance	chlorophyll content	bulk density	median grain size	very fine sediment
Alitta succinea	8.94	-1.04	-0.09 ***	-0.31	-0.04	0.13 *	-0.02 *	-0.02
Aphelochaeta	0.23	-2.78	0.1	0.34 **	0 *	3.33 ***	-0.01	0.03
Corophium volutator	7.89	0.32 *	0.03	-0.21	-0.05 **	4.7 ***	-0.01 **	-0.08 ***
Crangon crangon	7.2	-2.11	-0.33	-1.03	-0.03	1.33 **	0.03	0.01
Cyathura carinata	5.07	0.24	-0.01	0.13	0	-1.28 *	0.01 *	0.05 **
Eteone.spp	5.17	-0.51 **	0.07	0.11	-0.03 *	0.94	-0.01 ***	-0.04 **
Hediste diversicolor	5.35	-0.07	0.1 **	0.14	0.02 *	-2.81 ***	0.01	0.03
Heteromastus filiformis	7.78	-0.17	0.11 ***	0.07	0.01	0.3	0	-0.02
Limecola balthica	4.97	-0.88 **	0.13	-0.4	-0.02	1.59 ***	0	0
Nemertea	1.81	-1.15	0.05	0.16	-0.01	2.46 ***	0	0.01
Nereis	2.15	0.46	0.08 *	-0.1	0.02	0.24	0.01	0.01
Oligochaeta	-11.86	1.75	0.26	0.24 *	0.06	14.26 **	-0.01	-0.21
Peringia ulvae	6.61	-2.59	-0.11	-0.06	0.07 ***	-1.44	-0.01	0.04
Polydora cornuta	-0.47	1.76	0.06 *	0.14	0.07	3 **	-0.02 *	-0.03
Pygospio elegans	6.13	-0.21	0.09	0.36	-0.02 **	1 **	0	0
Scrobicularia plana	3.33	0.83	-0.22	0.25	0.06 *	-4.61 *	-0.02 *	0.2 **
Streblospio benedicti	-0.43	0.75	0.46 **	0.24	-0.06	11.6	-0.05	-0.54 ***

Table 19. The coefficients for the multivariate generalized linear model of taxa biomass explained by sediment characteristics. Significant negative coefficients are highlighted in blue, significant positive coefficients are highlighted in red. . The significance levels are: 0.1 > * > 0.05 > ** > 0.01 > ***

	(Intercept)	elevation	mud depth	penetration resistance	chlorophyll content	bulk density	median grain size	very fine sediment
Alitta succinea	10.46	-2.14	-0.19 **	-0.25	-0.01	-0.12	-0.02	0.01
Aphelochaeta	-0.27	-2.84	0.19 *	0.31	-0.02 *	1.73 **	-0.01	0.04
Corophium volutator	8.26	0.12 **	-0.03	-0.38	-0.05 **	4.03 ***	-0.01 ***	-0.08
Crangon crangon	4.83	-3.4	-0.3	-0.7	0	1.27 *	0.04 *	0.05
Cyathura carinata	4.72	0	-0.02	0.05	0	-0.94	0.01	0.04 **
Eteone.spp	2.25	-0.43	0.33 *	0.65	0	-3.08 **	0	0.08
Hediste diversicolor	8.2	0.03	0.05 *	0.06	0.03 **	-3.15 ***	0.01	0.01
Heteromastus filiformis	7.64	-0.16	0.13 ***	0.01	0.01	-0.54	0.01	-0.01
Limecola balthica	7.09	0.23	0.03	-0.09	0	-0.82 *	0.01	-0.02
Nemertea	2.88	-0.58	0.05	-0.21	-0.05	4.87 ***	0.01	-0.09
Nereis	-1.3	-1.69	0.18 *	0.23	0.06	-1.09	0.03 **	0.06
Oligochaeta	-9.9	1.42	0.04	-0.81 *	0.05	9.17 ***	-0.02	-0.02
Peringia ulvae	6.58	-3.29	-0.05	-0.09	0.07 **	-2.25 *	-0.01	0.05
Polydora cornuta	-1.21	1.81	-0.01	0.03	0.06	2.25 *	-0.02 *	-0.01
Pygospio elegans	2.84	-0.21	0.09	0.33	-0.01 *	1.23 ***	0	0
Scrobicularia plana	15.09	3.69	-0.32	-1.23 *	-0.11	-7.66 *	-0.05	0.22
Streblospio benedicti	-0.68	0.36	0.28 **	0.11	-0.03	6.34	-0.02 *	-0.35 ***

Table 20. The coefficients for the multivariate generalized linear model of taxa abundance explained by point, year, season, and an interaction between year and season. Both point and season were treated as factors, and while the coefficient for season is for sp is for spring, we did not include all the coefficients for the points as these were largely not significant. Significant negative coefficients are highlighted in blue, significant positive coefficients are highlighted in red. The significance levels are: 0.1 >* > 0.05 >** > 0.01 > ***

	(Intercept)	point	year	season (Spring)	Interaction between year and Spring
Alitta succinea	-72.95	3.91	0.04 ***	-2374.36 **	1.18 ***
Aphelochaeta	1396.02	-1.52 *	-0.69 ***	-4.76	0.00
Corophium volutator	2278.40	0.27	-1.13 ***	788.1 ***	-0.39
Crangon crangon	1565.67	-2.23	-0.78	-143.36 ***	0.07
Cyathura carinata	-2957.62	0.79	1.47 ***	-1808.3 ***	0.9 *
Eteone.spp	238.94	0.81	-0.12	-1257.05	0.62
Hediste diversicolor	-3825.97	-2.54	1.9 ***	-1907.69 **	0.95
Heteromastus filiformis	-112.75	0.25	0.06	-6541.78 ***	3.24 ***
Limecola balthica	671.19	-0.86	-0.33 ***	2761.05 ***	-1.37 ***
Nemertea	755.69	-0.30	-0.37 ***	2551.04	-1.26 **
Nereis	-2777.95	-3.23	1.38 **	7109.49 *	-3.53
Oligochaeta	7335.16	-2.33 **	-3.64 ***	6258.61	-3.1 *
Peringia ulvae	-2453.79	0.03	1.22 ***	-7346.24 ***	3.64 *
Polydora cornuta	1488.49	2.20	-0.74 ***	-1354.75 *	0.67
Pygospio elegans	-1042.42	-1.32 *	0.52	2324.41 ***	-1.15 ***
Scrobicularia plana	-7900.38	-2.00	3.92 ***	2526.09 *	-1.25
Streblospio benedicti	8712.01	22.02	-4.33 ***	-9578.15	4.75

5.3.5 BIRDS USAGE AT PERKPOLDER

During low tide 16 species of waders (including Common shelduck, *Tadorna tadorna*) and 18 other species of water birds were recorded foraging in the managed realignment area during low tide (Figure 92). In total more than a 1000 Black-headed gulls (*Chroicocephalus ridibundus*), Common shelducks (*Tadorna tadorna*) and Mallards (*Anas platyrhynchos*) were recorded foraging in the area over a one-year period. Waders like Eurasian curlew (*Numenius arquata*) and Eurasian oystercatcher (*Haematopus ostralegus*), and the Common shelduck (*Tadorna tadorna*) are foraging during low tide in the intertidal zone, while the creeks are used by ducks such as Mallard (*Anas platyrhynchos*) and Wigeon (*Mareca penelope*). Little egrets (*Egretta garzetta*)

look for small fish and crustaceans in the creeks. Figure 94 shows the diet of the different waders found within Perkpolder. The available food in the managed realignment area mainly consist of worms (green circle Figure 94). The presence of dunlins (*Calidris alpina*) corresponds with the presence of their preferred food source in the area.

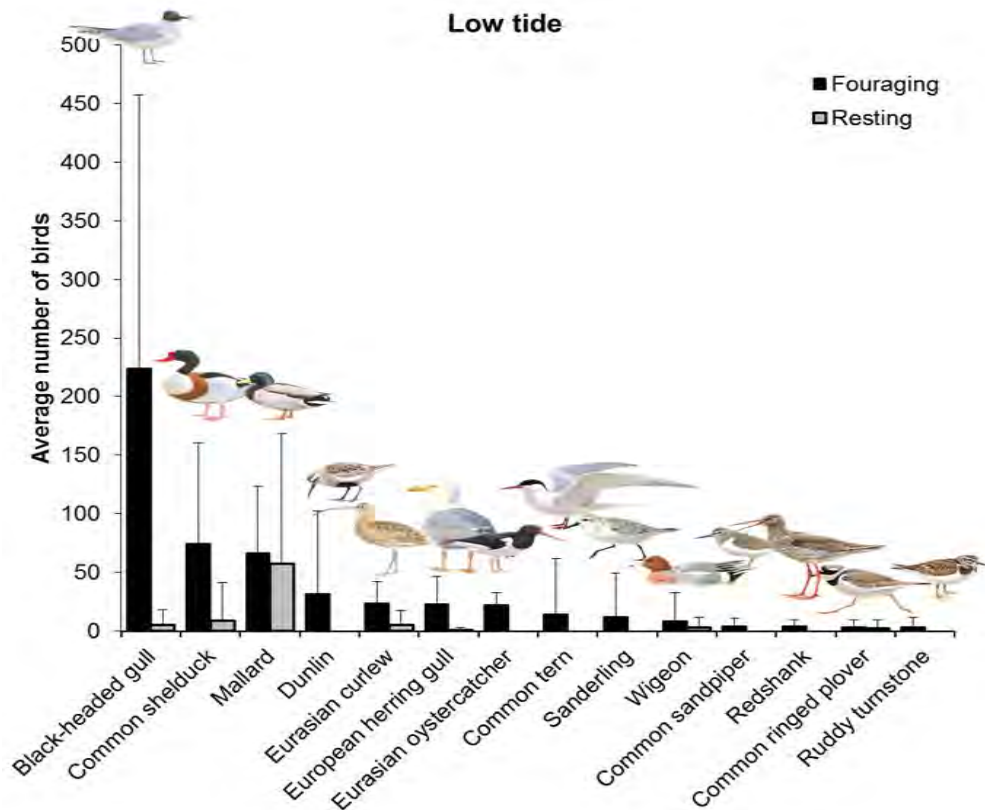


Figure 92. Average number of observed birds foraging and resting in the managed realignment area (75 ha) between September 2017 and September 2018.

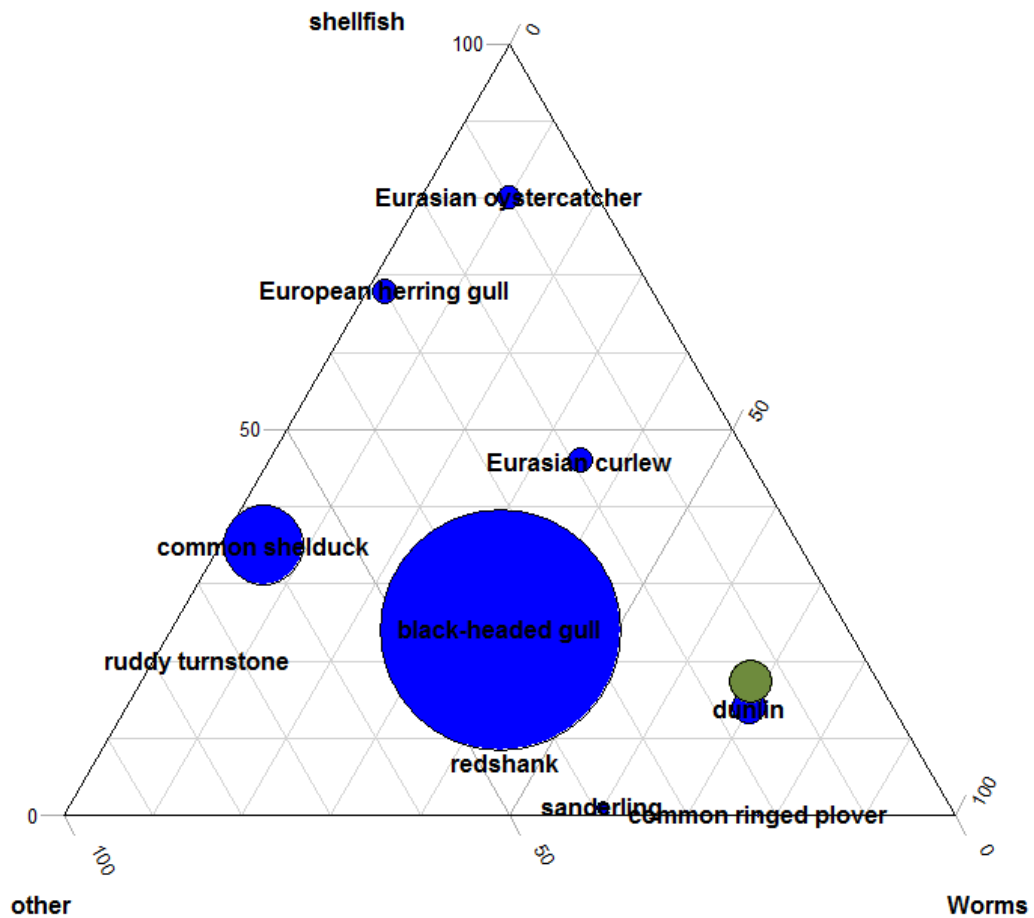


Figure 93. Diet and occurrence (ind. ha⁻²) of the top ten waders found in Perkpolder between September 2017 and September 2018. The location of the blue circle in the triangle indicate the diet composition. Distance to each corner represents relative importance of shellfish, worms or other macrobenthic organisms within their diet. Diet data was obtained from Leopold et al. 2004. The size of the circles indicates the relative density of species. The green circle indicate the benthic community composition and total biomass (size of the circles) in autumn 2018.

Dunlin, Mallard and Common shelduck, Bar-tailed godwit and Eurasian oystercatcher were the five most observed birds during high tide, using the dike around the managed realignment or the water as resting place (Figure 94). During each bird count all disturbances were counted (Figure 95). In September highest number of people (111) at the dikes surrounding Perkpolder were observed. Most of them were observed on the bike path at the west side of the area. On the east and south sides people are not permitted. Occasionally, people walk or bike there.

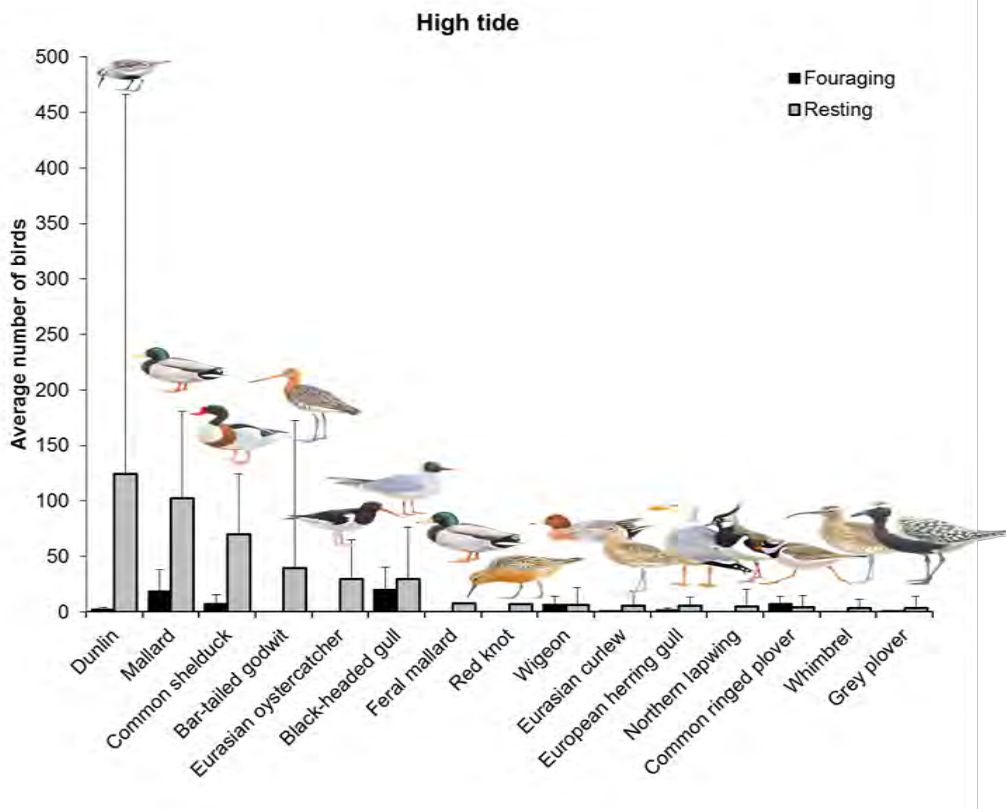


Figure 94. Average number of observed birds foraging and resting on the dikes surrounding the managed realignment area between September 2017 and September 2018.

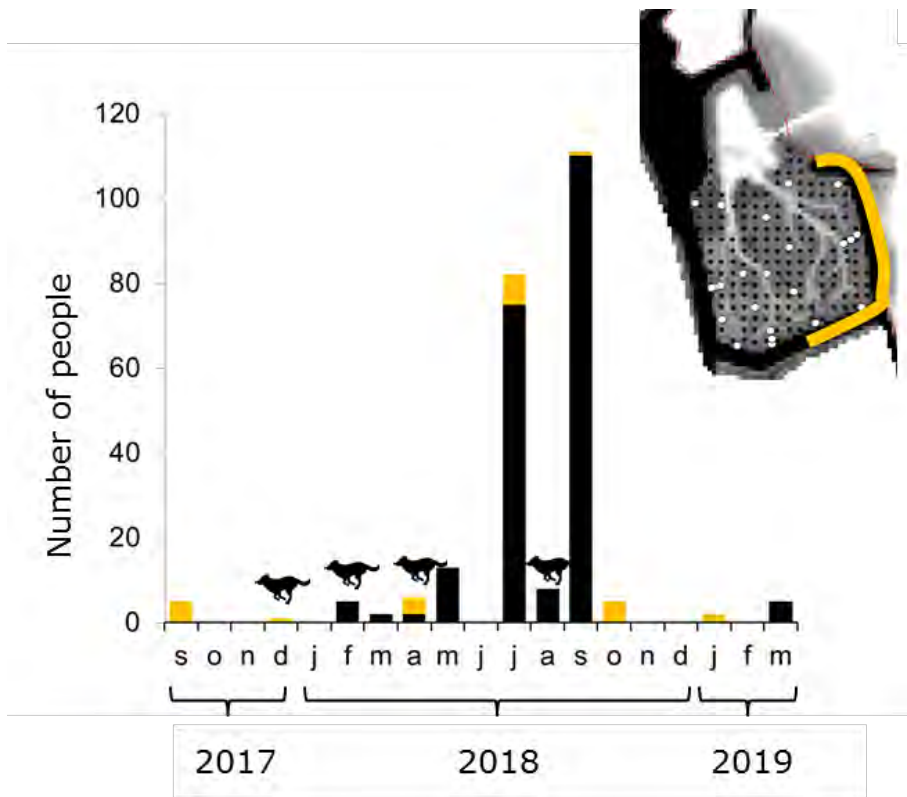


Figure 95. Number of people observed on the dikes surrounding Perkpolder. The west side is a bike path. On the east and south dike access is not permitted. For part of this stretch (yellow) it is known how many people visit do walk or bike here. At four occasions in time one dog was observed on the dike.

Table 21. Number of birds observed in the managed realignment Perkpolder (75 ha) during low tide and percentage showing foraging behaviour between September 2017 and September 2018.

species	spring		summer		autumn		winter		total
	n	%	n	%	n	%	n	%	
<i>Black-headed gull</i>	345	87	573	100	902	98	154	100	1974
<i>Mallard</i>	94	100	136	100	835	21	234	100	1299
<i>Common shelduck adult</i>	209	100	134	100	589	80	82	100	1014
<i>Eurasian curlew</i>	71	18	25	100	76	100	104	88	276
<i>European herring gull</i>	34	100	38	100	115	97	12	100	199
<i>Eurasian oystercatcher</i>	55	100	37	100	23	100	73	100	188
<i>Common tern</i>	154	100	6	100	0		0		160
<i>Dunlin</i>	60	100	0		68	100	0		128
<i>Wigeon</i>	0		0		3	100	114	91	117
<i>Redshank</i>	9	100	2	100	22	100	8	100	41
<i>Common shelduck juvenile</i>	0		37	100	0		0		37
<i>Common sandpiper</i>	0		0		37	100	0		37
<i>Ruddy turnstone</i>	34	100	0		0		0		34
<i>Sanderling</i>	0		0		22	100	5	100	27
<i>Common ringed plover</i>	0		0		4	100	18	100	22
<i>Great corn orant</i>	7	71	2	0	9	56	3	100	21
<i>Grey plover</i>	15	100	0		3	100	2	100	20
<i>Bar-tailed godwit</i>	18	100	0		1	0	0		19
<i>Common greenshank</i>	8	100	4	100	4	0	0		16
<i>Greylag goose</i>	0		0		14	0	0		14
<i>Lapwing</i>	0		9	100	0		0		9
<i>Little egret</i>	0		0		4	100	5	100	9
<i>Feral Mallard</i>					8	0			8
<i>Eurasian teal</i>	6	0	0		2	100	0		8
<i>Great crested grebe</i>	2	100	2	100	0		1	100	5
<i>Eurasian spoonbill</i>	2	100	3	100	0		0		5
<i>Whimbrel</i>	2	100	1	100	0		0		3
<i>Great black-backed gull</i>	0		0		2	100	0		2
<i>Eurasian Pied avocet</i>	2	100	0		0		0		2
<i>Mediterranean gull</i>	2	100	0		0		0		2
<i>Grey heron</i>	0		0		1	100	0		1
<i>Red-breasted merganser</i>	1	100	0		0		0		1
<i>Spotted redshank</i>	0		0		1	0	0		1

5.4 DISCUSSION

The inflow of water within the managed realignment area Perkpolder gave rise to morphological changes. Due to sediment import the resulting intertidal habitat is accretion over time. This enlarges the buffering function for flood protection as higher elevated intertidal habitat absorb and attenuate more wave energy. The fresh deposited layer of estuarine sediment also facilitated fast establishment and succession of the benthic macrofauna community. Initial colonisation of the realignment site by intertidal benthic macroinfauna was rapid with 19 species recorded during the first sampling, four months after the sea defences were breached in June 2015. This fast establishment can be related to both the planktonic stage of juveniles and the mobility of adults (Atkinson et al., 2001). Evans et al. (1999) showed for the Teesmouth managed realignment in the Tees estuary (UK), that establishment was slower when sediment was more compact. Here compaction was caused by earth moving equipment during the creation of the contours of the intertidal area. Increases in average abundance co-occurred with increase of depth of the mud layer on top of the former farmland in autumn 2016 and autumn 2018. Between autumn 2016 and spring 2018 the mud layer reduced in depth and penetration resistance increased indicating consolidation of the deposited sediment layer. During this period a decline in abundance was observed. Correspondingly at Tollesbury, in an estuary northwest of London, UK, Garbutt et al (2006) observed that invertebrate colonisation only occurred in newly accreted sediments within the realignment site.

The pioneering benthic community inside the managed realignment was structurally different from the estuarine area outside the managed realignment. The mud shrimp *Corophium volutator* was among the early colonizers. After three years of tidal inundation the benthic community of the realignment site is still in development and differs from that found on nearby tidal flats. Based on the current development in the direction of the community found on nearby tidal flats it can be expected that a stable community is reached within years rather than decades.

With the colonization of the benthic macrofauna into the Perkpolder area, also estuarine birds uses the area as foraging ground. Establishment of high numbers of *C. volutator* within four months after the breach contributes to the quality of this newly developing tidal area as foraging ground for birds as *C. volutator* is the main food of several small shorebird species. The most important food of large shorebirds, the ragworm *Hediste diversicolor*, appear in spring 2016 in low numbers, but did not become abundant until autumn 2018. Waders like Eurasian curlew (*Numenius arquata*) and Eurasian oystercatcher (*Haematopus ostralegus*), and the Common shelduck (*Tadorna tadorna*) are foraging during low tide in the intertidal zone, while the creeks are used by ducks such as Mallard (*Anas platyrhynchos*) and Wigeon (*Mareca penelope*). Little egrets (*Egretta garzetta*) look for small fish and crustaceans in the creeks.

For future coastal management it is important to understand how newly flooded coastal areas will develop. Our study shows that the managed realignment area Perkpolder was transformed into a biologically active intertidal area within a short time frame. The benthic community develops in the direction of a community found on nearby tidal flats. Birds use the area as foraging ground. High numbers of people on the surrounding dikes indicate that the area also has a recreational value. Insights in the rate of development could help predict how future managed realignment areas such as Hedwige-Prosper will develop over time.

5.5 CONCLUSION

For future coastal management it is important to understand how newly flooded coastal areas will develop. The development of the benthic community and the bird community within the managed realignment Perkpolder in the Scheldt estuary is encouraging. A former agricultural area has been transformed into a biologically active intertidal area within a short time frame. Within 3 years the benthic macro-infaunal community showed a development towards a community found on natural tidal mudflats and is expected to reach a stable community in years rather than decades. The area is frequently visited by birds which forage during low tide and rest on the surrounding dikes during high tide.

Recommendations:

To understand the relative importance of Perkpolder as foraging area for waders, comparison should be made with low water counts on nearby natural tidal flats. Low water counts are however rarely executed in the Scheldt estuary.

For this area, we recommend to perform another monitoring after 5 and 8 years, to see if the area has developed towards a fully natural intertidal area.

The uses of the area by fish is unknown. By catching the fish in the area, information can be obtained about the function of this area. A comparison between a newly created tidal area and natural tidal areas could provide insight in the expected development of this area for fish.

6 EDUCATION

6.1 RESEARCH PROJECTS AND FINAL THESIS

In Table 22 below the students are listed who were involved in the research at Perkpolder. The students who worked on their final thesis got the opportunity to do fieldwork and present their work at a project meeting.

Table 22. Overview of student projects as part of the Perkpolder project.

Study year	titel rapport	Names	Nr. Of students	Study Year	Type of assignment	Supervisors
2016	The tidal basin of Perkpolder - Monitoring the development of the inlet and an investigation of the basin characteristics	Marjolein van Vliet	1	3	Minor	Matthijs Boersema
2016	Height development in tidal areas, predicting the surface level accretion for a de-embanked basin, Perkpolder Scheldt Estuary	Mireille Martens	1	4	BSc. Thesis	Matthijs Boersema
2016	Groundwater in the new intertidal area Perkpolder	Jens Schouwenaars	1	4	BSc. Thesis	Carla Pesch, Tjeerd Bouma
2016	Morphological development of Perkpolder tidal basin	Rien Krielen, Yves Bonné, Lars van Duren, Owen de Vliieger, Ivory Mast, Ymke Tmmerman, Loes de Jong, Eva den Boer, Marie Wahl, Mathijs Dubbeldam, Mikayla Muizer, Beatriz	12	2	Lectorenopdracht (research assignment)	Matthijs Boersema en Edwin Pree
2016	Numerical modelling of morphological development in a managed realignment project. A case study of the Perkpolder project, Western Scheldt, The Netherlands	Xinyue Zhao	1	5	MSc. Thesis	
2017	Salt marsh development in tidal restoration projects	Lasse Gillisen	1	3	Minor	Carla Pesch, Tjeerd Bouma
2017	Development of Perkpolder tidal basin	Yingjie An, Chanyan Feng	2	4	BSc. Thesis	Joao Salvador de Paiva, Matthijs Boersema
2017	Changes in channel morphology Perkpolder	Riccardo Brunetta	2	3	Internship	Joao de Paiva
2018	Perkpolder tidal basin	Arne de Poorter, Scott Bodges	2	3	Minor	Joao de Paiva
2018	Morphological development of Perkpolder tidal basin	Carlo Alberto Carissimi, Elena Santirosi	2	3	Internship	Joao de Paiva
2019	Tidal propagation in aquifer of the restored Perkpolder. A numerical approach.	Jordy van der Drift	1	4	WUR MSc. Thesis	Perry de Louw



Figure 96. Mireille Martens (BSc. student HZ) busy with field measurements (April 2016).

6.2 EXCURSIONS FOR STUDENTS

On March 16, 2016 the HZ organized a recruitment event for new students. In total 40 potential students had a program during the day. The first part of the day consisted of presentations from partners (Yvo Provoost, Anton van Berchum from Rijkswaterstaat, and Matthijs Boersema from HZ). The second part of the day, the students went into the field looking at the development in the Perkpolder tidal basin, and exploring the salt water discharge facility (Perry de Louw, Deltares).

7 EXPOSURE

7.1 CONFERENCES

Aspects of this project were presented during the NCK days 2016 and at the ECSA Local Meeting 2016 (Estuarine Restoration: from theory to practice and back⁷⁾) in Antwerp. See the poster presentation below (Figure 97). An abstract of the research was printed in a 'book of abstracts'. Results were also presented during the 2018 Scheldesymposium in Antwerp.

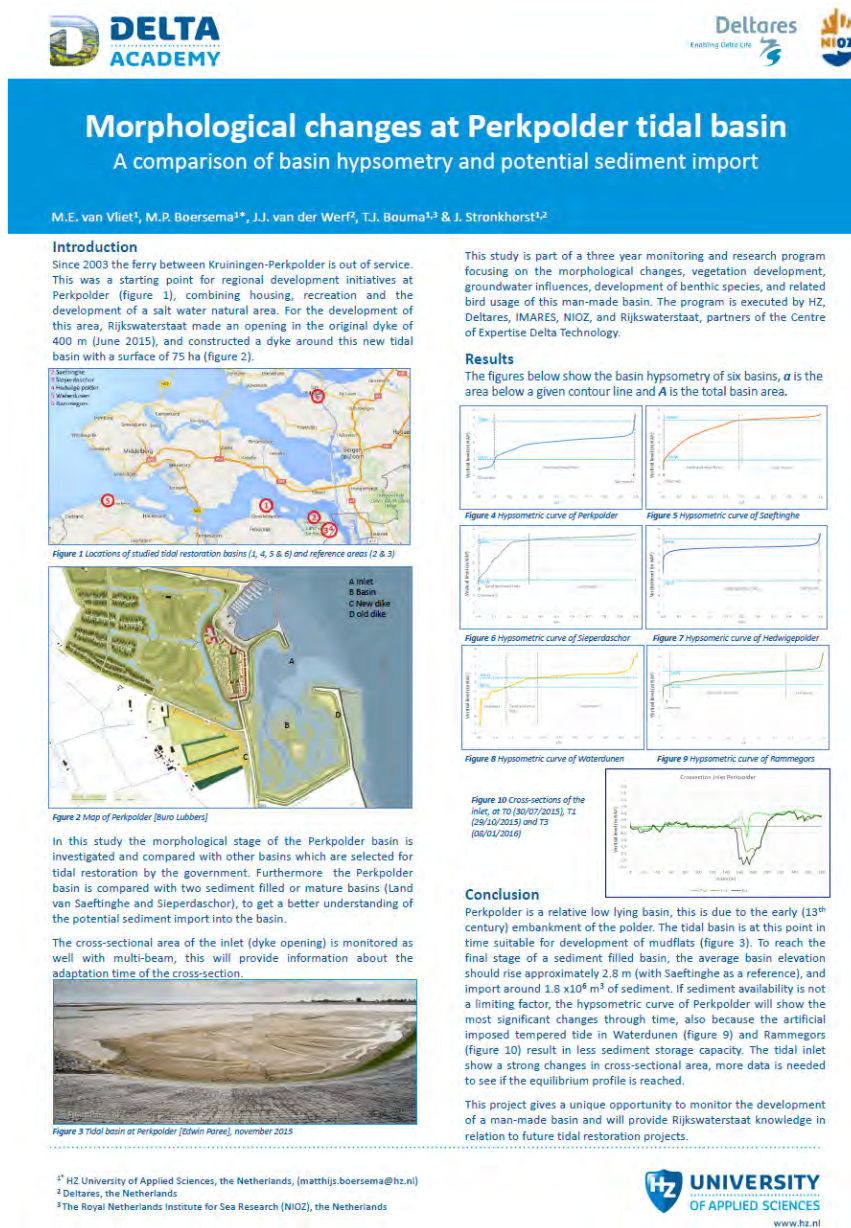
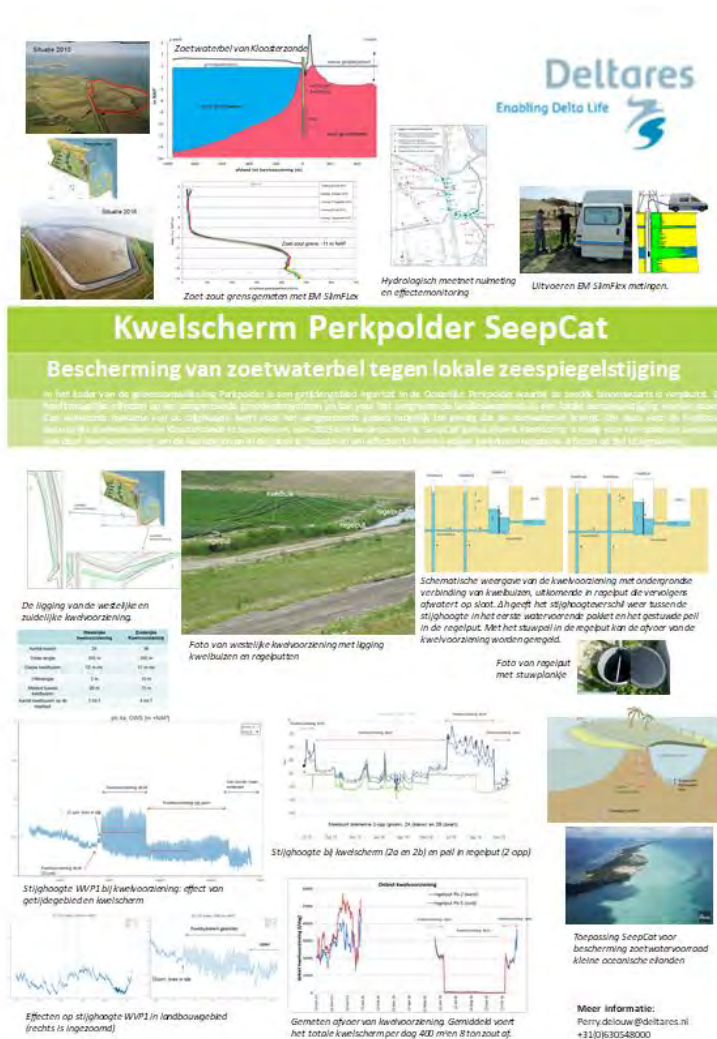


Figure 97. Example of a poster presentation resulting from the Perkpolder project.

The concept and first results of the mitigation measure SeepCat to protect the freshwater lens of Kloosterzande were presented at the SWIM-APCAM conference in Cairns 2016. The extended abstract was

published in: Werner, A.D. (ed.) (2016), Proceedings of the 24th Salt Water Intrusion Meeting and the 4th Asia-Pacific Coastal Aquifer Management Meeting, 4-8 July, 2016, Cairns, Australia).

At 15 June 2017, SeepCat was presented at the Proeftuin Zoetwater Zeeland infodag. The poster is given below.



Deltares made also a movie about SeepCat and published it on internet in their annual report. Via the following link, the movie can be seen (choose view highlight):

<http://annualreport2015.deltares.nl/freshwater-scarcity/>

SeepCat is possible an effective measure to mitigate the effects of sea level rise on freshwater lenses below small islands. Deltares made a youtube-movie to show the working and possibilities of SeepCat for such small islands. See the following link:

<https://www.youtube.com/watch?v=K3RbSjucxIk>

Aspects of the project were used in the course “ecological engineering” and “estuarine and coastal systems” at the University of Antwerp.

7.2 NEWSLETTERS

An article in the October 2016 newsletter of de VNSC was focusing on the Perkpolder research project.



Scheldetopics oktober 2016



Perkpolder: nieuw buitendijks natuurgebied vol leven

In de zomer van 2015 werd een bres gemaakt in de zeedijk van Perkpolder en is de omliggende dijk versterkt. Sindsdien stroomt de Westerschelde tweemaal per dag het voormalige poldergebied binnen. Zo ontstaat er een gloednieuw buitendijks natuurgebied...



In September 2017 a newsletter was made available by the “Zuidwestelijke Delta” website (<https://www.zwdelta.nl/>).

A newsletter article will be published in June 2019 about the results of project to date as reported in this document.

8 REFERENCES

- Aminot, A. & Rey F. (2000). Standard procedure for the determination of chlorophyll a by spectroscopic methods. International Council for the Exploration of the Sea. ISSN 0903-2606.
- Atkinson, P.W., S. Crooks, A. Grant, M.M. Rehfish (2001). The success of creation and restoration schemes in producing intertidal habitat suitable for water birds. *English Nature Research Report* No. 425. English Nature, Peterborough.
- Boersema, M.P, T. Ysebaert, P. de Louw, T.J. Bouma, J.J. van der Werf, C.J. Pesch, and G. Rosing (2015). Projectplan monitoring en onderzoek Perkpolder, de overgang van een zoetwaterlandbouwgebied naar een zoutwaternatuurgebied. Centre of Expertise Delta Technology, december 2015.
- Boon, J. D., & Byrne, R. J. (1981). On basin hyposmetry and the morphodynamic response of coastal inlet systems. *Marine Geology*, 40(1-2), 27–48.
- Bouma, H., D.J. de Jong, F. Twisk en K. Wolfstein (2005): "Zoute wateren EcotopenStelsel (ZES.1): Voor het in kaart brengen van het potentiële voorkomen van levensgemeenschappen in zoute en brakke rijkswateren", RIKZ rapport 2005.024, Middelburg.
- Buma, 2011. Plan Perkpolder. Nulmeting grondwater. Rapport, referentie 12017872-000-BGS-0005.
- Buma, 2014. Nulmeting grondwater Perkpolder. Eindrapport. Deltares-rapport 1205442-000-BGS-0010.
- Colen, C.V., et al. (2013). A bioturbation classification of European marine infaunal invertebrates. *Ecology and Evolution* 3, 3958–3985.
- Craeymeersch, J., & V. Escaravage (2014). Perceel Benthos. PMR Monitoring natuurcompensatie Voordelta. Eindrapport 1e fase 2009-2013 deel B. . In: T. Prins and G. van der Kolff. Delft D (ed) Deltares rapport 1200672-ZKS-0043.
- Craft, C., J. Sacco (2003). Long-term succession of benthic infauna communities on constructed *Spartina alterniflora* marshes. *Marine Ecology Progress Series* **257**: 45-58.
- De Jong, D.J., & V.N. De Jonge (1995). Dynamics and distribution of microphytobenthic chlorophyll-a in the Western Scheldt estuary (SW Netherlands). *Hydrobiologia* **311**: 21-30.
- De Louw, P.G.B., 2013. Zoute kwel in delta's. Preferente kwel via wellen en interacties tussen dunne regenwaterlenzen en zoute kwel. Academisch proefschrift, Vrije Universiteit Amsterdam, ISBN/EAN 9789461085429, 198 p.
- De Louw, 2014a. Monitoring protocol kwelvoorziening Perkpolder. Groeidocument – 3 oktober 2014. Deltares-rapport 1209917-000-BGS-0004.
- De Louw, 2014b. Second opinion kwelvoorziening Perkpolder. Deltares-rapport 1209917-000-BGS-0003.
- De Vet, P.L.M., B.C. van Prooijen, Z.B. Wang (2017). The differences in morphological development between the intertidal flats of the Eastern and Western Scheldt. *Geomorphology* **281**: 31-42.
- De Vriend H.J., Z.B. Wang, T. Ysebaert, P.M.J. Herman, P. Ding (2011). Eco-morphological problems in the Yangtze Estuary and the Western Scheldt. *Wetlands* **31**: 1033-1042.

- Esteves, L.S., 2014. Managed realignment: a viable long-term coastal management strategy? Springer Briefs in Environmental Science. Springer, New York, pp. 1–139. <http://dx.doi.org/10.1007/978-94-017-9029-1>.
- Evans, P.R. R.M. Ward, M. Bone, M. Leakey (1999). Creation of temperate-climate intertidal mudflats: factors affecting colonization and use by benthic invertebrates and their bird predators. *Marine Pollution Bulletin* **37**: 535-545.
- Ferreira, S.M., Pardal, M.A., Lillebø, A.I., Cardoso, P.G., and Marques, J.C. (2004). Population dynamics of *Cyathura carinata* (Isopoda) in a eutrophic temperate estuary. *Estuarine, Coastal and Shelf Science* **61**, 669–677.
- Garbutt R.A., C.J. Reading, M. Wolters, A.J. Gray, P. Rothery (2006). Monitoring the development of intertidal habitats on former agricultural land after the managed realignment of coastal defences at Tollesbury, Essex, UK. *Marine Pollution Bulletin* **53**: 155-164.
- Giere, O. (2006). Ecology and Biology of Marine Oligochaeta – an Inventory Rather than another Review. *Hydrobiologia* **564**, 103–116.
- Hamer, F., (2007). ComCoast WP3, ComCoast flood risk management schemes; ComCoast Interreg IIIb North Sea.
- Kessel, T. van, J. Vanlede, J.M. de Kok (2011). Development of a mud transport model for the Scheldt estuary. *Continental Shelf Research* **31** S165–S181 DOI: 10.1016/j.csr.2010.12.006.
- Kirby, R. (2000). Practical implications of tidal flat shape. *Cont. Shelf. Res.* **20**: 1061-1077.
- Leopold, M. F., Smit, C. J., Goedhart, P. W., Winden, A. J. V., Turnhout, C. V. (2004). Langjarige trend in aantallen wadvogels, in relatie tot de kokkelvisserij en het gevoerde beleid in deze. Alterra.
- Levin L.A., D. Talley, G. Thayer (1996). Succession of macrobenthos in a created salt marsh. *Marine Ecology Progress Series* **141**: 67-82.
- Marlin, 2016 BIOTIC - Biological Traits Information Catalogue. Marine Life Information Network. Plymouth: Marine Biological Association of the United Kingdom. [december 2018] Available from www.marlin.ac.uk/biotic
- Martens, M. (2016). Height development in tidal areas, understanding the development of surface elevation in de-embankment site Perkpolder, Scheldt estuary. BSc thesis, HZ University of Applied Sciences.
- Moseman S.M., L.A. Levin, C. Currin, C. Forder (2004). Colonization, succession, and nutrition of macrobenthic assemblages in a restored wetland at Tijuana Estuary, California. *Estuarine Coastal Shelf Science* **60**: 755-770.
- Mazik, K., J.E. Smith, A. Leighton, M. Elliott (2007). Physical and biological development of a newly breached managed realignment site, Humber estuary, UK. *Marine Pollution Bulletin* **55**: 564-578.
- Oksanen J, F.G. Blanchet, M. Friendly, R. Kindt, P. Legendre, D. McGlenn, P.R. Minchin, R.B. O'Hara, G.L. Simpson, P. Solymos, M.H.H. Stevens, E. Szoecs, H. Wagner (2018). Vegan: community ecology package. R package version 2.5-3
- Ontwerpbeheerplan, (2015). Natura 2000 Deltawateren, ontwerpbeheerplan 2015-2021, Westerschelde & Saeftinghe. Rijkswaterstaat i.s.m. Royal HaskoningDHV, juni 2015

- Oude Essink, G.H.P., van Baaren, E.S., Zuurbier, K.G., Velstra, J., Veraart, J., Brouwer, W., Faneca Sánchez, M., Pauw, P.S., de Louw, P.G.B., Vreke, J., Schoevers, M., 2014. GO-FRESH: Valorisatie kansrijke oplossingen voor een robuuste zoetwatervoorziening, KvK 151/2014, ISBN EAN 978-94-92100-12-2, 84 p.
- Pauw, P.S. (2015). Field and model investigations of freshwater lenses in coastal aquifers. Academisch proefschrift, Wageningen University, ISBN/EAN 9789462572928, 158 p.
- Pauw, P.S., Van Baaren, E.S., Visser, M. De Louw, P.G.B., Oude Essink, G.H.P., 2015, Increasing a freshwater lens below a creek ridge using a controlled artificial recharge and drainage system: a case study in the Netherlands, *Hydrogeology Journal*. doi: 10.1007/s10040-015-1264-z.
- Queirós, A.M., Birchenough, S.N.R., Bremner, J., Godbold, J.A., Parker, R.E., Romero-Ramirez, A., Reiss, H., Solan, M., Somerfield, P.J.,
- R core Team (2018). R: A language and environment for statistical computing. R Foundation for Statistical Computing, Vienna, Austria.
- van Rijn, L.C., Barth, R., 2018. Settling and Consolidation of Soft Mud–Sand Layers. *J. Waterw. Port Coast. Ocean Eng.* 145, 04018028. [https://doi.org/10.1061/\(ASCE\)WW.1943-5460.0000483](https://doi.org/10.1061/(ASCE)WW.1943-5460.0000483)
- Royal Haskoning, 2012. Afweging varianten kwelvoorziening. Notitie, referentie 9T9564.F0/N0004/LMOY/NTEK/Rott. Auteurs: Leslie Mooyaart en Leon Brouwer.
- Royal Haskoning, 2012. Kwelvoorziening Perkpolder. Toelichting op ontwerp diepdrainage. Conceptrapport, referentie 9T9564.F0/R0001/903703/Rott. Auteurs: Leslie Mooyaart en Leon Brouwer.
- Soetaert, K. & Herman, P. M. J. (1995). Estimating estuarine residence times in the Westerschelde (The Netherlands) using a box model with fixed dispersion coefficients. *Hydrobiologia* **311**, 215–224.
- Verbeek, H., (2005). Ontwikkelingsschets 2010 Schelde-estuarium, Besluiten van de Nederlandse en Vlaamse regering. versie 8 – definitief, Projectdirectie ontwikkelingsschets Schelde-estuarium
- Vroom, J., De Vet, L., Van der Werf, J. (2015). Validatie waterbeweging Delft3D-NeVla model Westerscheldemonding. Rapport 1210301-001-ZKS-0001, Deltares, Nederland.
- van der Wal, D., van Kessel, T., Eleveld, M.A., Vanlede, J., 2010. Spatial heterogeneity in estuarine mud dynamics. *Ocean Dyn.* 60, 519–533. <https://doi.org/10.1007/s10236-010-0271-9>
- Wallis, B., Brummelhuis, E., van der Pool, J., Wiesebron, L., Ysebaert, T. (2019) Development of benthos and birds in an intertidal area created for coastal defence (Scheldt estuary, the Netherlands, Wageningen Marine Research report C043/19, <https://doi.org/10.18174/475792>.
- Wang, Y., Naumann, U., Eddelbuettel, D., D. Warton (2018). Mvabund: Statistical methods for analysing multivariate abundance data. R packages version 3.13.1
- Witteveen+Bos, 2010. Analyse varianten watersysteem Perkpolder. Rapport, referentie MDB221-11/boeg3/009.
- Witteveen+Bos & Royal Haskoning, 2010. Geohydrologisch effect omputten oostelijke Perkpolder. Rapport, referentie MDB221-16/abdm/008.

- Ysebaert T, J.A.M. Craeymeersch, D. van der Wal (2016). De relatie tussen bodemdieren en hydro- en morfodynamiek in het sublitoraal en litoraal van de Westerschelde. In: IMARES (ed), Book (Rapport / IMARES C066/16)
- Ysebaert, T., Fettweis, M., Meire, P., and Sas, M. (2005). Benthic variability in intertidal soft-sediments in the mesohaline part of the Schelde estuary. *Hydrobiologia* 540.
- Zhao, X. (2016). Numerical modelling of morphological development in a managed realignment project, A case study of the Perkpolder project, Western Scheldt, The Netherlands. MSc thesis, University of Twente.
- Zagwijn, W. H. (1986). *Nederland in het Holoceen* (2nd ed.). Rijks geologische dienst.

ACKNOWLEDGEMENT

This report is part of the Perkpolder monitoring project that was executed by the Centre of Expertise Delta Technology. This is a consortium formed by the HZ University of Applied Sciences, Wageningen Marine Research (WMR), NIOZ, Deltares and Rijkswaterstaat. WMR research was also partly financed by the Ministry of Public Affairs, within the framework of the Kennisbasis Programme System Earth Management (project KB-24-001-14). We would like to thank *Natuurbeschermingsvereniging De Steltkluut* for executing low and high water bird counts.

9 APPENDICES

9.1 GEGEVENS VAN MEETPUNTEN EN MONITORINGFREQUENTIE

In onderstaande tabel staan enkele gegevens van de meetpunten en de frequentie van monitoring.

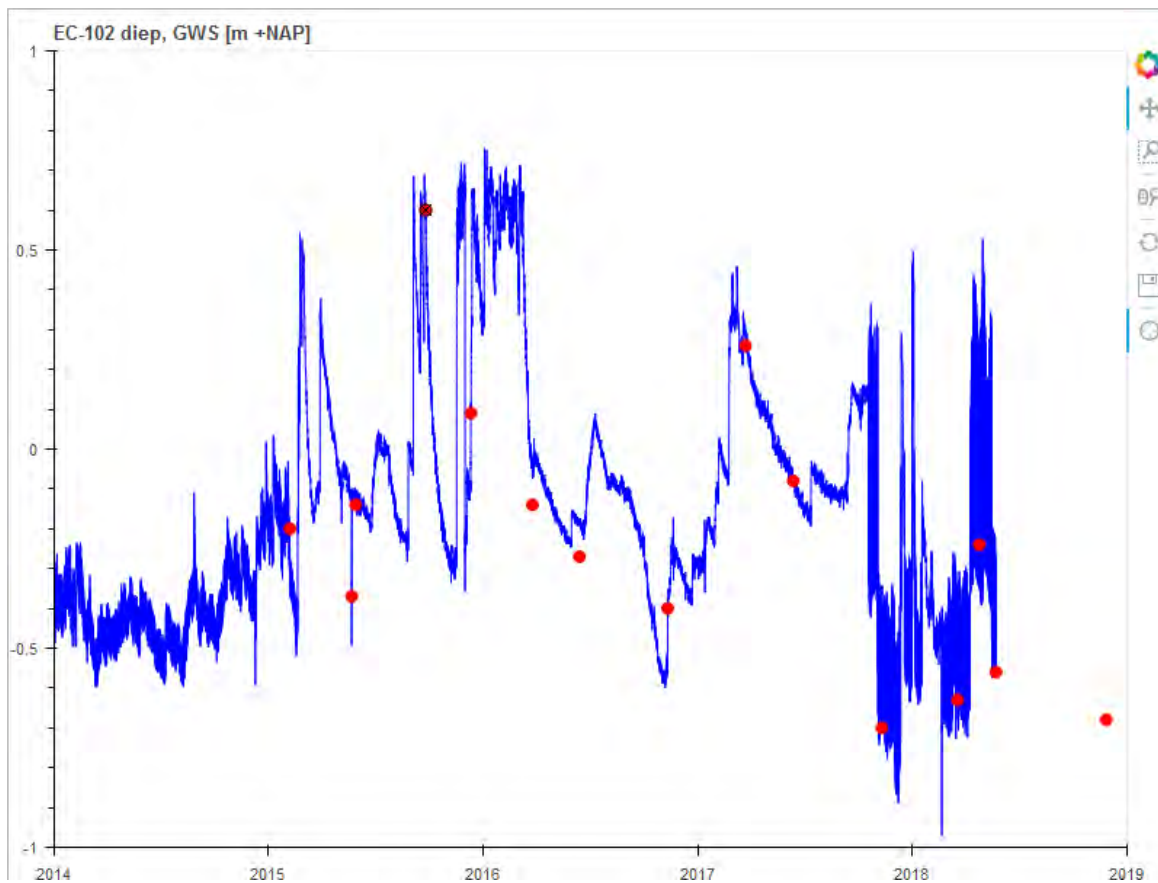
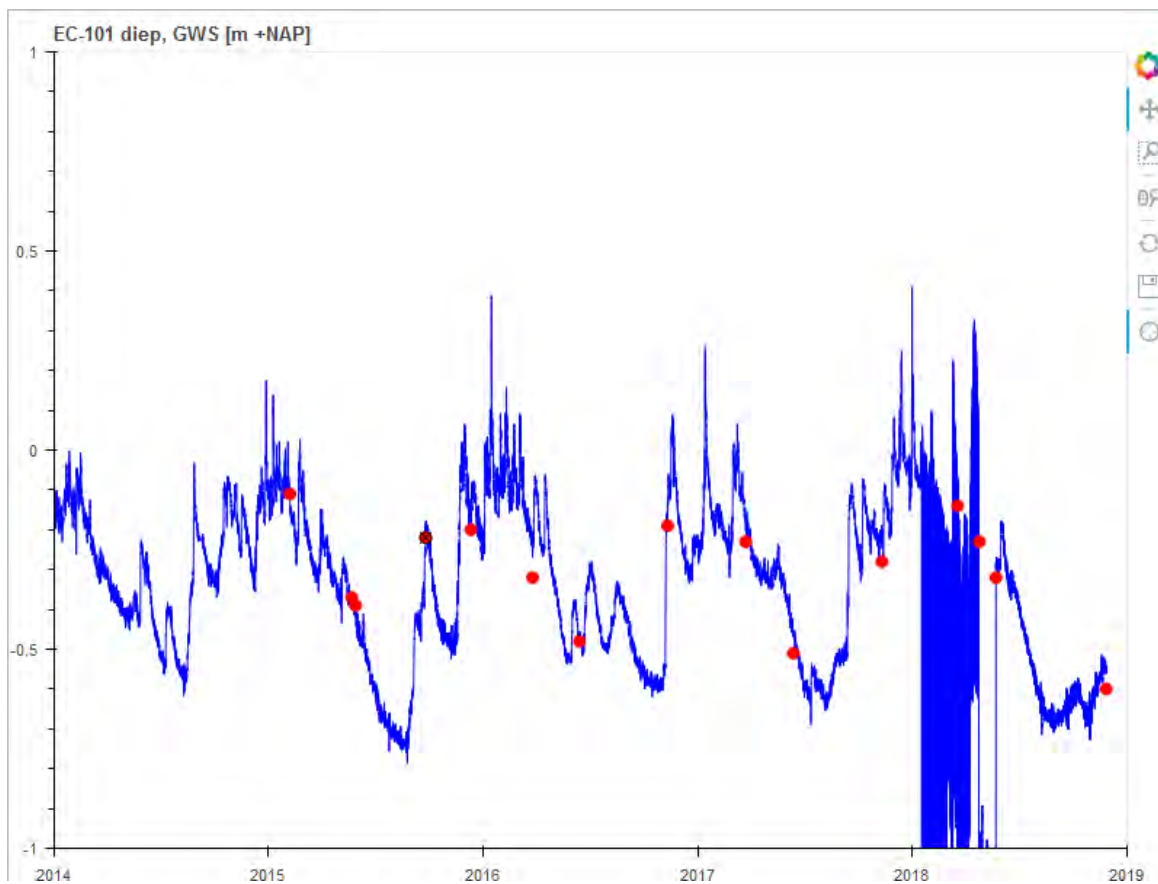
		Onderkant	Eind-	Diver-nr dec 2015	Bovenkant	Maaiveld-	Stijghoogte		Zoet-zout	Kwelvoorziening		
		filter	diepte		peilbuis	hoogte	Frequentie	Handmeting	grensvlak	Debiet	EC	Peil
		m-mv	m-mv		m NAP	m NAP	Diver	en uitlezen	SlimFlex	regelput	regelput	regelput
EC-101 ondiep	V	4.5	4.5	geen	?	0.80		kwartaal				
EC-101 diep	V	6.0	12.0	D7175	?	0.80	ieder uur	kwartaal	jaarlijks			
EC-102 ondiep	V	4.5	4.5	H2437	?	0.23	ieder uur	kwartaal				
EC-102 diep	V	9.0	10.0	D7158	?	0.23	ieder uur	kwartaal	jaarlijks			
EC-106 diep	V	8.5	20.0	D7174	1.62	1.15	ieder uur	kwartaal	jaarlijks			
EC-107 diep	V	10.0	12.0	J1328	1.18	0.77	ieder uur	kwartaal	jaarlijks			
EC-111 ondiep	V	4.5	4.5	J2695	1.43	1.08	ieder uur	kwartaal				
EC-111 diep	V	9.0	11.0	G6197	1.57	1.08	ieder uur	kwartaal	jaarlijks			
EC-118 ondiep	V	4.5	4.5	geen	?	0.90		kwartaal				
EC-118 diep	V	11.0	11.0	D7182	1.51	0.90	ieder uur	kwartaal	jaarlijks			
EC-119 ondiep	V	4.5	4.5	geen	?	1.01		kwartaal				
EC-119 diep	V	12.0	12.0	D7173	1.47	1.01	ieder uur	kwartaal	jaarlijks			
EC-121 diep	V	~10.0	~10.0	D7183	0.66	0.66	ieder uur	kwartaal	jaarlijks			
Kalverdijk 3	V	3.2	3.2	S7119	1.55	1.23	ieder uur	kwartaal				
Walsoorden-ondiep	V	3.0	3.0	T1551	2.03	1.50	ieder uur	kwartaal				
Walsoorden-diep	V	10.0	14.0	T1549	2.01	1.52	ieder uur	kwartaal	jaarlijks			
pb 1a	K	12.0	12.0	U1646	0.52	0.45	ieder uur	kwartaal				
pb 1b	K	12.0	12.0	geen	0.54	0.39		kwartaal				
pb 2a-laag	K	8.0	8.0	geen	0.34	0.22		kwartaal				
pb 2a-midden	K	12.0	12.0	U1797	0.31	0.22	ieder uur	kwartaal	jaarlijks			
pb 2a-hoog	K	18.0	18.0	geen	0.20	0.22		kwartaal				
pb 2b	K	12.0	12.0	U1813	0.13	0.06	ieder uur	kwartaal				
pb 3a	K	12.0	12.0	U1817	0.94	0.89	ieder uur	kwartaal				
pb 3b	K	12.0	12.0	geen	0.98	0.80		kwartaal				
pb 4a	K	12.0	12.0	U1801	0.26	0.26	ieder uur	kwartaal	jaarlijks			
pb 4b	K	12.0	12.0	geen	0.30	0.20		kwartaal				
pb 5a-laag	K	8.0	8.0	geen	0.87	0.70		kwartaal	jaarlijks			
pb 5a-midden	K	12.0	12.0	T1540	0.83	0.70	ieder uur	kwartaal				
pb 5a-hoog	K	18.0	18.0	geen	0.78	0.70		kwartaal				
pb 5b	K	12.0	12.0	T1547	0.83	0.51	ieder uur	kwartaal				
pb 6a	K	12.0	12.0	T1541	0.74	0.66	ieder uur	kwartaal				
pb 6b	K	12.0	12.0	geen	0.81	0.54		kwartaal				
Regelput bij Pb 2	K									ieder uur	ieder uur	ieder uur
Regelput bij Pb 5	K									ieder uur	ieder uur	ieder uur
Het doel van het meetpunt wordt aangegeven met de letter V (vervolmonitoring) of K (volgen van de werking van de kwelvoorziening)												
<i>Opm1. Voor een aantal meetpunt (aangegeven met ?) is de NAP-hoogte niet exact bekend ivm verlengen peilbuis. Voor deze meetpunten dient een nieuwe NAP-meting te worden gedaan</i>												
<i>Opm2. De vetgedrukte meetpunten zijn uitgerust met een telemetrisch systeem voor verzenden van de meetdata.</i>												

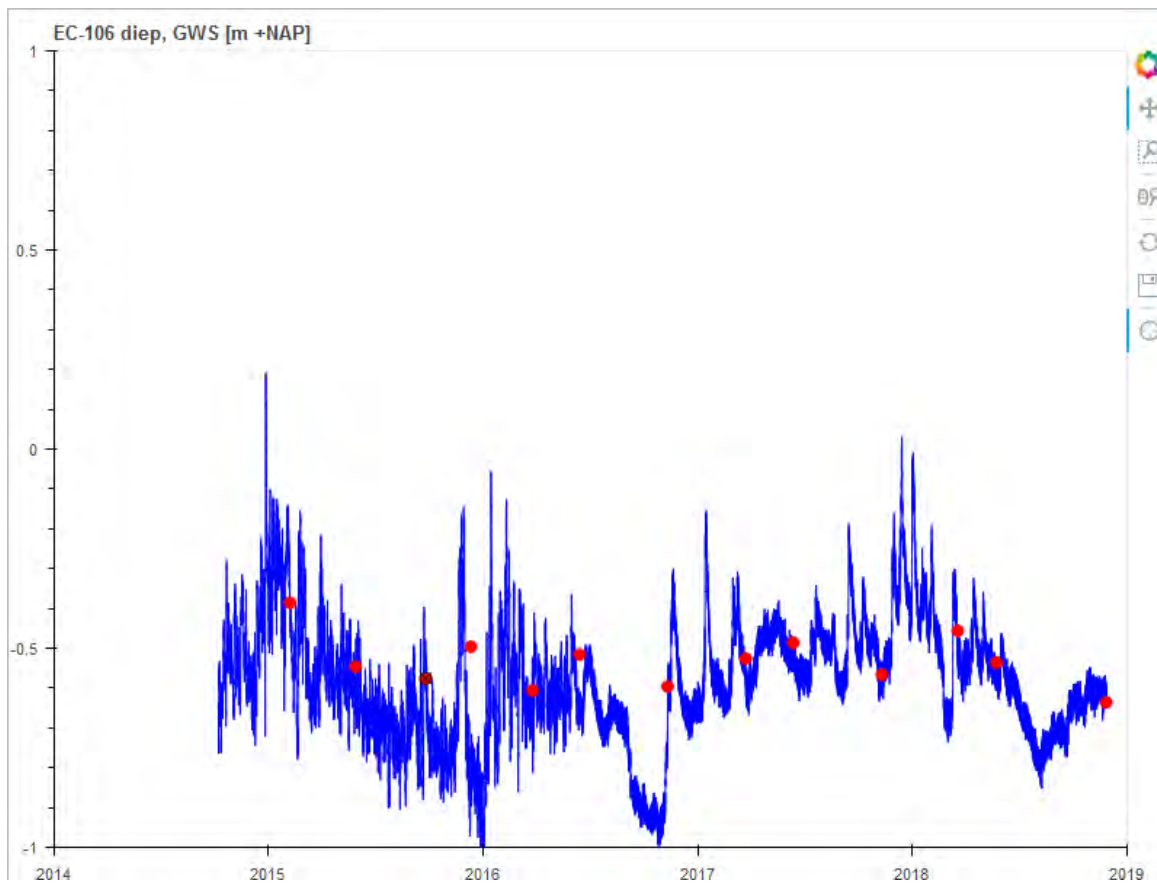
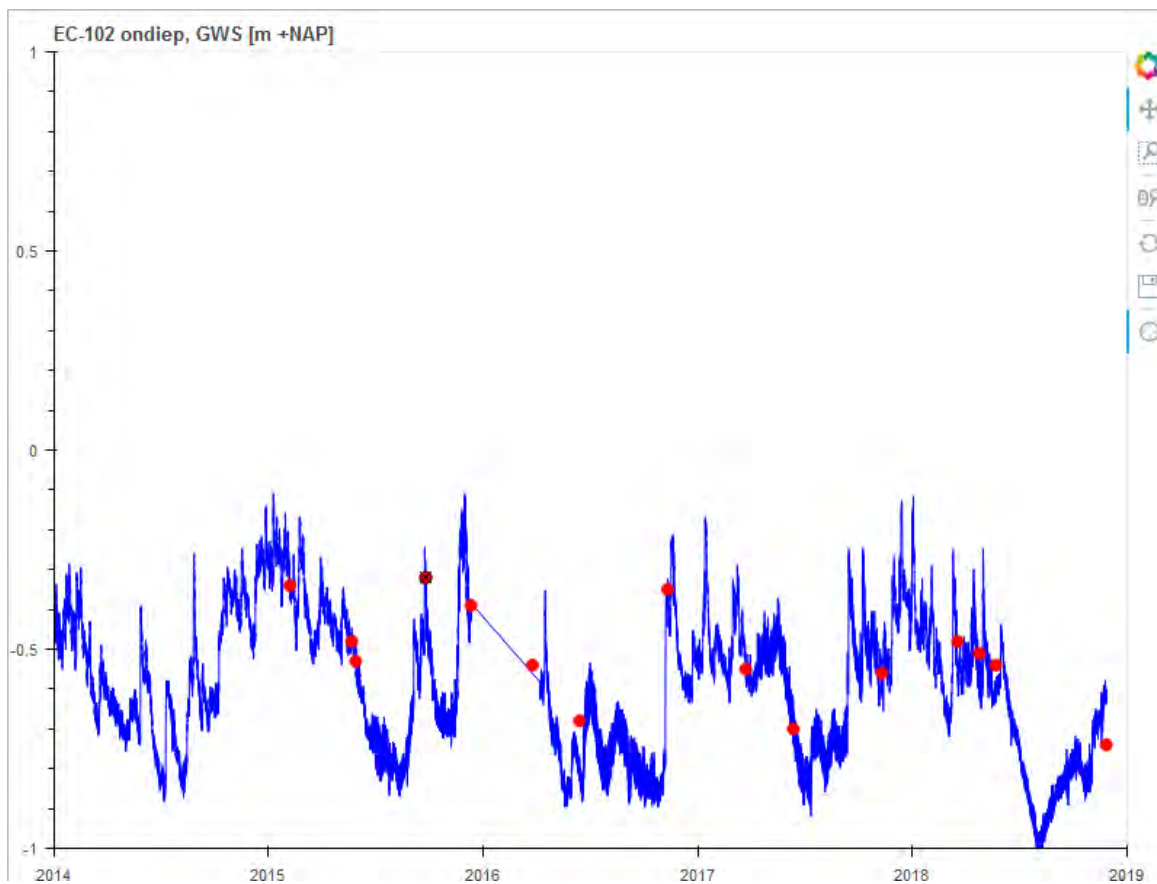
9.2 STIJGHOOGTEMETINGEN

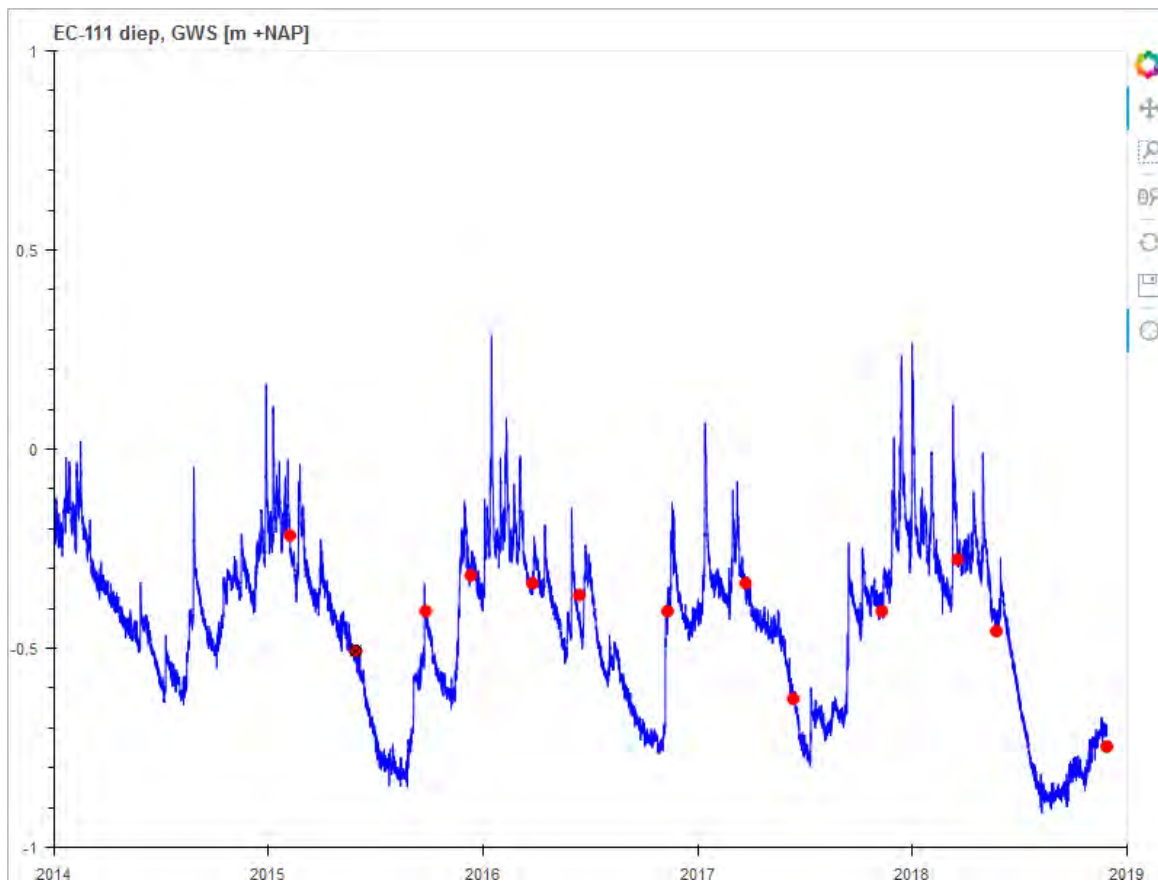
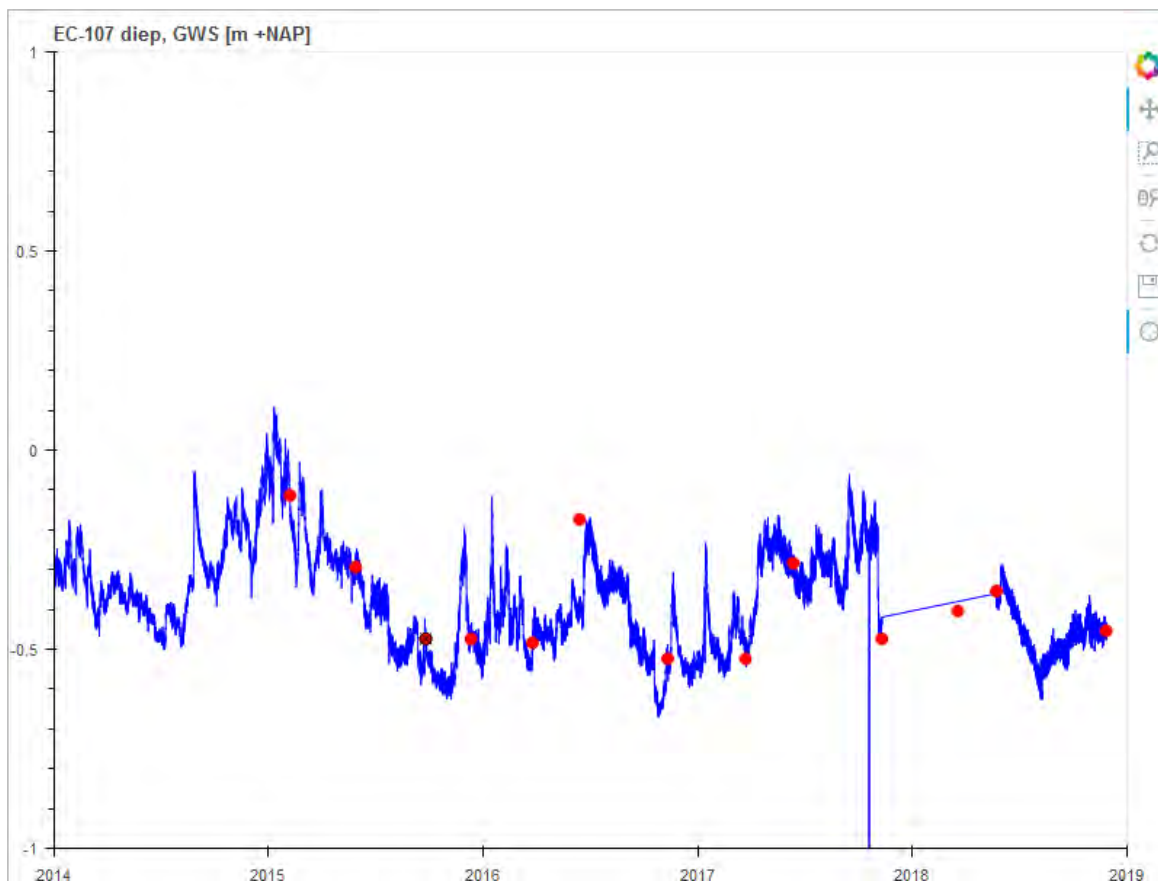
In deze bijlage staan alle meetreeksen weergegeven van de meetpunten uitgerust met een automatische drukopnemer ('Diver'). De rode punten geven de handmetingen aan.

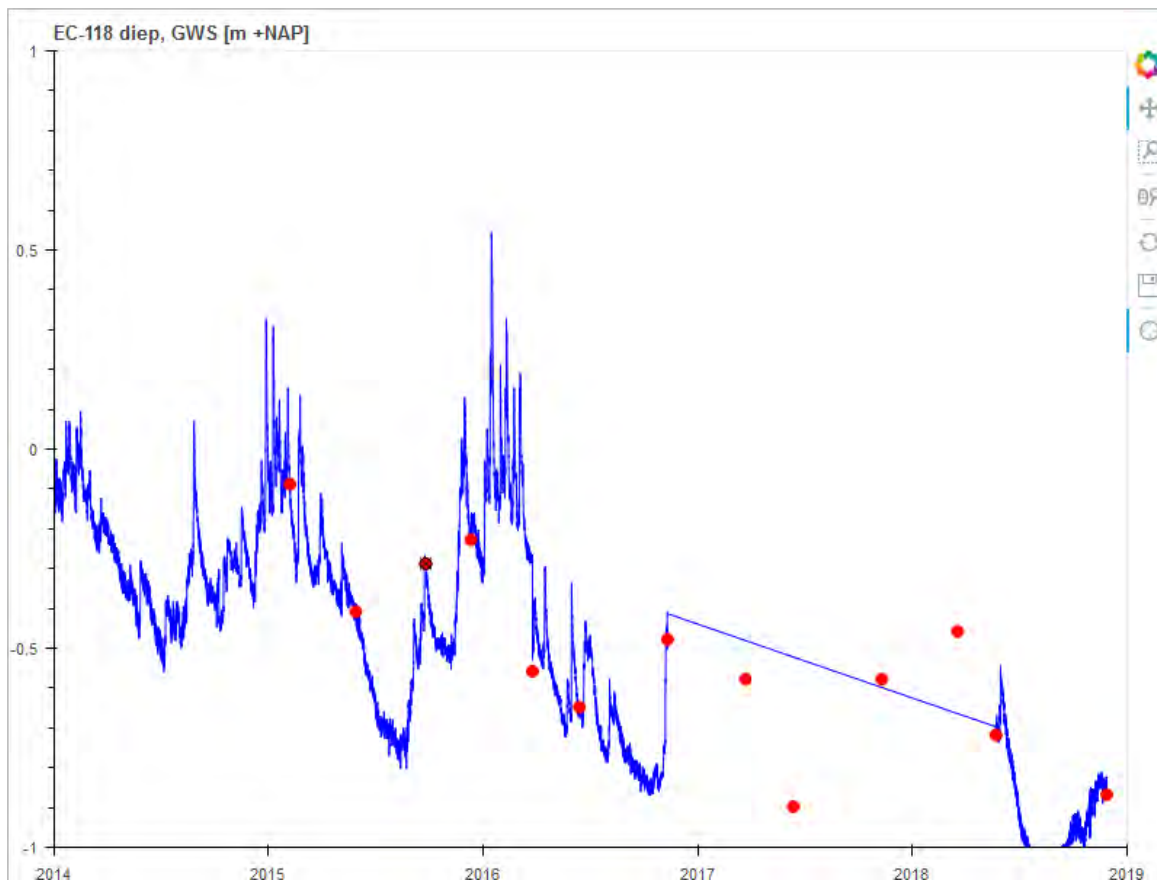
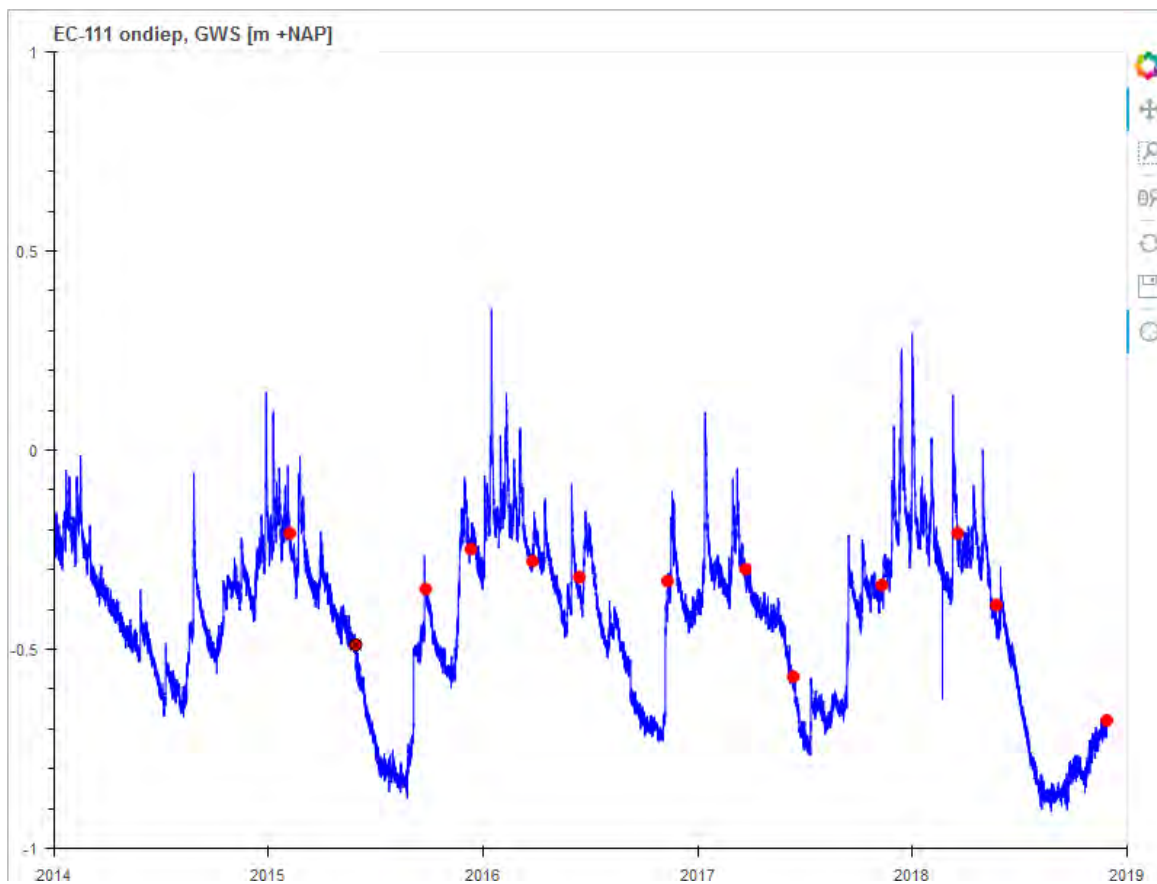
Tevens zijn enkele grafieken weergegeven waarin de meetreeksen van enkele meetpunten zijn gecombineerd.

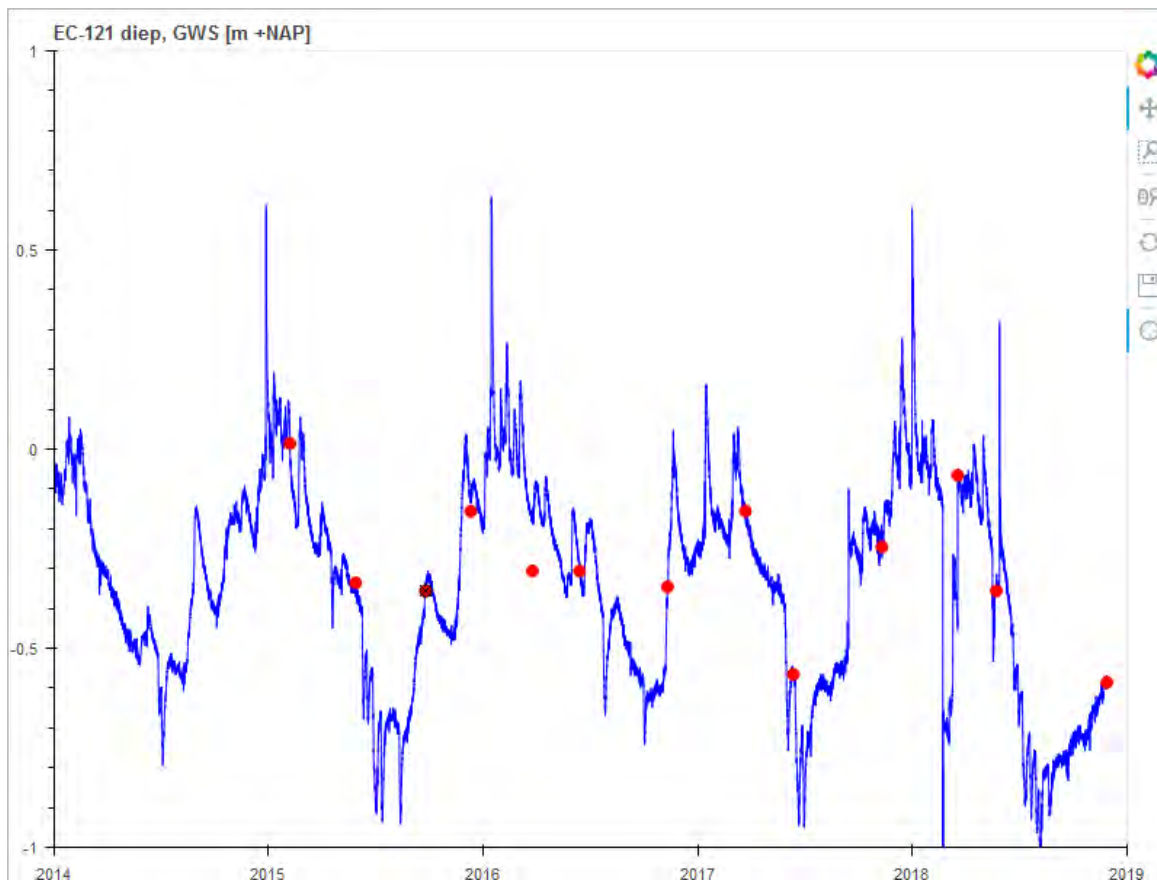
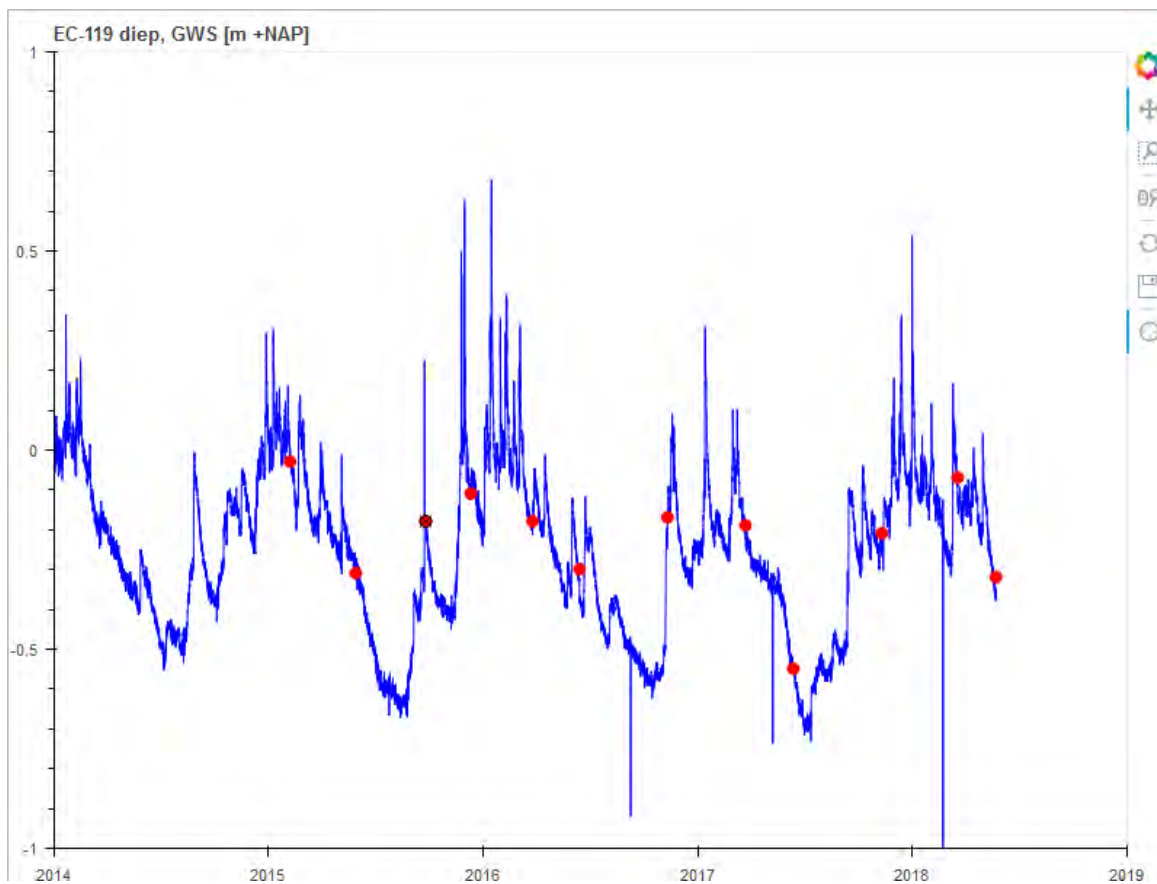
De meetpunten aangeduid met 2-2EC en 5-5EC geven het peil in de regelput aan bij de meetpunten Pb2 en Pb5.

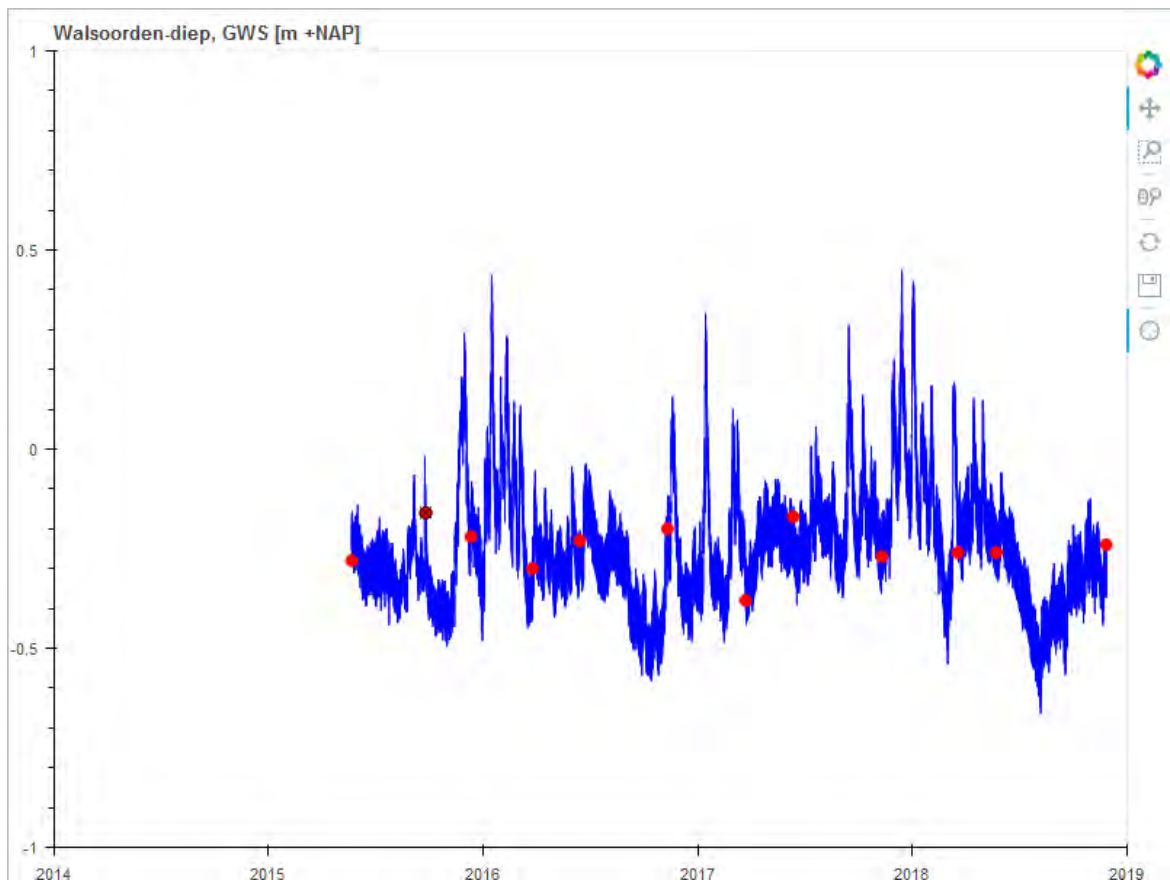
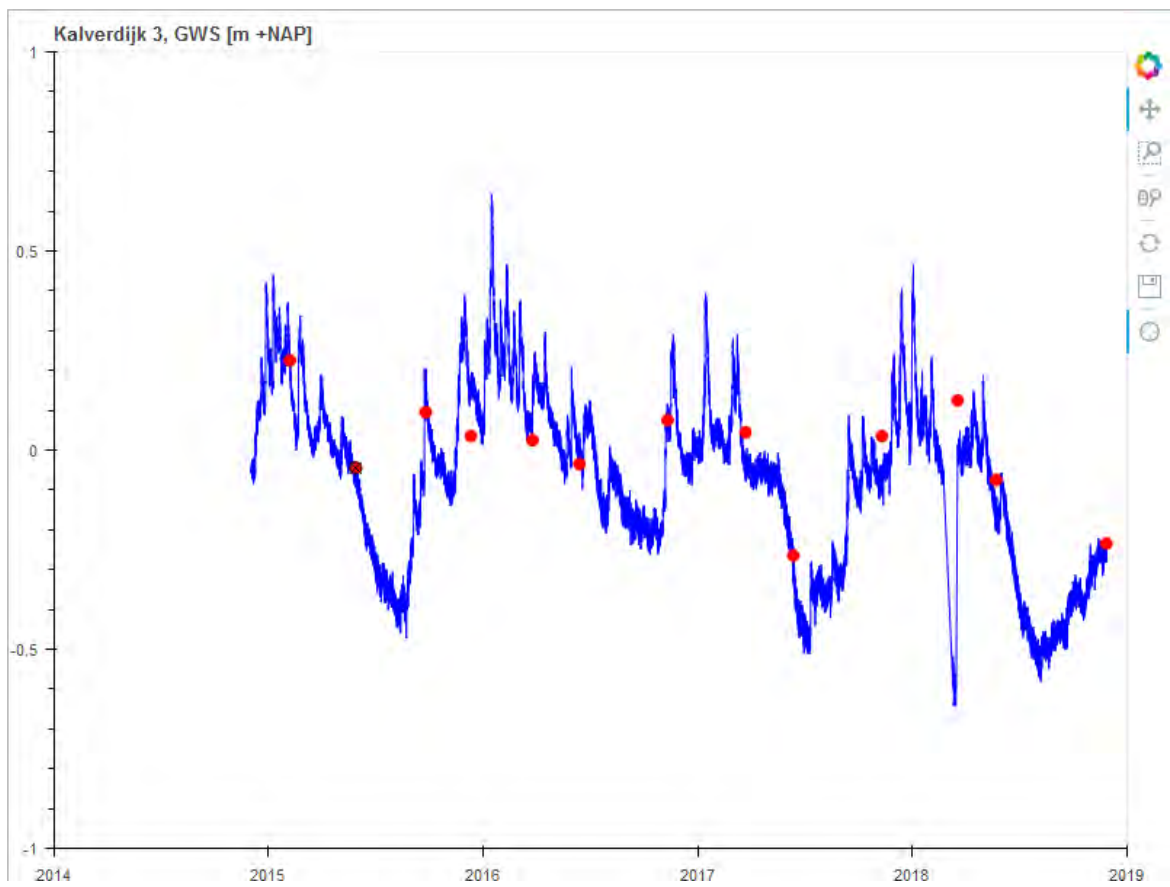


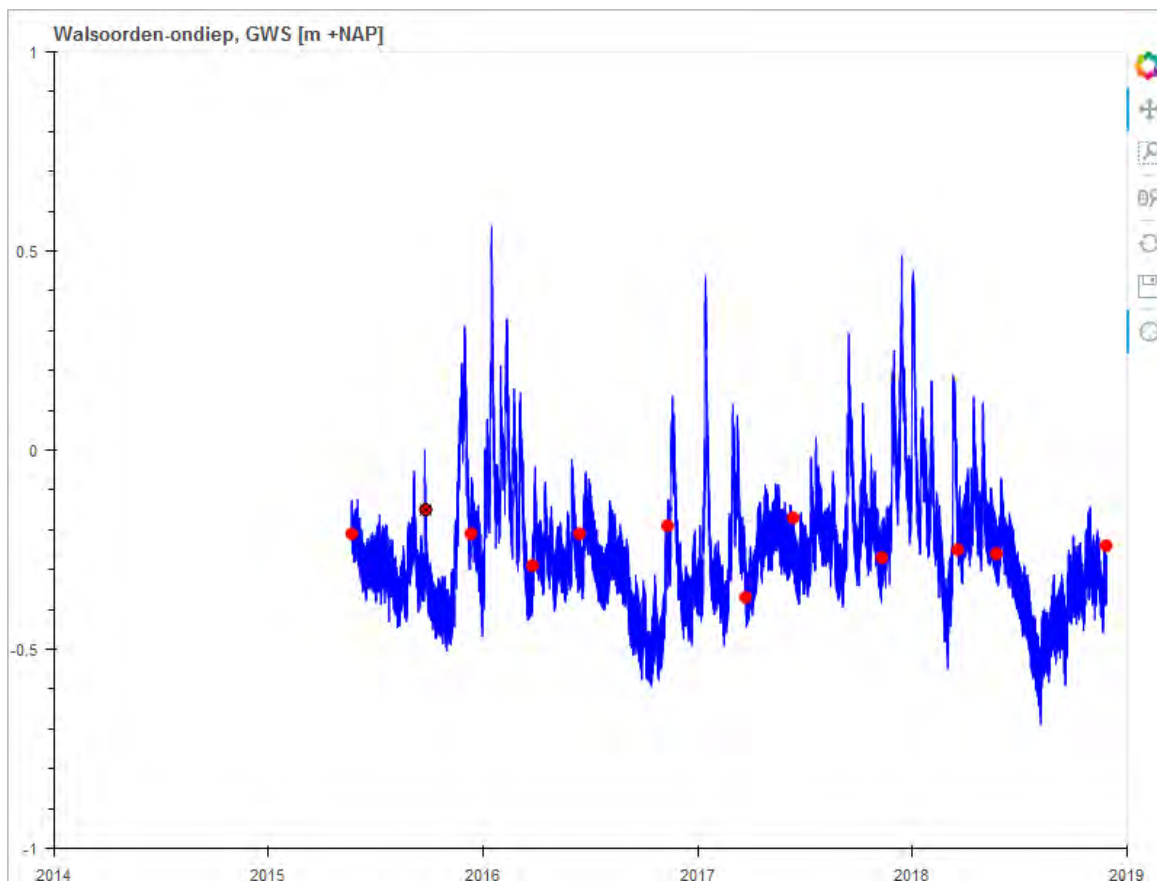


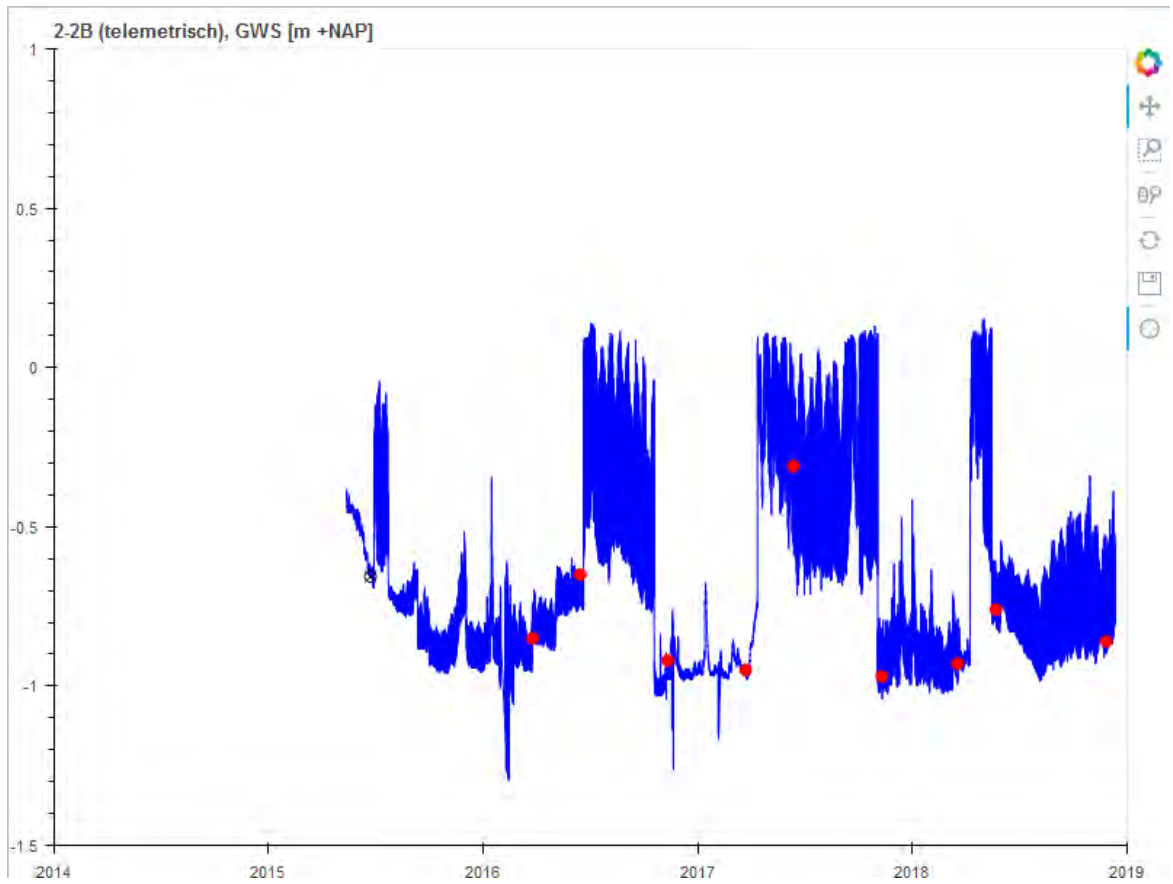
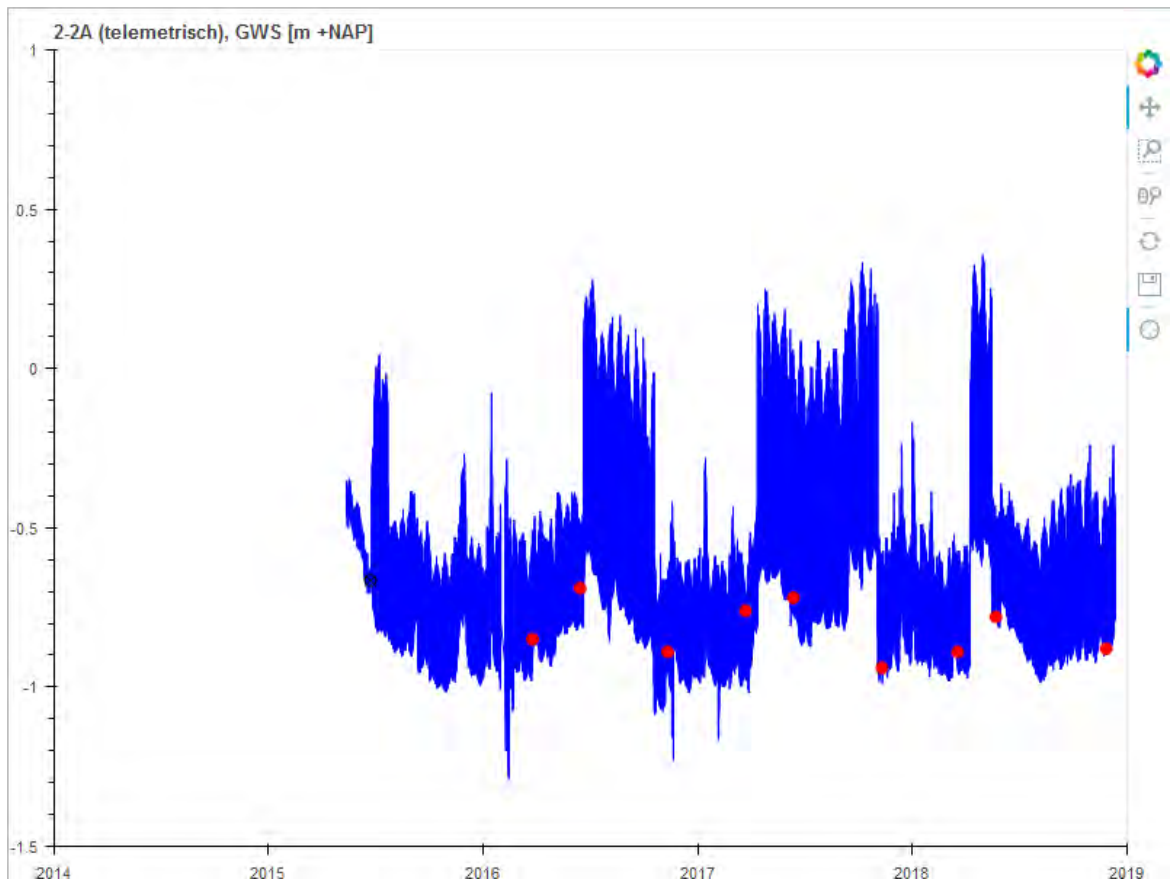


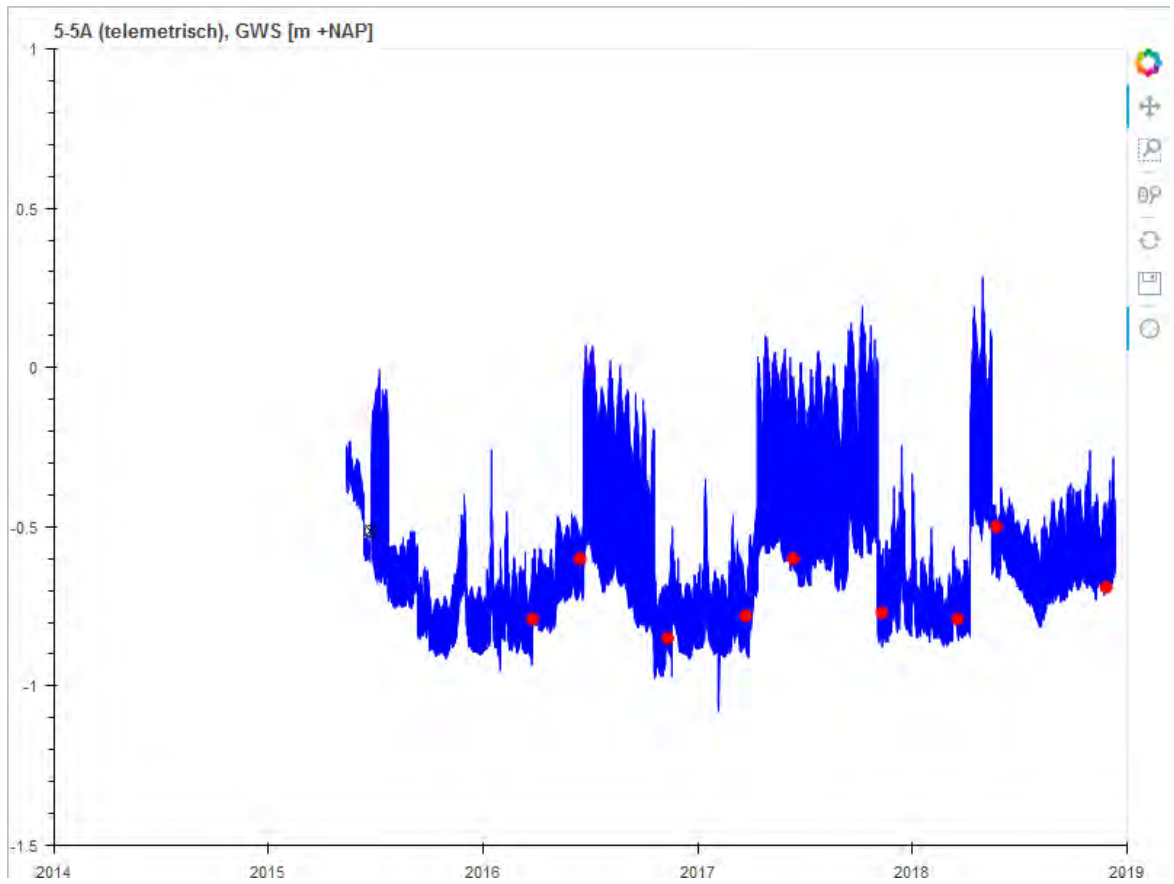
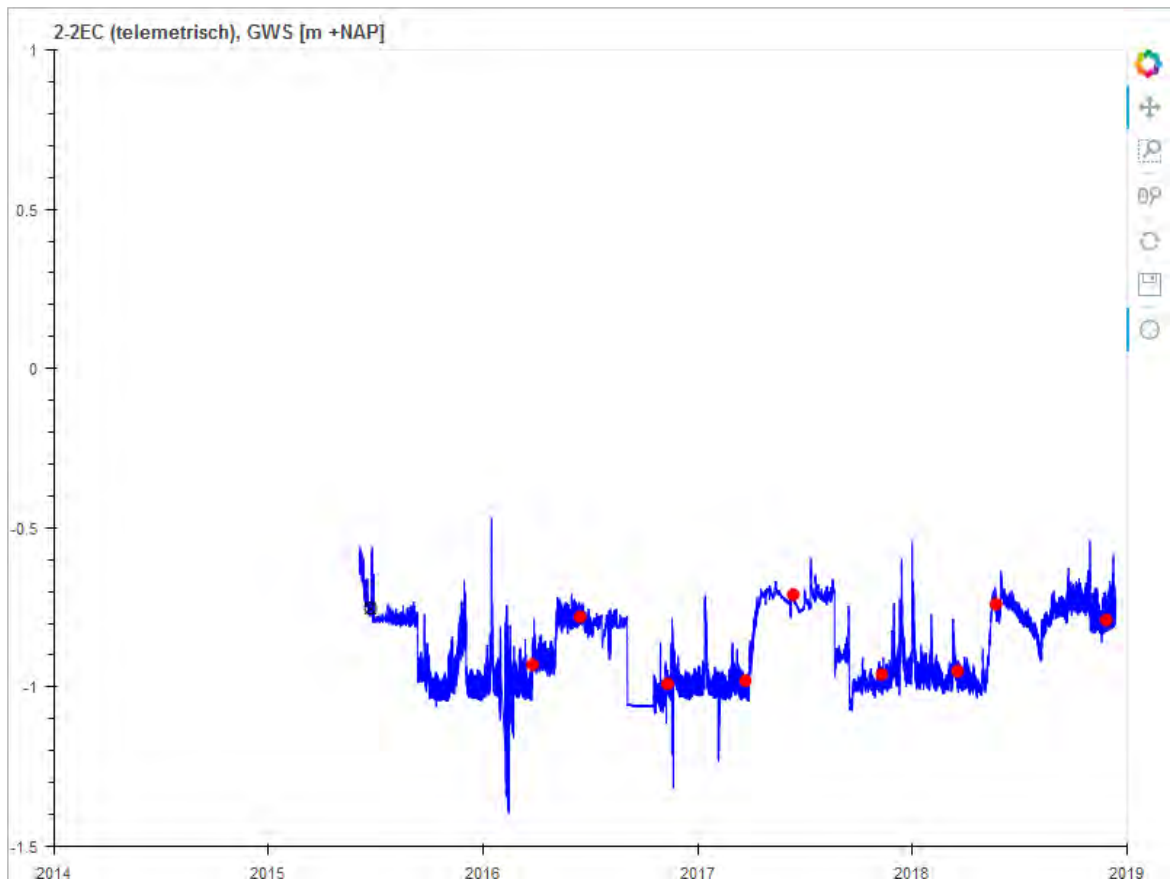


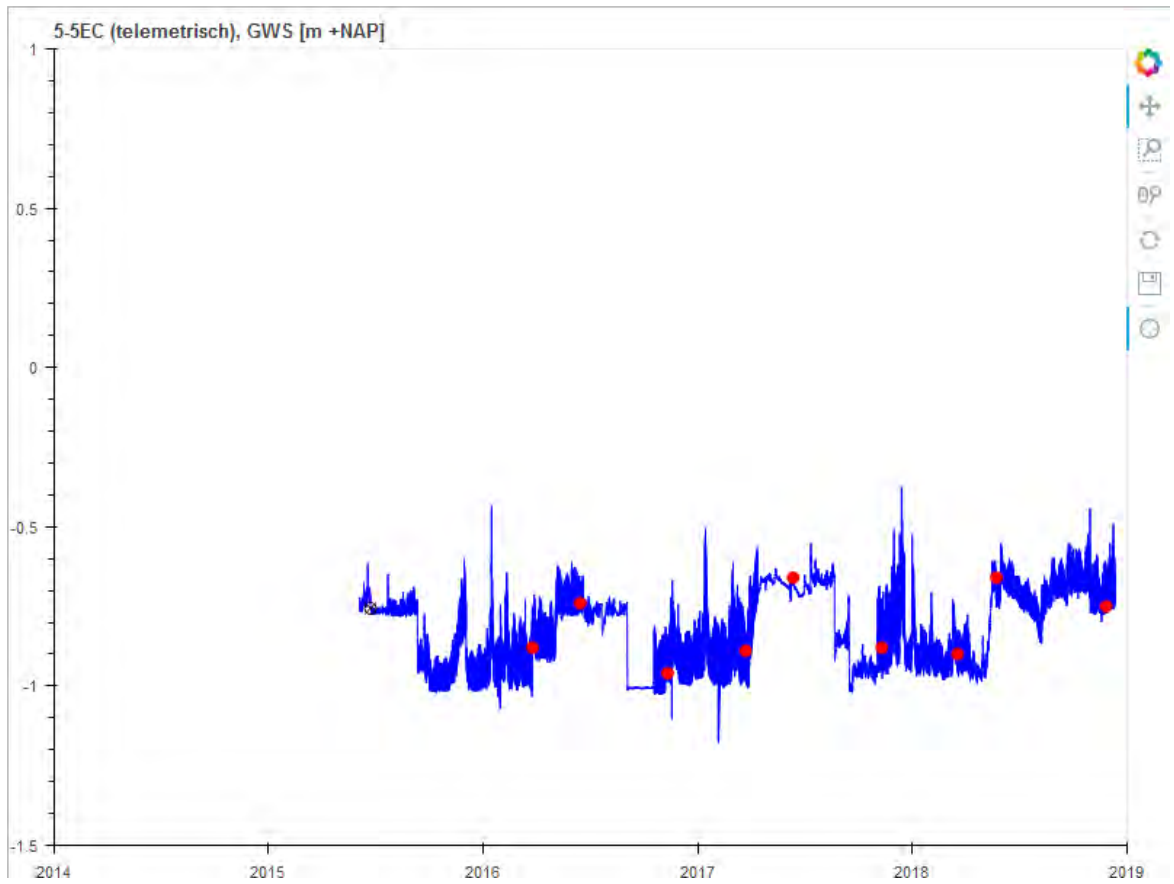
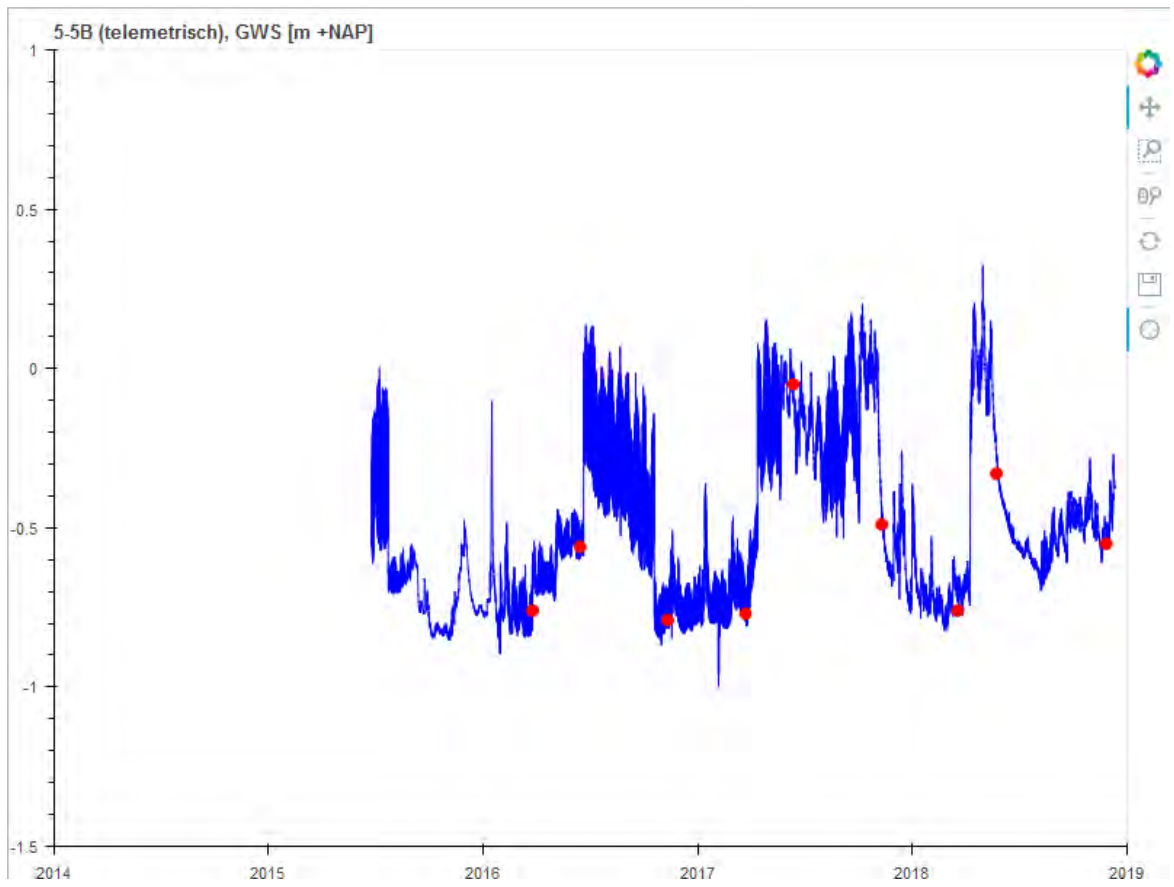


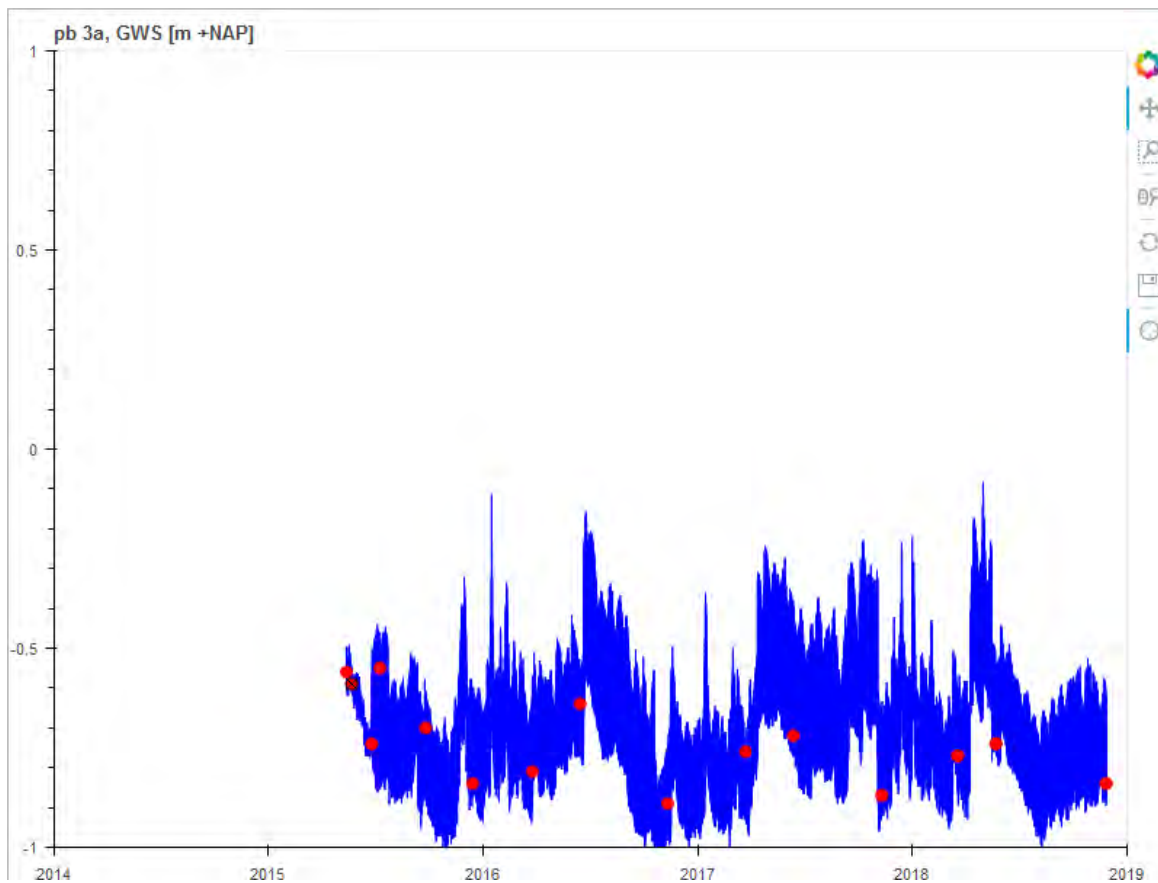
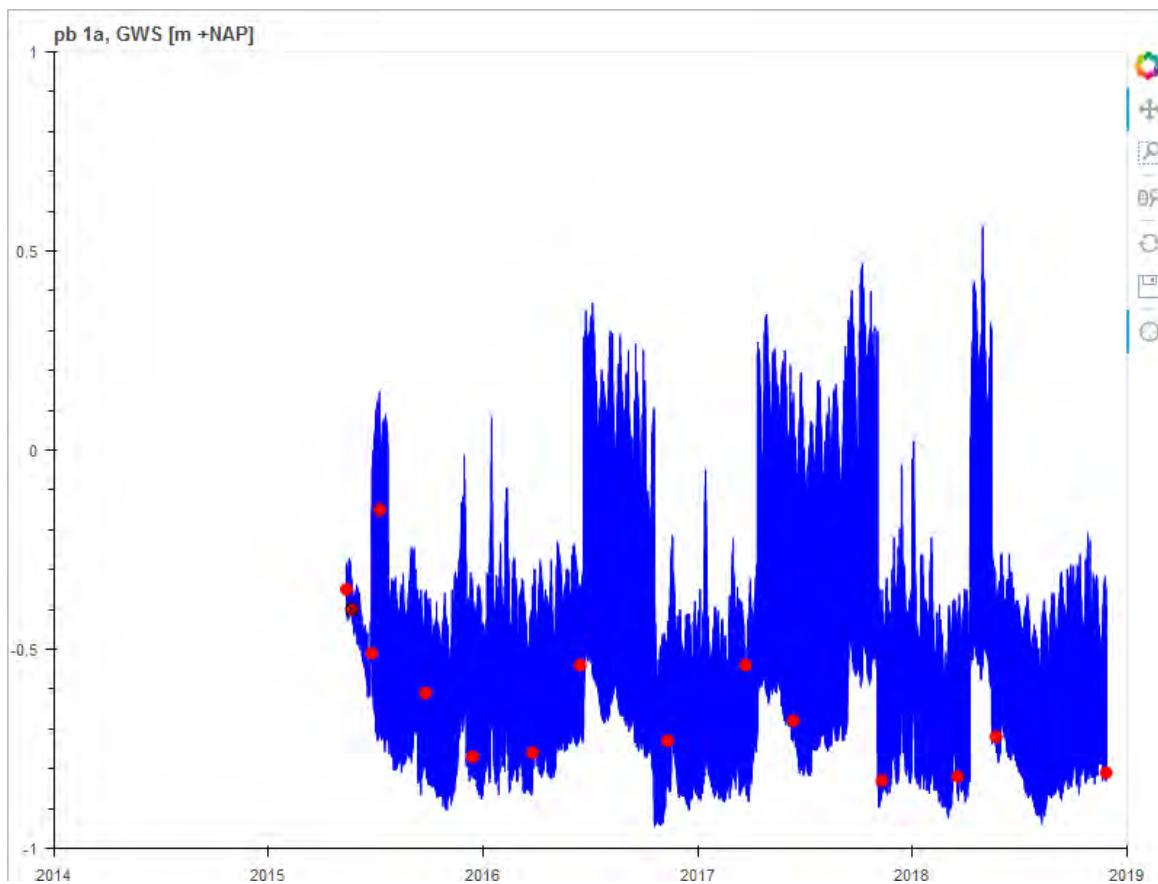


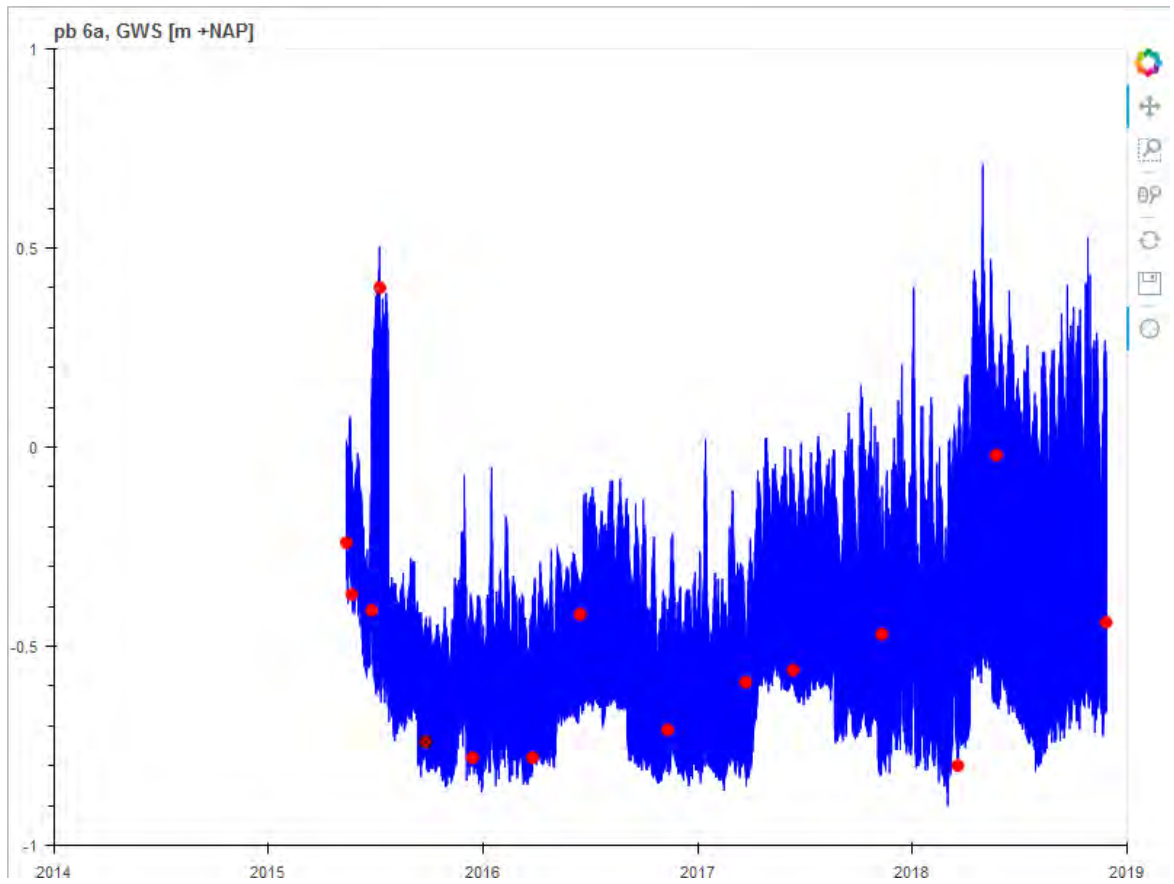
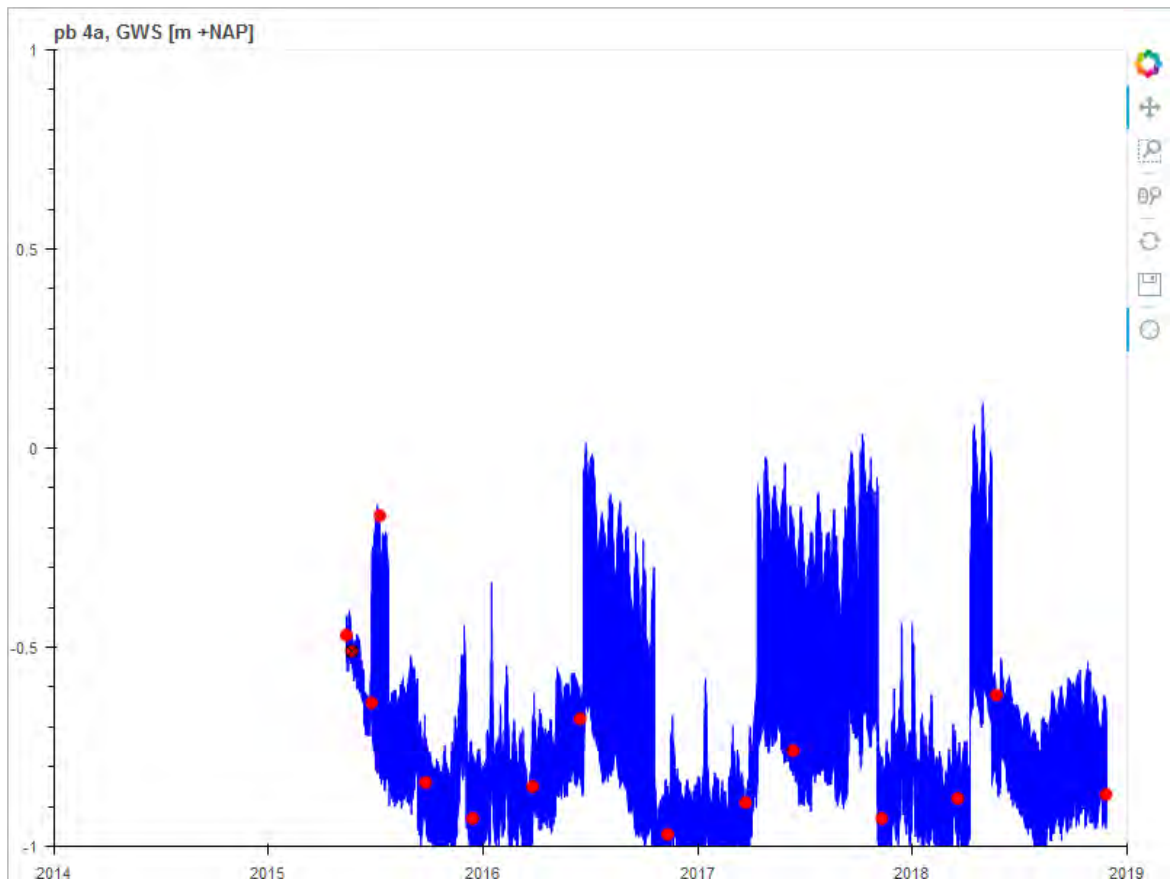


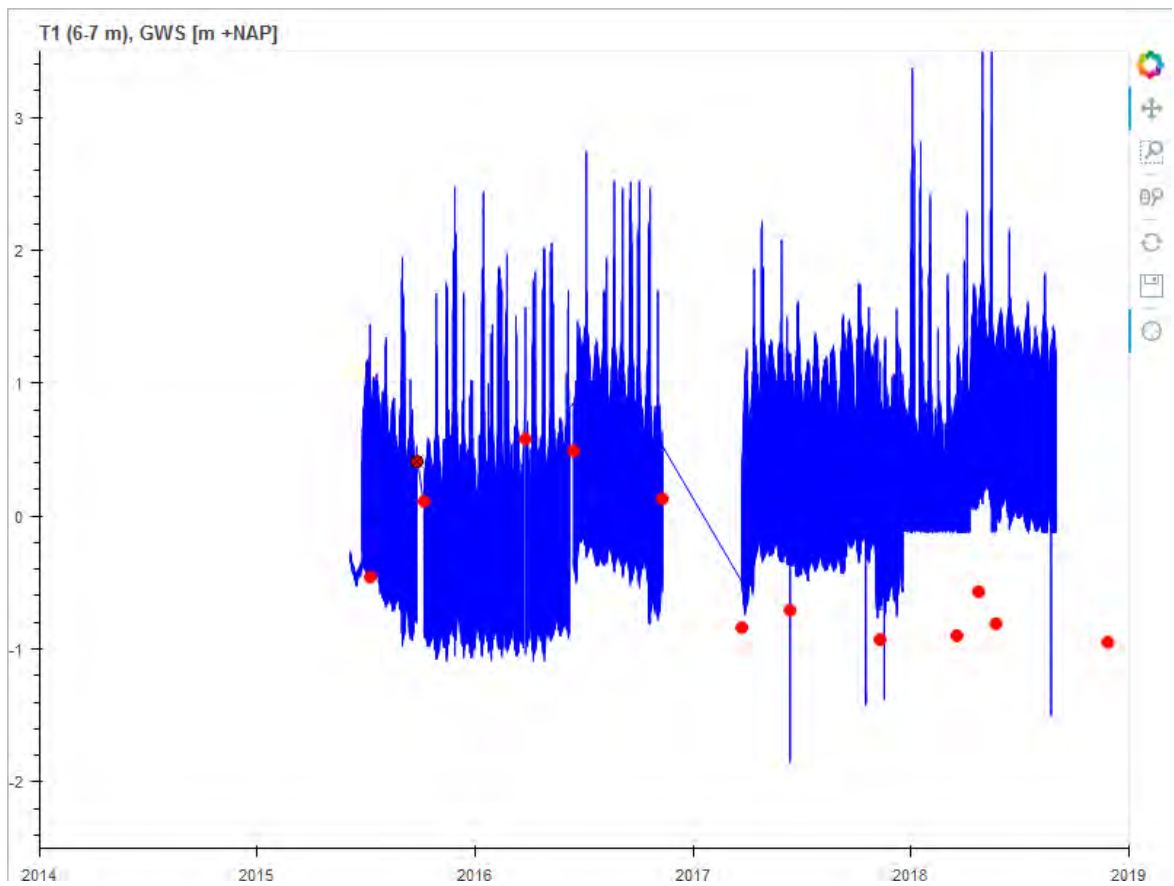
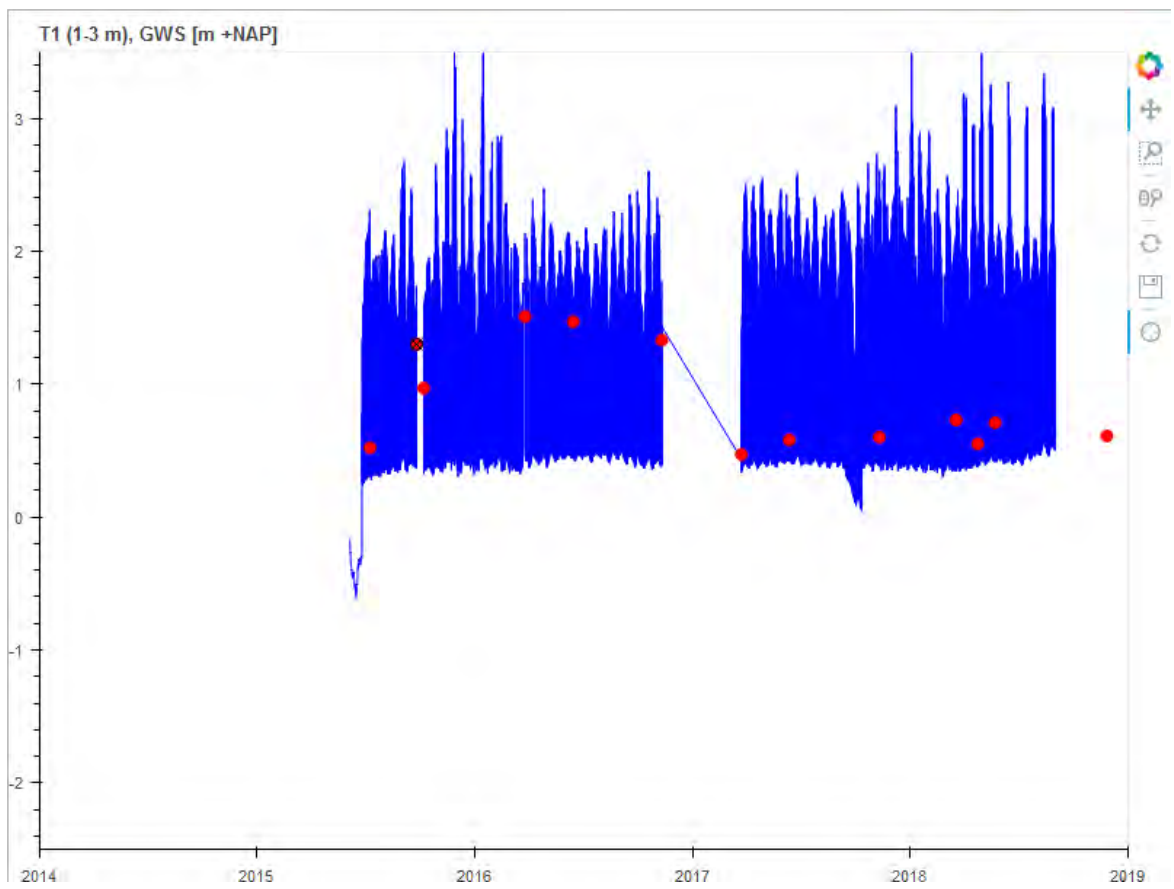


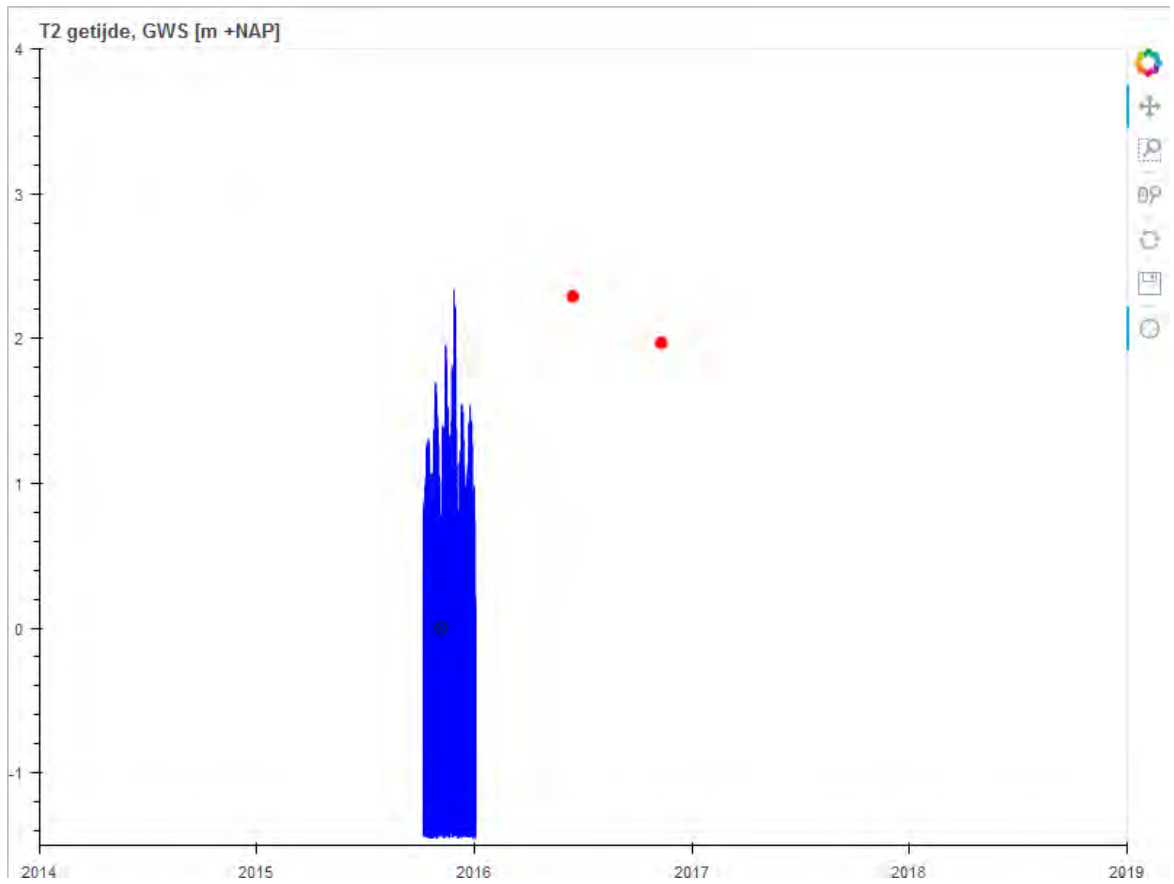
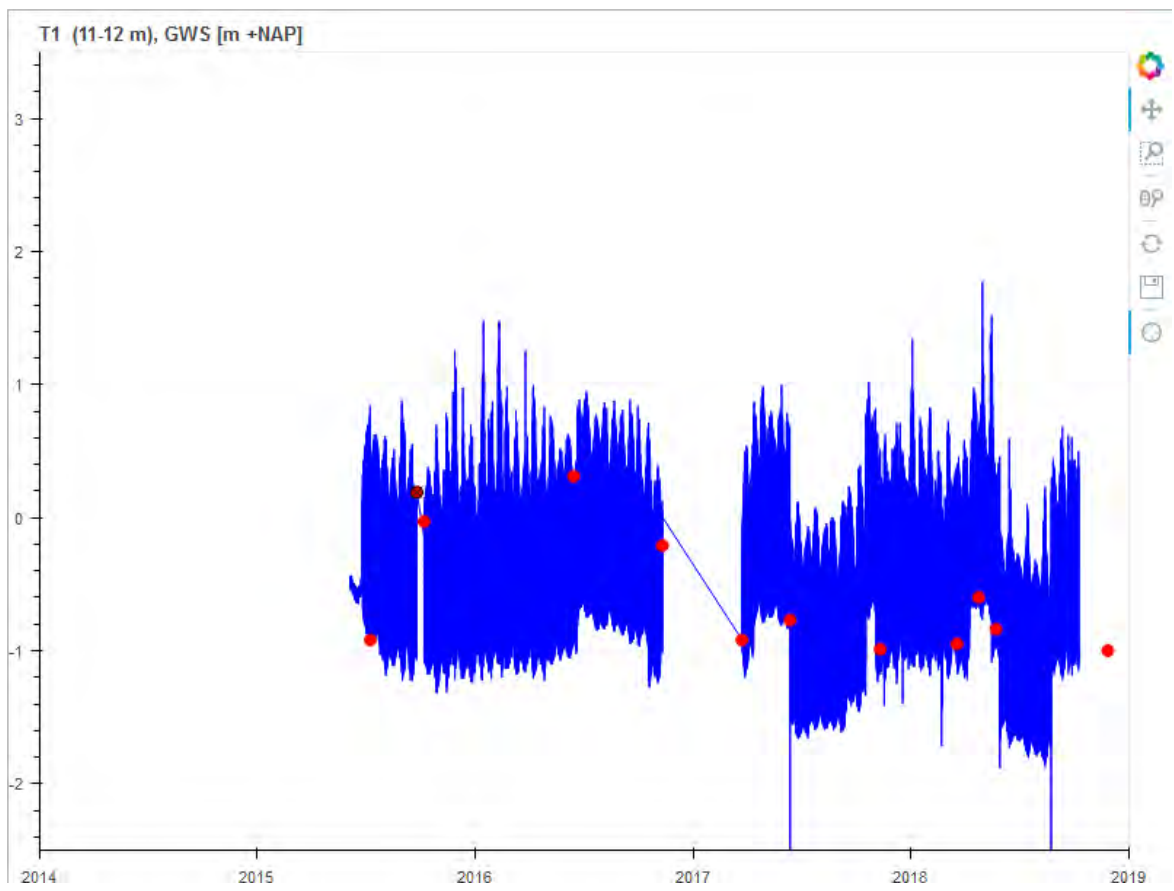


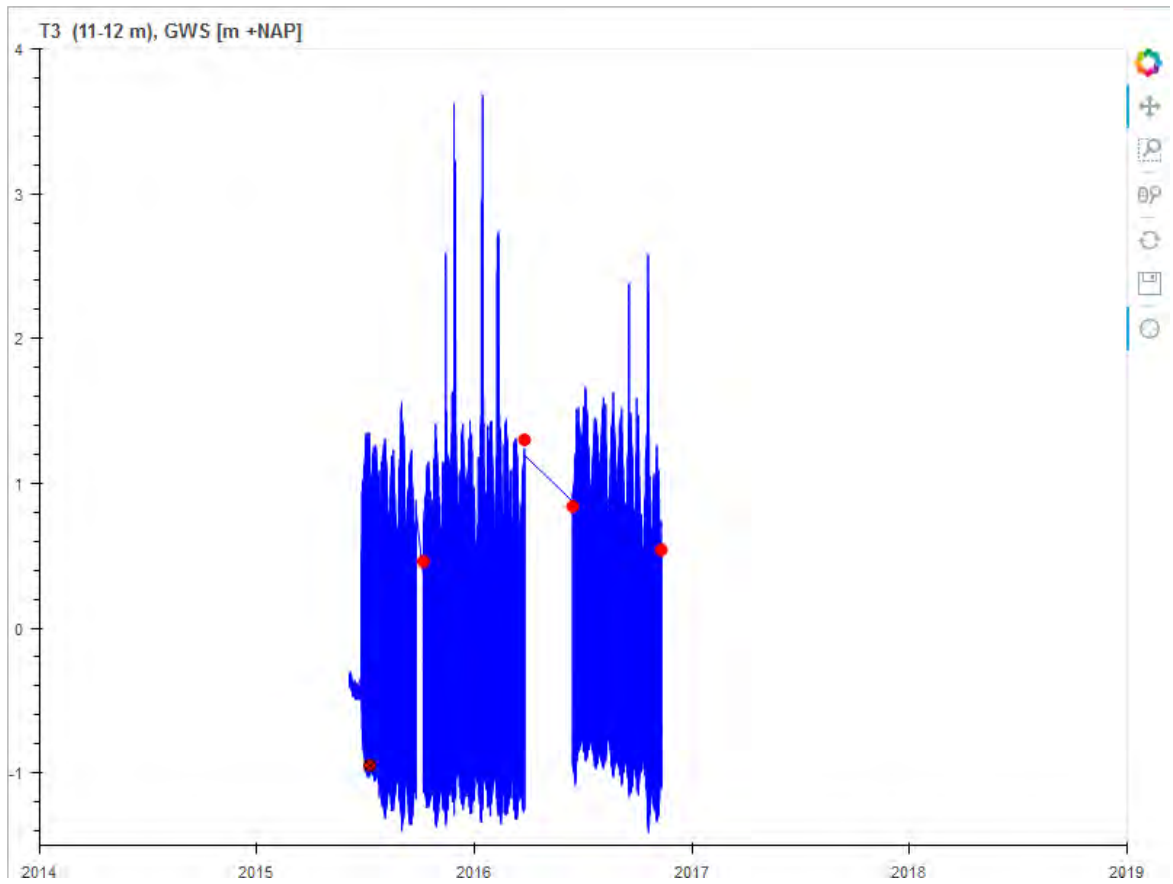
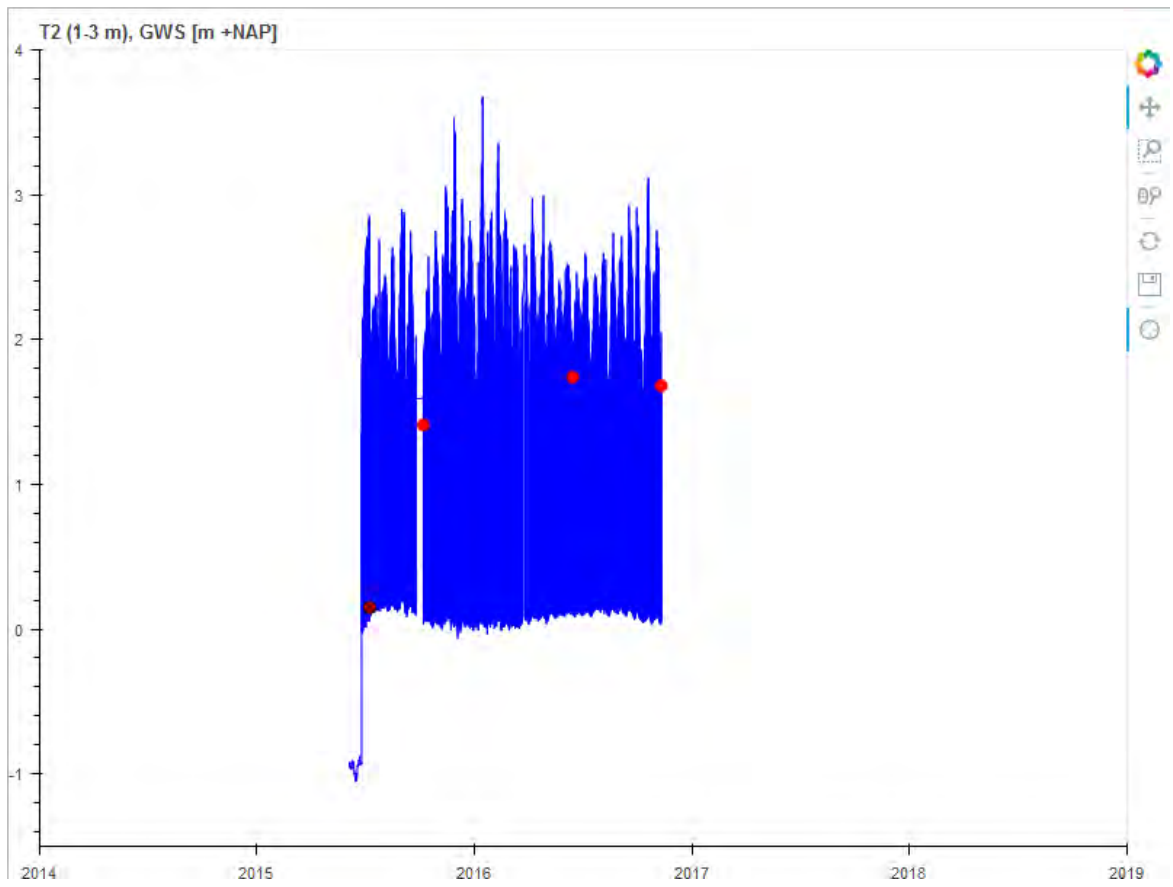


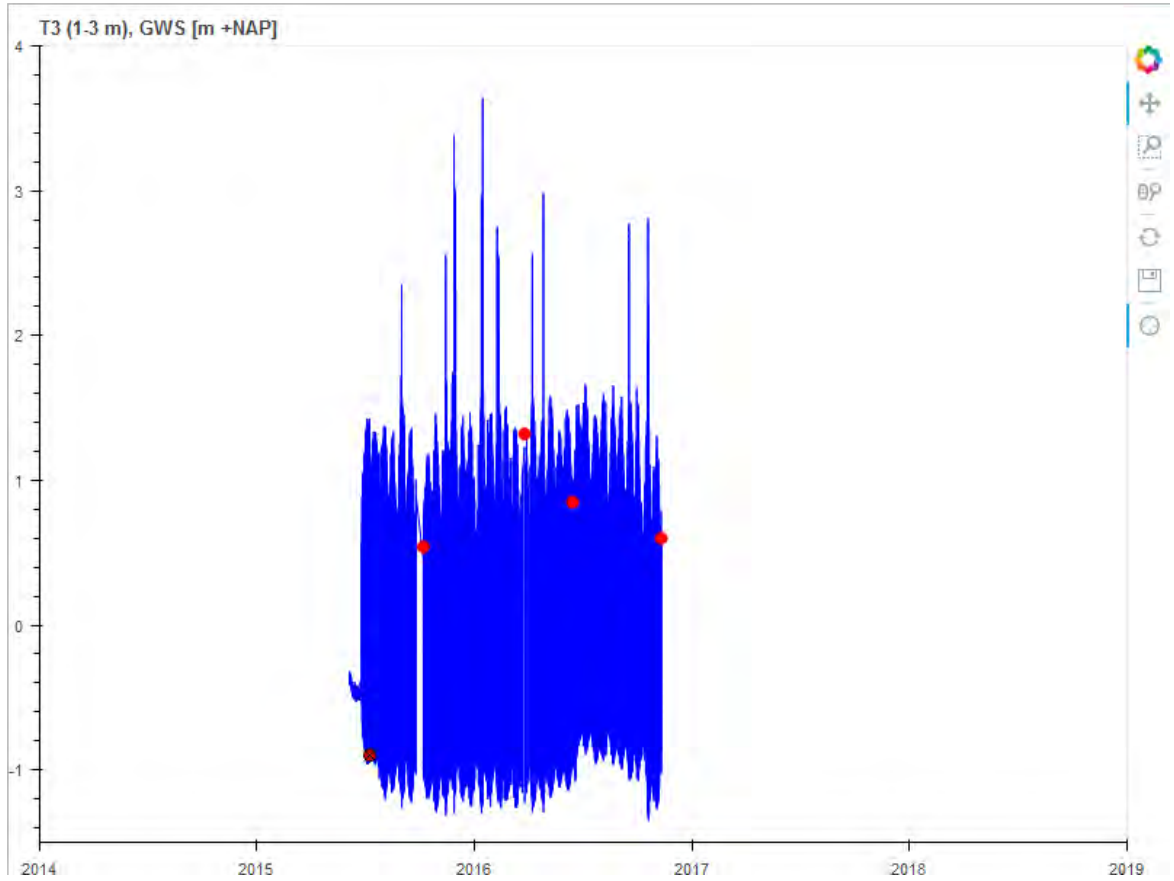
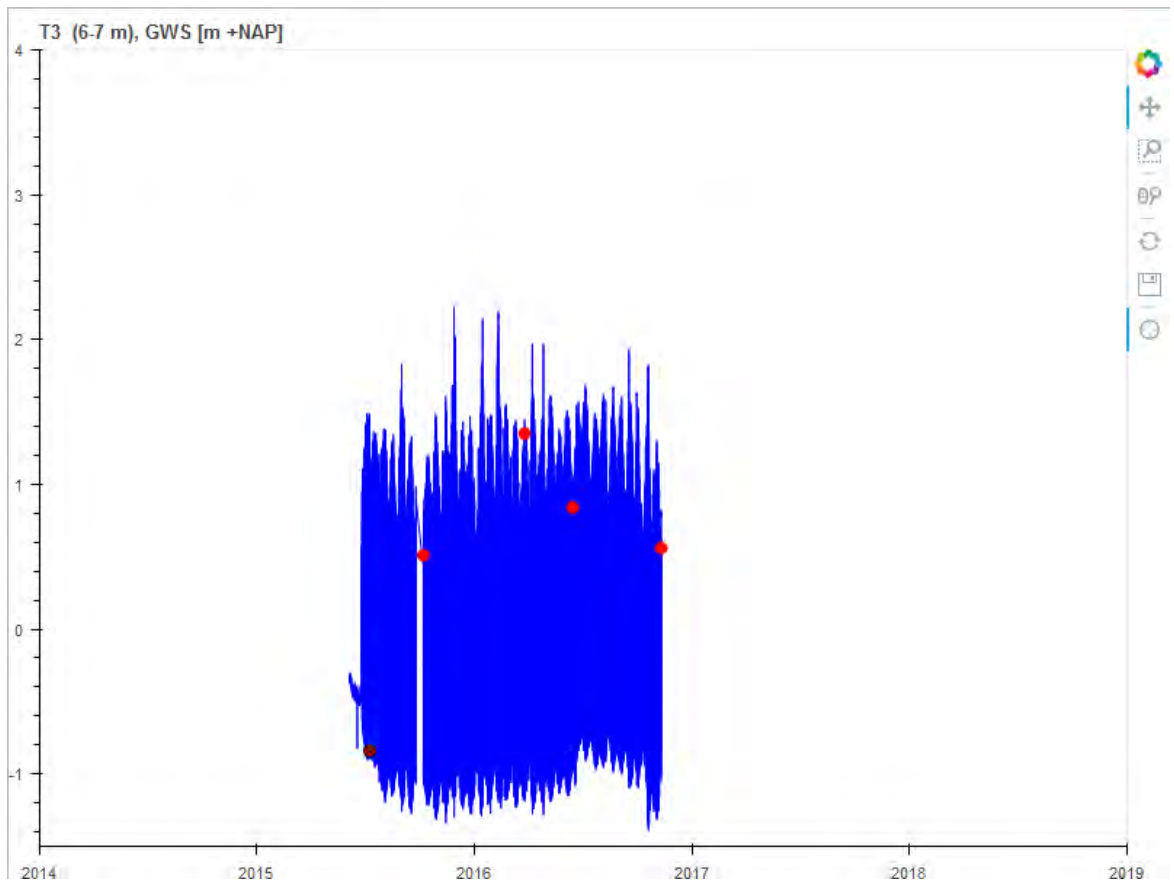


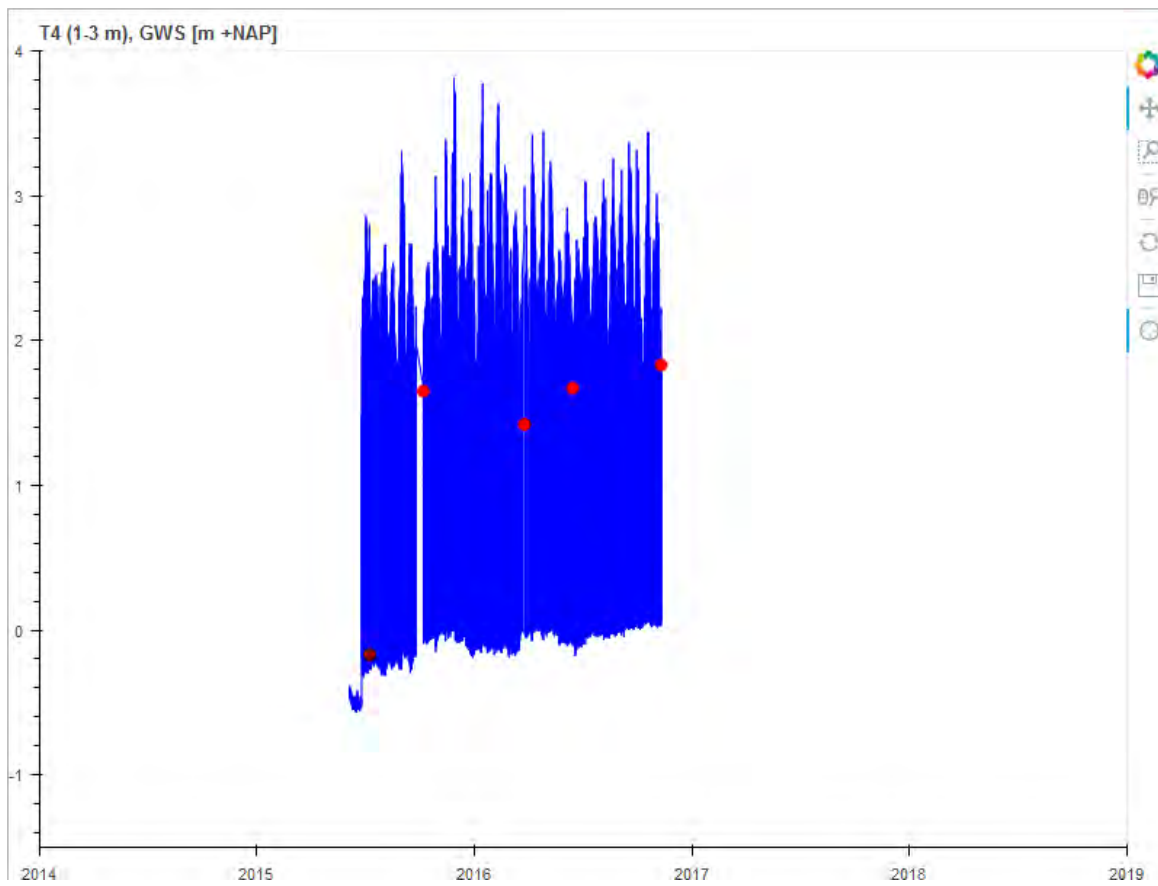
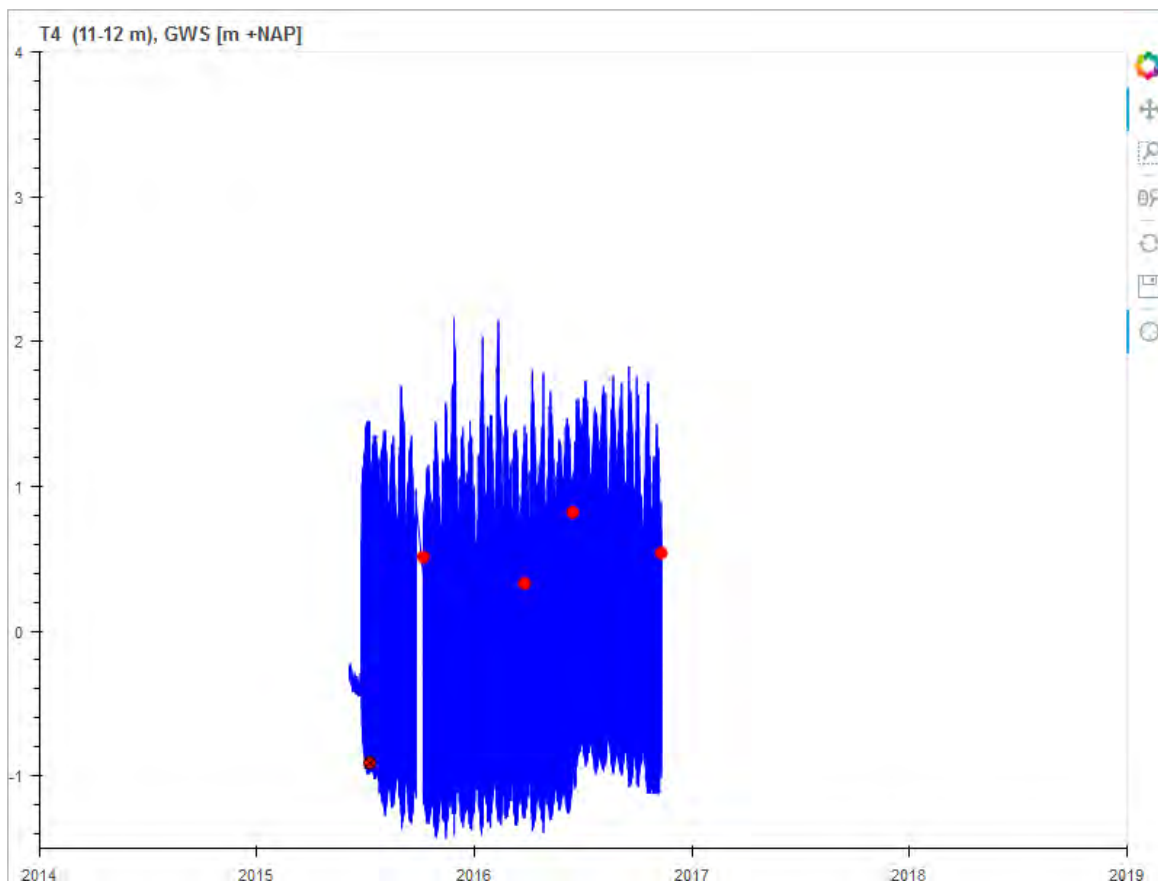


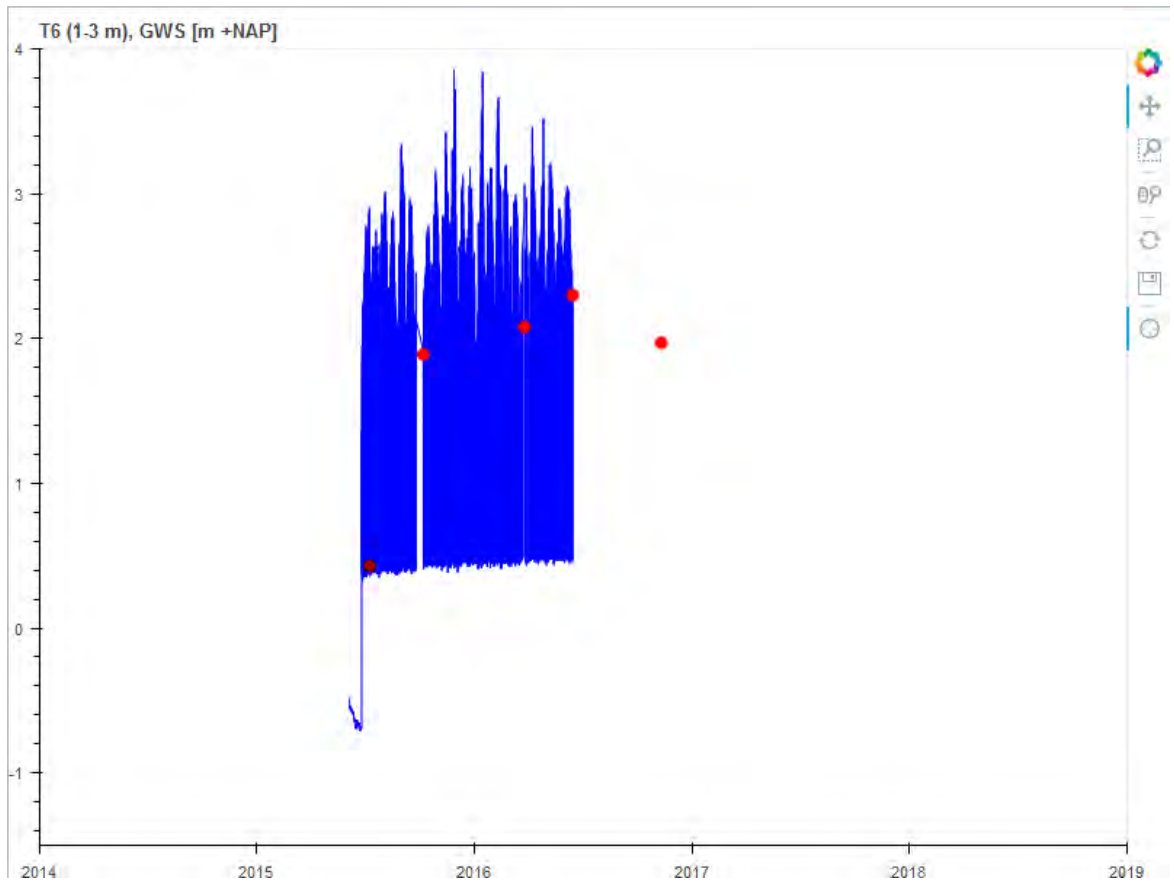
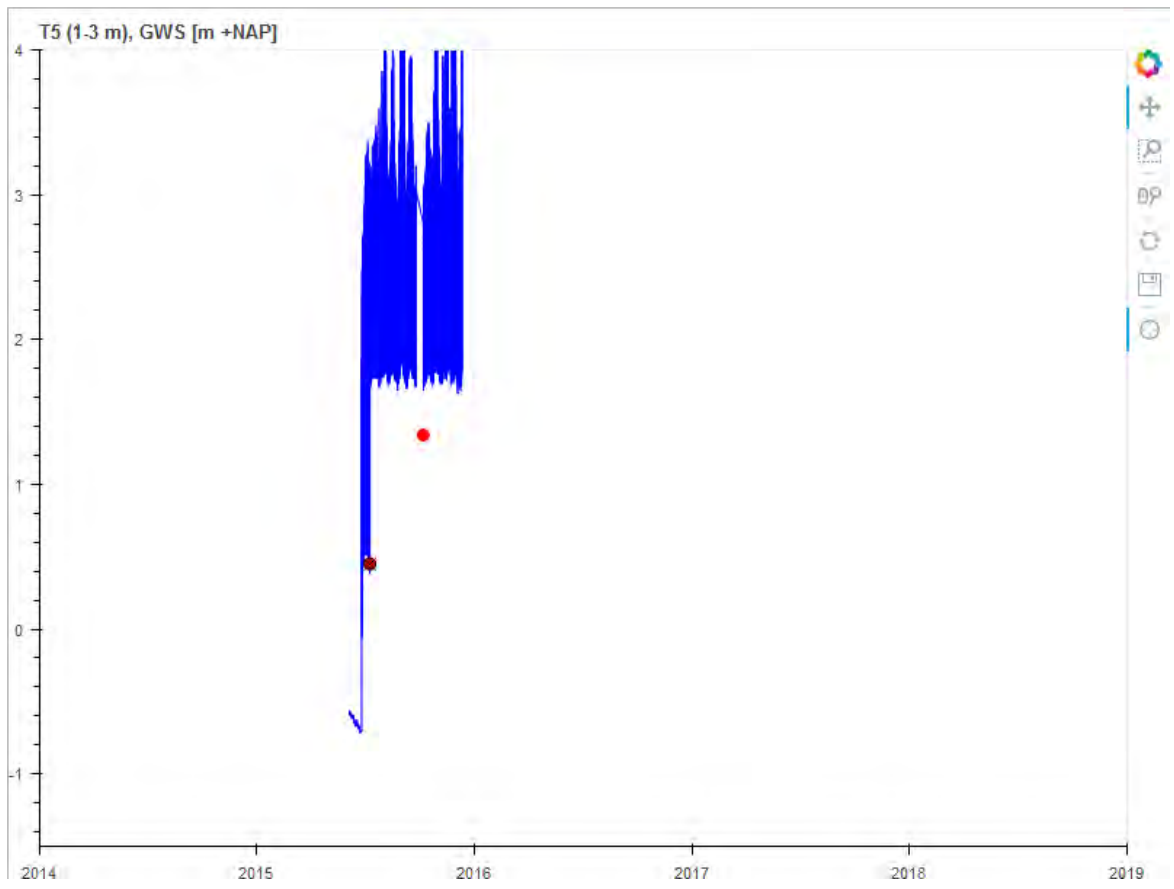


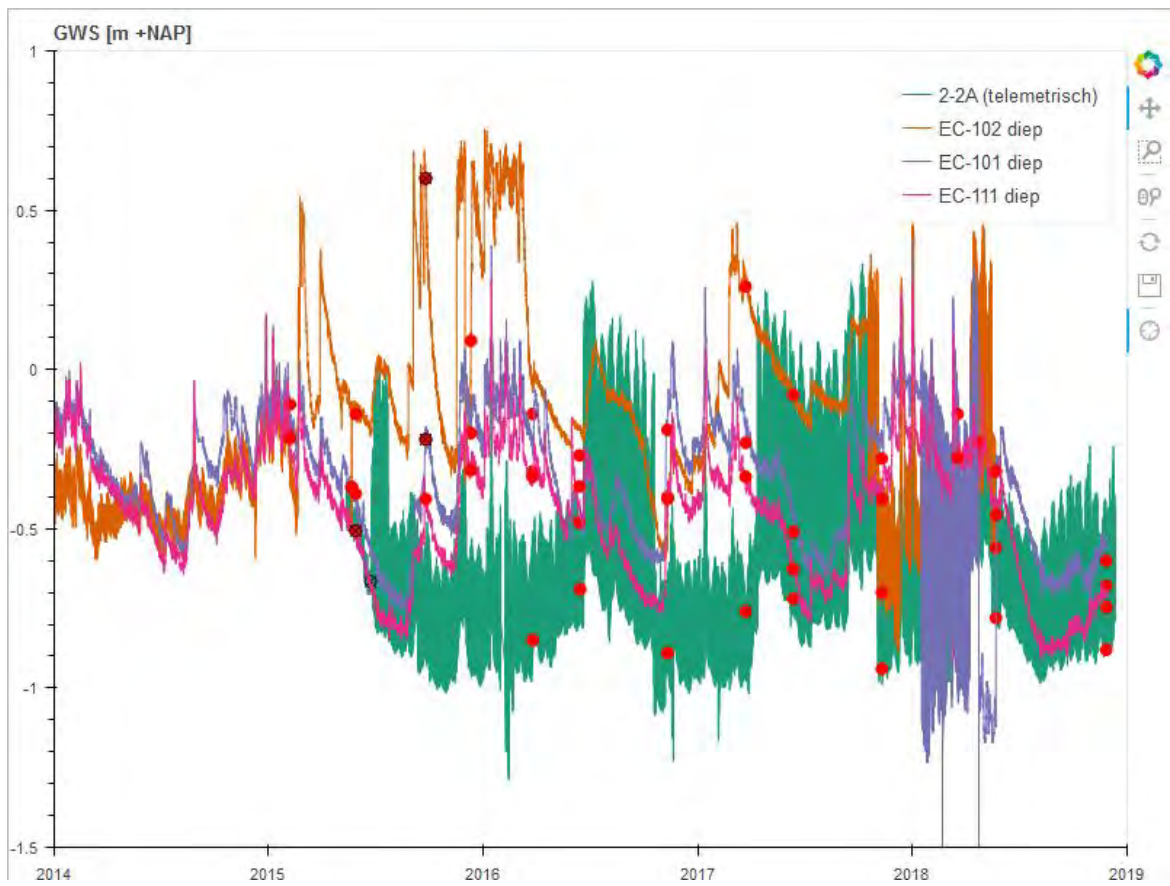
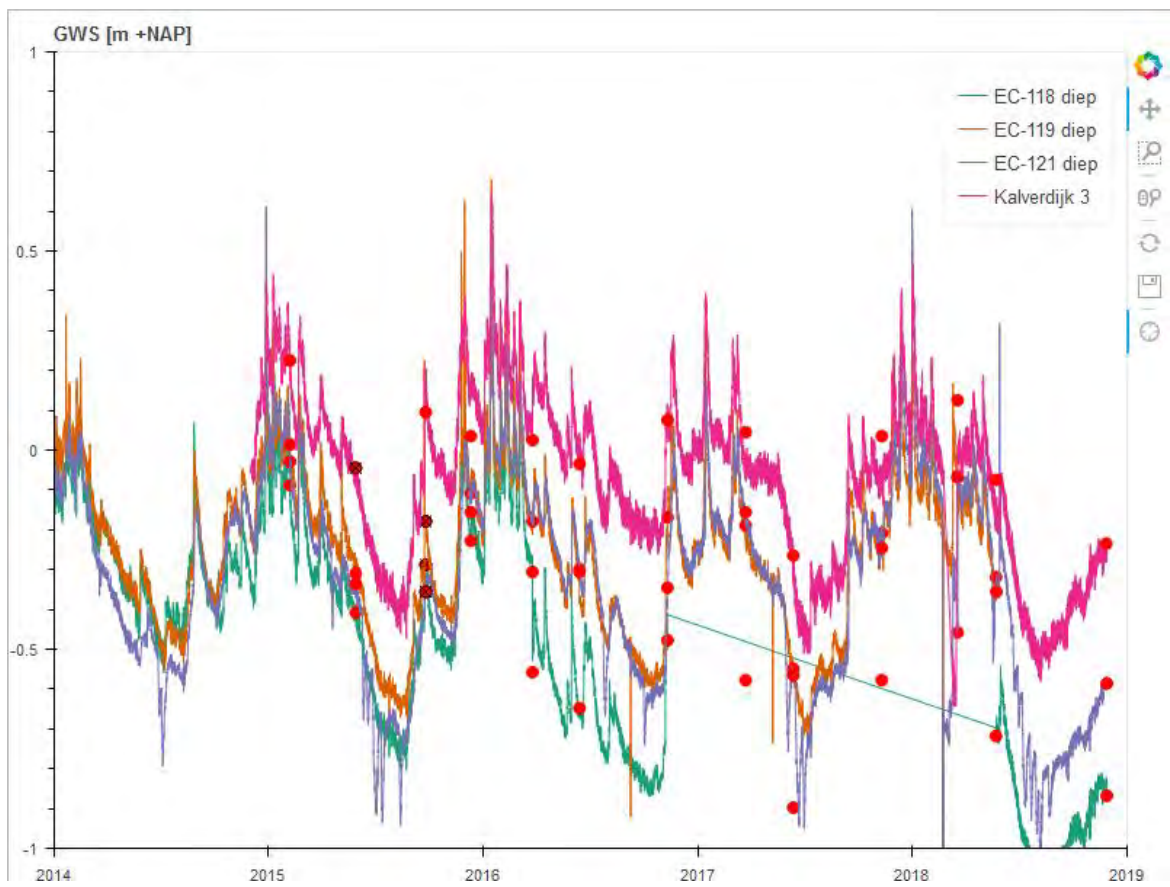


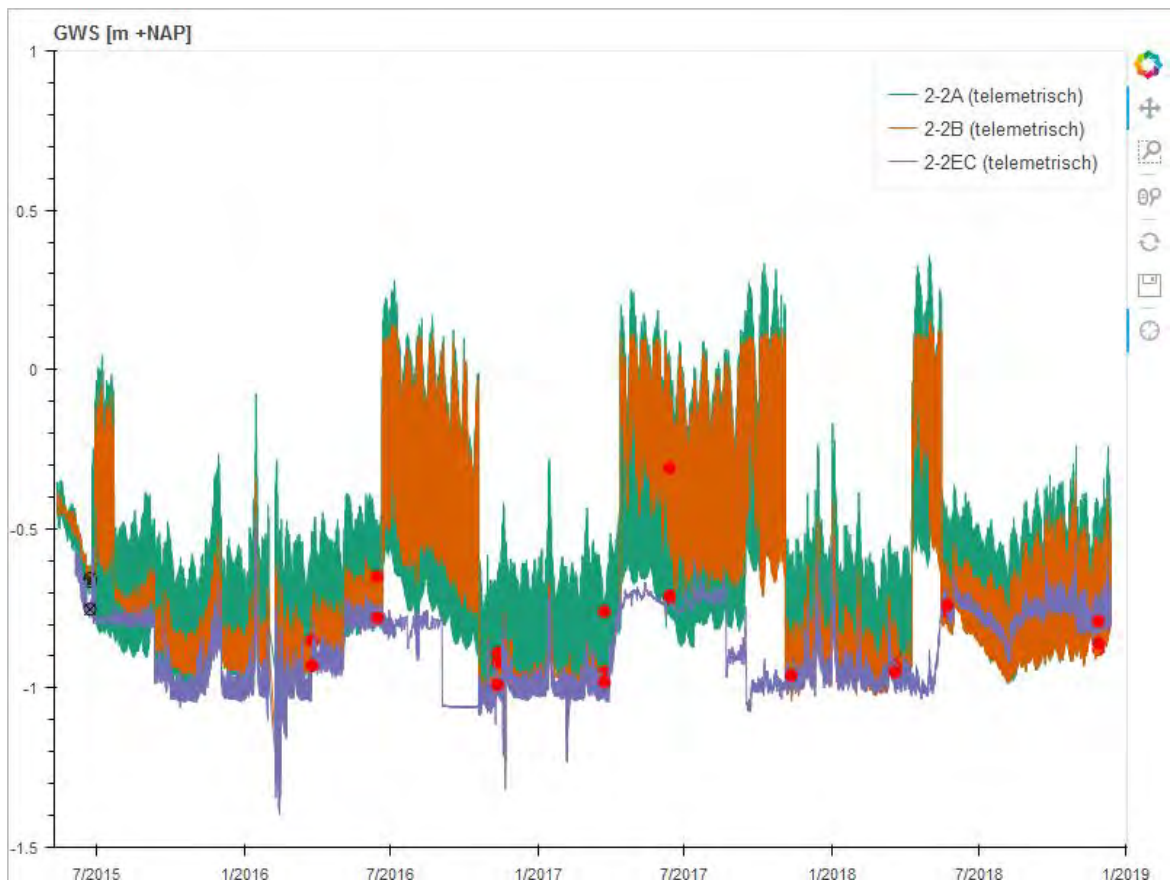
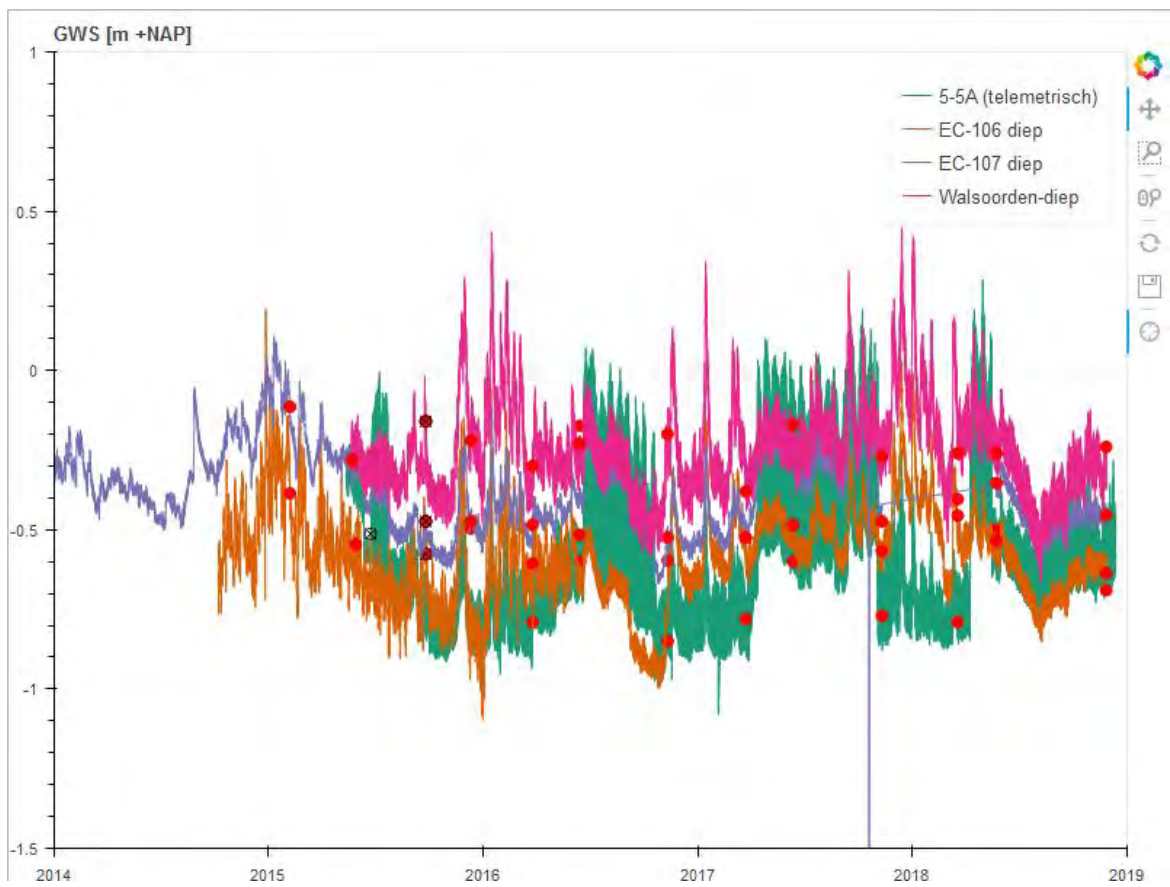


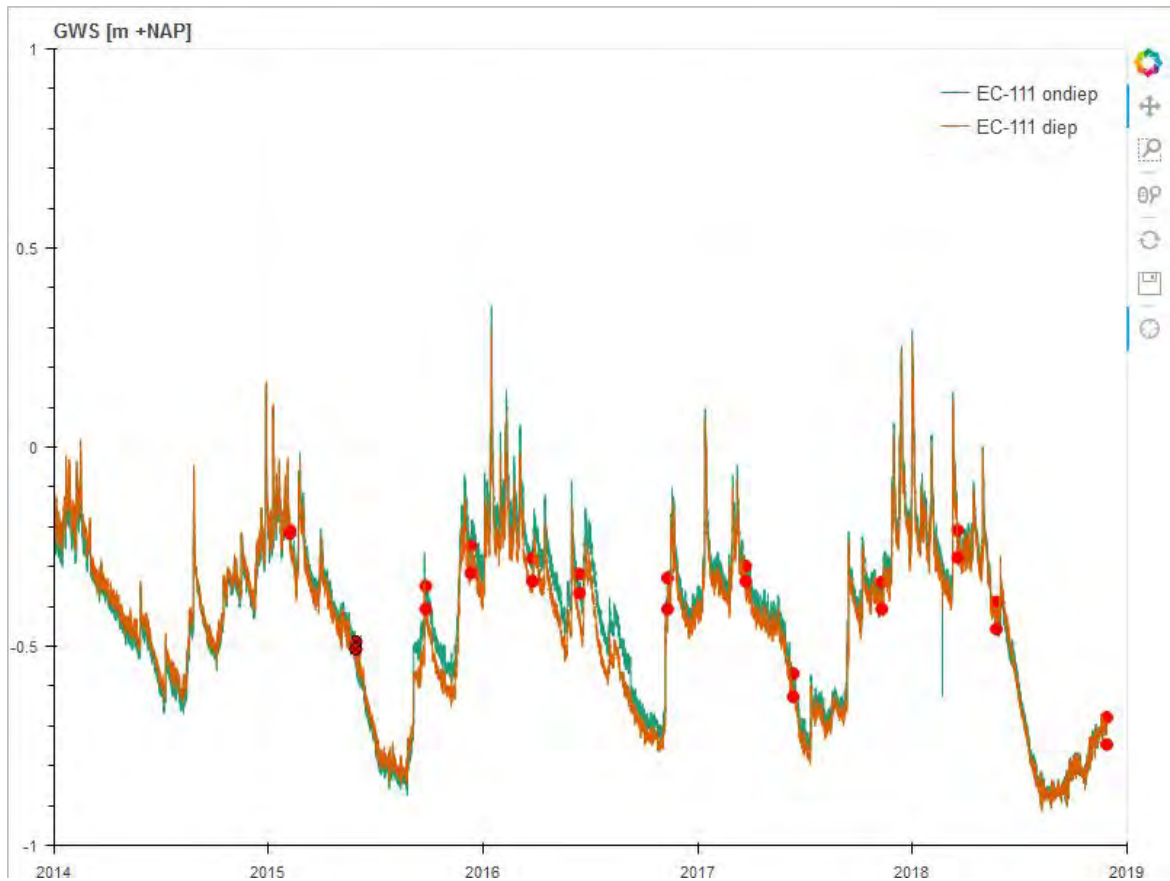
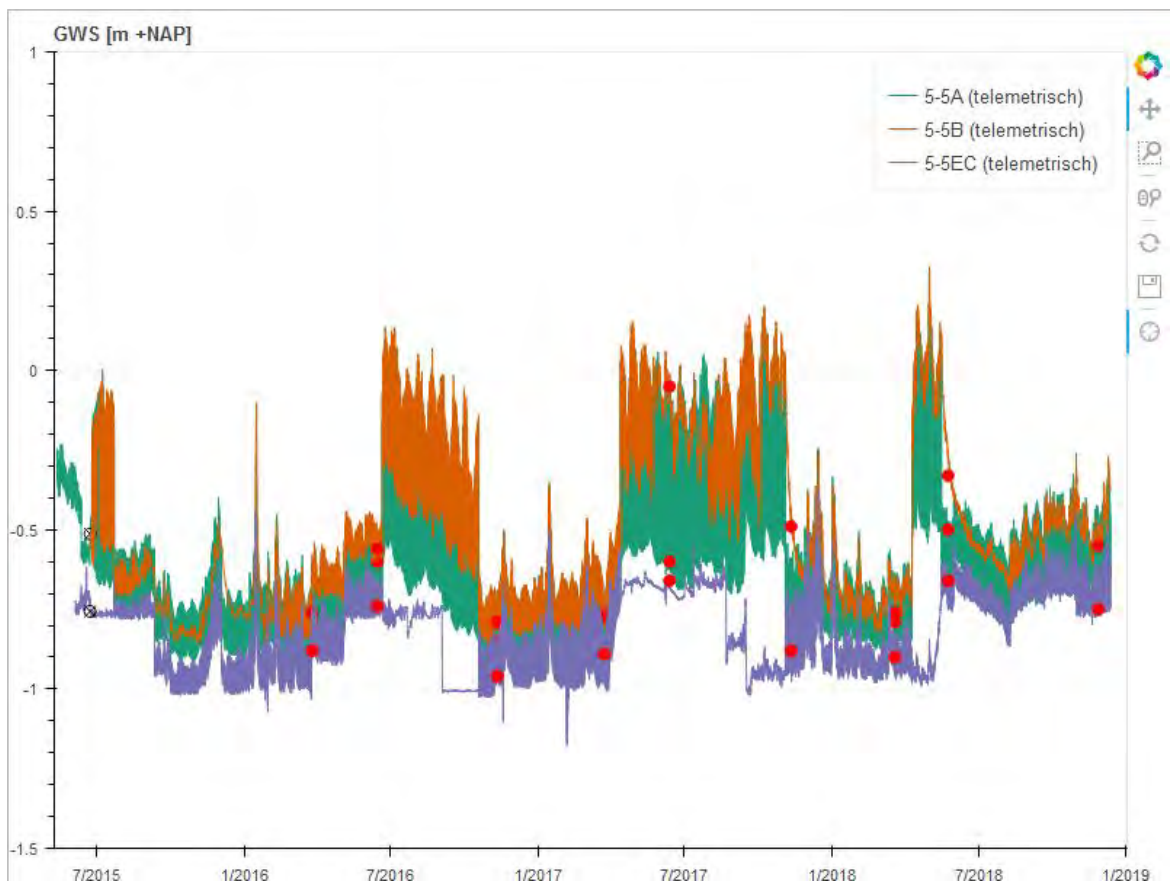


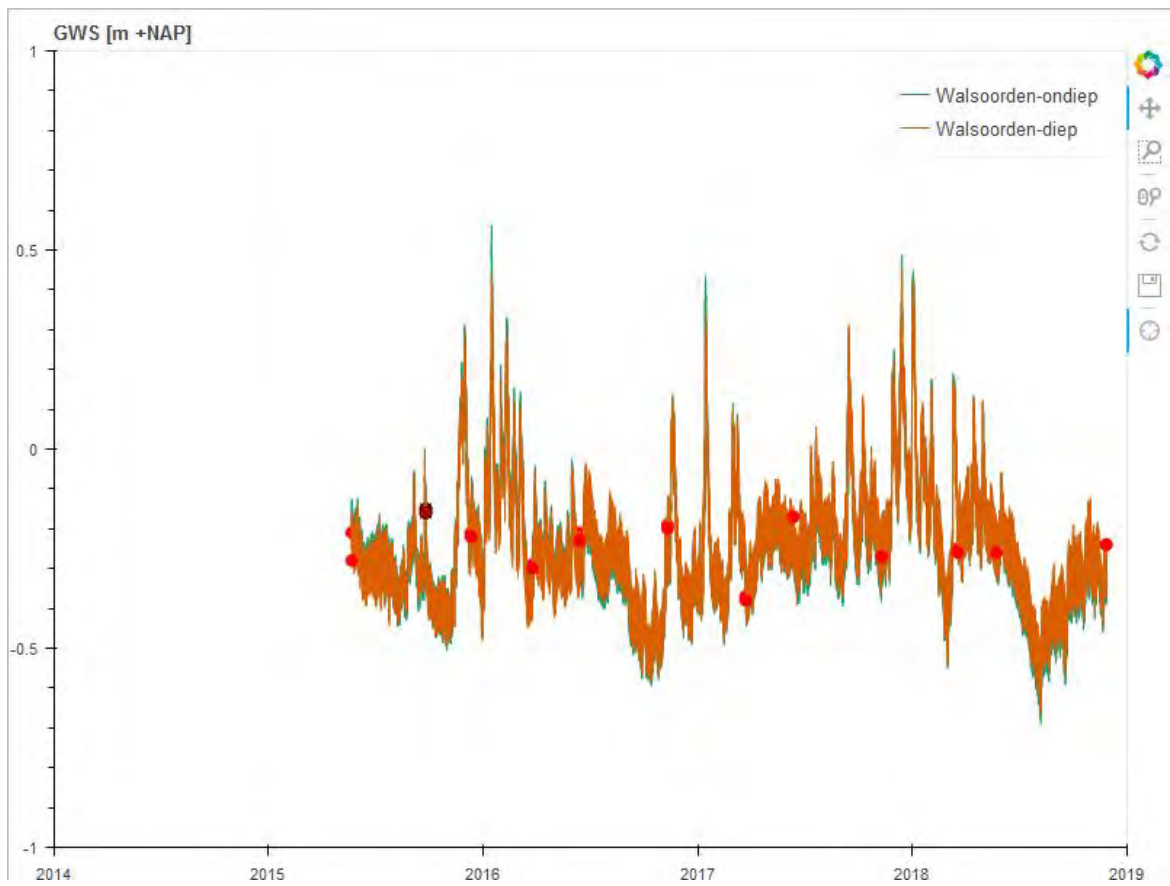
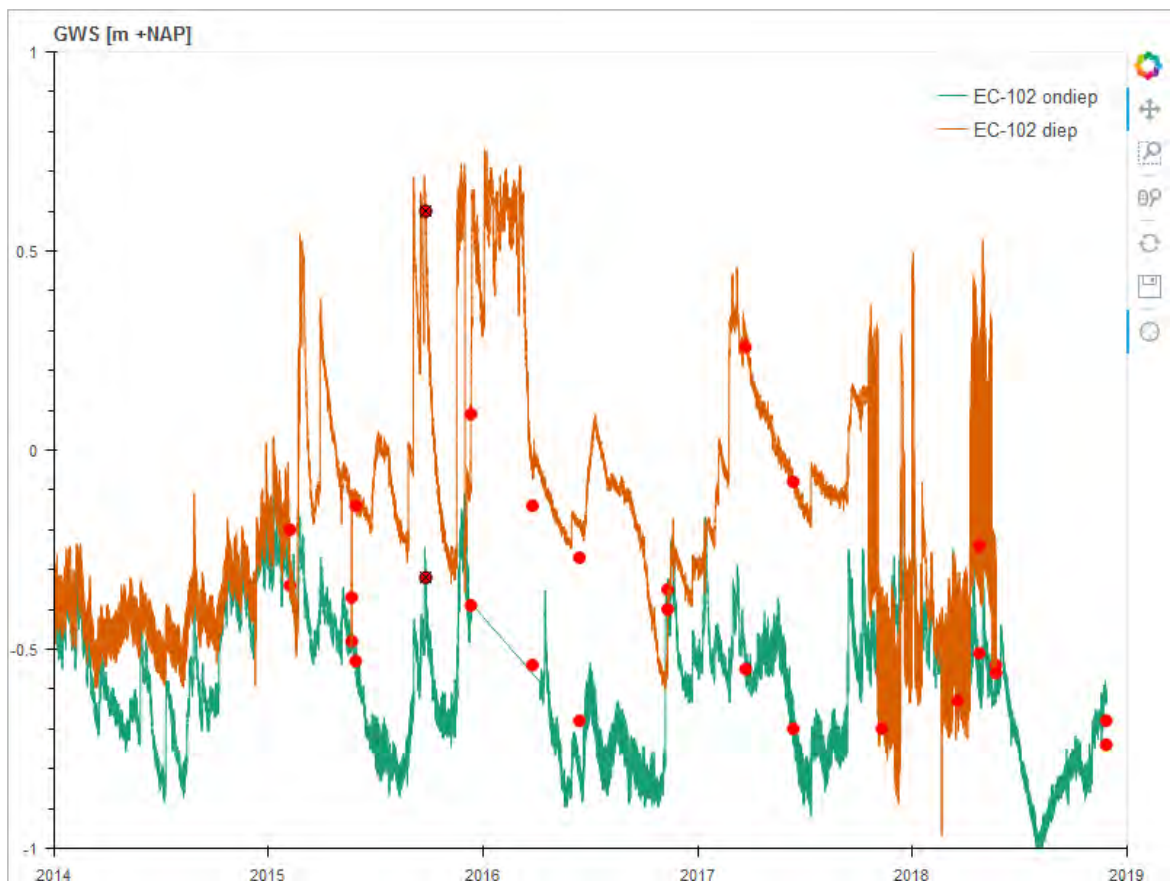






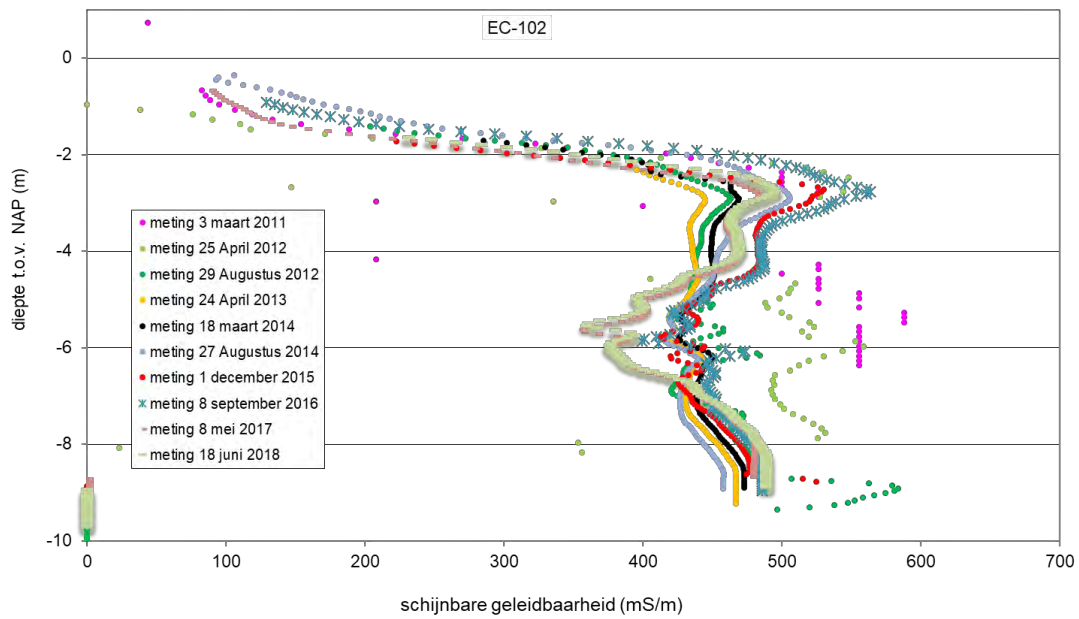
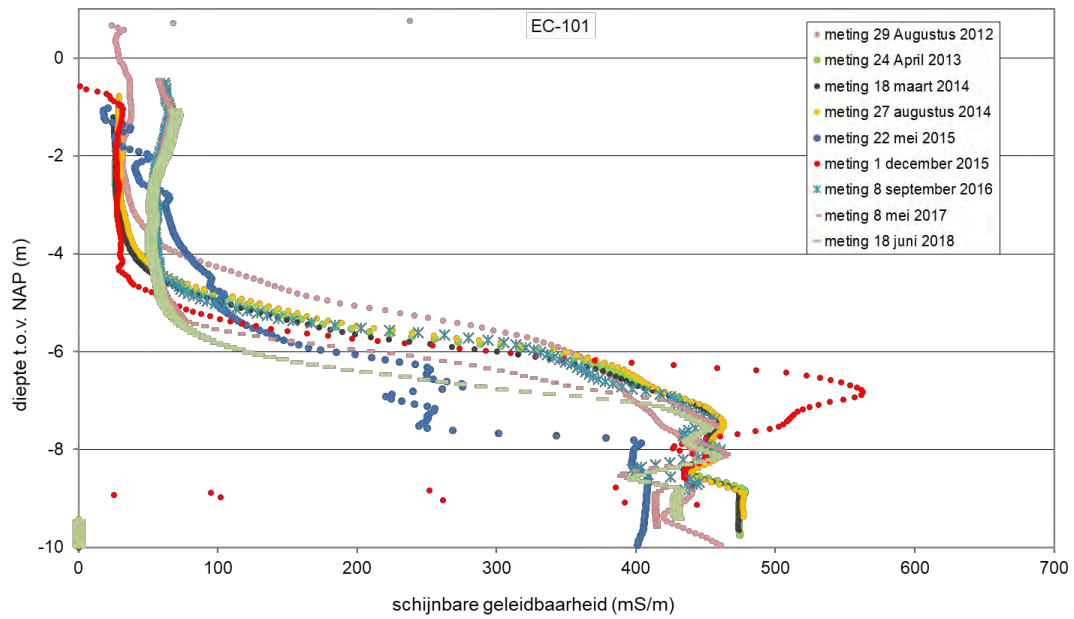


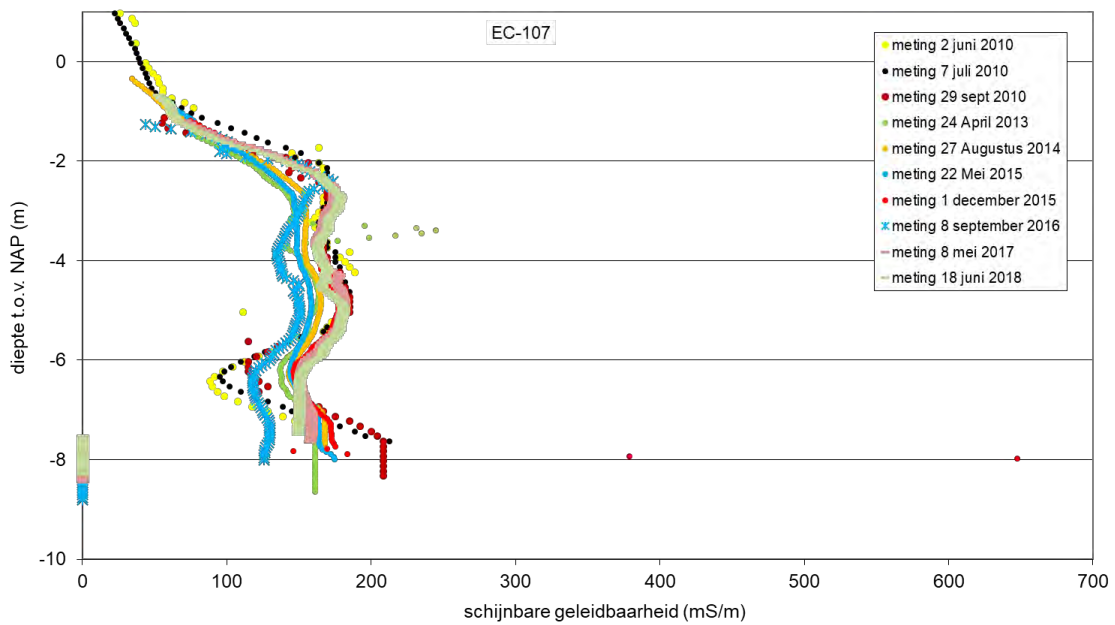
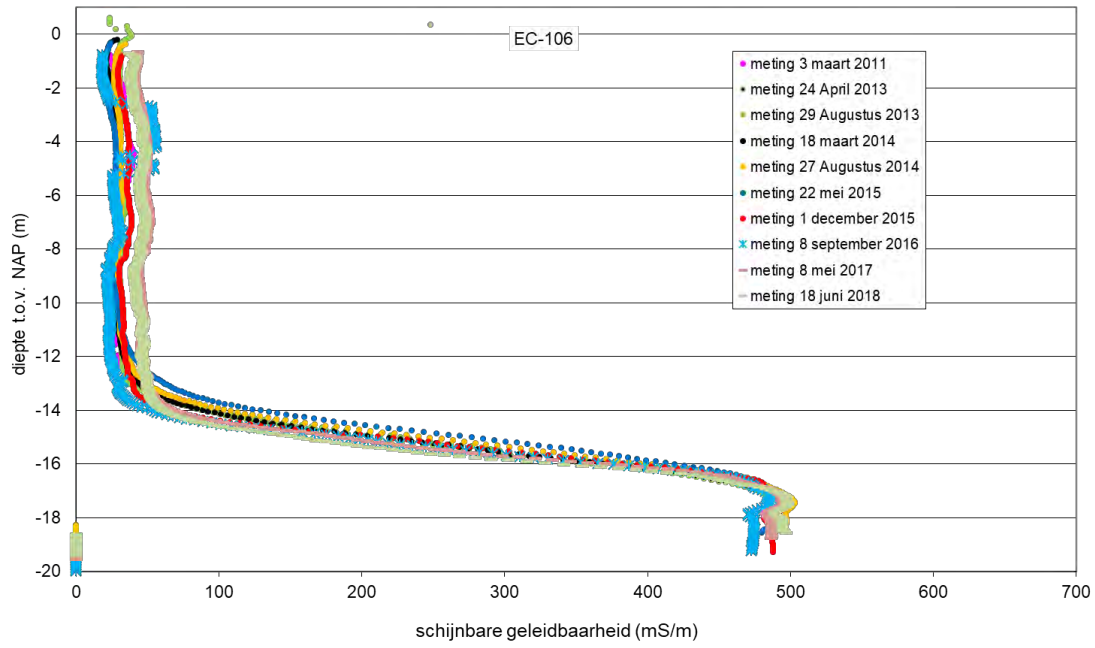


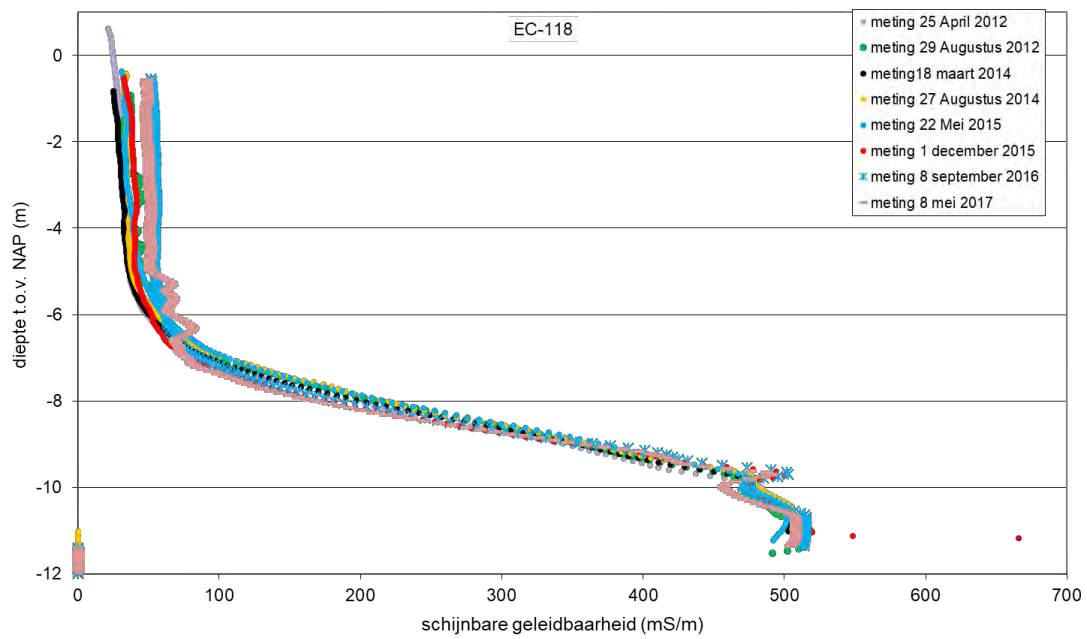
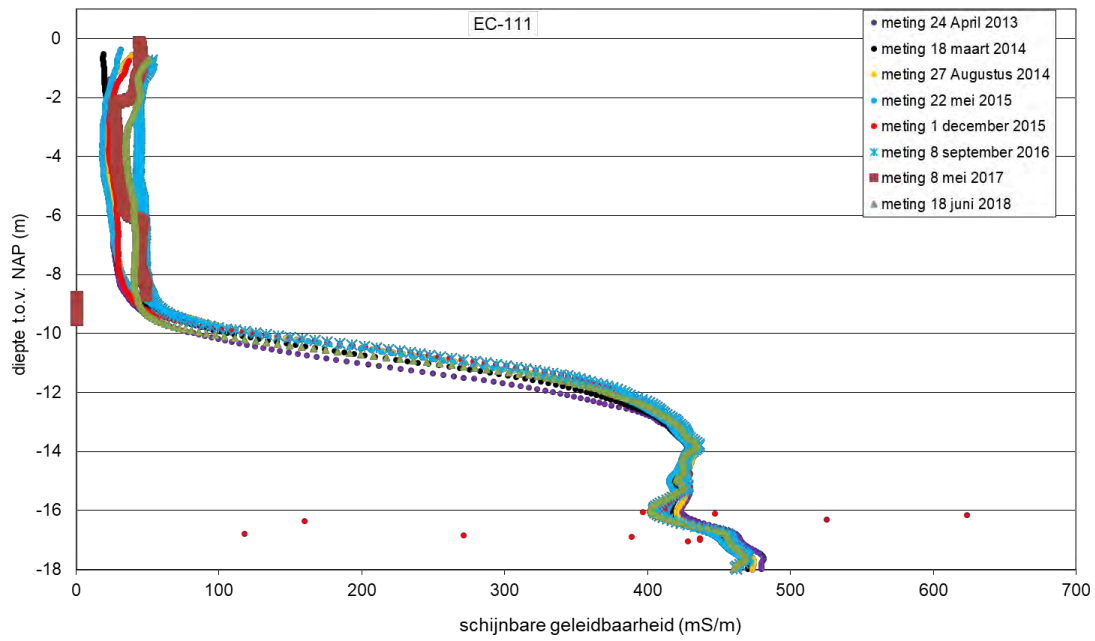


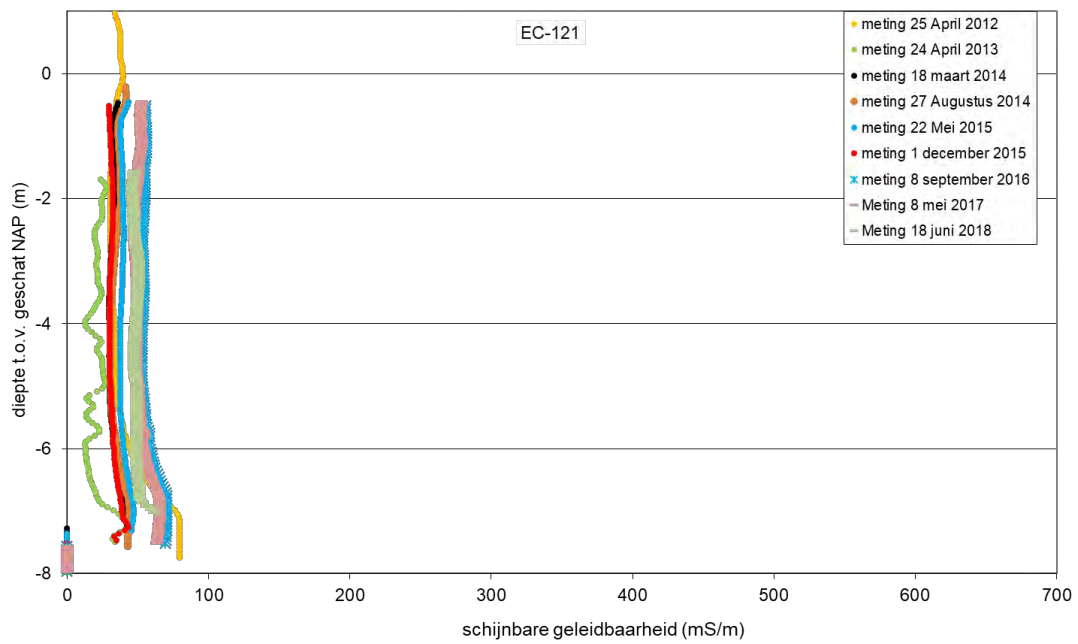
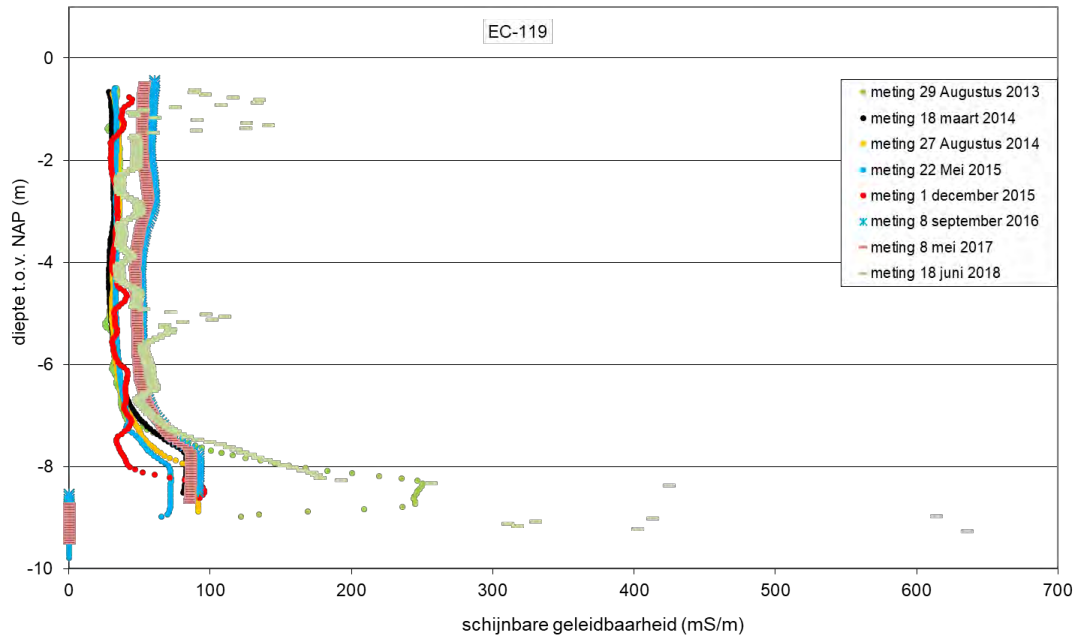
9.3 SLIMFLEX-METINGEN

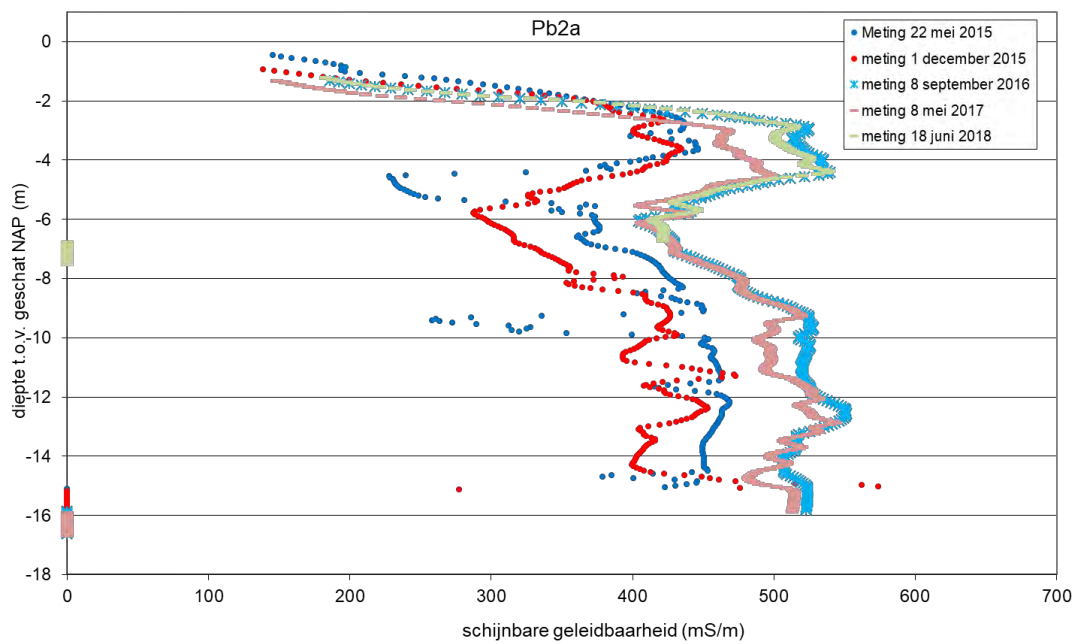
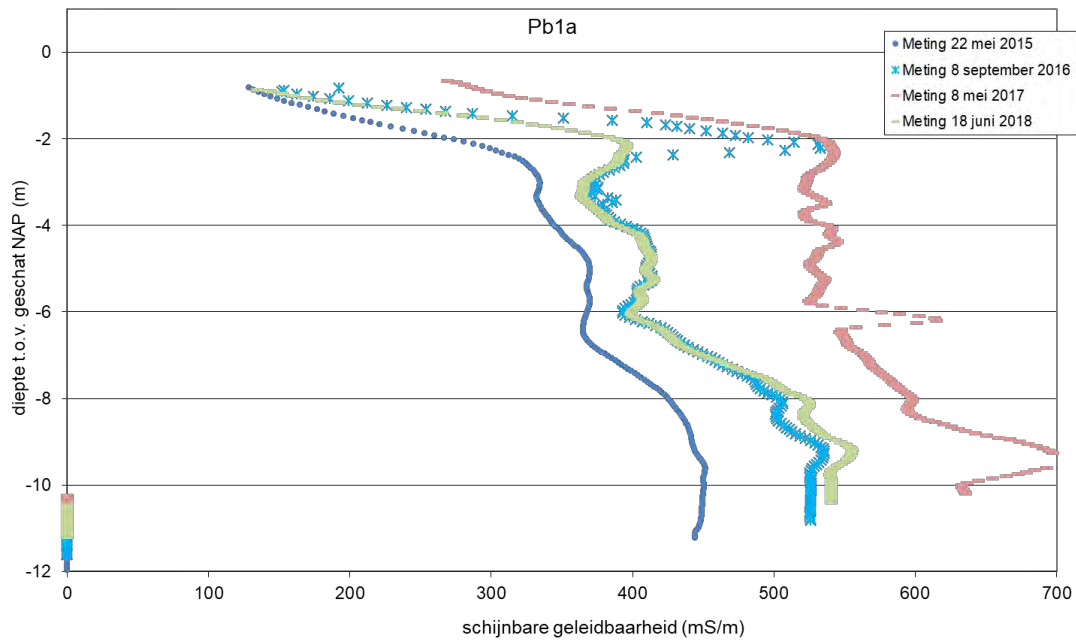
In deze bijlage staan de SlimFlex meting weergegeven.

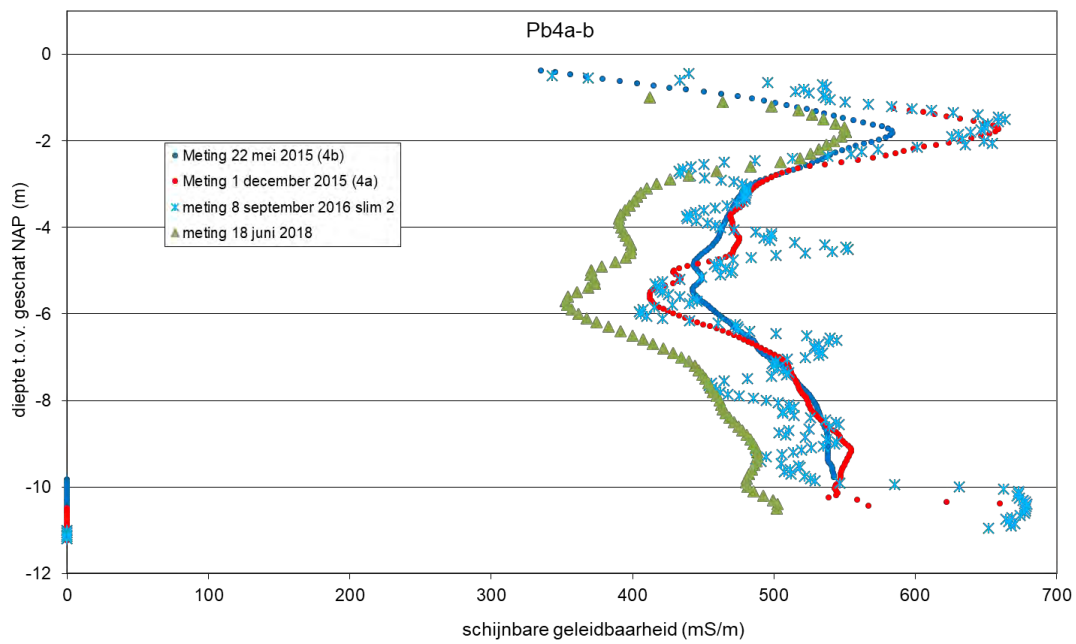
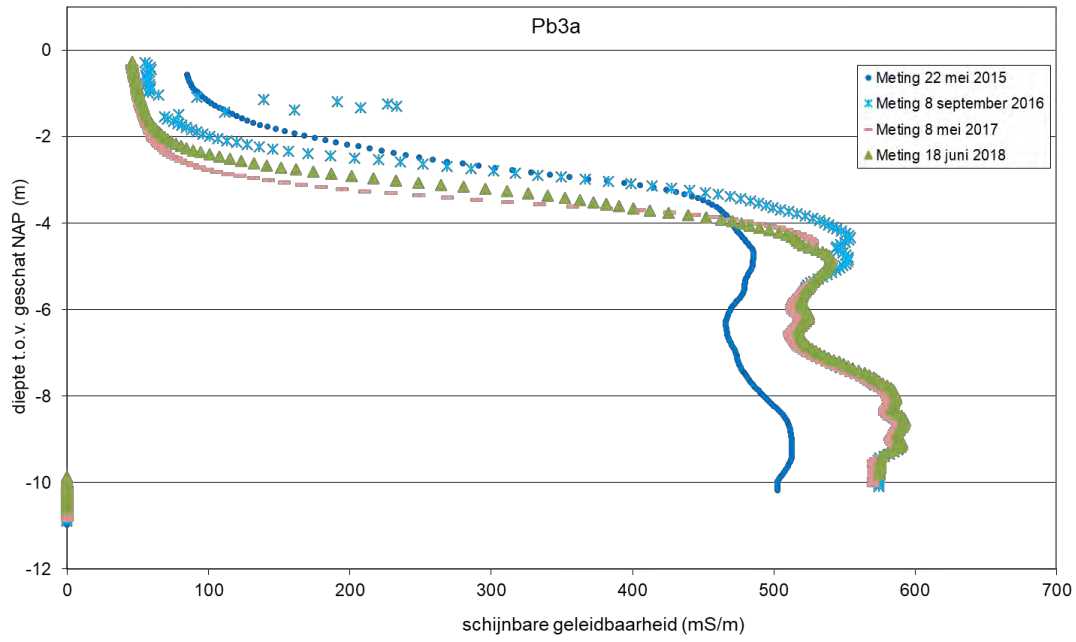


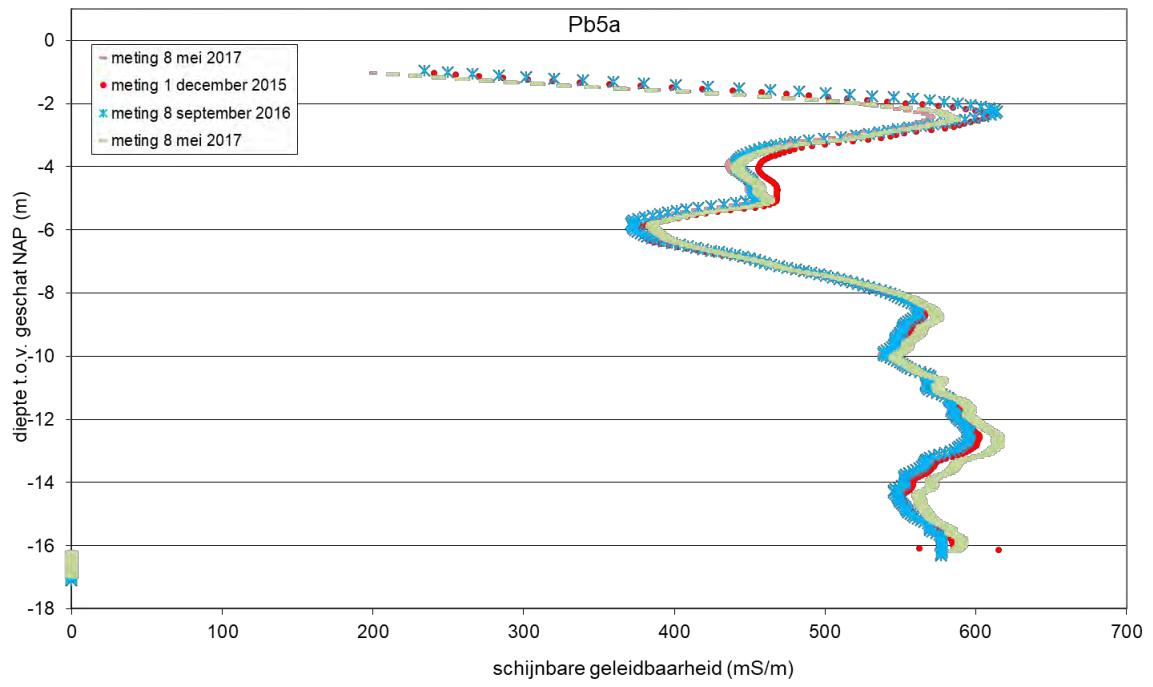












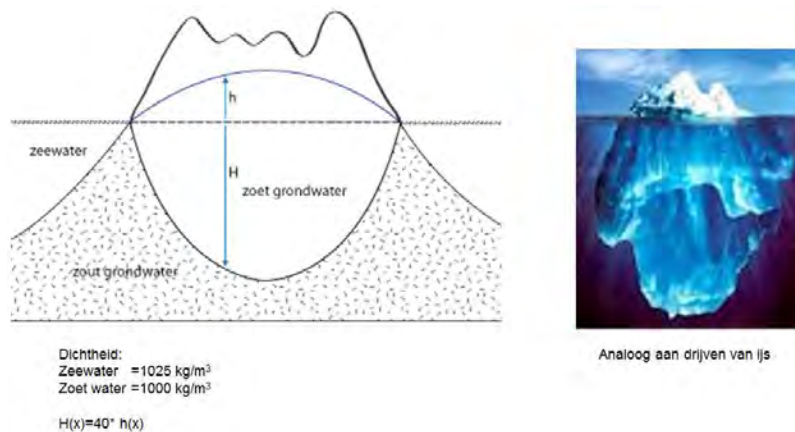
9.4 KRIMPEN EN GROEIEN VAN EEN ZOETWATERLENS IN ZOUTE OMGEVING

Badon-Ghyben Herzberg (BGH) relatie en zoetwaterbel van Kloosterzande

In de onderstaande figuur is een zoetwaterbel onder een eiland in zee te zien. Door de opwaartse druk van het zwaardere zoute water drijft de lichtere zoetwaterbel als het ware in het zoute grondwater, analoog aan het drijven van het lichtere ijs in water. Afhankelijk van de dichtheid van het zoete en zoute water is er een evenwicht tussen het zoete water wat boven de zeespiegel uitsteekt (h), aan de bovenkant begrenst door de freatische grondwaterstand, en wat onder de zeespiegel wordt aangetroffen (H). De wet van Archimedes is hierop van toepassing waarbij de opwaartse kracht die de zoetwaterbel in het zoute water ondervindt, even groot is als het gewicht van de verplaatst hoeveelheid zout water. Deze wet toepassend en uitgaande van zoetwater met dichtheid 1000 kg/m^3 en zout water met dichtheid 1025 kg/m^3 , is de dikte van de zoetwaterbel H (vanaf zeeniveau) ongeveer 40 keer de opbolling van het freatische grondwater h ten opzichte van zeeniveau ($H = 40 \times h$). Dit wordt de BGH-relatie genoemd. Hierbij dient te worden opgemerkt dat wordt uitgegaan van ideale, homogene omstandigheden die in werkelijkheid bijna nooit optreden en dat de werkelijke dikte dus zal afwijken van de theoretische dikte volgens de BGH-relatie.

Als we dit voorbeeld toepassen op de zoetwaterbel van Kloosterzande, dan kunnen we zeggen dat de stijghoogte in het zoute deel van het eerste watervoerend pakket analoog is aan de zeespiegel in het voorbeeld. h is dan gelijk aan de freatische grondwaterstand ten opzichte van deze stijghoogte. Hieruit blijkt dat de dikte van de lens is te beïnvloeden door veranderingen van h (de freatische grondwaterstand) of veranderingen van de stijghoogte. Bij een gemiddeld hogere freatische grondwaterstand (h) zal de zoetwaterlens een nieuwe evenwicht zoeken en groeien, immers de dikte van de lens moet volgens het evenwicht gelijk zijn aan $41 \times h$. In de situatie dat de stijghoogte (in het voorbeeld zeeniveau) stijgt en de freatische grondwaterstand blijft gemiddeld op hetzelfde absolute niveau (bijvoorbeeld door drainage), dan zal h (ten opzichte van de stijghoogte) afnemen met als gevolg dat de dikte van de lens afneemt. Dit is gelijk aan de situatie in Perkpolder zonder kwelvoorziening omdat de ontwikkeling van het getijdegebied leidt tot een gemiddeld hogere stijghoogte. Met de kwelvoorziening proberen we de extra stijging van deze stijghoogte te compenseren. Dit betekent ook dat als we de stijghoogte juist extra zouden verlagen door de kwelvoorziening harder te laten werken (daardoor neemt h toe ten opzichte van de stijghoogte), we de lens zelfs zouden kunnen laten groeien.

Het groeien en krimpen van de lens is een langzaam proces omdat het hierbij gaat om het daadwerkelijk verplaatsten van water, in tegenstelling tot veranderingen in de stijghoogte die voornamelijk door drukverplaatsing plaatsvinden (vrijwel instantaan). Bij het groeien van een lens gaat het om aanvulling van extra zoetwater. Als daarvoor het natuurlijk jaarlijks neerslagoverschot van bijvoorbeeld 200 mm / jaar beschikbaar is, dan zou de lens kunnen groeien met maximaal 60 cm per jaar (bij een porositeit van $1/3$). Nu is nooit het totale neerslagoverschot beschikbaar door de efficiënte afvoer via drains en sloten. Echter, wanneer extra water wordt aangevoerd en geïnfiltreerd, kan de lens veel sneller groeien. Dit test Deltares op Walcheren met de Go-Fresh kreekruuginfiltratieproef (Oude Essink et al., 2014).



Figuur beschrijving: Een zoetwaterbel onder een eiland in de zee. Volgens het Badon-Ghyben Herzberg principe is in het gegeven voorbeeld de dikte van de zoetwaterbel gelijk aan 41 keer de opbolling van de freatische grondwaterstand boven de zeewaterspiegel (links). Een zoetwaterbel in zout grondwater is analoog aan het drijven van ijs in water (rechts).

9.5 GROUNDWATERMODELLING OF THE FRESHWATER LENS OF KLOOSTERZANDE

9.5.1 PERKPOLDER MODELLING

The numerical model developed for Perkpolder is a simplified model that aims at representing the general groundwater conditions, i.e. heads and concentrations distribution of a “typical” cross section in Perkpolder and to represent the impacts of the flooding area and the effects of the seepage facility. The model was developed to represent the average conditions under the creek ridge, where the freshwater lens develops and observed measurements are available. It must be noted that a rigorous calibration was not performed as it was beyond the scope of this project. For this reason, the results presented here must be seen as general indicators of the seawater/freshwater interactions occurring under those scenarios rather than as precise representation of the lens behaviour.

9.5.2 MODEL CONSTRUCTION

The model was developed using the U.S. Geological Survey computer code SEAWAT (Langevin et al., 2008). SEAWAT is a finite-difference code of public domain, design to simulate variable density groundwater flow and solute transport. It combines MODFLOW for groundwater flow and MT3DMS for solute transport into a single program, which conserves fluid mass instead of fluid volume, and uses the equivalent freshwater head as the principal dependent variable (Guo and Langevin, 2002). The model was developed by using the script-based, computer modelling platform FloPy (Bakker et al. 2016) that is based on the programming language Python.

The model grid represents a thin cross section (A-A') of 3700m length and 20 m width (Figure 98). The model extends 3300 m inland from the coast and 400 m offshore and it is aligned to the transect formed by monitoring bores EC-101, EC-102, EC-100 and EC-111. The model width of 20 m corresponds to the distance between the installed drains of the seepage facility.

For reference purposes the model is divided in four sections (Figure 99 and Table 23). Section A represents the more inland part of the model with an extension of 1100 m, section B corresponds to a creek ridge located towards the west of the dike and has a length of 1400 m, section C corresponds to the tidal flooded area located east of the dike and a length of 800 m, and section D represents the Western Scheldt estuary.



Figure 98: Model cross section representation.

9.5.3 DISCRETIZATION

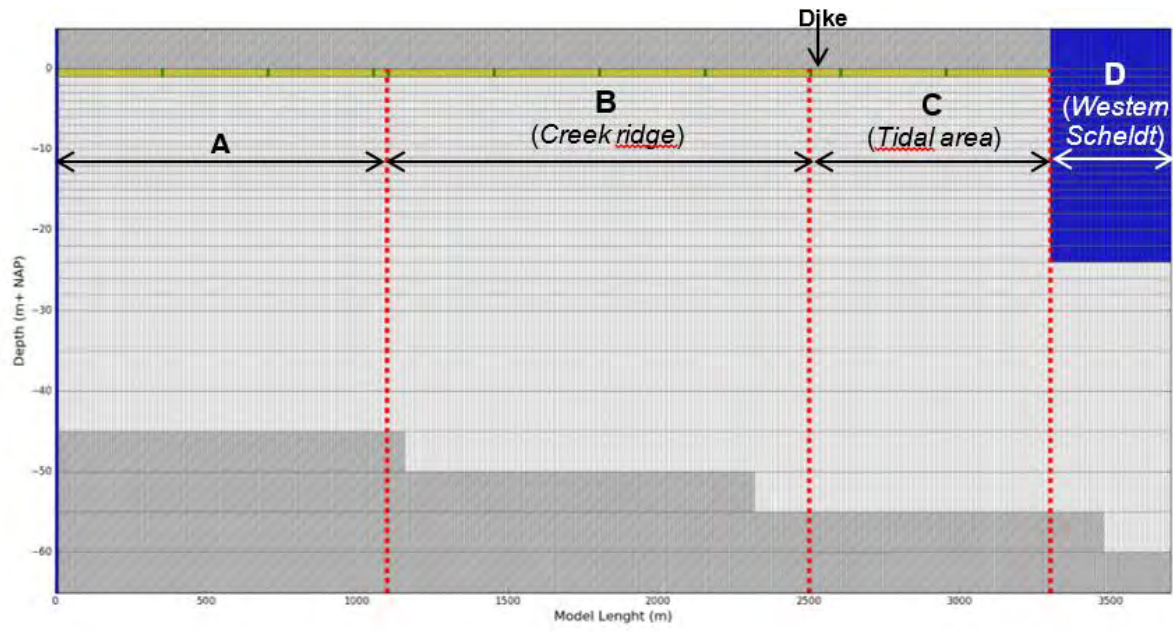
Table below presents the general model discretization details. Vertically the thickness of the cells increased with depth, resulting in a finer discretised zone where the concentration gradients were expected to be larger, i.e. top 16 meters where the freshwater lens occurs (Table 23).

- Layer 1: 5 m thick. From 5 m NAP to 0 m NAP
- Layers 2 to 17: 1 m thick, from 0 m NAP to -16 m NAP
- Layers 18 to 24: 2 m tick, from -16 m NAP to -30 m NAP
- Layers 25 to 31: 5 m tick, from -30 m NAP to -65 m NAP

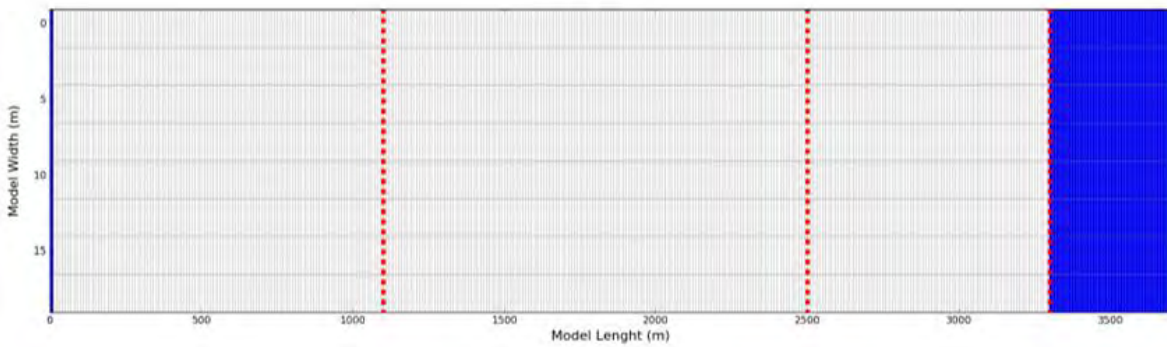
Table 23: Model discretization.

Model length (m)	3700
Number of columns	370
Columns width (m)	10
Model width	20
Number of rows	8

Rows width (m)	2.5
Total Depth (m)	70
Number of layers	31



(a)



(b)

Figure 99: Discretization and boundary conditions. In blue - general head boundary, green – rivers, yellow – drains, and grey with diagonal hatch - inactive cells. (a) Cross section trough row 4, (b) plant view of layer 10.

9.5.4 HYDRAULIC PARAMETERS

Hydraulic conductivities were distributed in zones of uniform values to represent the hydrogeological conditions of tidal deposits of sand and clay identified in previous studies (Figure 100).

- Layers 1 to 8: Shallow clay of the Naaldwijk formation with varying thickness from 0 m, in the creek ridge at section B, up to 8 m.
- Layers 9 to 21: Fine sands of the Oosterhout formation.
- Layers 22 to 24: Clay of the formation Oosterhout that occurs between -24 to -30 m NAP.
- Layers 25 to 31: Deep sandy layer of the formation Oosterhout identified between -30 to -50 m NAP.
- The Rupel/Boom clay that occurs from -40 and -50 m NAP was represented with inactive cells (no flow) to the deep layers, as indicated in Figure 100.

A constant anisotropy factor of 0.2 was used to define the vertical hydraulic conductivities. The storage coefficient was defined as 1×10^{-6} for layers 3 to 31 and 0.12 for layers 0 and 1 representing and unconfined aquifer.

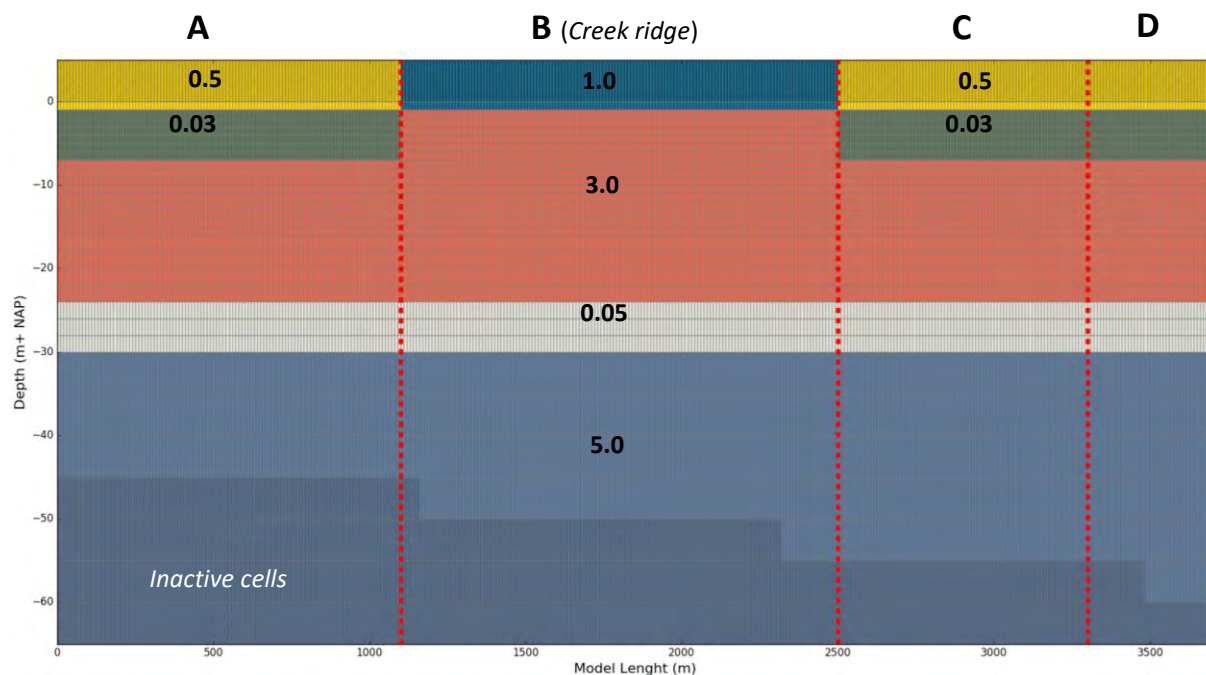


Figure 100: Zones of assigned hydraulic conductivity (m/d) and inactive cells at the bottom layers representing the Rupel/Boom clay.

9.5.5 BOUNDARY CONDITIONS

Boundary conditions are summarised in the following table. The Westerschelde and the inland boundaries were represented as source concentration cells, with a concentration of 12 mg/L, which corresponds to measured concentrations at Perkpolder estuary.

Table 24: Boundary conditions applied to the model.

Boundary (type)	Stage (m NAP)	Conductance (m ² /d)	Conc. (mg/L)	Assigned to cells	Observations
Western Scheldt (GHB)	0.15	600	12	Layers 1–20 Rows 1-8 Columns 330-370	Applied to cells in section D Stage corresponds to mean level.
Inland (GHB)	-0.6	500	12	Layers 1–31 Rows 1-8 Column 1	Stage is representative of observed heads at monitoring locations between 1990 and 2000.
Ditches Sect. A (River)	-1.8	2	-	Layer 2 Rows 1-8 Spaced every 35 columns	Ditches were represented as rivers and were assigned every 350 m. The elevation of the bottom of the riverbed was defined as equal to the river stage.
Ditches Sect. B (River)	-0.5	2	-	Layer 2 Rows 1-8 Spaced every 35 columns	
Ditches Sect. C (River)	-1.1	2	-	Layer 2 Rows 1-8 Spaced every 35 columns	
Drains Sect. A	-1.1	0.16	-	Layer 2 Rows 1-8 Spaced every column (10m)	Drains were assigned every 10 m. The conductance of the drains is constant for all drains.
Drains Sect. B	-0.5 and -0.85	0.16	-	Layer 2 Rows 1-8 Spaced every column (10m)	
Drains Sect. C	-1.0	0.16	-	Layer 2 Rows 1-8 Spaced every column (10m)	
Tidal Area (GHB)	0.15	600	12	Layers 1 and 2 Rows 1–8 Columns 254-329	Boundary applied to simulate the flooding of the tidal area (Figure 4).
Seepage facility (Drains)	-1.2 m NAP	0.31	-	Layers 9-13 Column 249 Rows 1 and 8	The drainages were assigned between -7.0 and -12.0 m NAP, i.e. 7.5 and 12.5 m below ground level. Drains assigned to rows 1 and 8 representing the real distance between the seepage points of 20 m (Figure 4).

9.5.6 SEEPAGE FACILITY:

The seepage facility SeepCat was simulated assigning drains in column 249 (approximately 50 m from the flooded area) between depths of -7 and -12 m + NAP, corresponding to layers 9 and 13 in rows 1 and 8, i.e. separated 20 m. The stage of the drains was set to -1.2 m + NAP with a conductance of 0.31 m²/d.

9.5.7 RECHARGE

An average annual recharge of 131 mm/year was distributed in winter and summer periods. Winter recharge was estimated as 264 mm for a 6-month period (October-March), and -131 mm for the 6-month summer period (April-September). The negative value used for summer represents a physical loss of water from the water table caused by evapotranspiration and or evaporation from the shallow water table. Recharge was applied to sections A, B and C of the model (Figure 100).

9.5.8 TRANSPORT PARAMETERS

The assigned transport parameters are summarised in the following Table.

Table 25: Transport parameters.

Longitudinal dispersivity (m)	0.1
Horizontal transverse dispersivity (m)	0.01
Vertical transverse dispersivity (m)	0.01
Porosity [-]	0.27

9.6 MODEL SCENARIOS

9.6.1 REFERENCE MODEL

The reference model aims at representing the conditions prior the open and flooding of the tidal area. Initial heads and initial concentrations were assigned as 0.15 m NAP and 12 mg/L respectively for the entire model domain. The model was run for a simulation time of 750 years allowing the freshwater lens to develop and reach steady state conditions, i.e. no changes in heads and concentrations were observed with time. The model was discretized in 1500 stress periods of 182.5 days (6-month).

Observed concentrations and heads were used to manually calibrate the model to represent the salinity distributions and the occurrence of the freshwater lens in the creek ridge area. A sensitivity analysis was conducted by systematically changing assigned parameters of recharge, hydraulic conductivity, drains depth, inland GHB stage, longitudinal and transverse dispersivity, and assessing the performance of the model to observed data.

9.6.2 FLOODING

This scenario simulates the transformation of the agricultural area into a tidal area without implementing the seepage facility. The objective of this scenario is to understand the longterm effect of inundating the area without any mitigation, in order to compare the efficiency and impacts of the seepage facility. Freshwater heads and concentration's distributions of the calibrated reference model were used as initial conditions. The model was run for a simulated period of 100 years, i.e. 200 stress period of 182.5 days length.

The boundary conditions assigned to simulate the flooding of the tidal area are summarised in **Figure 101** and Table 24.

9.6.3 FLOODING WITH SEEPAGE FACILITY

This scenario represents the operation of the seepage facility, which was represented by drains located between -7.0 and -12 m NAP and 20 meters west of the dike (**Figure 101**). Initial conditions correspond to the calculated freshwater heads and concentrations of the calibrated reference model. The model was run for a simulated period of 100 years. The boundary conditions assigned to simulate the seepage facility are summarised in Table 24.

Two simulations were developed for this scenario. The first simulation has the seepage facility operating all year round, while the second simulation is more representative of the current operation of the facility, with the seepage operating only for the winter period, 6-months when head levels are higher, and is off during summer months.

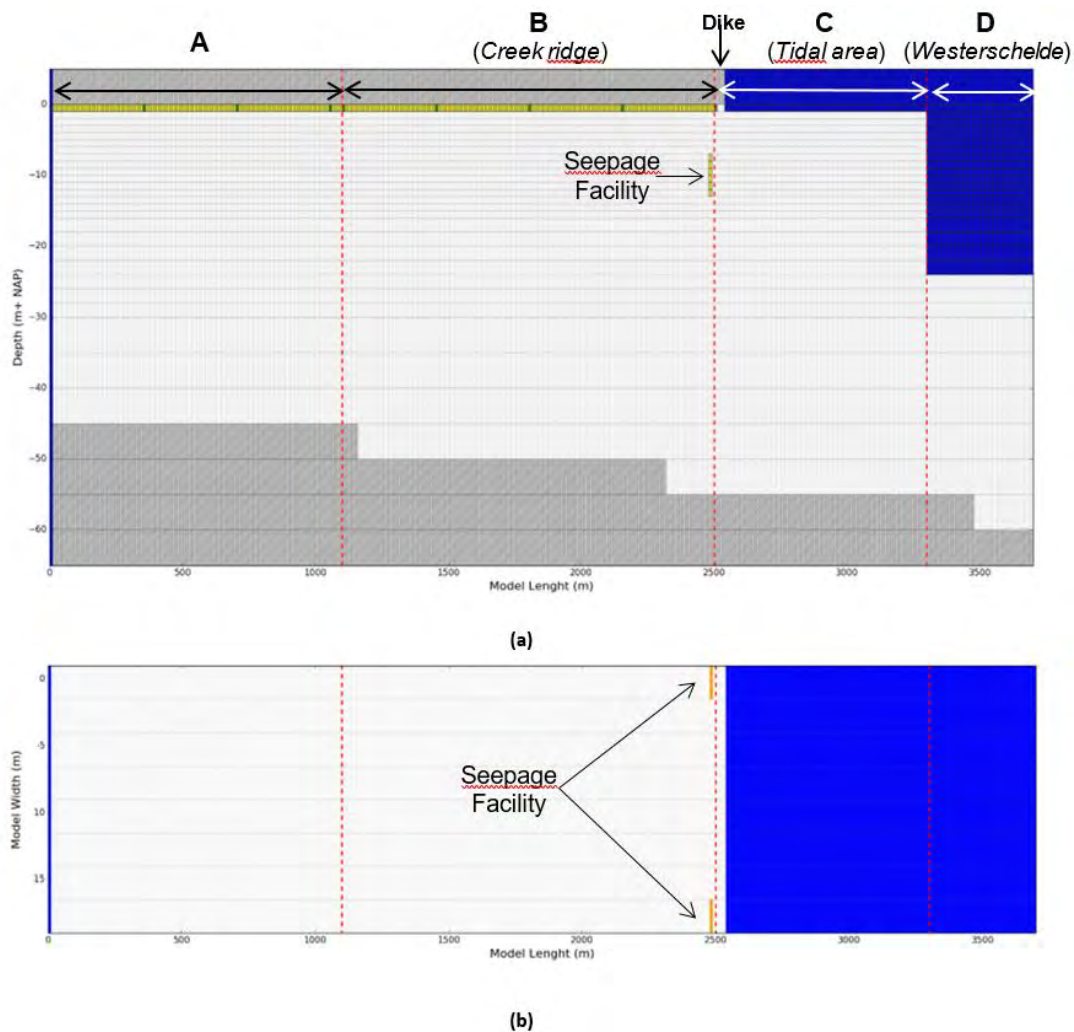


Figure 101: Assigned boundary conditions of the flooding scenario and the flooding + seepage facility. In blue - general head boundary, green - rivers, yellow - drains, and grey with diagonal hatch - inactive cells. (a) Cross section through row 4, (b) plant view of layer 10.

9.7 MODEL RESULTS

9.7.1 REFERENCE MODEL

Quasi steady state conditions in the developing of the lens were established after 700 years of simulation. The lens develops in the creek ridge section resulting from the higher water table caused by the higher elevation of the drains and ground level in this section. In sections A and C fresh recharge does not infiltrates deep further because of the permanent upward flow of saline groundwater (saline seepage) (Figure 102).

The ditches cause an up-coning process, with the upwards movement of saltwater from the bottom of the lens towards the ditches. On the thinnest part of the lens the up-coning reaches the ditches, forming in depending thin and narrow lenses, while inland the lens is continuous

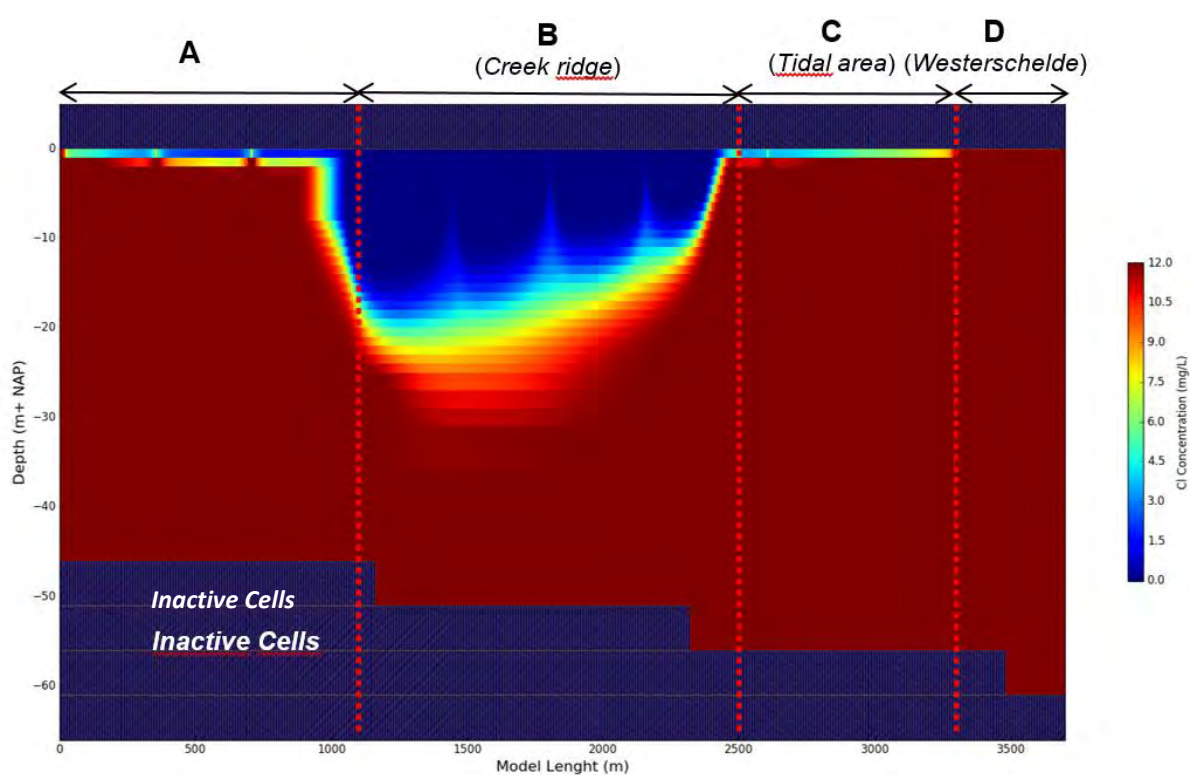


Figure 102: Modelled freshwater lens in the creek ridge zone with steady state conditions reached after 500 years.

Figure 103 shows the concentration contours from 0.15 mg/L, corresponding to the freshwater limit, to 6 mg/L which is 50% of the maximum salinity at Perkpolder. The lens is asymmetric, with the freshwater limit depth varying from -7 m NAP towards the estuary and -14 m NAP inland.

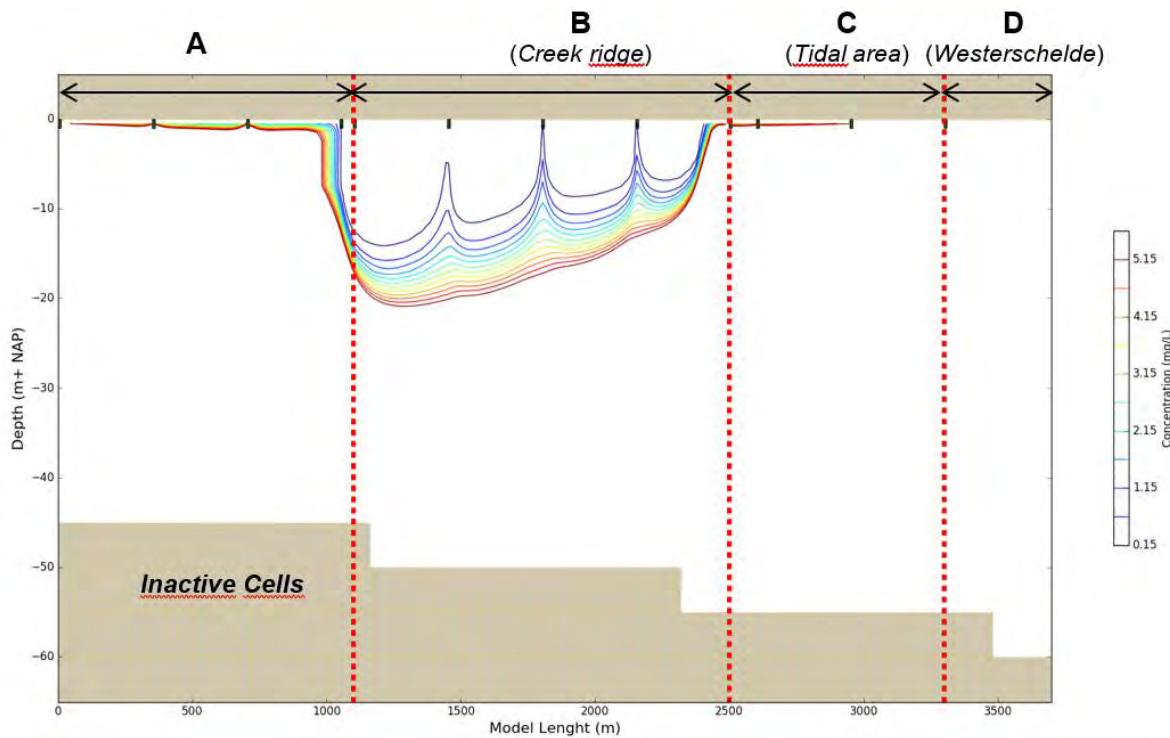


Figure 103: Concentration contours between the freshwater limit 0.15 mg/l (blue) and 6 mg/L (red).

The head distributions vary considerably between winter and summer (Figure 104). On the ridge creek section the simulated water table and aquifer heads vary approximately 0.55 m between summer and winter (Figure 104a). This result corresponds with the average seasonal variations observed in the monitoring bores EC-101, EC-102 and EC-111, located along the model line, which ranges between 0.5 and 0.65 m (De Louw et al., 2016).

Figure 105 presents a comparison between the observed and simulated heads and concentration at the monitoring bores location. The model underestimates the observed heads, especially towards the edge of the ridge creek, where differences of observed and simulated heads are up to -0.49m in EC-102 in winter. Towards the west –inland- the model performance improves, with smaller differences between observed and simulated heads, and a minimum of -0.06 m at EC-111 in summer.

In the ridge creek zone the aquifer head is always lower than the water table elevation (Figure 104b), indicating a downward movement of water, which allows recharge to penetrate and form the lens. The gradient between the water table and the aquifer head in the ridge creek is slightly larger in winter and reduces in summer as a result of the simulated negative recharged for summer. In sections A and C (tidal area) the water movement is always upwards, resulting in a permanent saline seepage.

In terms of concentration the model performs better at replicating the observed distributions, with a thin (< 2 m) lens at EC-102, and a thicker 5 and 9 m lens in EC-101 and EC-111 respectively (see Figure 105).

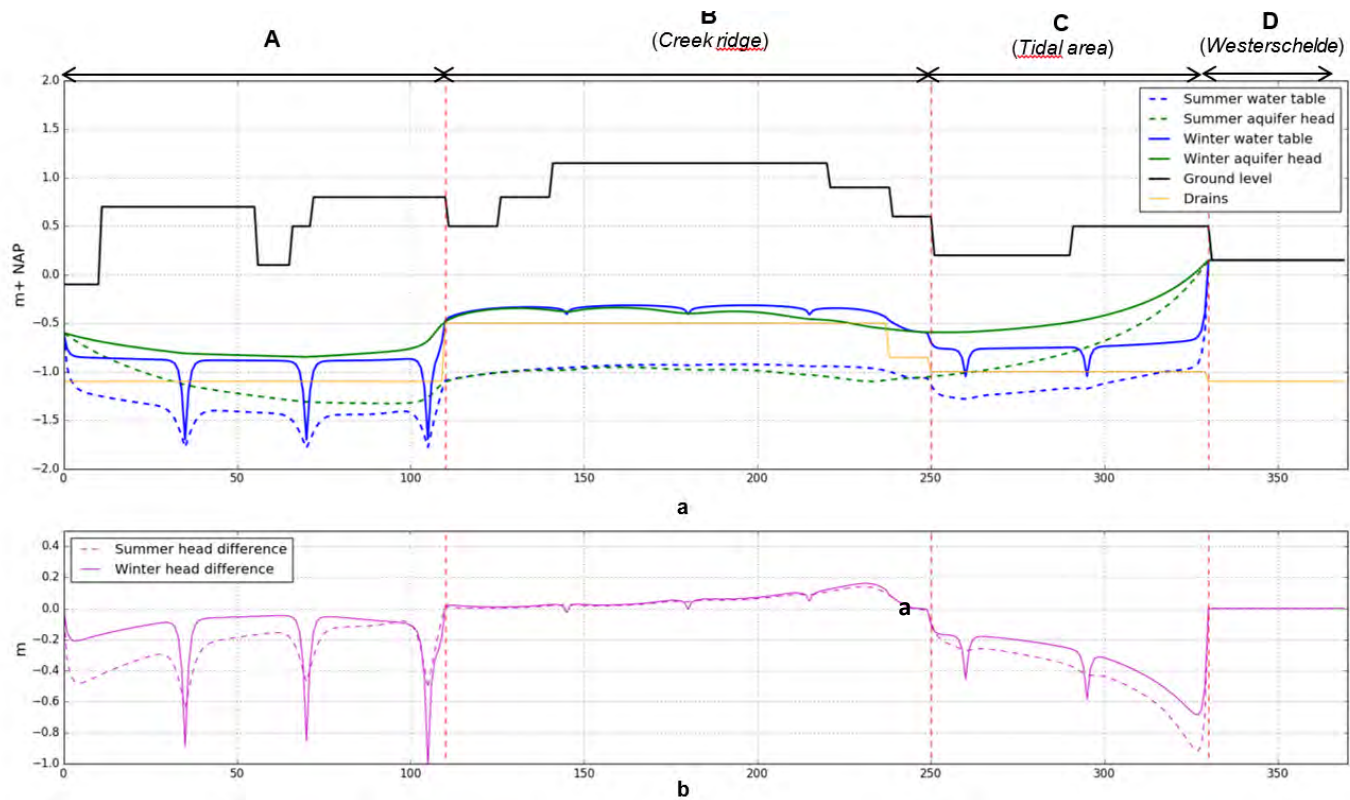


Figure 104: Groundwater head distributions for winter and summer a) Simulated aquifer freshwater heads (at -14.5 m NAP) and water table along the model section; b) head differences between the water table and the aquifer (>0 downward movement, <0 upward movement). Note: X axis is presented as columns numbers.

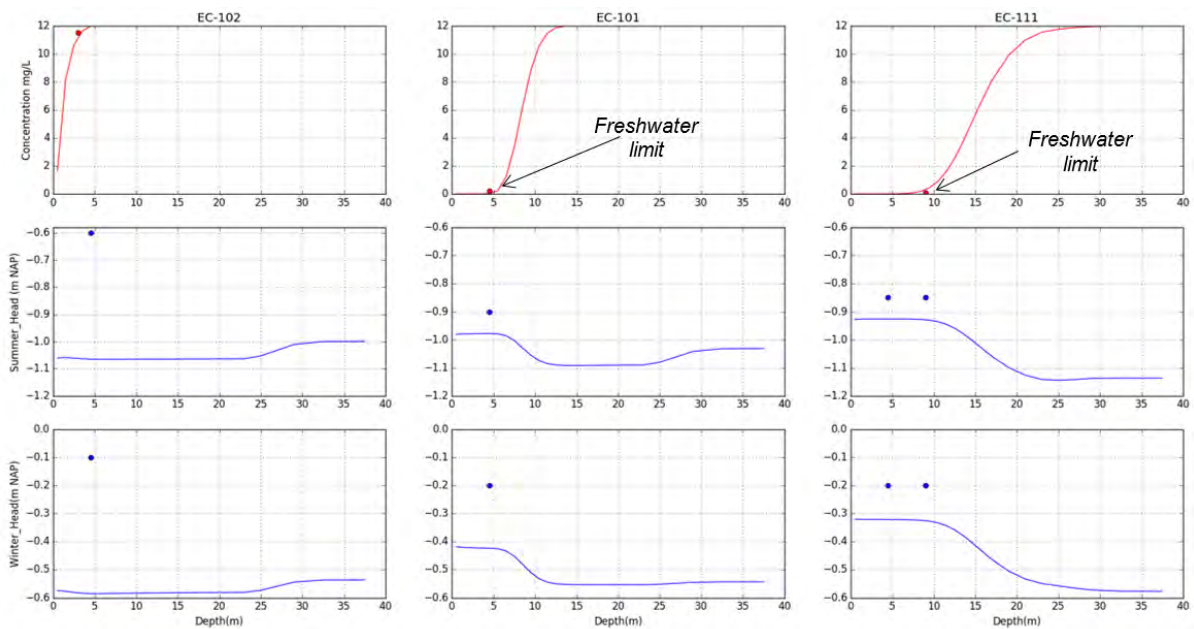


Figure 105: Observed and simulated concentrations and heads profiles at the monitoring bores EC-102, EC-101 and EC-111 located along the model line. Lines correspond to simulated profiles and points represent average of observed values.

9.7.2 SCENARIO MODELS

Figure 106 presents a comparison on the freshwater lens limit for the reference, flooding, and flooding with seepage facility scenarios at different simulation times. The impacts of flooding the tidal area are long-term observed. The simulation results indicate that a new steady state is not yet established after 100 years. After one year of flooding the tidal area the freshwater limit is moved inland, away from the flooded area, approximately 10 meters and the thickness of the lens remains equal (Figure 107a). The progressive inland-upward movement of the interface continues at a slow rate, resulting in a reduction of the freshwater lens thickness of approximately 1 meter after 5 years of simulation, and a complete salinization of the freshwater lens, within a distance of 700 m from the flooded area, after 100 years of simulation (Figure 108d).

The scenario simulating the seepage facility indicates that this measure reduces significantly, in the long-term, the impacts of flooding the tidal area in the freshwater lens. After 5 years the thickness of the lens remains as on the reference simulation, and after 25 years the upward movement of the limit of the freshwater lens is of approximately 0.9 m, which is comparable to the 5 years effects of flooding without the seepage facility scenario. After 100 years the lens shows a reduction in thickness of 2 m and a complete extension over the ridge creek resulting in a large benefit of available volume of freshwater compared to the situation without the seepage facility.

The effects of the scenarios in the head distribution in the aquifer are presented in Figure 107 and Figure 108 for 6 months and 100 years of simulation respectively. The flooding scenario shows that aquifer heads rise on the edge of zone B caused by the boundary condition of the tidal area. This rising heads effect is localised, extended 250 m inland from the flooding area after 6 months (Figure 107a), and extended up to 600 m after 100 years of simulation (Figure 108a).

The drainage from the seepage maintains the aquifer heads low, avoiding the increment on the head pressure caused by the closer boundary of the estuary. The long term effect of the seepage is shown Figure 108b, where the difference between the water table and the aquifer heads differ considerably from the flooding scenario, i.e. the seepage facility maintains the hydraulic pressure in the aquifer low, allowing a downward movement of groundwater that helps to keep the formed lens in this area. The simulated heads in the seepage scenario fall below the heads on the reference model (Figure 107a and Figure 108a) on the vicinity of the seepage facility, which was also observed in monitoring location Pb-2 (De Louw et al., 2016).

Simulated and average observed head variations at PB-2, located next to the seepage facility, are compared in Figure 109. Flooding of the tidal area resulted in an average observed head increment of 0.3 m, comparable with the 0.22 m rise simulated by the model. The seepage facility lowered the heads by 0.45 m which is correspondent to the 0.46 m simulated by the model. It is to note that the model is not able to replicate the observed heads at the monitoring bores, but in a sense it represents the head rise and lowering on the range of the observed measures.

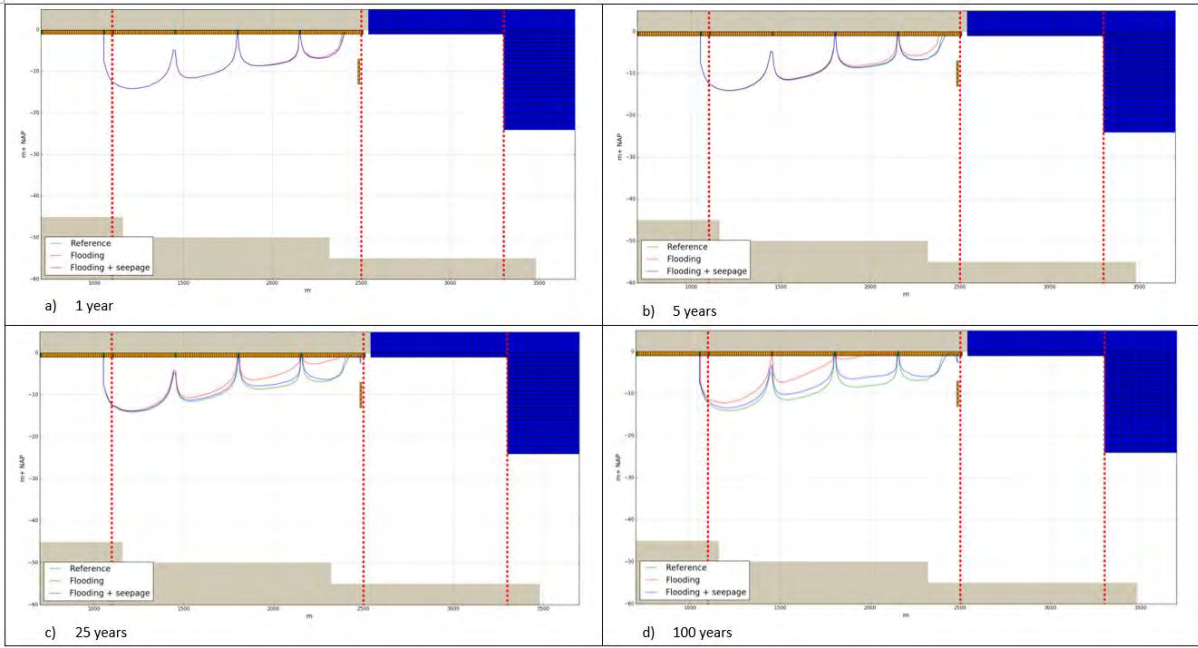


Figure 106: Results of scenarios simulations at different simulations times.

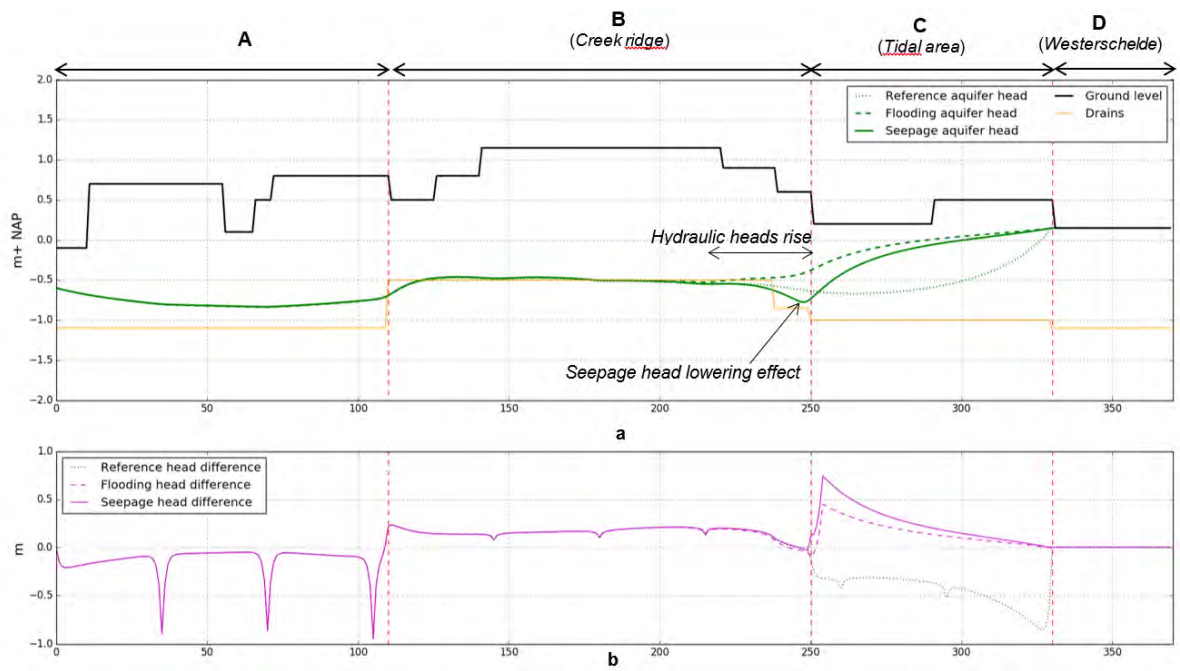


Figure 107: Groundwater head distributions after 6 months for scenarios. a) Simulated aquifer freshwater heads (at -20.5 m NAP) and water table along the model section; b) head differences between the water table and the aquifer (>0 downward movement, <0 upward movement). Note: X axis is presented as columns numbers.

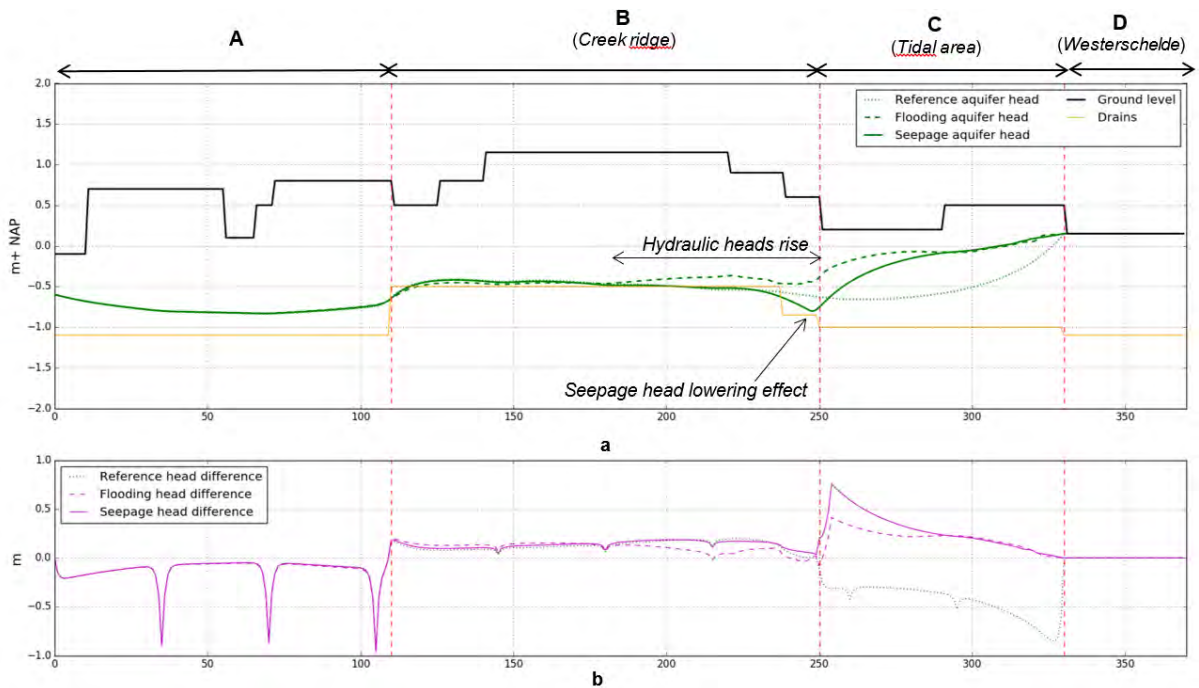


Figure 108: Groundwater head distributions after 100 years for scenarios. a) Simulated aquifer freshwater heads (at -20.5 m NAP) and water table along the model section; b) head differences between the water table and the aquifer (>0 downward movement, <0 upward movement). Note: X axis is presented as columns numbers.

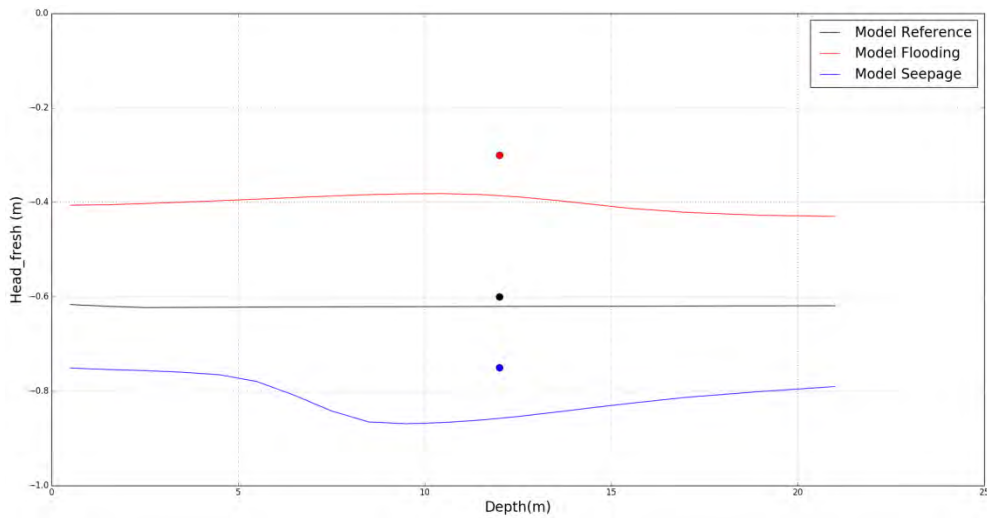


Figure 109: Observed and simulated head profile at monitoring location PB-2 for the reference, flooding and seepage scenarios.

9.7.3 SEEPAGE FACILITY OPERATING ONLY DURING WINTER PERIOD

The results from the additional simulation of the seepage facility operating only during winter months are presented in Figure 110. The effect of the facility is reduced compare to the scenario where it operates all year round, however, benefits are still observed in preserving the lens in the immediate vicinity of the tidal area compared to the flooding - no seepage facility scenario.

The differences between operating the seepage facility all year round and only in winter are observed on the long term, after 25 years, when the upward movement of the limit of the freshwater lens is of approximately 1.2 m, which is comparable to the 100 years effects of operating the seepage facility all year. After 100 years the lens thickness reduced by approximately 3.5 m and moved inland 20 m. Figure 111 presents the head distributions after 100 year of simulation, i.e. at the end of the summer period. It shows that the simulation in which the seepage operates only in winter shows a similar head aquifer head distribution to that observed in the scenario without the seepage facility, with higher heads than those observed on the seepage facility operating in summer and winter.

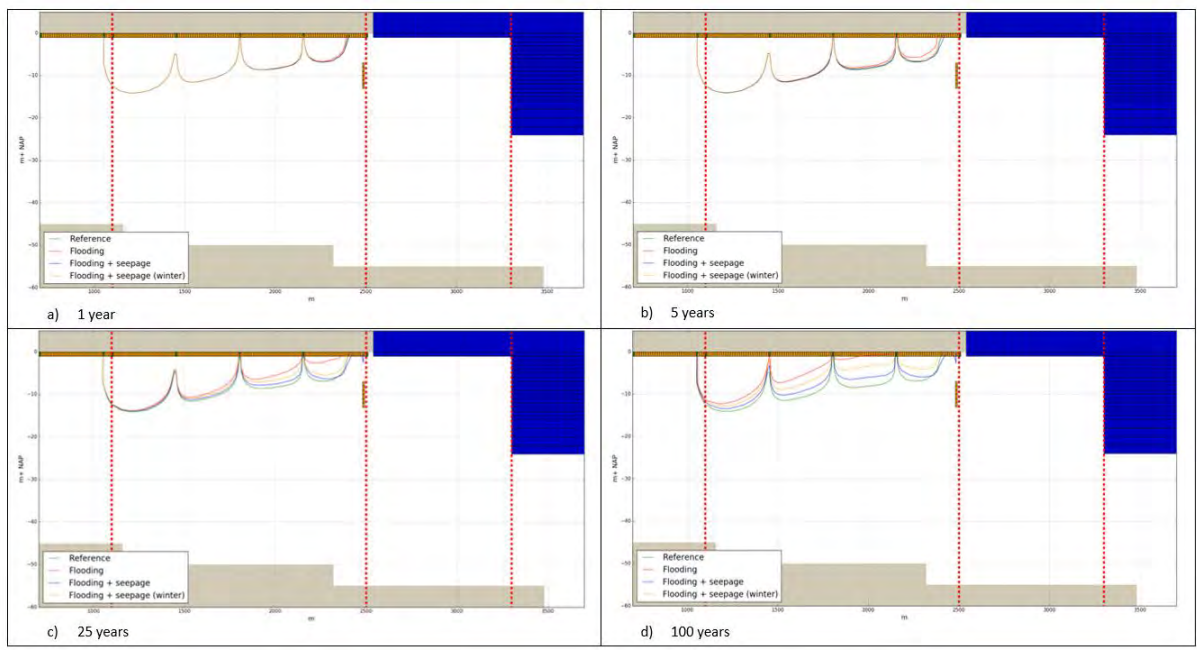


Figure 110: Results of scenarios simulations at different simulation times with the seepage facility operating 6-months a year, during the winter period.

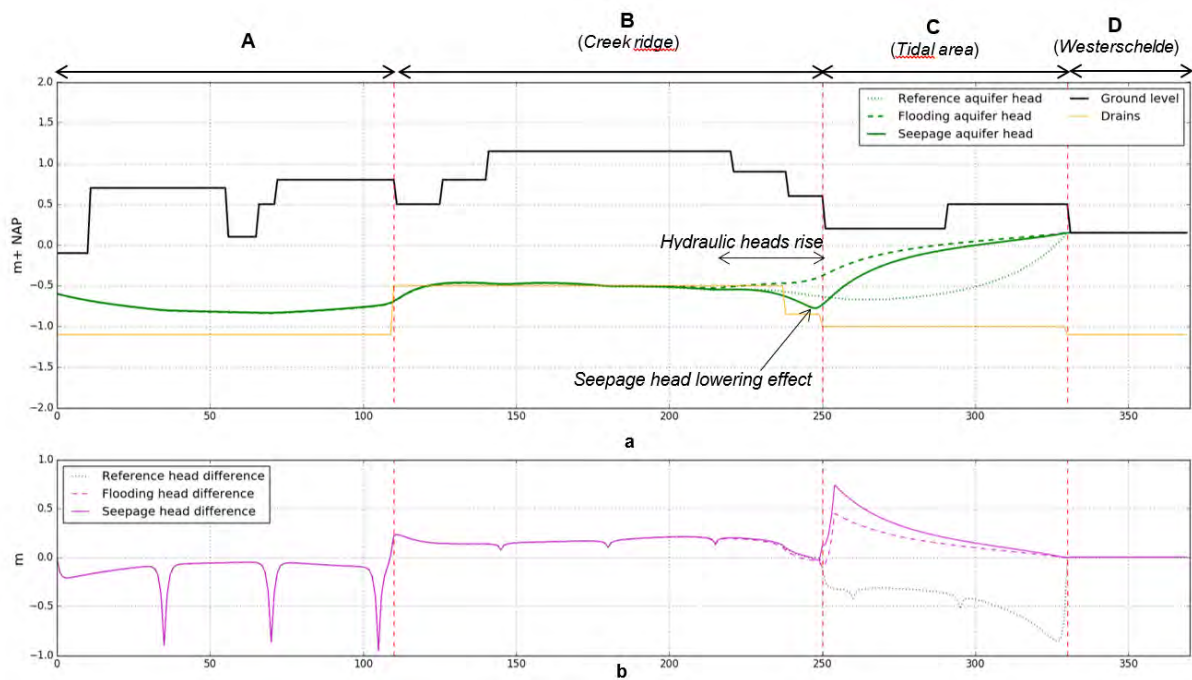


Figure 111: Groundwater head distributions after 100 years for scenarios. a) Simulated aquifer freshwater heads (at -20.5 m NAP) and water table along the model section; b) head differences between the water table and the aquifer (>0 downward movement, <0 upward movement). Note: X axis is presented as columns numbers.

9.8 CONCLUSIONS

- The model is a simple representation of the freshwater lens in Perkpolder. It aims at representing the occurrence of the freshwater lens in the creek ridge area, the effect of flooding the tidal area on the lens, and the mitigation of seawater intrusion with the seepage facility.
- A rigorous calibration was not performed, but in general terms the model is able to represent the concentration distribution adequately, however it underestimated the heads. Further sensitivity analysis would be required to improve the representation of Perkpolder heads distribution.
- Despite the discrepancies between simulated and observed heads, the model is able to reproduce the general groundwater head distributions on the lens and is within the magnitude of orders of heads variations under the different scenarios simulated.
- Flooding the tidal area without any mitigation action will result in a gradual reduction of the freshwater lens, as the interface moves inland and upwards. After 100 years of simulation the lens had disappeared from a 700 m distance from the tidal area.
- The seepage facility is able to lower the hydraulic heads in the aquifer, resulting in a long-term solution that prevents seawater intrusion into the lens. This measure seems much more effective in the long term when the seepage facility operates permanently and not in periods, winter and summer.
- It should be remarked that the model was built with a 2D-concept which means that effects can only migrate perpendicular to the tidal area and to the seepage facility. Since in this way diffuse 3D-effects are neglected, the possibility exists that the 2D-results are a little bit exaggerated.